SWIL Hydrological and Water Quality Calibration Basins

Draft Memorandum

TASK 6 AND TASK 7 OF THE SPATIAL WATERSHED ITERATIVE LOADING MODEL UPDATE

PREPARED FOR:

PREPARED BY:

April 5, 2023

Table of Contents

LIST OF FIGURES

List of Tables

List of Acronyms

DRO	Direct runoff
ET	Evapotranspiration
in	Inches
IRL	Indian River Lagoon
L	Liter
LULC	Land Use Land Cover
mg	Milligram
mm	Millimeter
NASA	National Aeronautics and Space Administration
NRCS	Natural Resources Conservation Service
POR	Period of record
SJRWMD	St. Johns River Water Management District
SNP	Sebastian North Prong
SSP	Sebastian South Prong
SWIL	Spatial Watershed Iterative Loading
TN	Total nitrogen
TP	Total phosphorus
USDA	United States Department of Agriculture
USGS	United States Geological Survey
WHAT	Web-based hydrograph analysis tool

1 Introduction

As there were large-scale land use changes in the Indian River Lagoon (IRL) watershed since the original calibration and changes in the subsurface flow components of the model based on newly available data, there was anticipation that calibration factors would need to be regenerated for Spatial Watershed Iterative Loading (SWIL) 5.0 model. Included in this memorandum is a characterization of the seven basins used to calibrate and evaluate SWIL.

2 Calibration Basin Characterization

The subsections below provide a brief characterization of the model inputs for each basin used during the calibration process, including land use land cover (LULC), soil hydrologic types, precipitation, evapotranspiration (ET), treatments, hydrology, and water quality characteristics.

2.1 Big Flounder

2.1.1 LULC Change

The Big Flounder calibration basin is the smallest of the seven calibration basins, covering approximately 1,890 acres. It has been predominately composed of low density residential (~27%), improved pasture (~25%), hydric hammock (~8%), industrial (~6%), and dry prairie (~5%) land use consolidation types (Table 1). The western portion of the basin is characterized mostly by residential areas, while the eastern portion is pasture and natural (upland and wetland) types (Figure 1, Figure 2, Figure 3). Overall, the largest changes to the total area occurred between 2010 (Figure 1) and 2015 (Figure 2), with increases in pasture (~9%) and institutional (~5%) land use types after the development of the Cape Canaveral National Cemetery, accompanied by minor decreases in the citrus (~4%) and rangeland (~2%) types.

Table 1. Total area (in acres and percentage) of each land use consolidation type in the Big Flounder calibration basins for the 2010, 2015, and 2020 years.

Land Use Consolidation	Land Use Area (Acres)			Percent of Total Land Use (%)			Percent Change (%)	
	2010	2015	2020	2010	2015	2020	2015-2010	2020-2010
Citrus	**111.24**	40.62	39.20	**5.89**	2.15	2.07	-3.74	-3.81
Commercial	40.01	40.05	41.29	2.12	2.12	2.19	0.00	0.07
Dry Prairie	**111.98**	**94.65**	**94.65**	**5.93**	**5.01**	**5.01**	-0.92	-0.92
Field Crop	86.79	--	--	4.59	--	--	--	--
High Density Residential	0.94	7.50	7.50	0.05	0.40	0.40	0.35	0.35
Hydric Hammock	**173.02**	**154.02**	**154.02**	**9.16**	**8.15**	**8.15**	-1.01	-1.01

Land Use Consolidation	Land Use Area (Acres)			Percent of Total Land Use (%)			Percent Change (%)	
	2010	2015	2020	2010	2015	2020	2015-2010	2020-2010
Improved Pasture	**345.20**	**523.64**	**523.72**	**18.27**	**27.71**	**27.72**	9.44	9.45
Industrial	111.24	**112.29**	**112.29**	5.89	**5.94**	**5.94**	0.06	0.06
Institutional	0.43	91.69	91.69	0.02	4.85	4.85	4.83	4.83
Low Density Residential	**501.63**	**503.60**	**508.99**	**26.55**	**26.65**	**26.94**	0.10	0.39
Medium Density Residential	15.19	18.96	17.72	0.80	1.00	0.94	0.20	0.13
Mesic Flatwoods	6.59	6.54	6.54	0.35	0.35	0.35	0.00	0.00
Open	39.88	34.99	35.01	2.11	1.85	1.85	-0.26	-0.26
Other Agriculture	49.61	13.54	8.66	2.63	0.72	0.46	-1.91	-2.17
Rangeland	94.21	48.49	48.49	4.99	2.57	2.57	-2.42	-2.42
Scrub	18.79	18.15	18.15	0.99	0.96	0.96	-0.03	-0.03
Transportation	23.67	23.66	23.66	1.25	1.25	1.25	0.00	0.00
Upland Flatwoods	53.04	48.45	48.08	2.81	2.56	2.54	-0.24	-0.26
Water	8.53	13.01	13.01	0.45	0.69	0.69	0.24	0.24
Wet Flatwoods	11.98	7.86	7.83	0.63	0.42	0.41	-0.22	-0.22
Wet Prairies	0.38	6.27	6.27	0.02	0.33	0.33	0.31	0.31
Wetland	85.26	81.64	82.84	4.51	4.32	4.38	-0.19	-0.13

**The top five land uses that make up a majority of the area have been bolded for each year. The percent change between land use years is also included.*

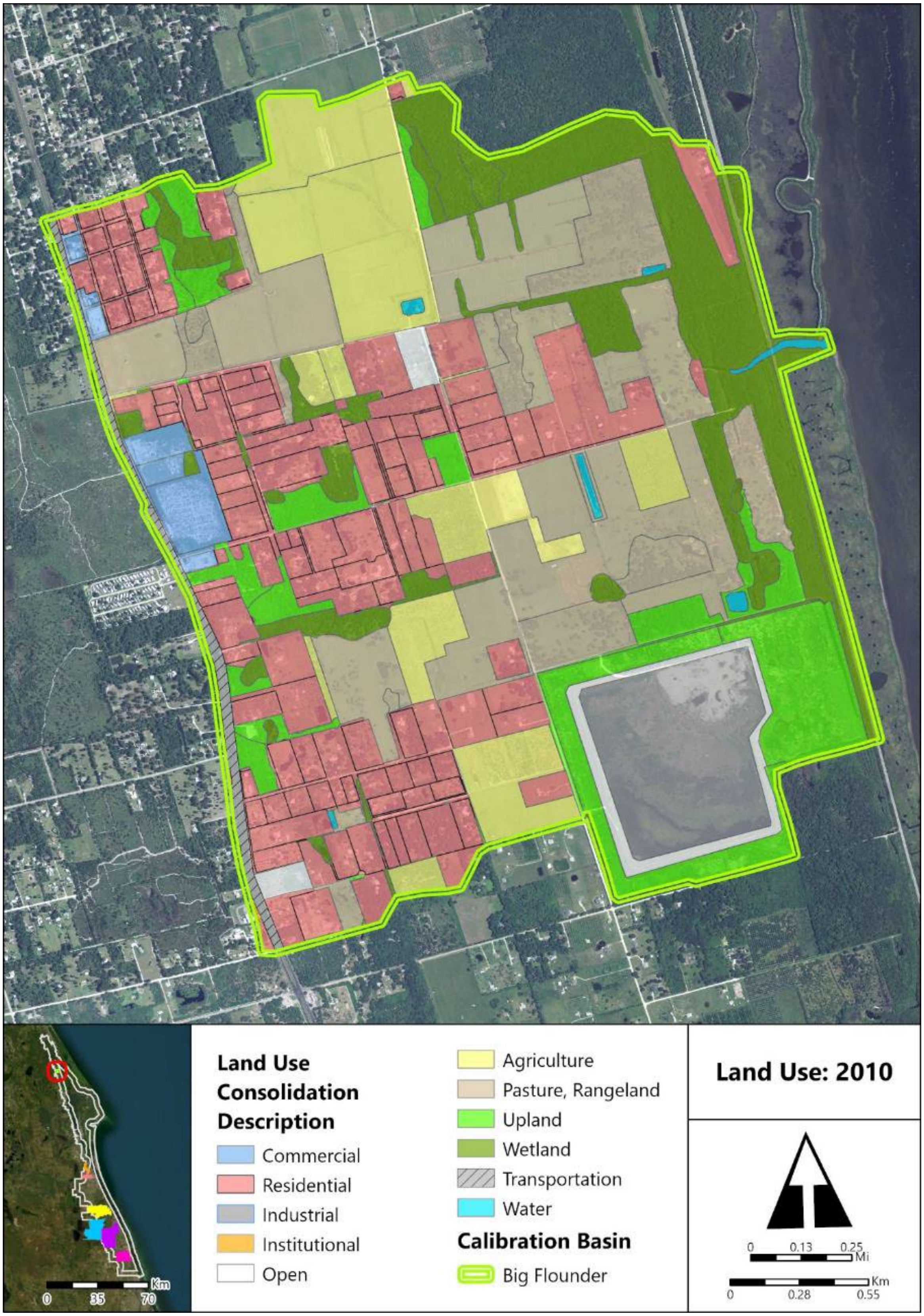

Figure 1. Land use within the Big Flounder calibration basin for 2010.

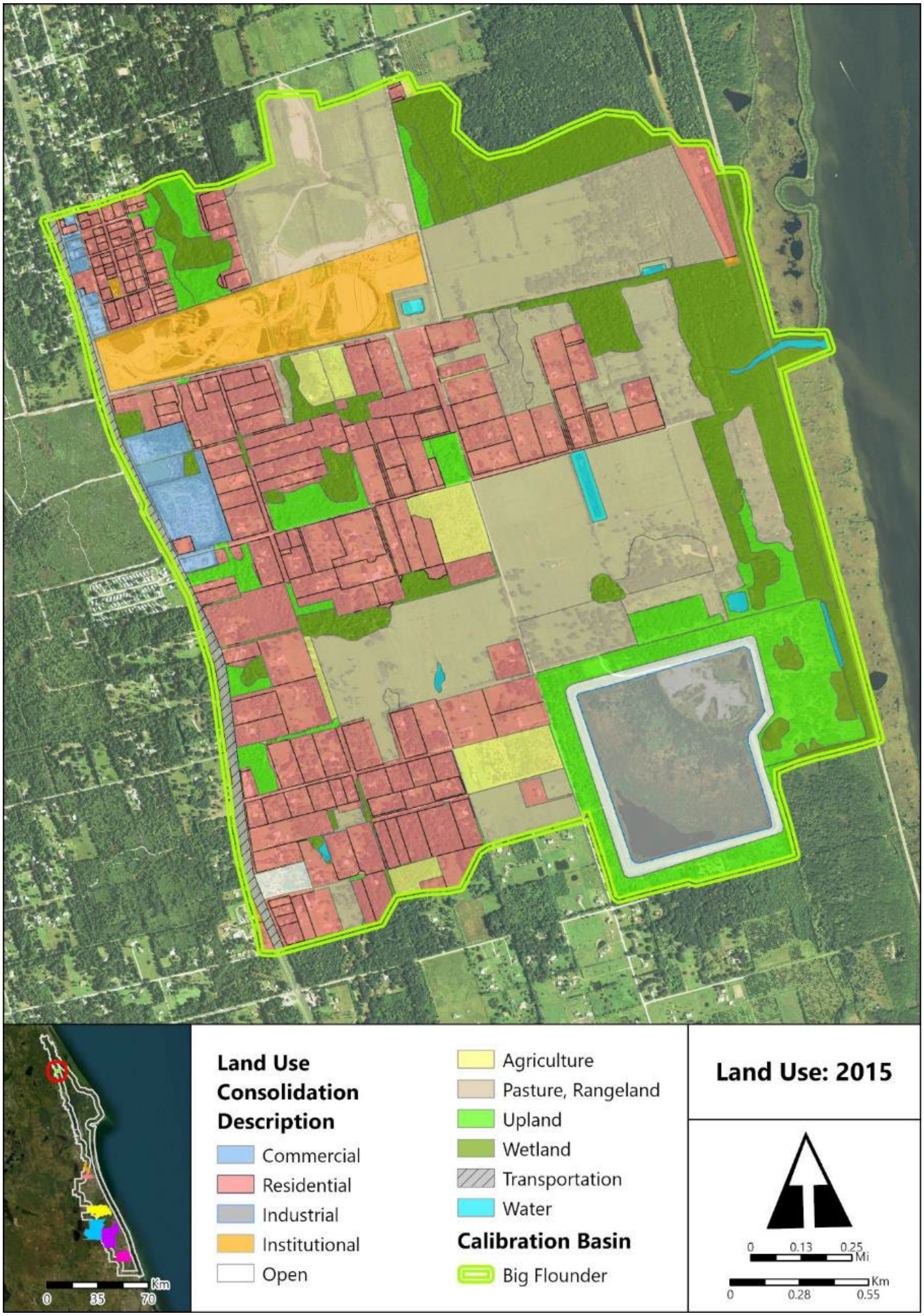

Figure 2. Land use within the Big Flounder calibration basin for 2015.

Figure 3. Land use within the Big Flounder calibration basin for 2020.

2.1.2 Soil Hydrologic Group

The Big Flounder calibration basin is primarily composed of the A/D hydrologic soil group (67%), followed by C/D (20%), A (8%), B/D (3%), D (2%), and water (<1%) (Figure 4). The D soils are centralized in the area directly surrounding Big Flounder Creek, C/D soils are located on the eastern portion of the basin, A soils are on the western portion of the basin, and A/D soils encompass the central areas; B/D soils have smaller patches along the east and northern regions of the basin (Figure 5).

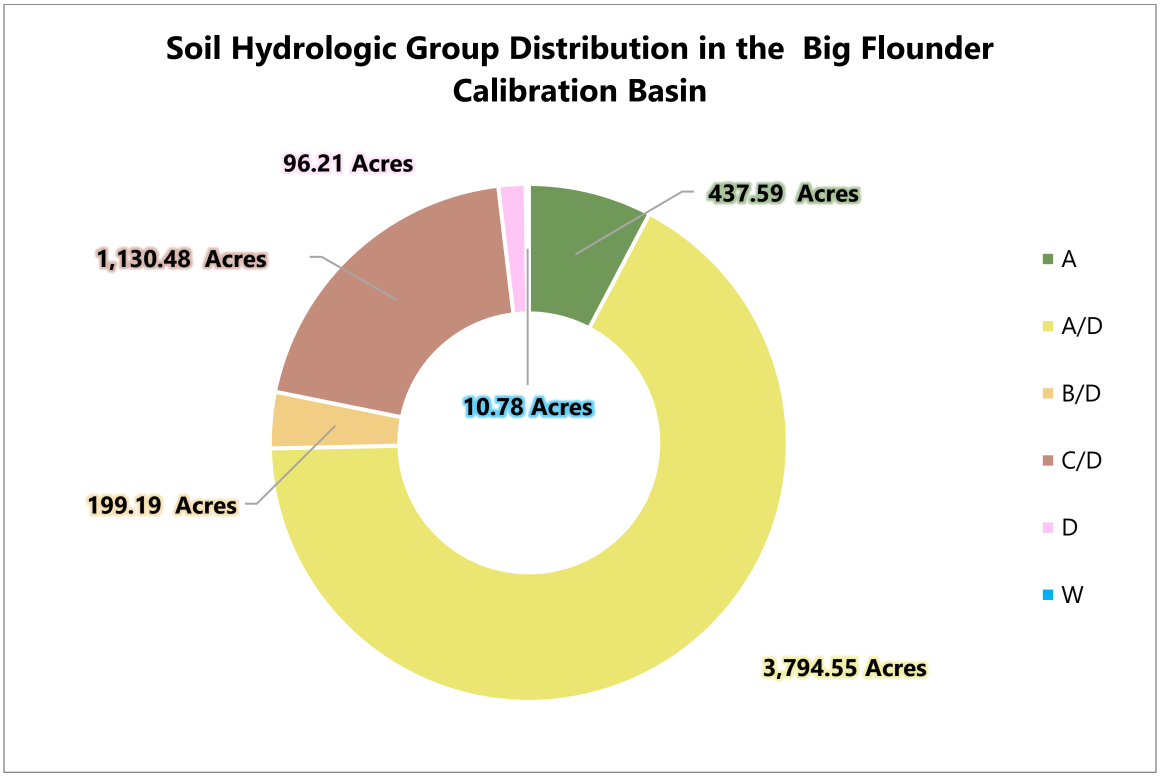

Figure 4. Pie chart (acres) of the soil hydrologic group distribution in the Big Flounder calibration basin using United States Department of Agriculture (USDA) Natural Resources Conservation Service (NRCS) data.

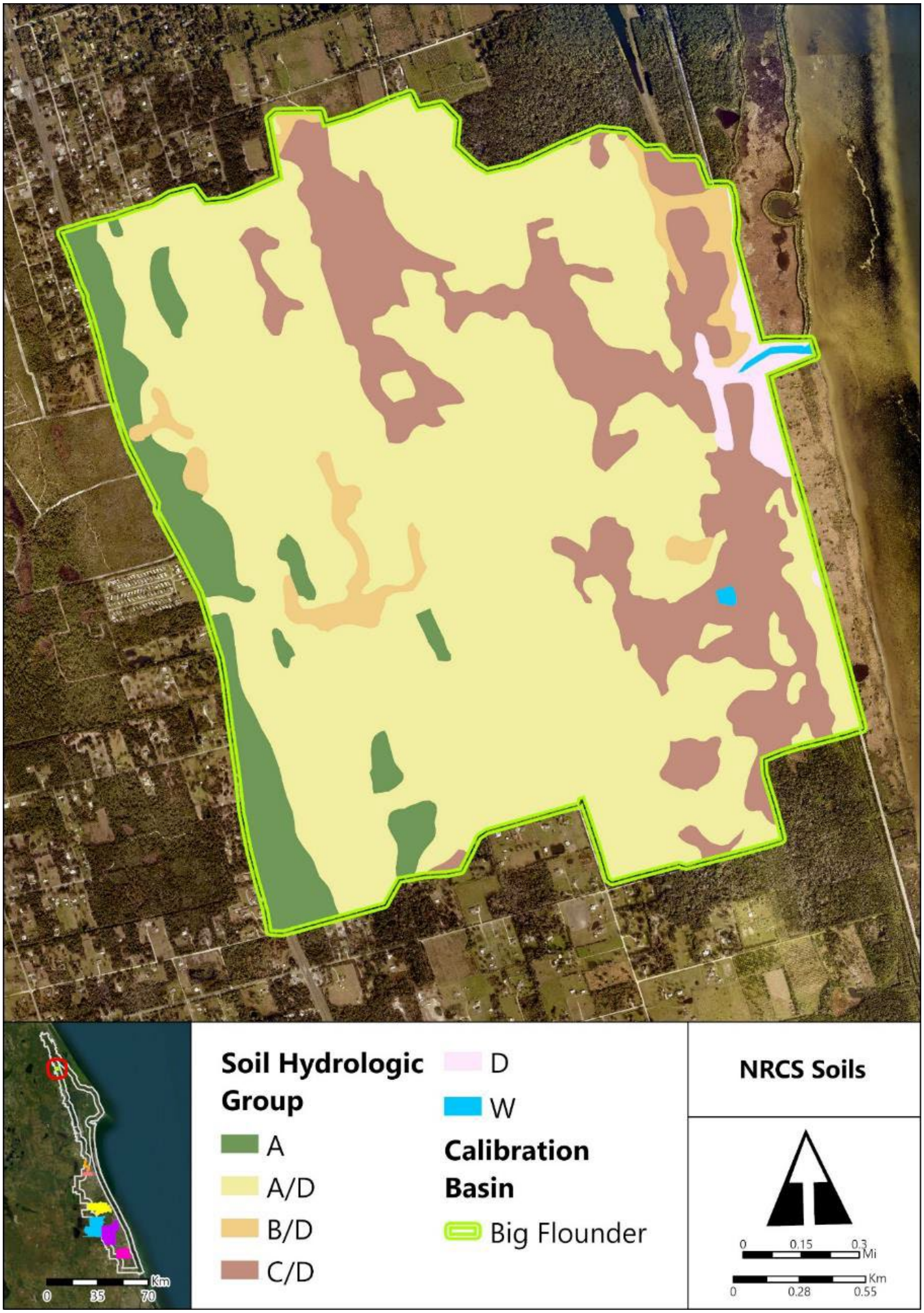

Figure 5. Distribution of soil hydrologic groups within the Big Flounder calibration basin.

2.1.3 PRECIPITATION

The annual total precipitation for Big Flounder ranges from the lowest annual total of 22 inches in 2010 to the highest annual total of 62 inches in 2014 (Figure 6). Wet (June to October) and dry (November to May) seasonal summaries are provided in Figure 7. For all years, with the exception of 2018, the dry season has a lower total seasonal rainfall as compared to the wet seasons of the same years. The average monthly precipitation values are higher from May to October and lower from November to April (Figure 8). Maps of February and September monthly precipitation averages (inches/month) across the period of record (POR) for the Big Flounder calibration basin are provided in Figure 9 and Figure 10, respectively.

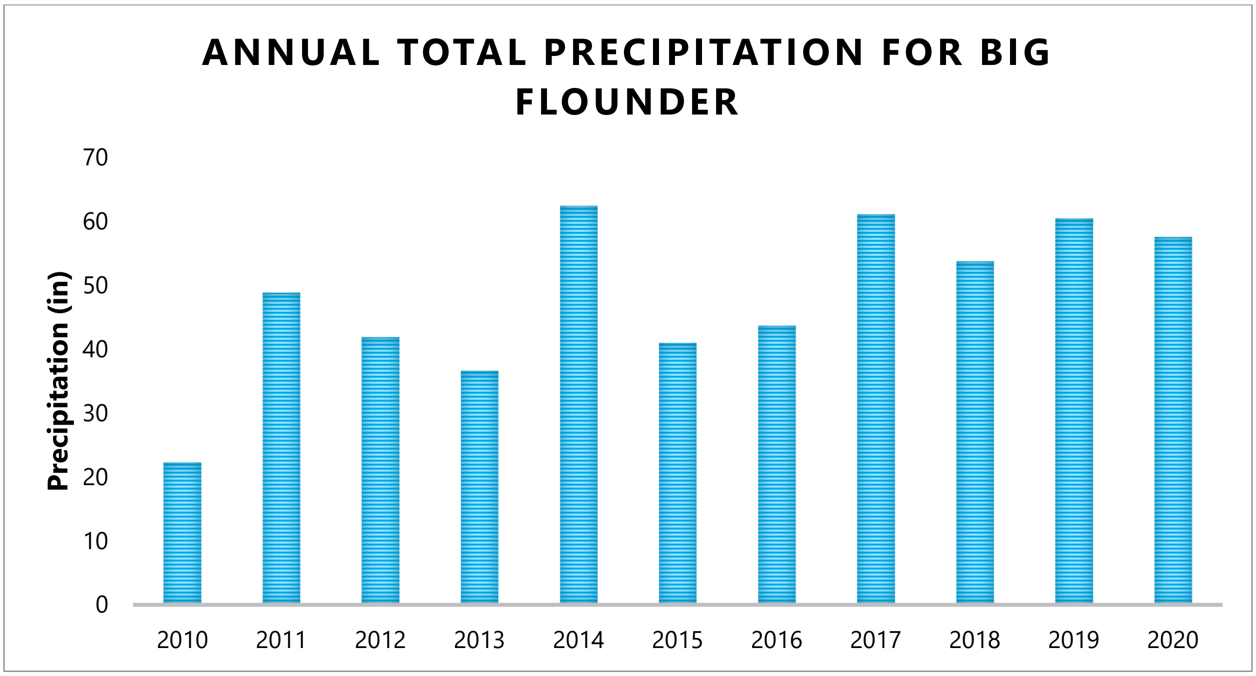

Figure 6. Annual total precipitation (in) for the Big Flounder calibration basin from 2010 to 2020 derived from St. Johns River Water Management District (SJRWMD) Next Generation Weather Radar (NEXRAD) data.

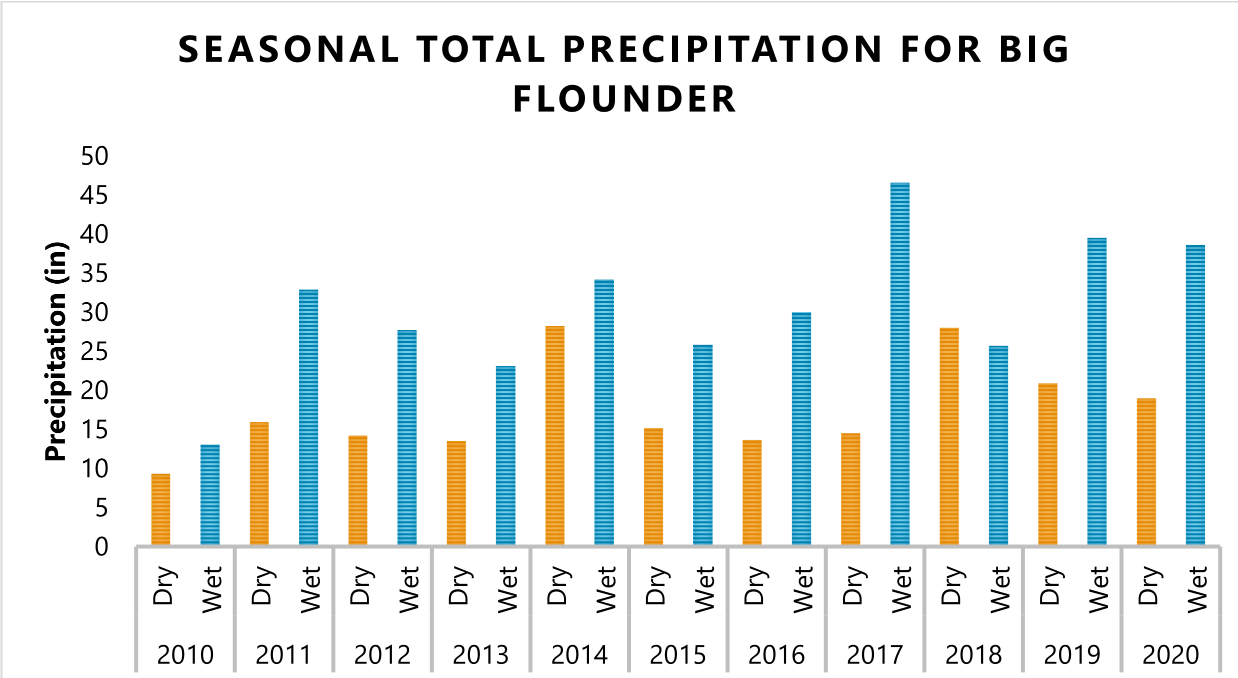

Figure 7. Seasonal total precipitation (in) for the Big Flounder calibration basin from 2010 to 2020 derived from SJRWMD NEXRAD data.

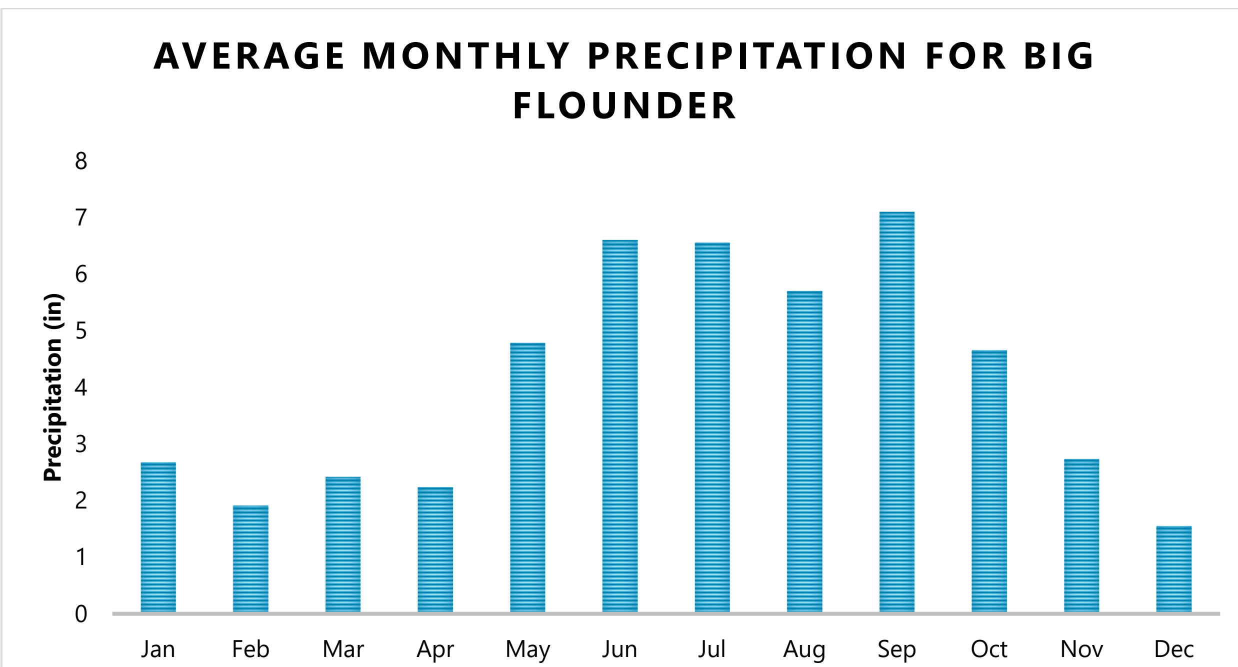

Figure 8. Average monthly precipitation (in) for the Big Flounder calibration basin derived from SJRWMD NEXRAD data.

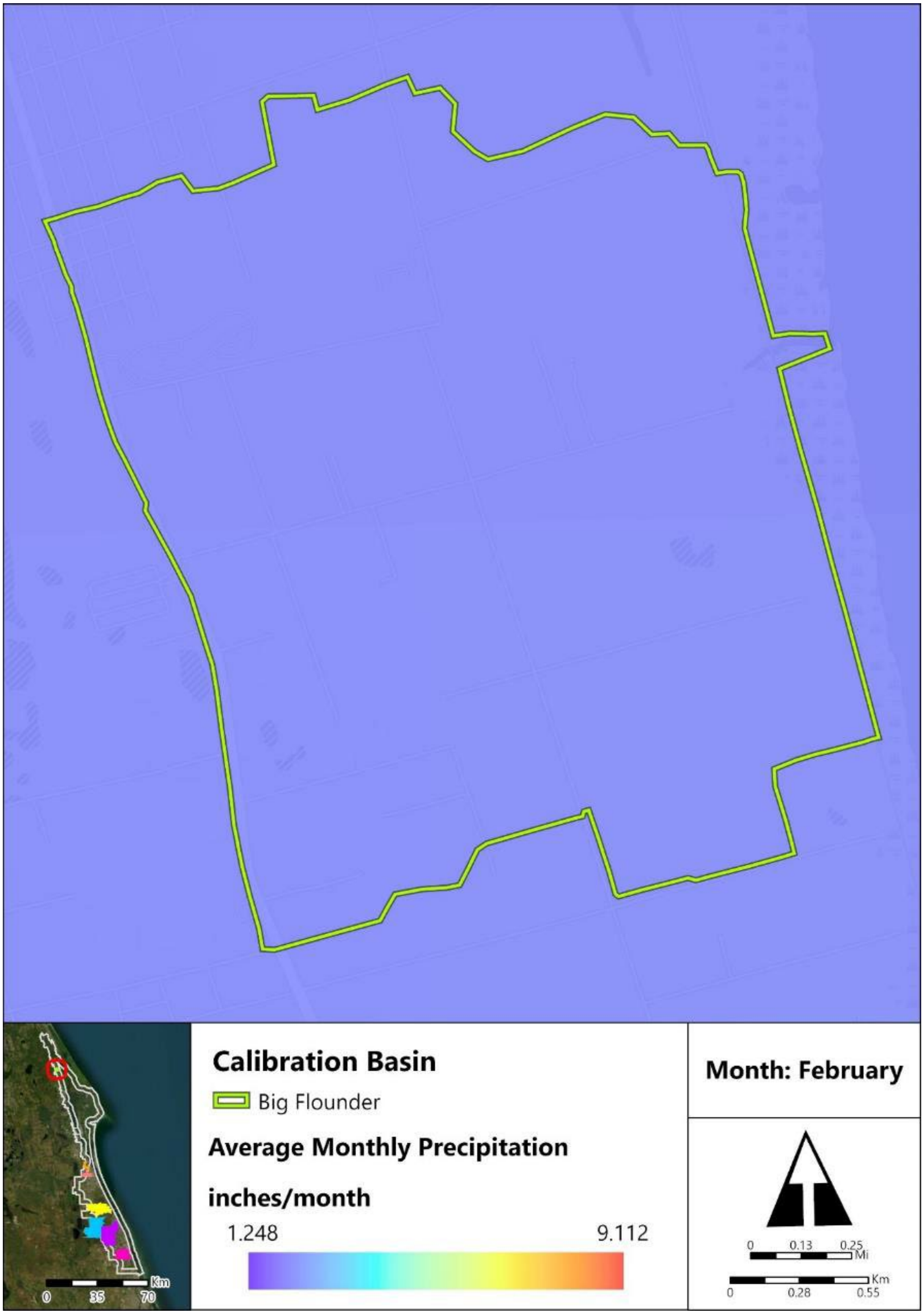

Figure 9. Average monthly precipitation (inches/month) for February across the period of record in the Big Flounder calibration basin.

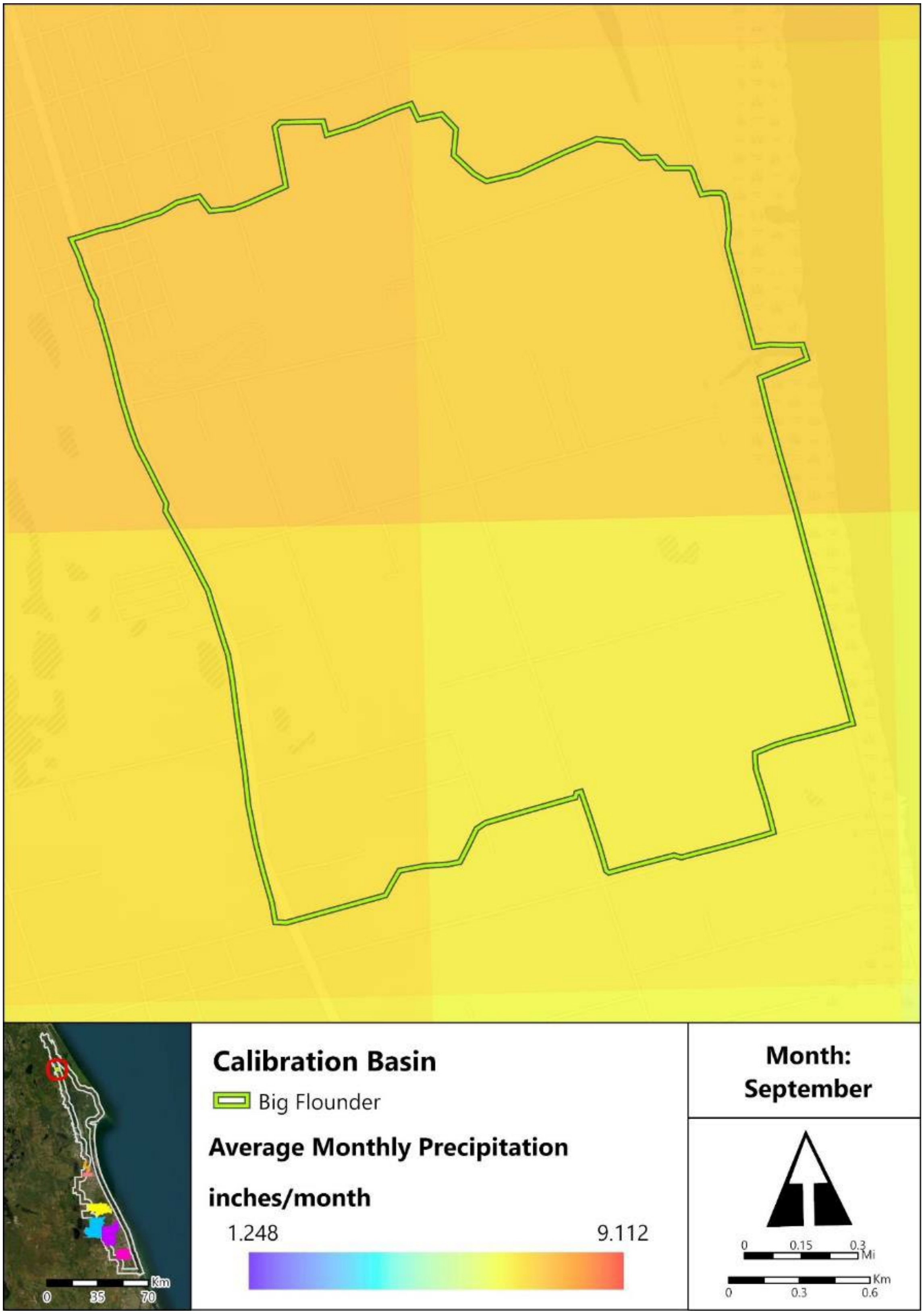

Figure 10. Average monthly precipitation (inches/month) for September across the period of record in the Big Flounder calibration basin.

2.1.4 ET

Summary statistics for the monthly mean ET in the Big Flounder calibration basin are provided as a boxplot (Figure 11). For Big Flounder, there is a distinct difference in the wet and dry seasonal ET, with rates increasing through the wet season and decreasing in the dry season. The lowest median value and lowest variability in ET rates are seen in the dry season, where there are generally lower temperatures. The greatest median ET and highest variability are seen in the wet season, where there are generally higher temperatures. The lowest median value was observed in January (1.15 millimeters [mm]/day), whereas the highest median was observed in August (2.99 mm/day). The highest variability was observed in July with a difference of 1.23 mm/day difference within the interquartile range, and the lowest variability was observed in November with a difference of 0.16 mm/day within the interquartile range. Maps for mean monthly ET rates (mm/day) during February and September across the POR in the Big Flounder calibration basin are provided in Figure 12 and Figure 13, respectively.

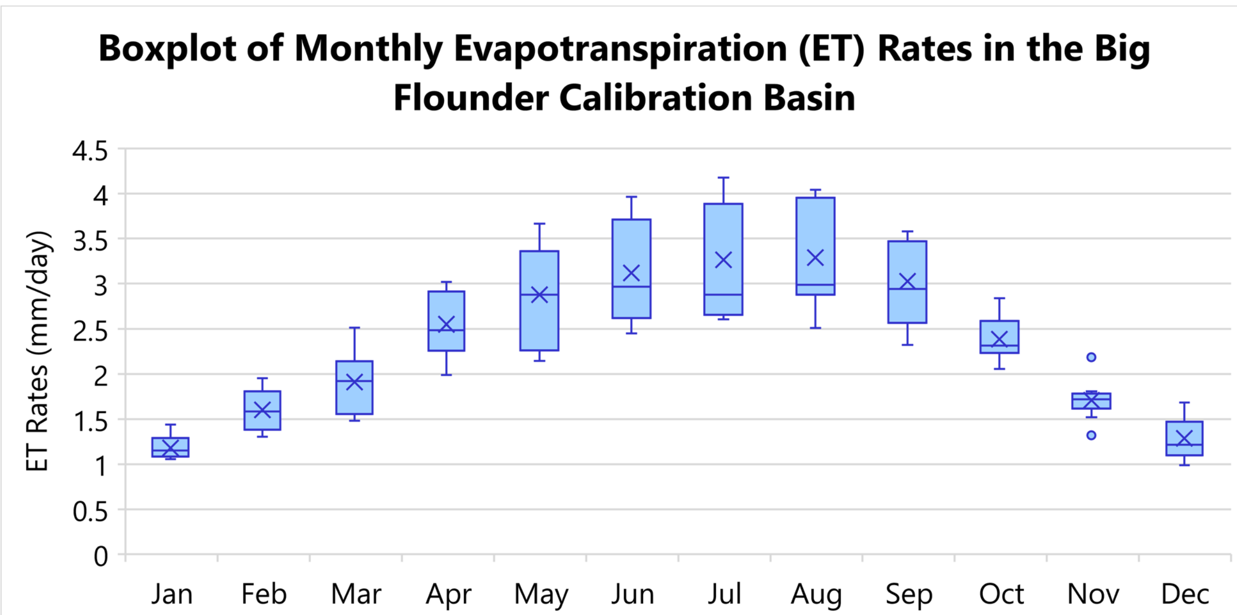

Figure 11. Boxplot of monthly mean ET rates in the Big Flounder calibration basin derived from National Aeronautics and Space Administration (NASA) EarthData and the University of Montana data.

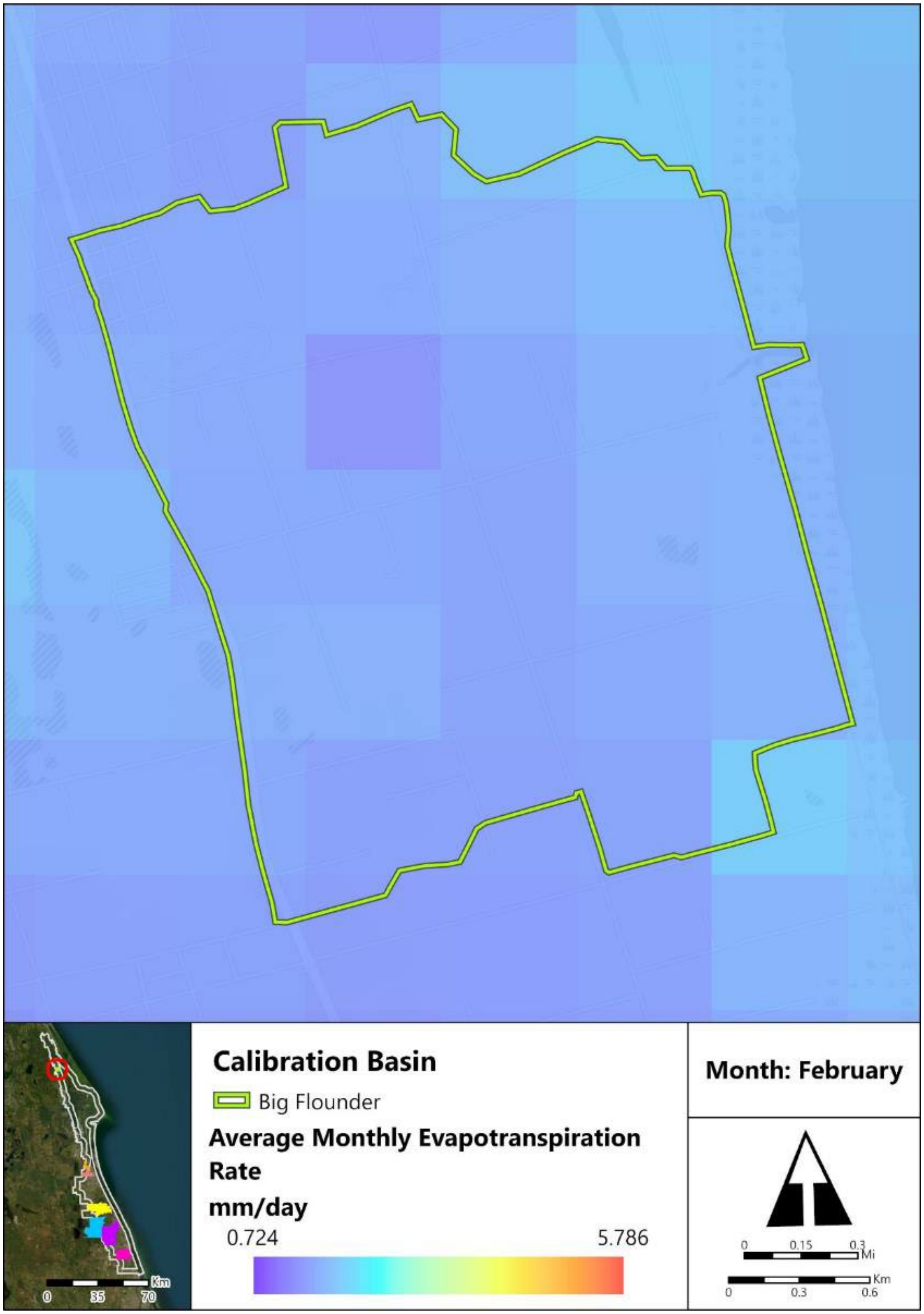

Figure 12. Average monthly ET rates (mm/day) for February across the period of record in the Big Flounder calibration basin.

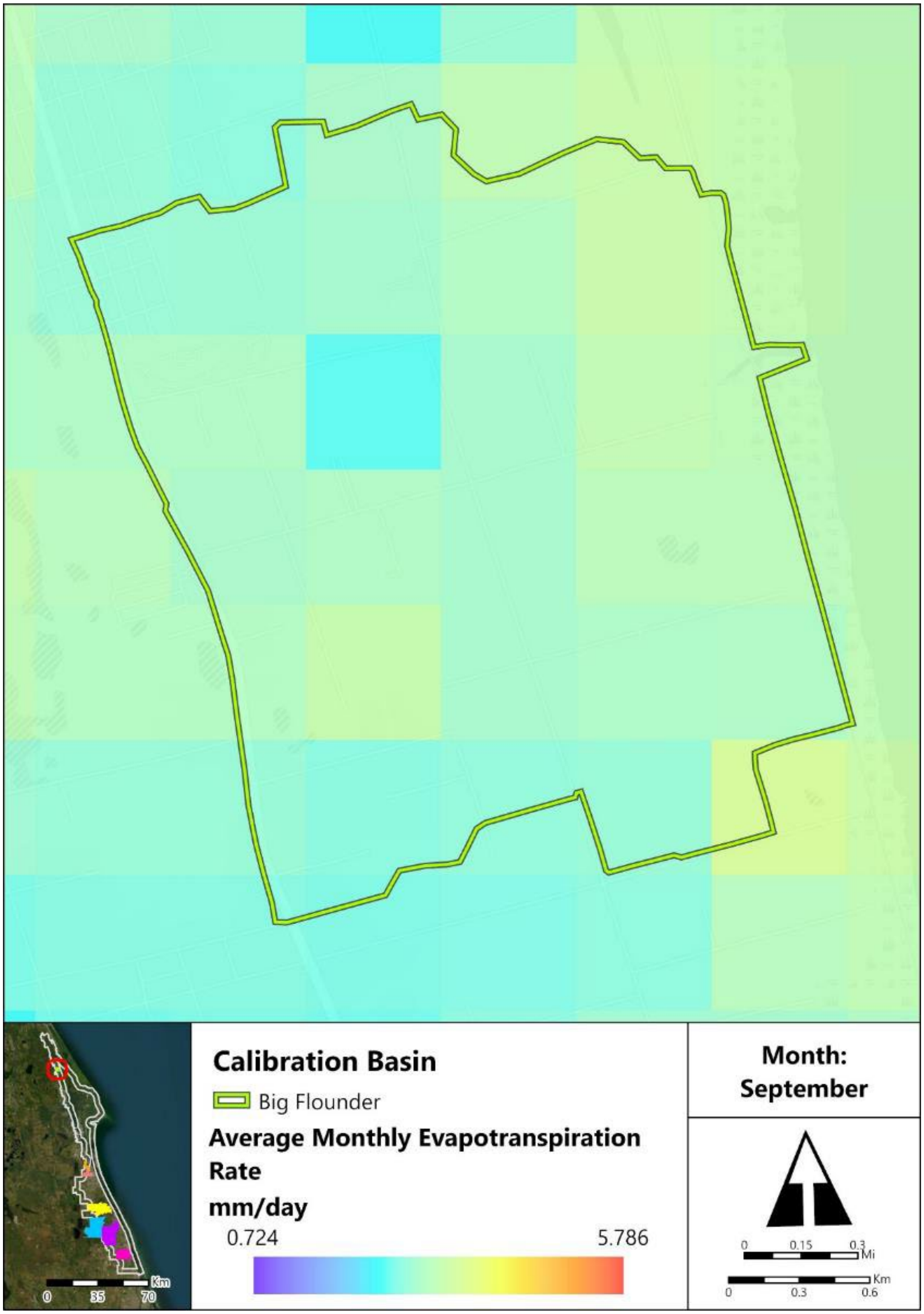

Figure 13. Average monthly ET rates (mm/day) for September across the period of record in the Big Flounder calibration basin.

2.1.5 TREATMENTS

Within Big Flounder, approximately 34% of basin's total area is treated (Table 2), with a majority being wet treatments (22%) versus dry treatments (12%). Overall, the largest changes to the total area of treatments occurred between 2010 and 2015, with increases in wet treatments (~6%) after the development of the Cape Canaveral National Cemetery (Figure 14, Figure 15, Figure 16).

Table 2. Total area (acres) of each treatment type in the Big Flounder calibration basin for the 2010, 2015, and 2020 years.

Treatment Type	Treatment Area (Acres)			Percent of Total Basin Area (%)			Percent Change (%)	
	2010	2015	2020	2010	2015	2020	2015-2010	2020-2010
Dry	219.27	222.25	236.11	11.60	11.76	12.50	0.16	0.89
Wet	358.17	449.24	464.73	18.95	23.77	24.59	4.82	5.64
Total	*577.44*	*671.49*	*700.85*	*30.56*	*35.54*	*37.09*	*4.98*	*6.53*

**The percentage of the total basin area and the percent change from the overall area between 2010 and 2015, as well as 2010 and 2020, have also been provided.*

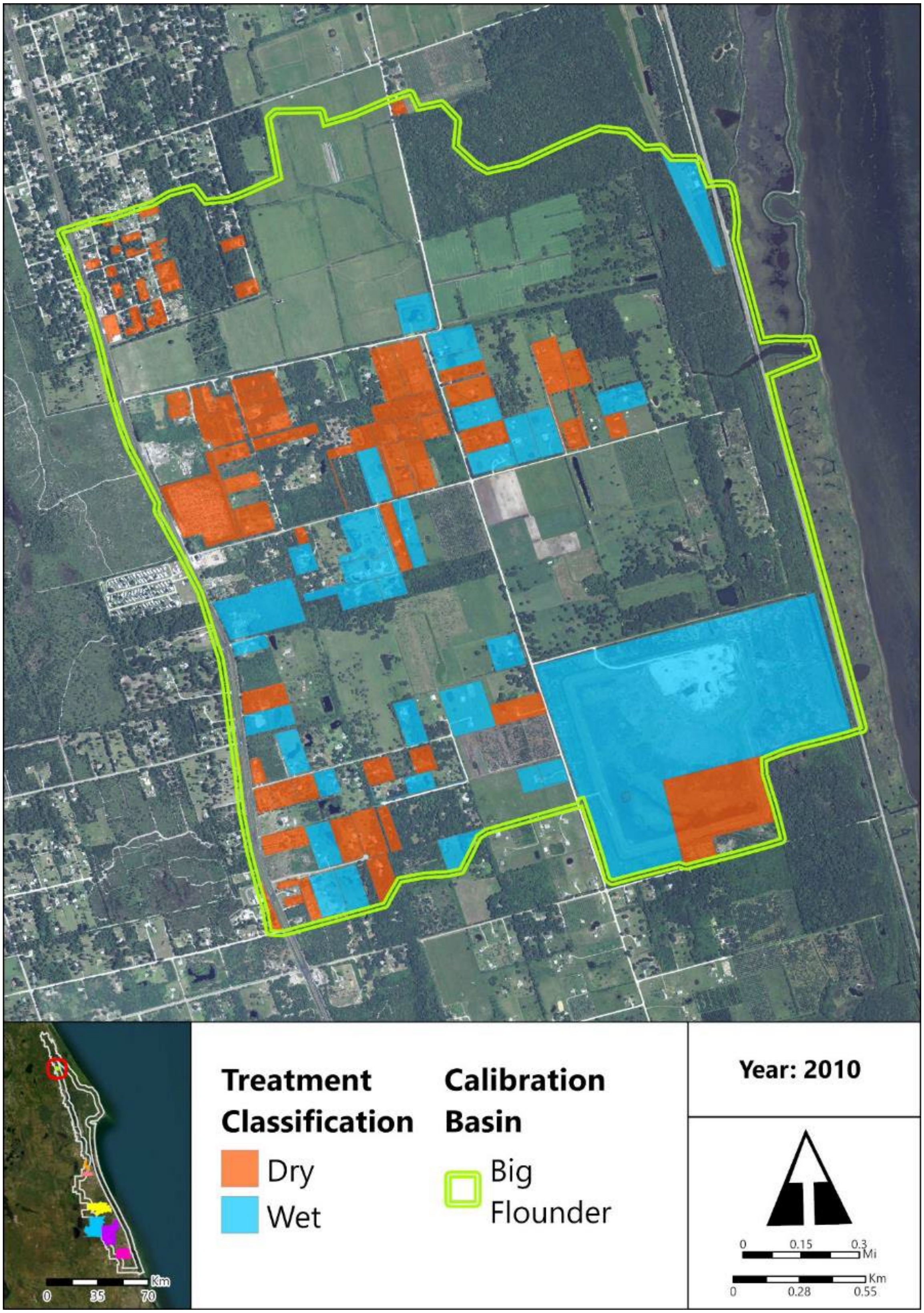

Figure 14. Treatments within the Big Flounder calibration basin for 2010.

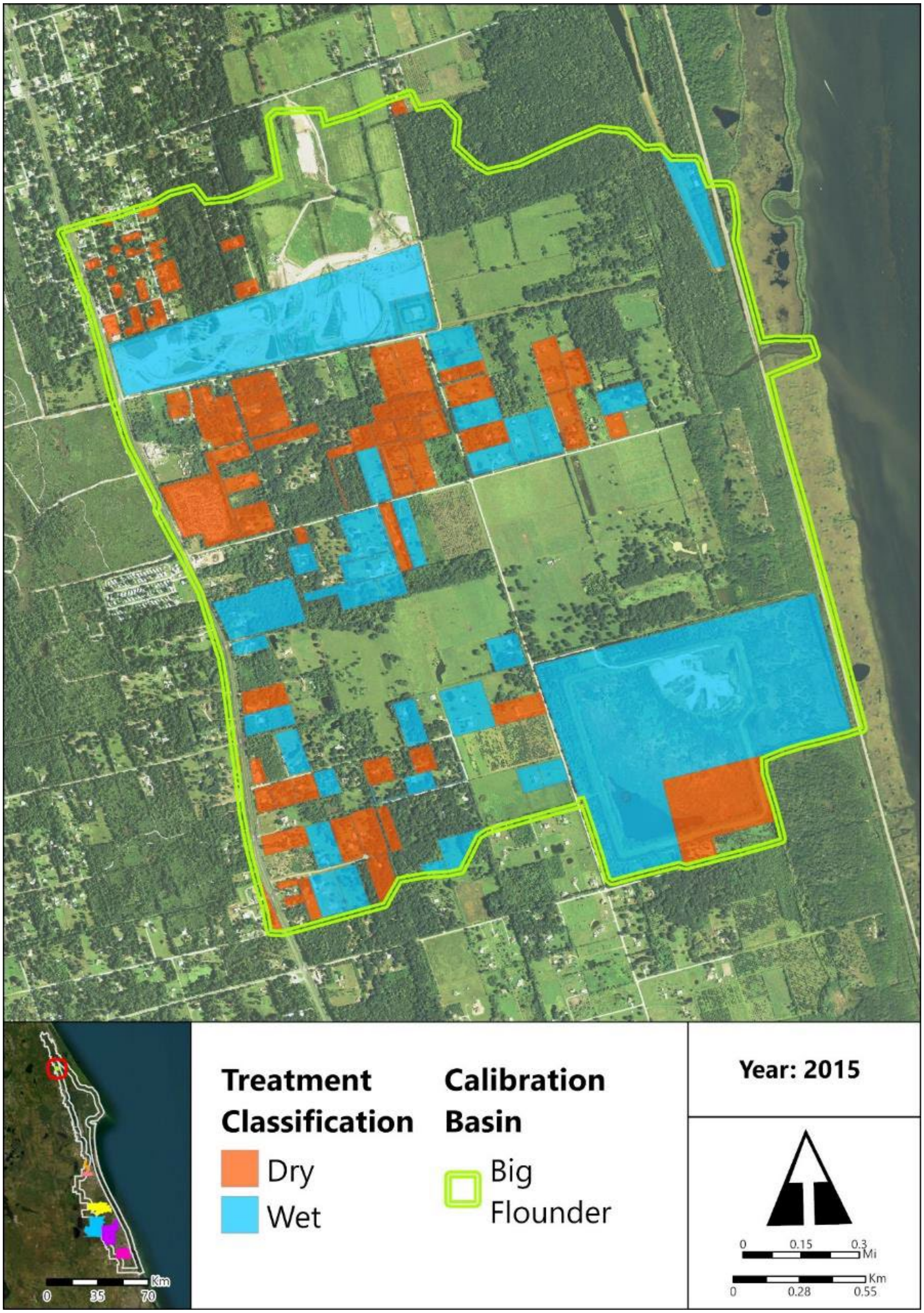

Figure 15. Treatments within the Big Flounder calibration basin for 2015.

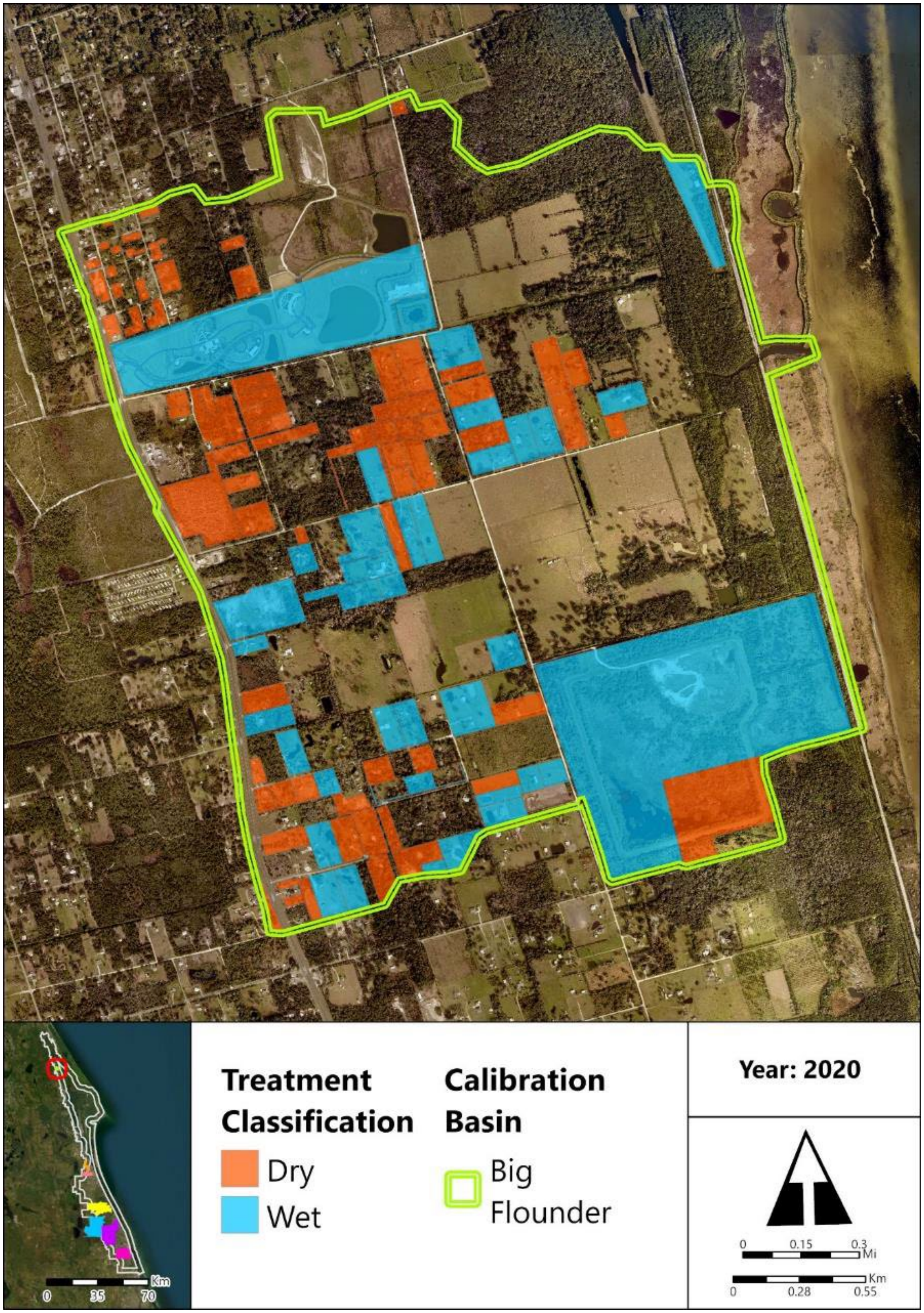

Figure 16. Treatments within the Big Flounder calibration basin for 2020.

2.1.6 Hydrology

Due to a lack of a hydrological monitoring station, the volume of flow for this basin could not be determined, and the Big Flounder calibration basin was not used for hydrological calibration. However, for water quality calibration, it was important to define which water quality measurements were associated with subsurface flow versus direct runoff (DRO) conditions. The segregation of subsurface flow versus DRO was determined using a NEXRAD radar rainfall method which was described in the previous Task 1 Memorandum (Applied Ecology, Inc., 2022).

DRO conditions were determined by identifying which days had more than 0.7 inches of rainfall accumulation during the preceding 72 hours. Subsurface flow conditions were in turn determined by which dates had less than 0.7 inches of rainfall accumulation 72 hours prior. Within the Big Flounder calibration basin, there appears to be a trend of increasing days of DRO events (Table 3), with an increased variation in the percentage of DRO days between 2013 and 2017. From 2010 to 2020, the months with the most days of DRO occurred between June and September (Table 4).

Table 3. Percentage of days per year from 2010 to 2020 that were under DRO or subsurface flow conditions as determined by NEXRAD estimated rainfall.

Years	DRO	Subsurface Flow
2010	32%	68%
2011	38%	62%
2012	39%	61%
2013	38%	62%
2014	45%	55%
2015	40%	60%
2016	33%	67%
2017	43%	57%
2018	42%	58%
2019	46%	54%
2020	45%	55%

Table 4. Percentage of days in a month from 2010 to 2020 that were under DRO or subsurface flow conditions as determined by NEXRAD estimated rainfall.

Months	DRO	Subsurface flow
Jan	25%	75%
Feb	32%	68%
Mar	26%	74%
Apr	30%	70%
May	38%	62%
Jun	61%	39%
Jul	60%	40%
Aug	67%	33%
Sep	57%	43%
Oct	37%	63%
Nov	27%	73%
Dec	20%	80%

2.1.7 Water Quality

The Big Flounder calibration basin had considerable variation in the measured total nitrogen (TN) and total phosphorus (TP) concentrations from 2010 to 2020 (Table 5, Figure 17). In general, there is a higher degree of variability between DRO and subsurface flow for TN in comparison to TP, whose geometric means are extremely similar.

Trends between DRO and subsurface flow for TN fluctuate and contrast one another for a majority of the POR, although there were years in which subsurface flow had elevated concentrations. The highest geometric mean concentrations for subsurface TN concentrations occurred during the first three years of the POR (2010-2012) while the highest DRO concentrations occurred between 2013 and 2017.

Geometric means are quite similar for both the DRO and subsurface flow concentrations of TP throughout the POR, although a higher degree of variation is found amongst the DRO component. The highest geometric mean concentrations for subsurface TP concentrations occurred from 2017 to 2019, while the highest DRO concentrations occurred sporadically in 2011, 2015, and 2020.

Table 5. Comparison of measured DRO and subsurface flow annual geometric mean of TP (mg/L) and TN (mg/L) for the Big Flounder calibration basin as measured by the SJRWMD.

Year	TN - DRO	TN – Subsurface	TP - DRO	TP - Subsurface
2010	1.821	2.562	0.189	0.172
2011	2.509	2.828	0.247	0.210
2012	2.375	2.773	0.184	0.198
2013	2.446	2.416	0.187	0.178
2014	2.208	1.738	0.216	0.161
2015	2.735	1.591	0.277	0.171
2016	2.710	2.276	0.218	0.193
2017	2.496	2.240	0.176	0.277
2018	1.548	2.528	0.203	0.238
2019	1.626	2.169	0.176	0.224
2020	2.451	1.867	0.270	0.178

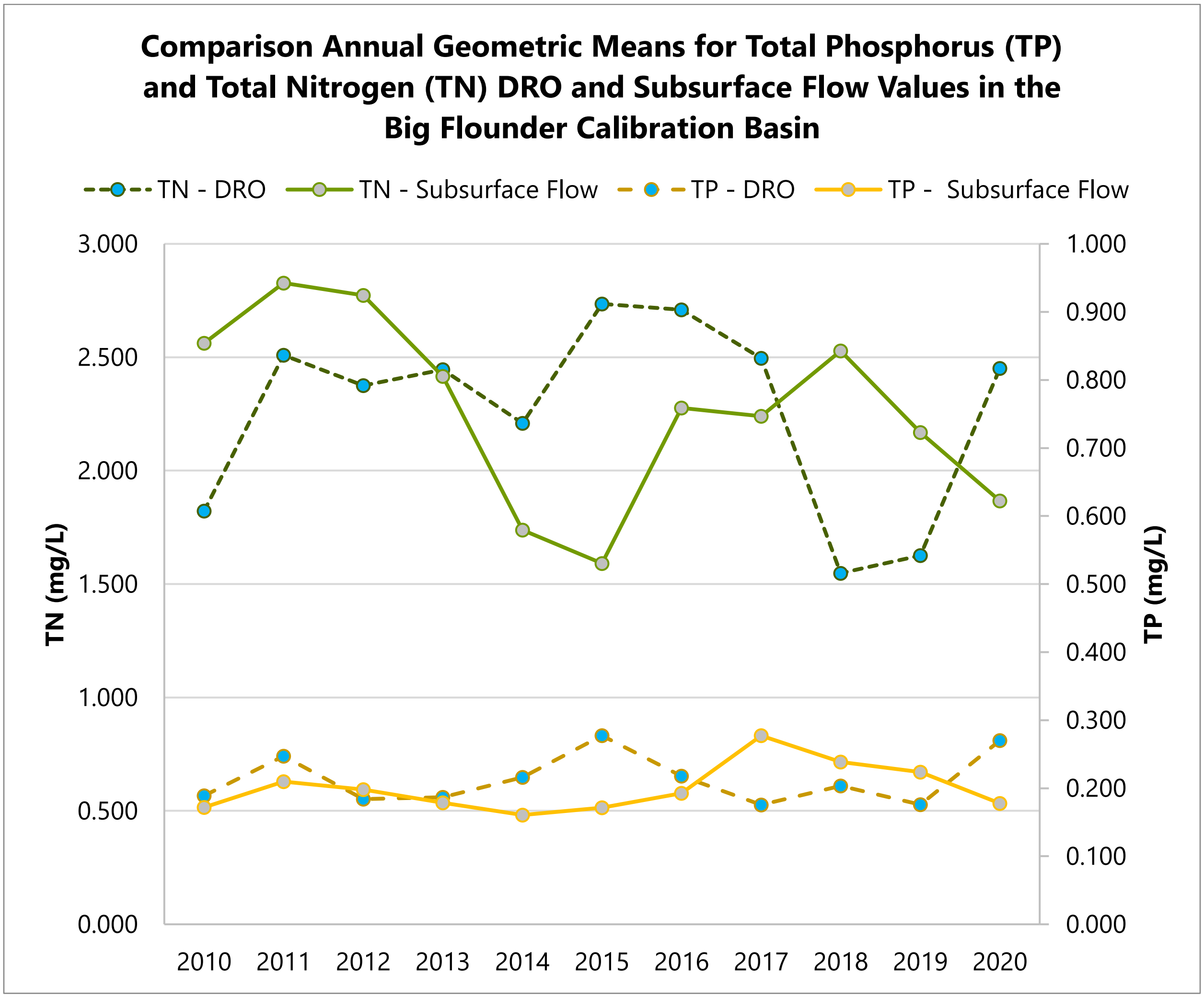

Figure 17. Comparison of measured runoff and subsurface flow annual geometric mean of total phosphorus and total nitrogen for the Big Flounder calibration basin as measured by the SJRWMD.

The overall annual patterns can also be observed at the seasonal scale (Figure 18). Generally, the samples associated with subsurface flow conditions were elevated over the DRO conditions, except for the period between 2014 and 2017, when DRO was higher than subsurface flow. Elevated values for both the DRO and subsurface components are observed during the wet season in comparison to the dry season for a majority of the POR for both TN and TP. Higher degrees of seasonal variability are observed within the subsurface flow in comparison to DRO. Gaps in the times series data for DRO are due to a lack of measured data at the monitoring location, which typically occur during the dry season as there is either no flow or limited flow, which would not be truly representative of the flow conditions.

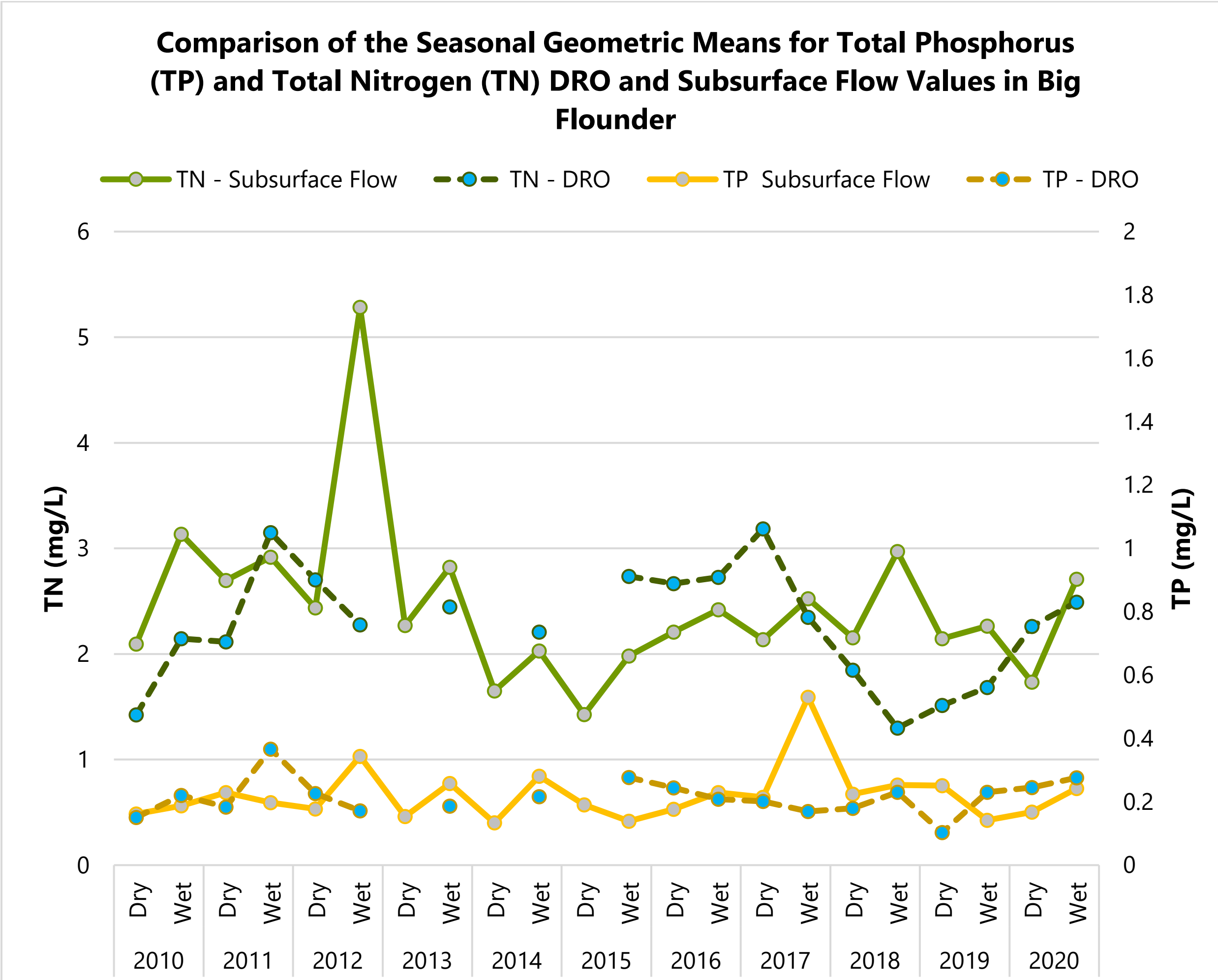

Figure 18. Comparison of the seasonal geometric means of TN (mg/L) and TP (mg/L) for subsurface flow and DRO between 2010 and 2020 for the Big Flounder calibration basin.

2.2 Eau Gallie

2.2.1 LULC Change

The Eau Gallie calibration basin is ~3,763 acres in size and has been predominately composed of medium density residential (~26%), high density residential (~22%), low density residential (~20%), commercial (~10%), and institutional (~6%) land use consolidation types (Table 6). The residential areas (of all densities) are widely distributed throughout the basin, as they make up almost 70% of the total area (Figure 19, Figure 20, Figure 21). Commercial areas are distributed along the central portion of the basin along the major roadways. Overall, relatively minor changes have occurred within the Eau Gallie calibration basin from 2010 to 2020, with the exception of some conversions from natural (scrub and uplands) to residential areas between 2015 and 2020, albeit these changes affected less than 2% of the total area of the basin.

Table 6. Total area (in acres and percentage) of each land use consolidation type in the Eau Gallie calibration basin for the 2010, 2015, and 2020 years.

Land Use Consolidation	Land Use Area (Acres)			Percent of Total Land Use (%)			Percent Change (%)	
	2010	2015	2020	2010	2015	2020	2015-2010	2020-2010
Citrus	1.17	1.17	1.17	0.03	0.03	0.03	0.00	0.00
Commercial	**384.02**	**380.69**	**399.14**	**10.21**	**10.12**	**10.61**	-0.09	0.40
Dry Prairie	3.35	--	--	0.09	--	--	--	--
High Density Residential	**827.30**	**809.65**	**853.07**	**21.99**	**21.52**	**22.67**	-0.47	0.69
Improved Pasture	3.76	0.07	0.07	0.10	0.00	0.00	-0.10	-0.10
Industrial	6.62	6.64	6.64	0.18	0.18	0.18	0.00	0.00
Institutional	**236.22**	**214.32**	**211.84**	**6.28**	**5.70**	**5.63**	-0.58	-0.65
Low Density Residential	**765.19**	**758.08**	**767.23**	**20.34**	**20.15**	**20.39**	-0.19	0.05
Medium Density Residential	**962.82**	**1,008.82**	**1,016.25**	**25.59**	**26.81**	**27.01**	1.22	1.42
Open	90.75	70.32	53.45	2.41	1.87	1.42	-0.54	-0.99
Other Agriculture	1.72	1.71	1.71	0.05	0.05	0.05	0.00	0.00
Rangeland	4.51	4.50	4.50	0.12	0.12	0.12	0.00	0.00
Recreational 2	3.80	24.72	24.72	0.10	0.66	0.66	0.56	0.56
Row Crops	--	1.65	1.65	--	0.04	0.04	--	--
Scrub	48.58	35.52	8.00	1.29	0.94	0.21	-0.35	-1.08
Transportation	51.92	51.20	51.20	1.38	1.36	1.36	-0.02	-0.02
Upland Flatwoods	49.50	54.63	37.49	1.32	1.45	1.00	0.14	-0.32
Water	80.29	92.14	95.64	2.13	2.45	2.54	0.32	0.41
Wet Flatwoods	28.76	33.43	18.94	0.76	0.89	0.50	0.12	-0.26
Wet Prairies	9.07	4.48	--	0.24	0.12	--	-0.12	--
Wetland	203.38	208.98	209.99	5.41	5.55	5.58	0.15	0.18

**The top five land uses that make up a majority of the area have been bolded for each year. Percent change from the overall area between 2010 and 2015, as well as 2010 and 2020 have also been provided.*

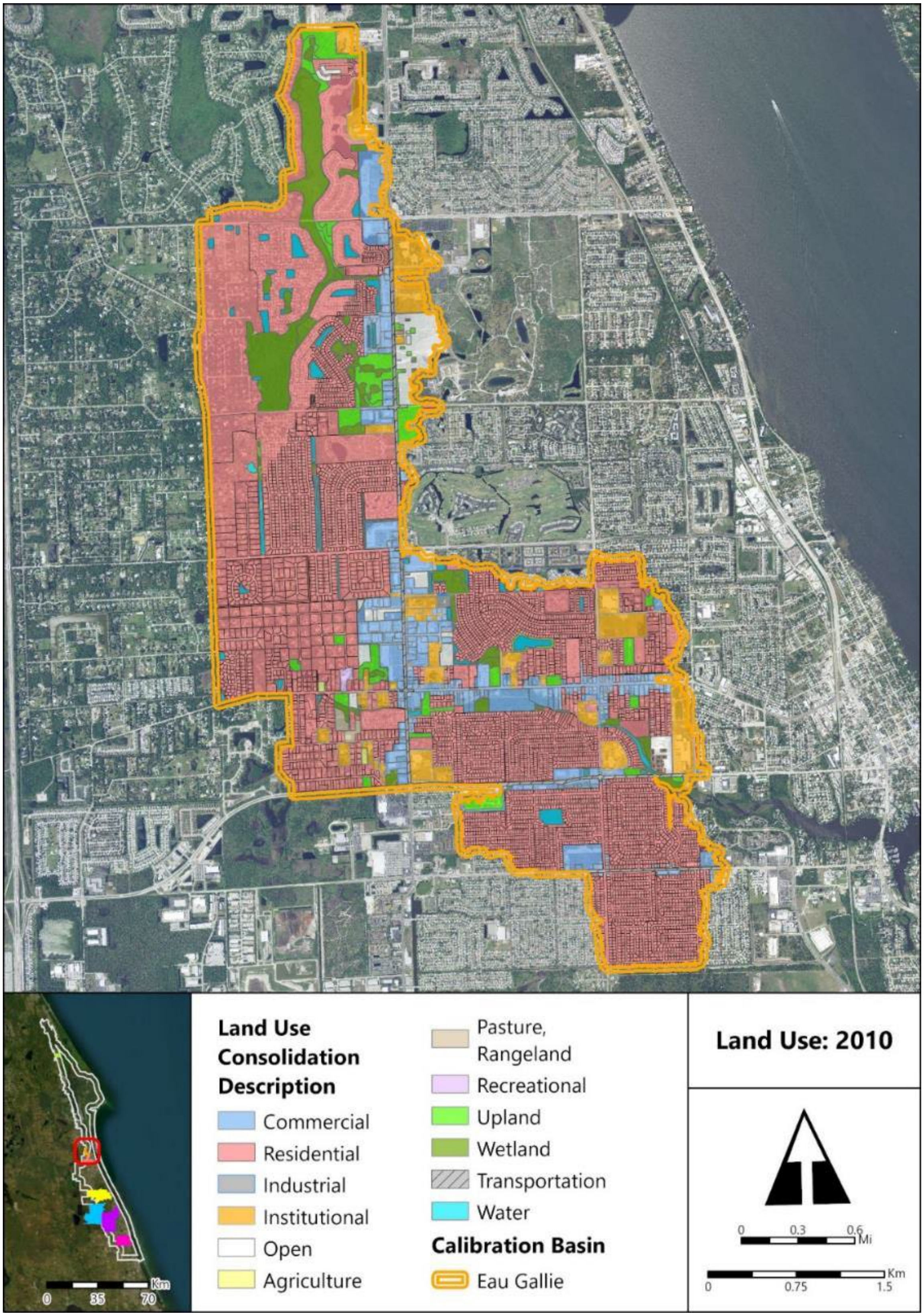

Figure 19. Land use within the Eau Gallie calibration basin for 2010.

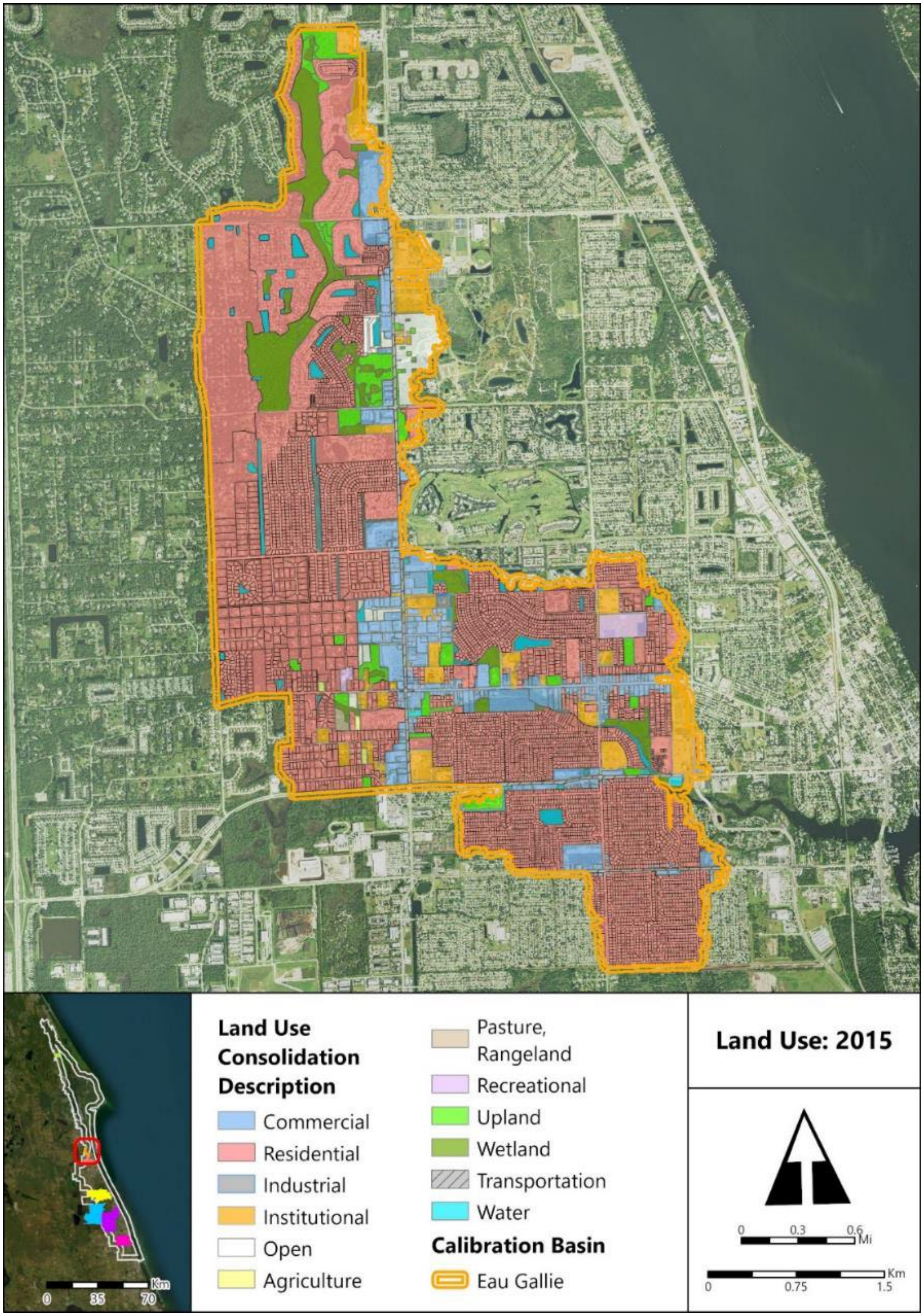

Figure 20. Land use within the Eau Gallie calibration basin for 2015.

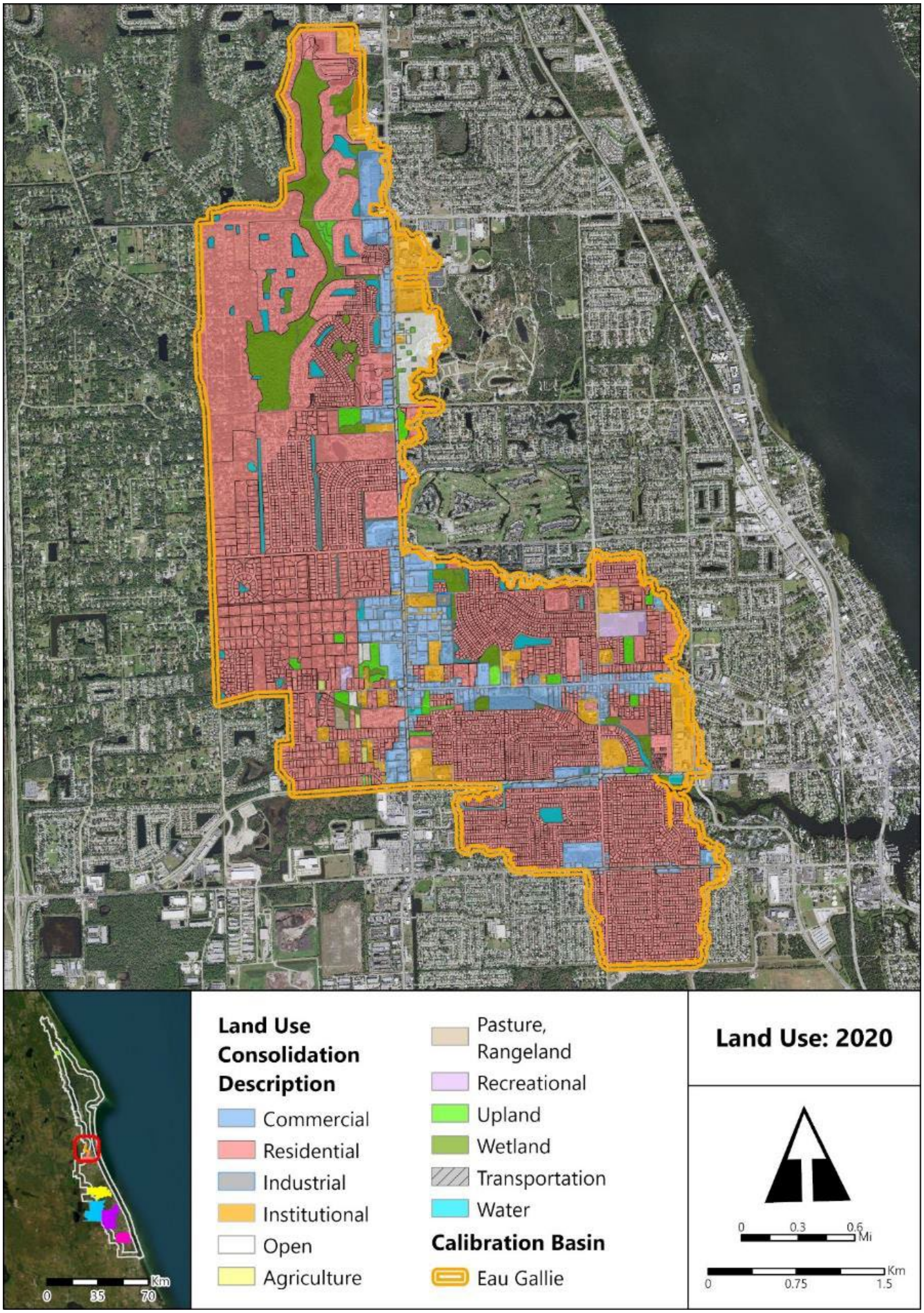

Figure 21. Land use within the Eau Gallie calibration basin for 2020.

2.2.2 Soil Hydrologic Group

The Eau Gallie calibration basin is primarily composed of the A/D (53%) and A (45%) hydrologic soil groups, with the remaining groups making up less than 3% of the total area (Figure 22). The A soils are in the southeast and northwest corners, while the A/D soils are found in the remaining areas (Figure 23).

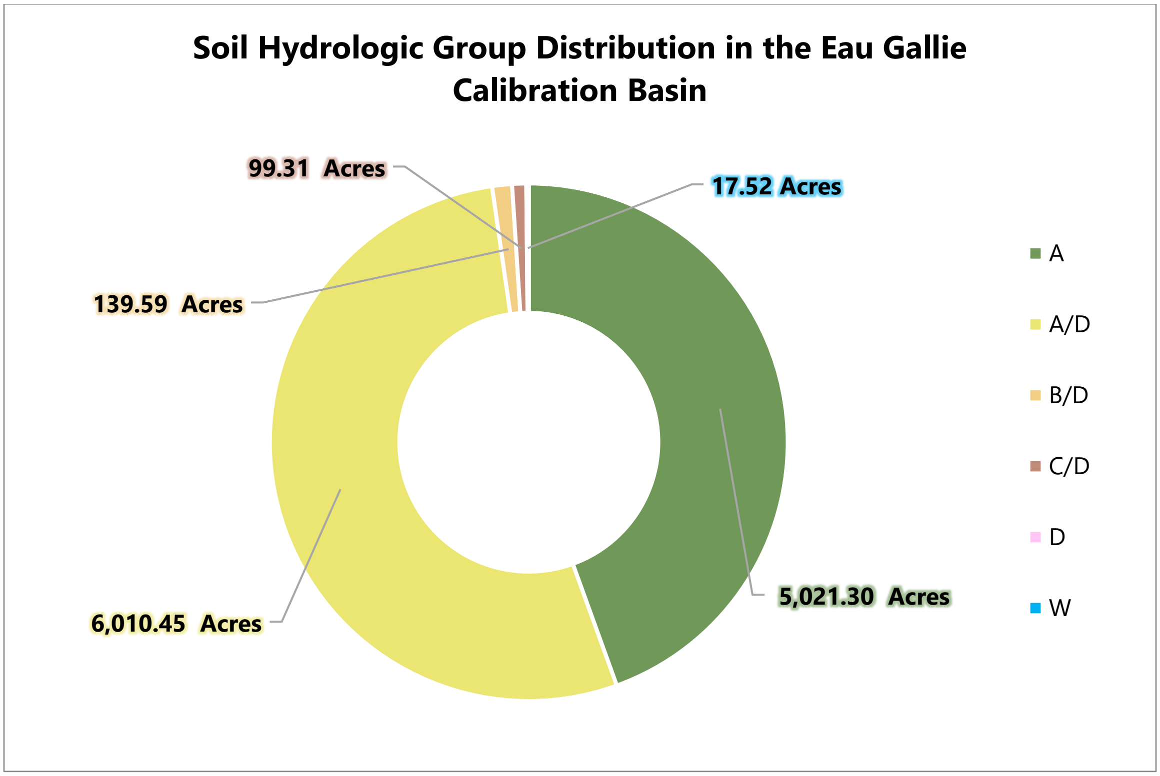

Figure 22. Pie chart (acres) of the soil hydrologic group distribution in the Eau Gallie calibration basin using USDA NRCS data.

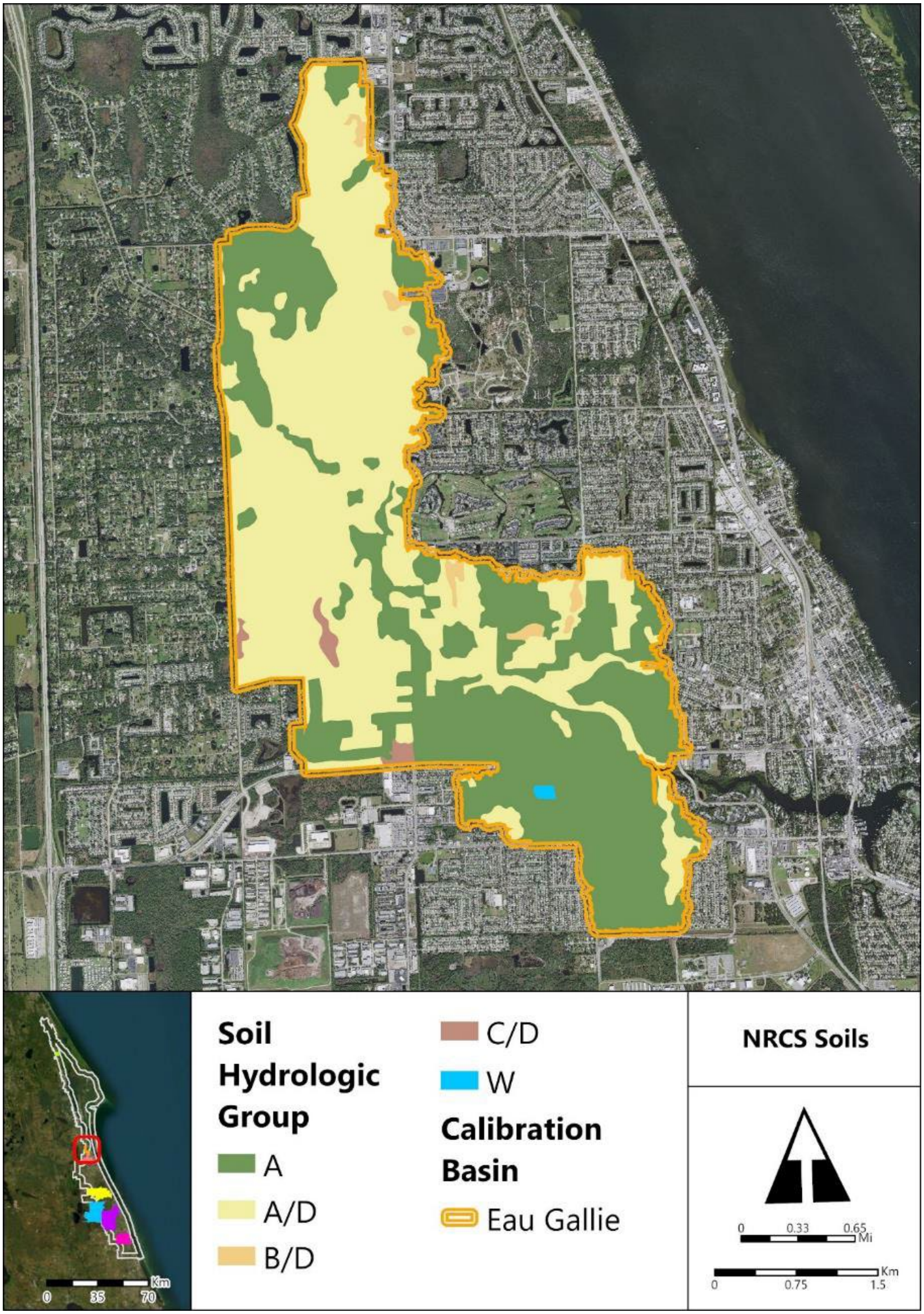

Figure 23. Distribution of soil hydrologic groups within the Eau Gallie calibration basin.

2.2.3 Precipitation

The annual total precipitation for the Eau Gallie calibration basin ranges from the lowest annual total of 21 inches in 2010 to the highest annual total of 56 inches in 2017 (Figure 24). For all years, the dry season has a lower total seasonal rainfall as compared to the wet seasons of the same year (Figure 25). The average monthly precipitation values are higher from May to October and lower from November to April (Figure 26). Maps for the February and September monthly precipitation averages (inches/month) across the POR in Eau Gallie are provided in Figure 27 and Figure 28, respectively.

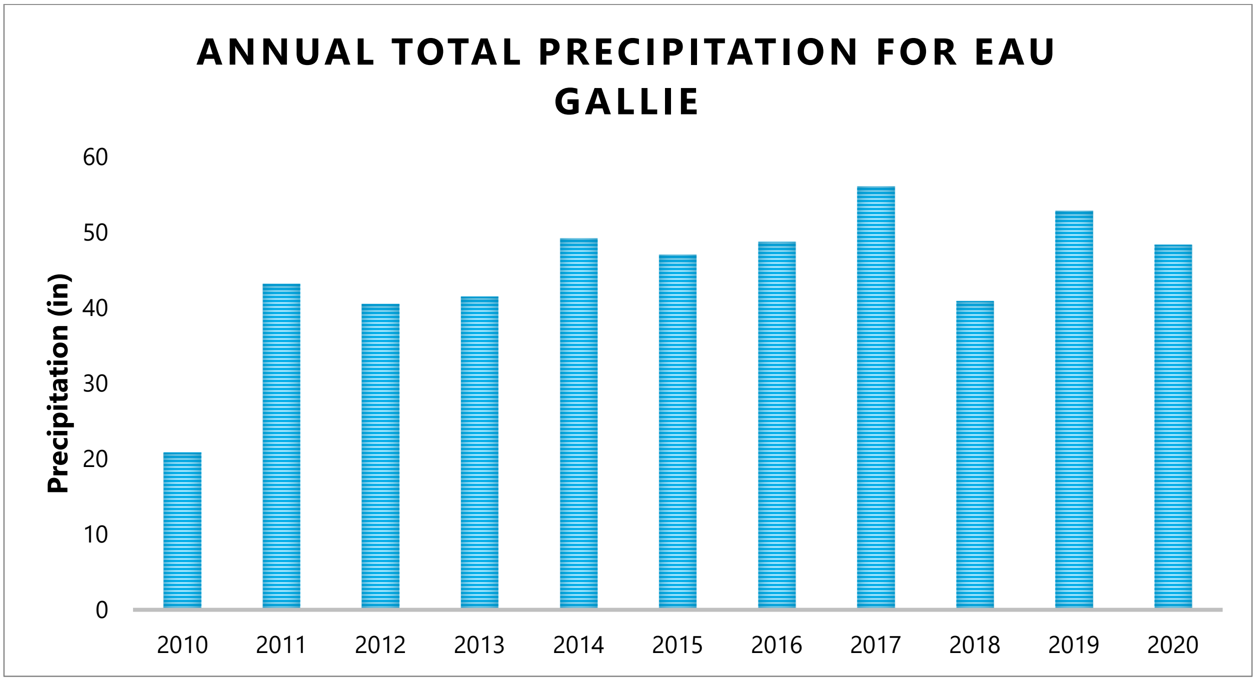

Figure 24. Annual total precipitation (in) for the Eau Gallie calibration basin from 2010 to 2020 derived from SJRWMD NEXRAD data.

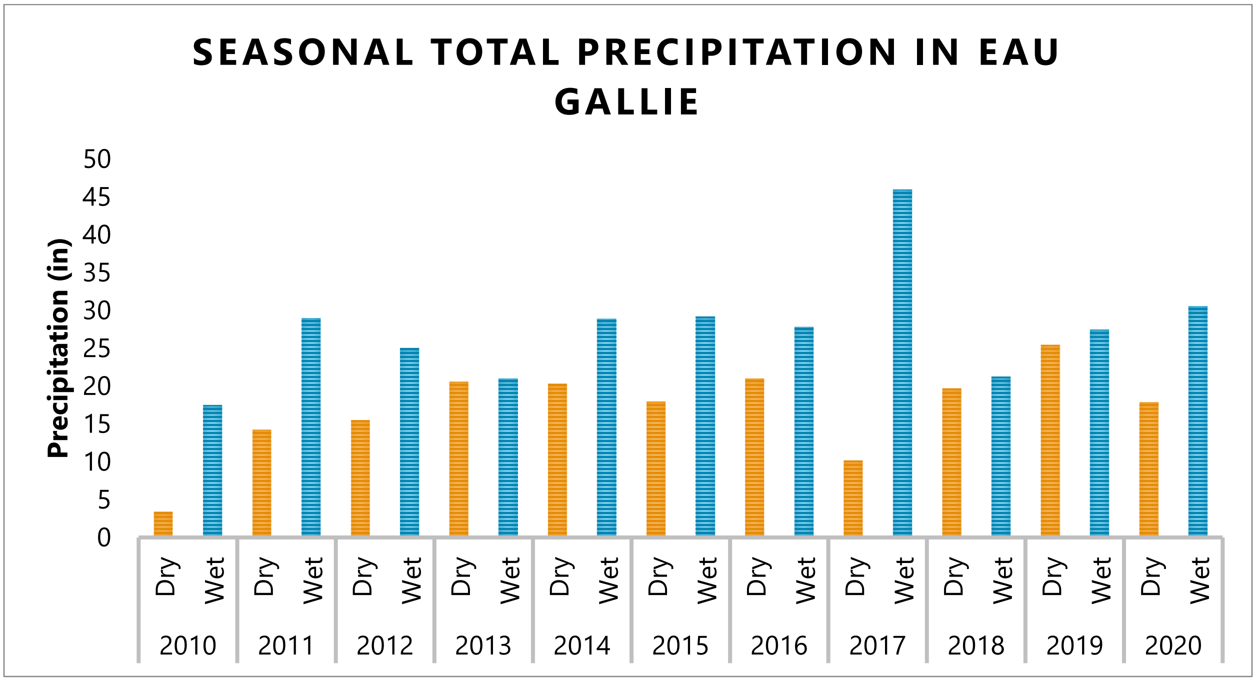

Figure 25. Seasonal total precipitation (in) for the Eau Gallie calibration basin from 2010 to 2020 derived from SJRWMD NEXRAD data.

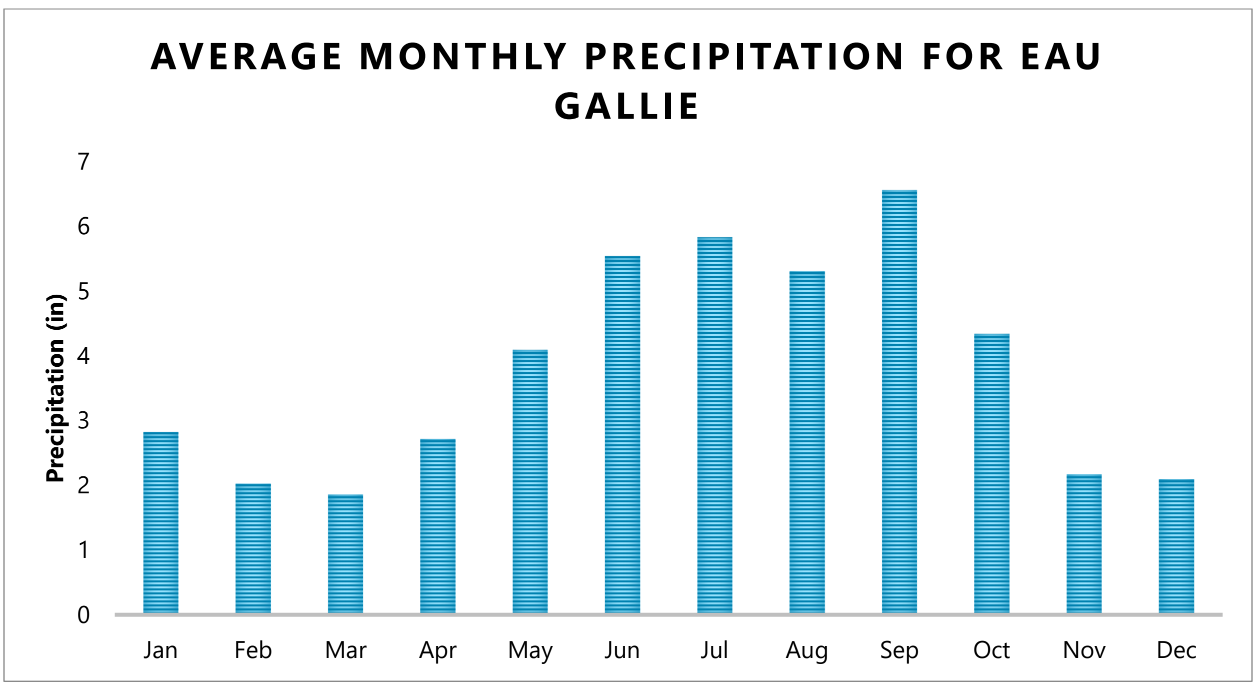

Figure 26. Average monthly precipitation (in) for the Eau Gallie calibration basin derived from SJRWMD NEXRAD data.

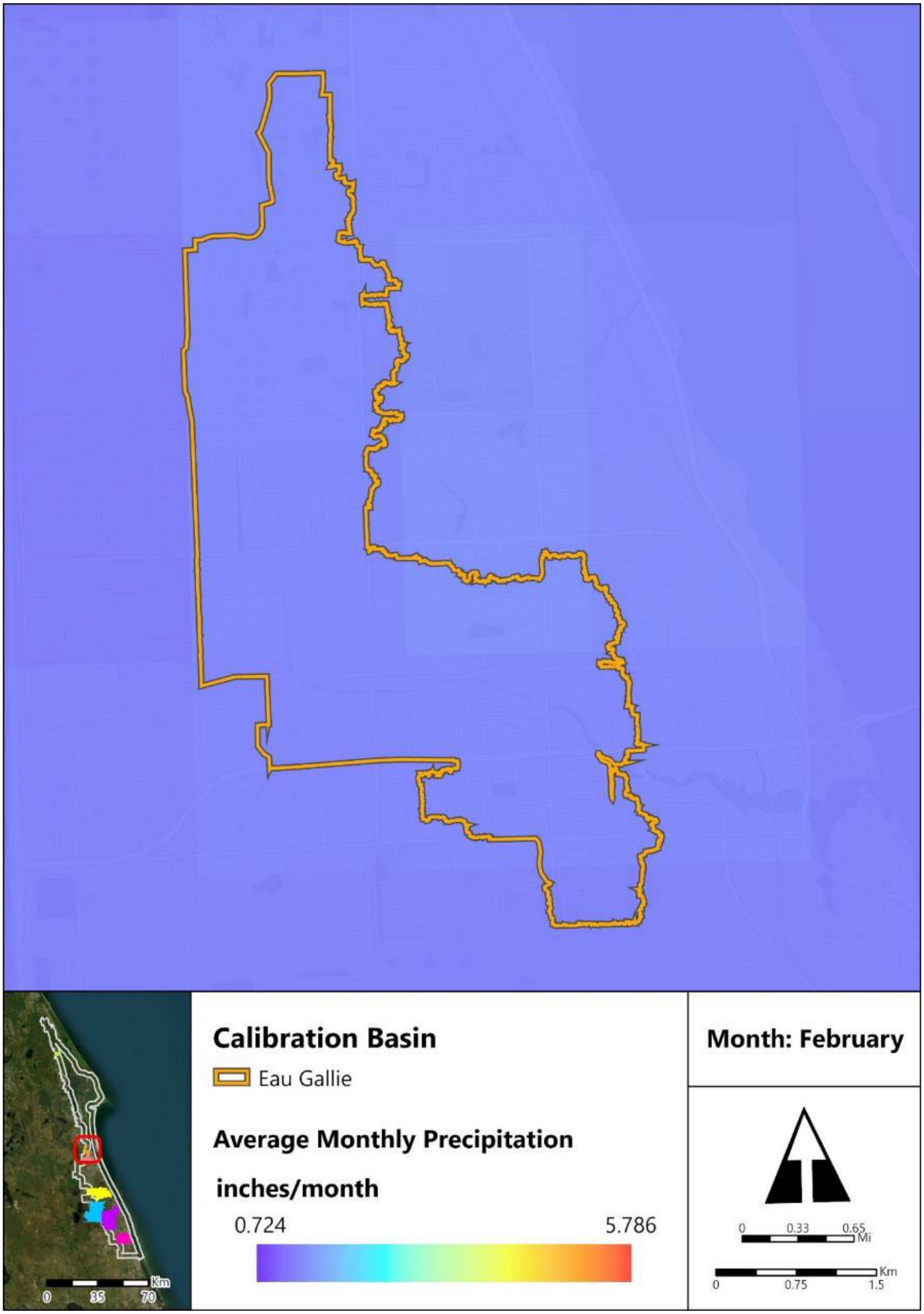

Figure 27. Average monthly precipitation (inches/month) for February across the period of record in the Eau Gallie calibration basin.

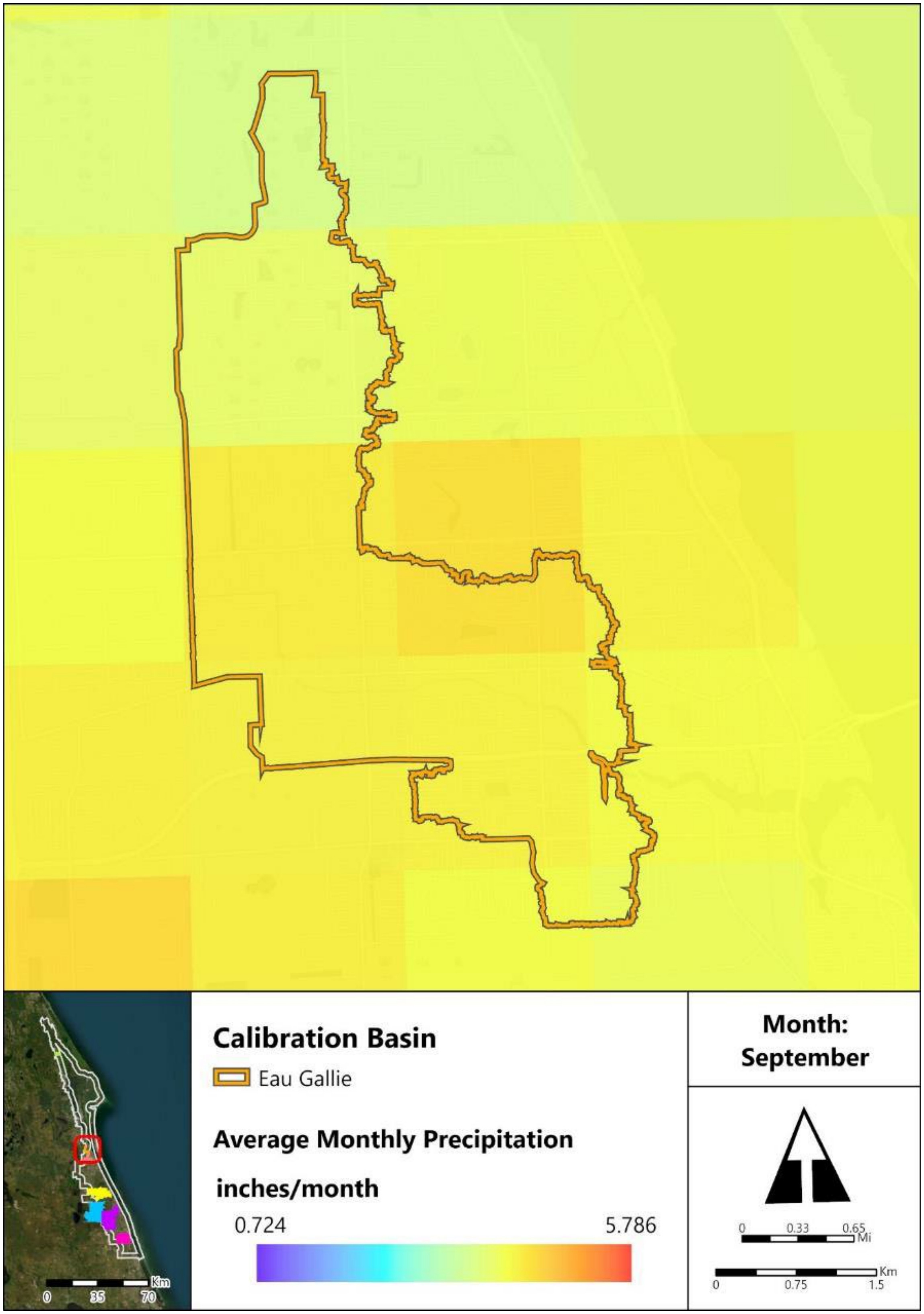

Figure 28. Average monthly precipitation (inches/month) for September across the period of record in the Eau Gallie calibration basin.

2.2.4 ET

Summary statistics for the monthly mean ET in the Eau Gallie calibration basin are provided as a boxplot (Figure 29). There is a lower variation in the wet and dry seasonal ET rates in comparison to those of the Big Flounder calibration basin. A general trend can be seen where ET increases through the wet season and decreases in the dry season. The lowest median ET and lowest variability in ET are seen in the dry season, where there are generally lower temperatures. The greatest median ET and highest variability are seen in the wet season, where there are generally higher temperatures. The lowest median value was observed in January (1.11 mm/day), whereas the highest medians were observed in July and August (2.42 mm/day). The highest variability was observed in July, with a 1.11 mm/day interquartile range difference, and the lowest variability was observed in January, with a 0.2 mm/day difference within the interquartile range. Maps for mean monthly ET rates (mm/day) during February and September across the POR in the Eau Gallie calibration basin are provided in Figure 30 and Figure 31, respectively.

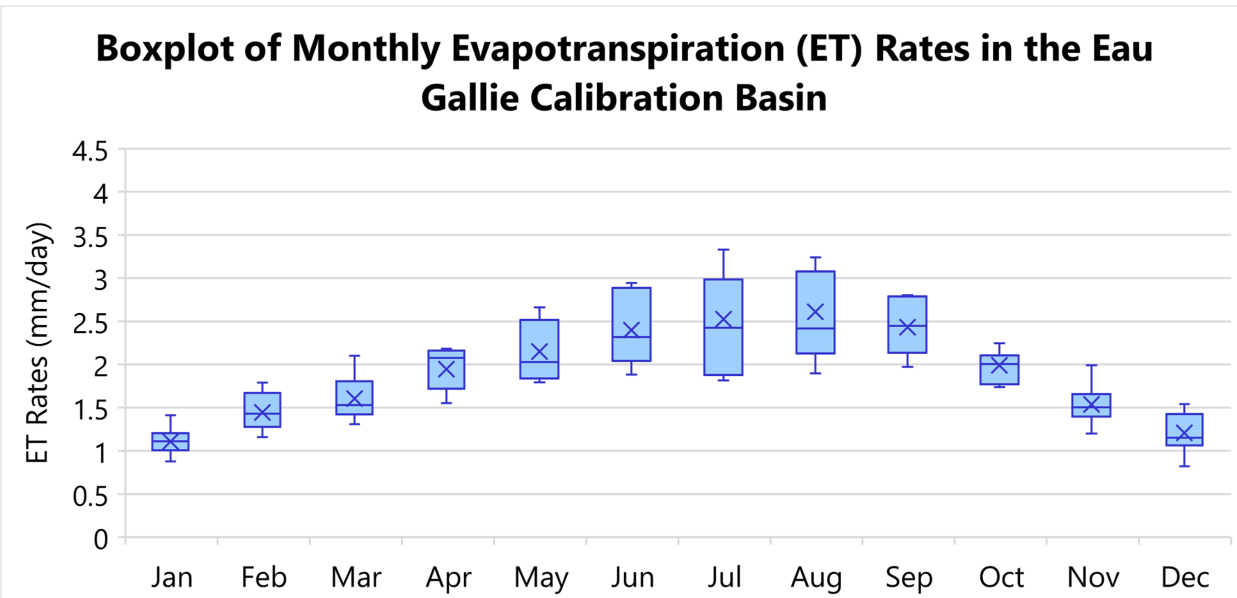

Figure 29. Boxplot of monthly mean ET rates in the Eau Gallie calibration basin derived from NASA EarthData and the University of Montana data.

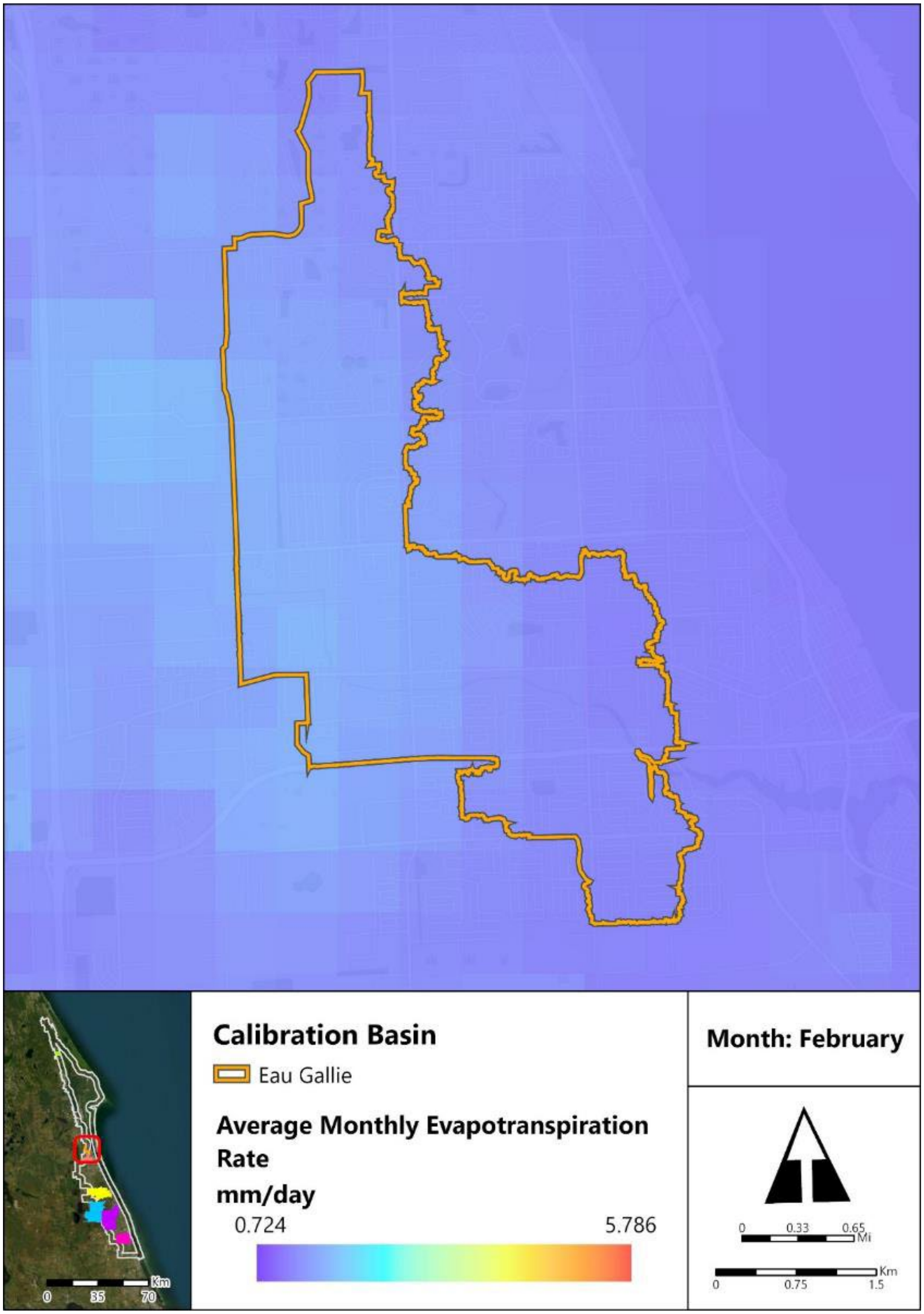

Figure 30. Average monthly ET rates (mm/day) for February across the period of record in the Eau Gallie calibration basin.

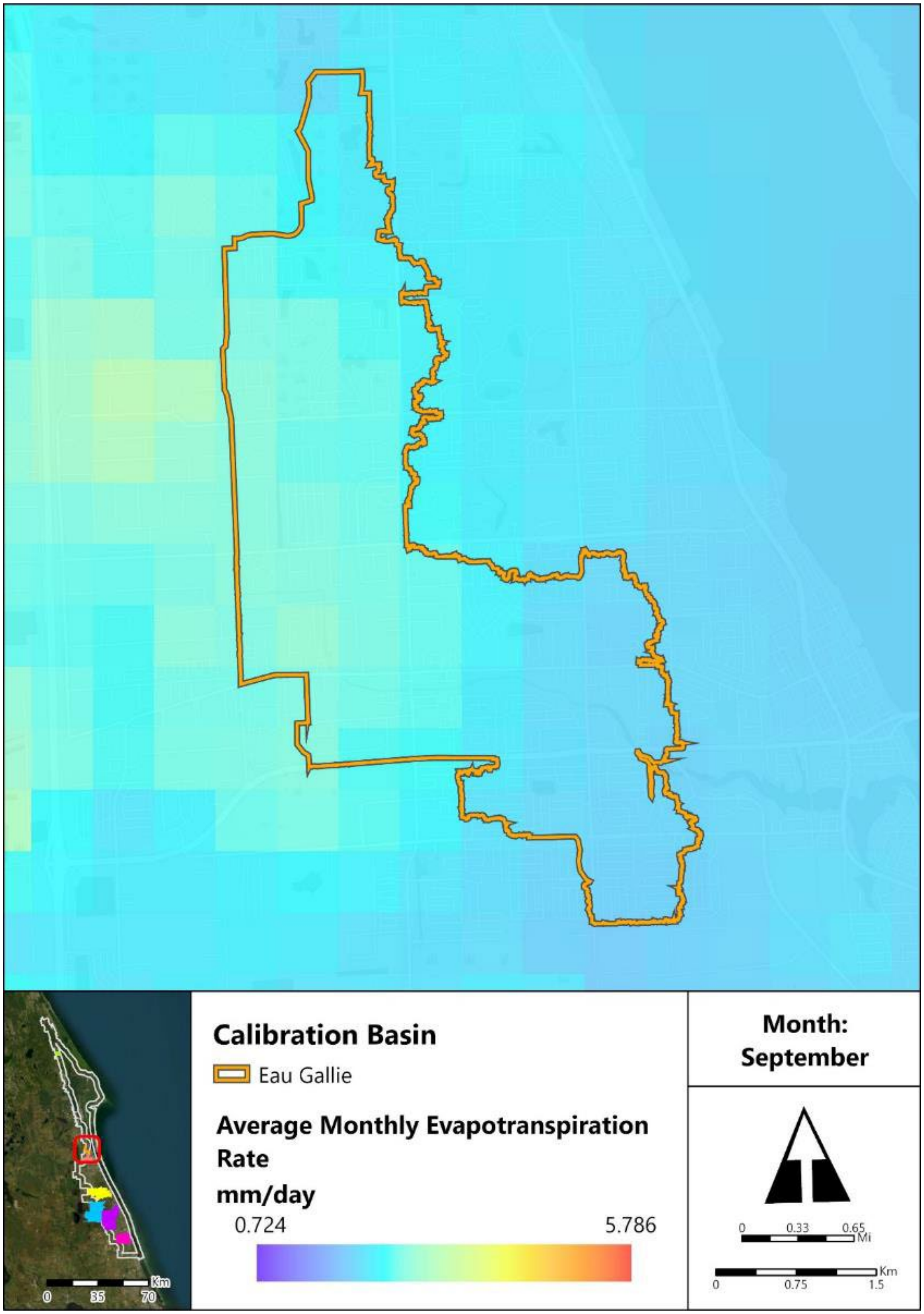

Figure 31. Average monthly ET rates (mm/day) for September across the period of record in the Eau Gallie calibration basin.

2.2.5 TREATMENTS

Within Eau Gallie, approximately 52% of the calibration basin's total area is treated (Table 7), with a majority being wet treatments (35%) versus dry treatments (16%). Overall, the largest changes occurred between 2010 and 2020, with increases in wet treatments (~2%) which is a result of increases in residential land use types (Figure 32, Figure 33, Figure 34).

Table 7. Total area (acres) of each treatment type in the Eau Gallie calibration basin for the 2010, 2015, and 2020 years.

Treatment Type	Treatment Area (Acres)			Percent of Total Basin Area (%)			Percent Change (%)	
	2010	2015	2020	2010	2015	2020	2015-2010	2020-2010
Dry	607.97	619.50	635.86	16.16	16.46	16.84	0.31	0.68
Wet	1,307.40	1,311.15	1,370.92	34.75	34.85	36.30	0.10	1.56
Total	*1,915.37*	*1,930.65*	*2,006.78*	*50.90*	*51.31*	*53.14*	*0.41*	*2.24*

**The percentage of the total basin area and the percent change from the overall area between 2010 and 2015, as well as 2010 and 2020, have also been provided.*

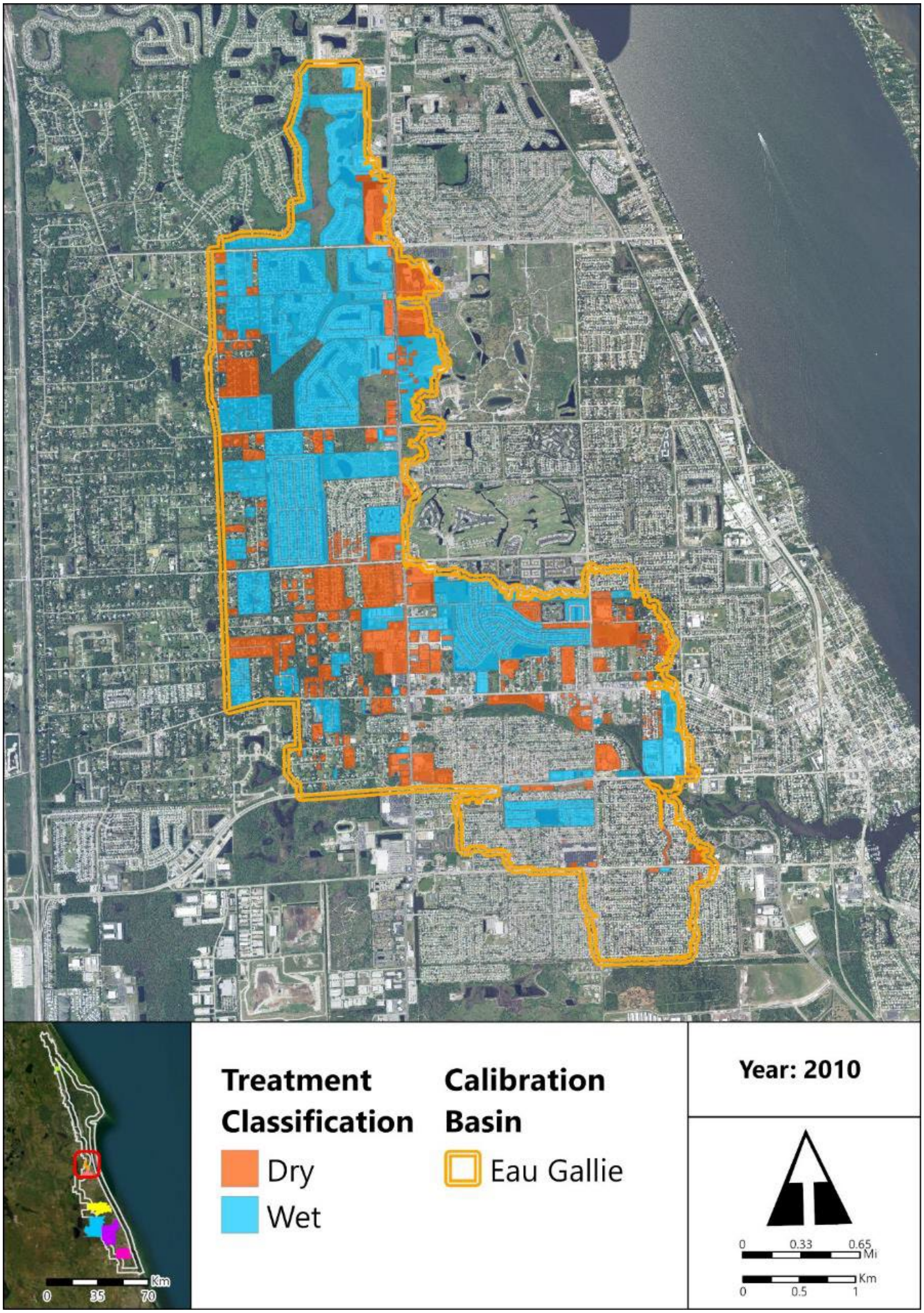

Figure 32. Treatments within the Eau Gallie calibration basin for 2010.

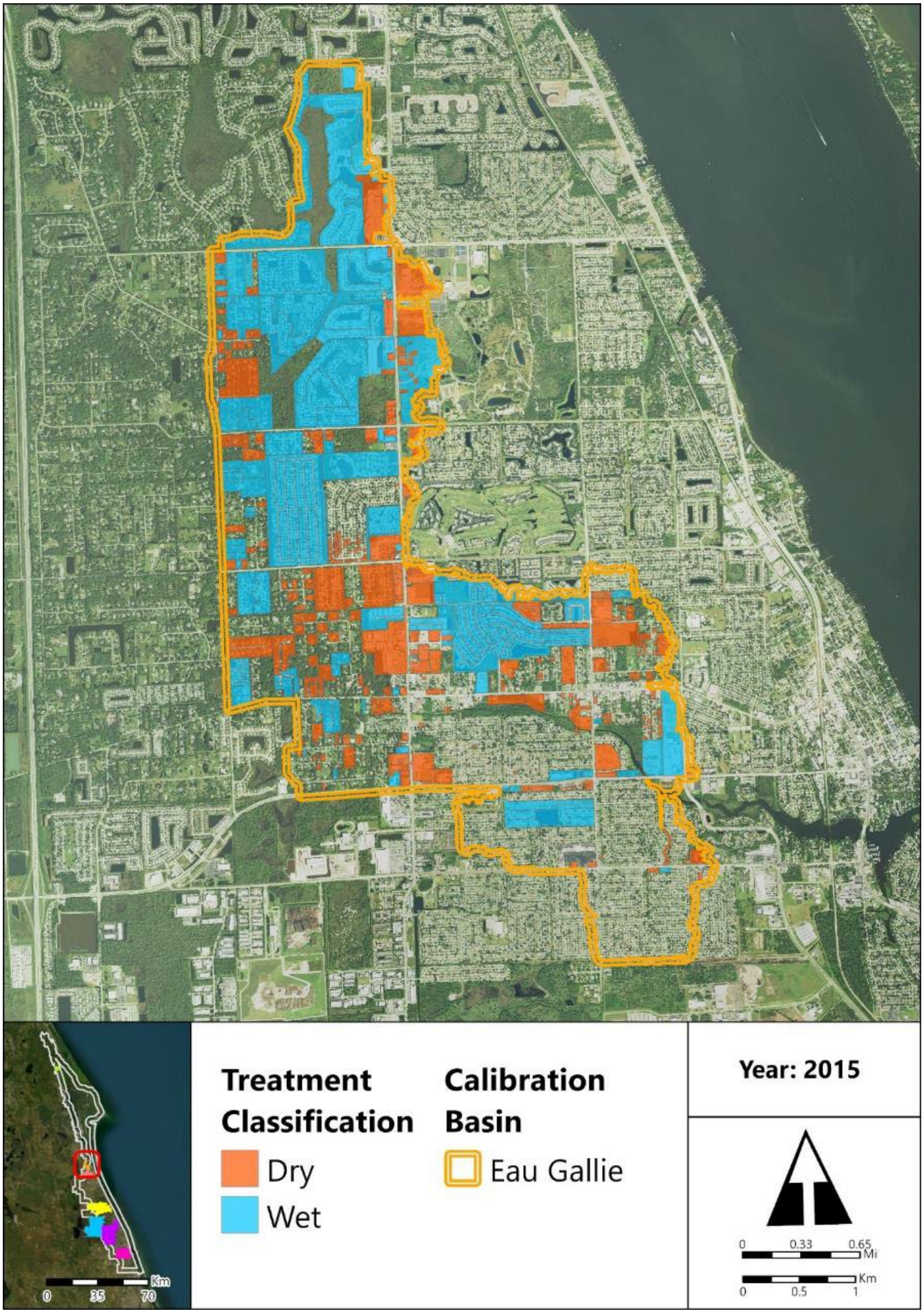

Figure 33. Treatments within the Eau Gallie calibration basin for 2015.

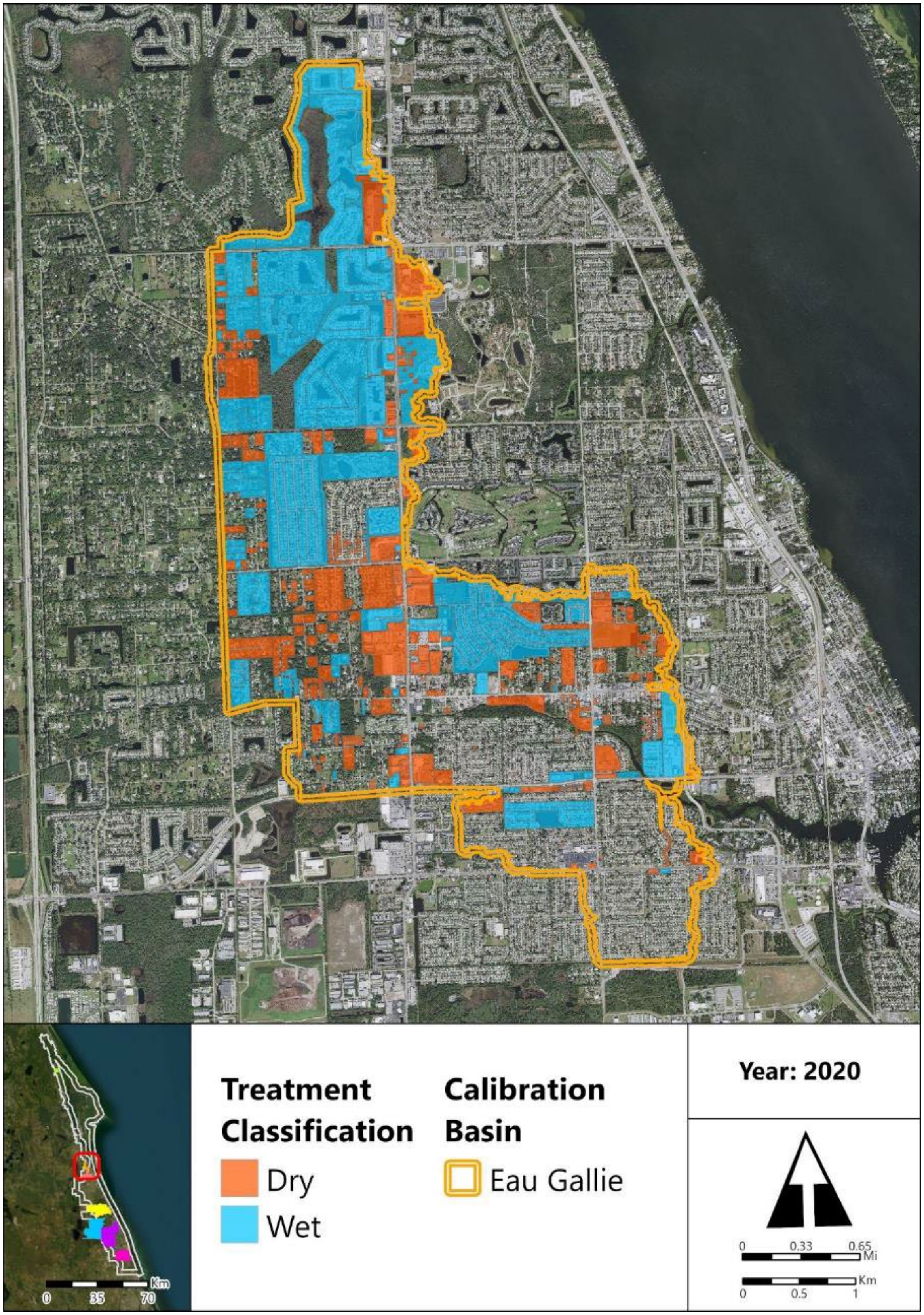

Figure 34. Treatments within the Eau Gallie calibration basin for 2020.

2.2.6 Hydrology

The Eau Gallie calibration basin volume is dominated by subsurface flow monthly (~76%), seasonally (~74% in the wet season and ~78% in the dry season), and annually (~75%) from 2010 to 2020. The average monthly volumes are higher from June to October, with lower volumes from November to May for the POR (Figure 36). The 2011 and 2017 wet seasons showed the highest discharge volumes, and the lowest was observed in the 2015 and 2017 dry seasons (Figure 37). The greatest annual volumes were observed in 2011 and 2017, coinciding with the highest volumes observed in the seasonal data, as the lowest volumes were observed in 2012 (Figure 35).

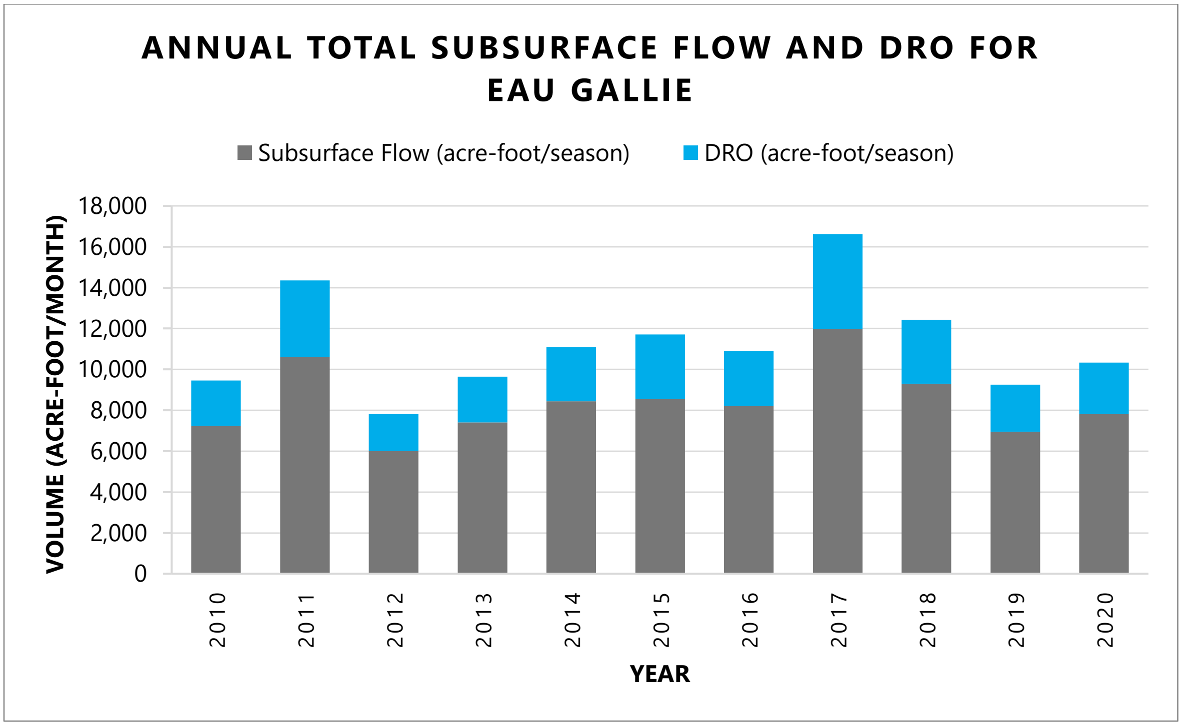

Figure 35. Annual subsurface flow (acre-foot/year) and DRO (acre-foot/year) for the Eau Gallie calibration basin derived from United States Geological Survey (USGS) web-based hydrograph analysis tool (WHAT) data.

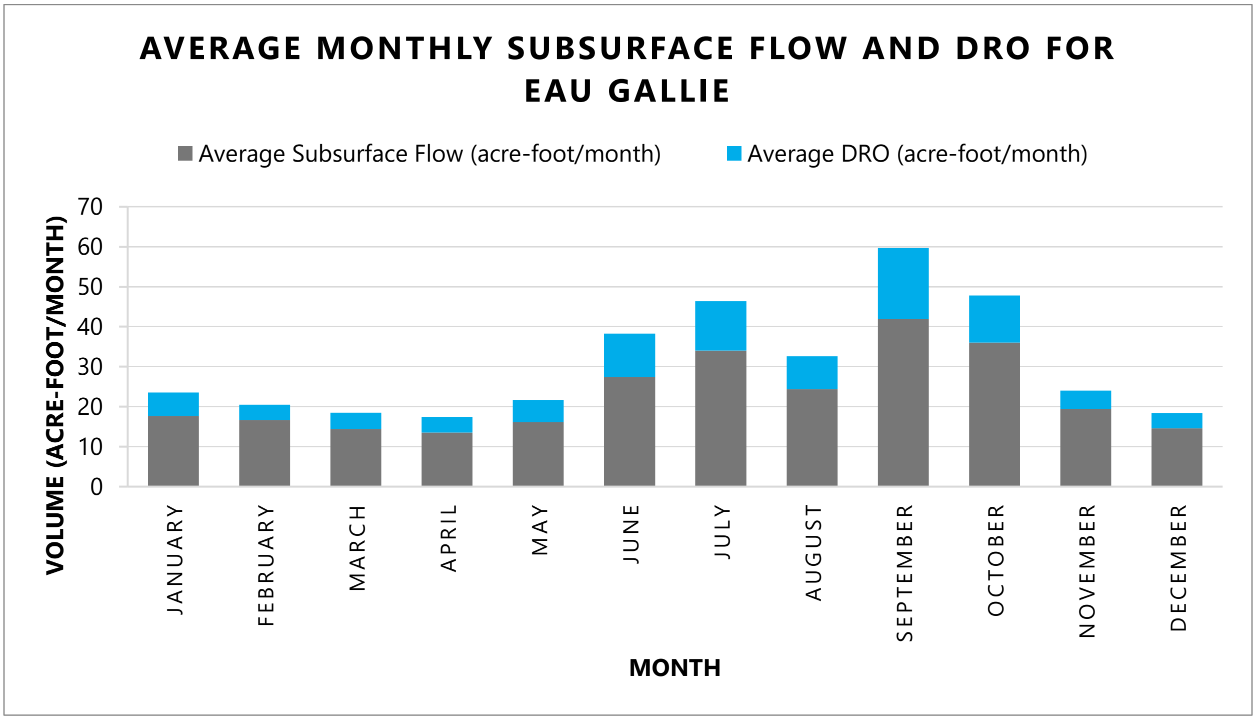

Figure 36. Average monthly subsurface flow (acre-foot/month) and DRO (acre-foot/month) for the Eau Gallie calibration basin derived from USGS WHAT data.

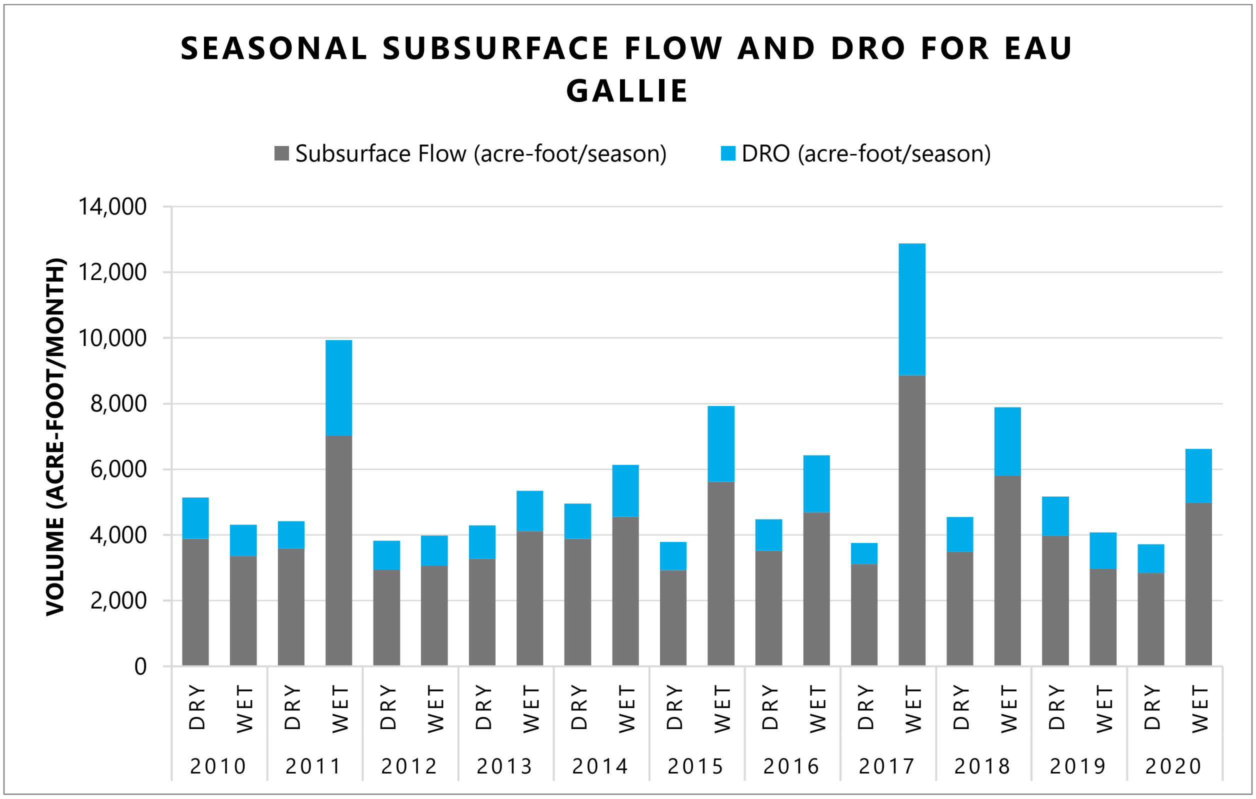

Figure 37. Seasonal subsurface flow (acre-foot/season) and DRO (acre-foot/season) for the Eau Gallie calibration basin derived from USGS WHAT data.

2.2.7 Water Quality

From 2010 to 2020, there were a total of 112 samples collected from Eau Gallie River at IRLUPEGWR by SJRWMD. Only two samples coincided with DRO conditions, 83 coincided with subsurface flow conditions, and the remaining 26 were under mixed conditions; gaps in the times series data for DRO is due to a lack of measured data at the monitoring locations (Table 8). The Eau Gallie calibration basin has little variation in its TN and TP subsurface flow concentrations from 2010 to 2020, with TN annual mean subsurface flow ranging from 0.83 to 1.13 mg/L and the TP annual mean subsurface flow ranging from 0.16 to 0.24 mg/L. Annual TN and TP annual mean subsurface flow do not appear to have any extreme patterns over the period of record, but the seasonal concentrations of both nutrients appear to have higher concentrations and degrees of variability in the wet season, with lower concentrations and less variability in the dry season (Figure 38, Figure 39).

Table 8. Comparison of DRO and subsurface flow annual geometric mean of TN (mg/L) and TP (mg/L) for the Eau Gallie River calibration basin as measured by the SJRWMD.

Year	TN - DRO	TP - DRO	TN - Subsurface flow	TP - Subsurface flow
2010			1.048	0.221
2011			0.834	0.240
2012				
2013			1.036	0.191
2014			1.052	0.195

Year	TN - DRO	TP - DRO	TN - Subsurface flow	TP - Subsurface flow
2015	0.925	0.288	1.067	0.199
2016	1.043	0.266	1.129	0.224
2017			0.928	0.161
2018			0.917	0.225
2019			0.898	0.208
2020			1.107	0.233

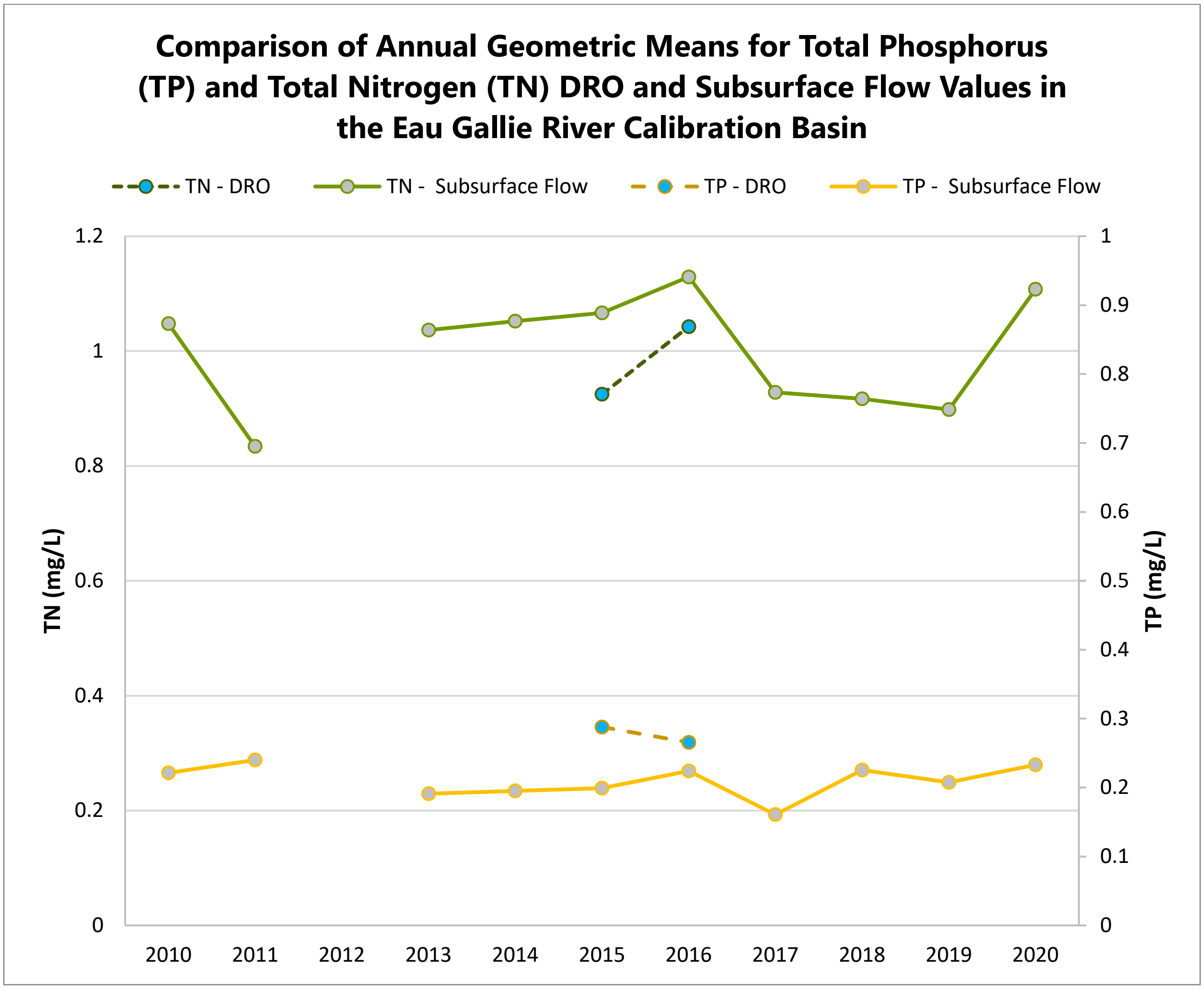

Figure 38. Comparison of DRO and subsurface flow annual geometric means for TN(mg/L) and TP (mg/L) for the Eau Gallie River calibration basin.

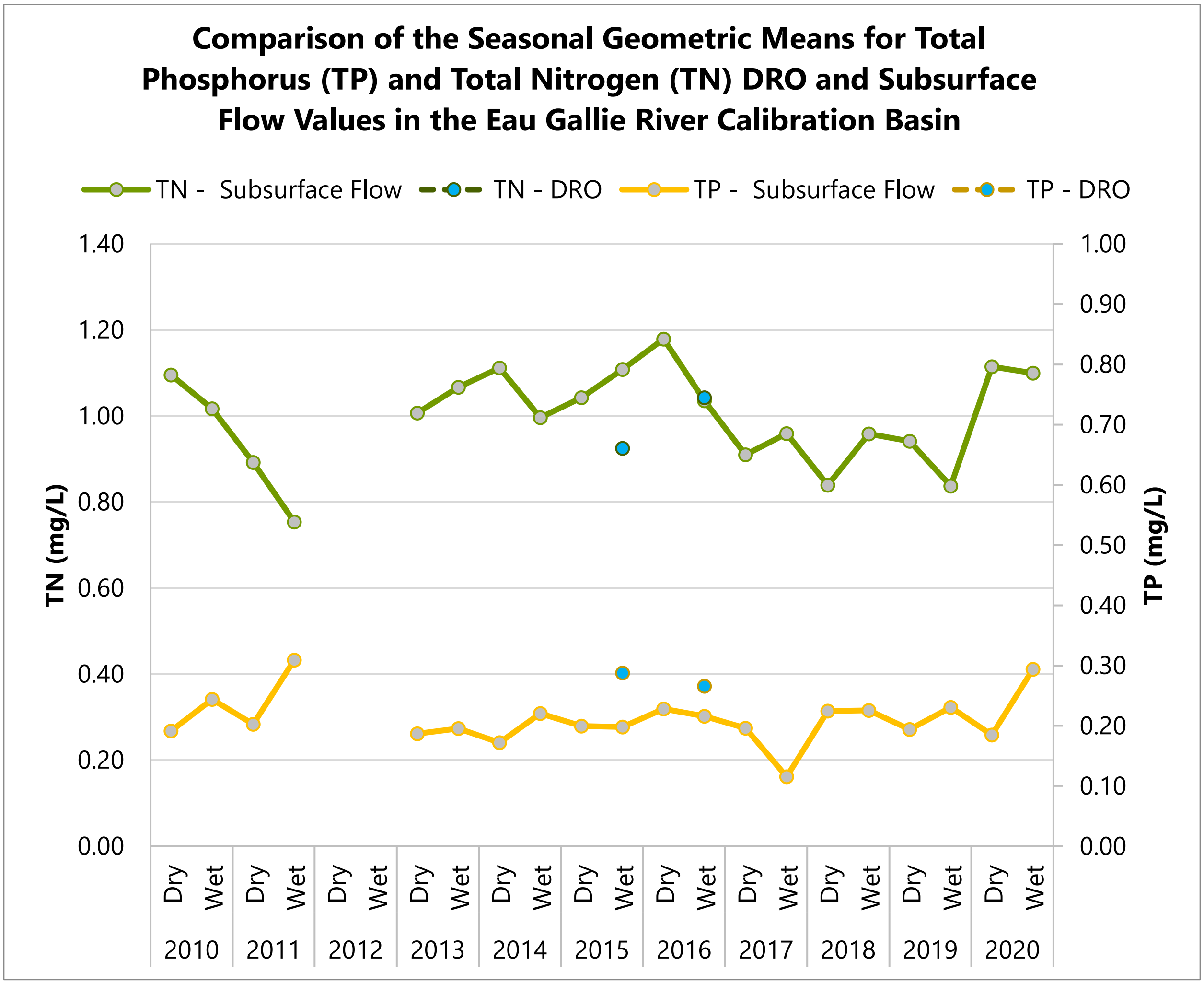

Figure 39. Comparison of the seasonal DRO and subsurface flow annual geometric means of TN (mg/L) and TP (mg/L) for the Eau Gallie River calibration basin. The two TN and TP DRO points consist of a single event.

2.3 CRANE CREEK

2.3.1 LULC CHANGE

The Crane Creek calibration basin is approximately 5,465 acres in size and has been predominately composed of commercial (~19%), medium density residential (~17%), institutional (~16%), high density residential (~12%), and low density residential (~10%) land use consolidation types (Table 9). The residential areas (of all densities) are widely distributed throughout the basin, as they make up almost 70% of the total area (Figure 40, Figure 41, Figure 42). The residential areas are concentrated in the southwest region of the basin, as well as smaller neighborhoods within the northern and southeast corners. The institutional areas within the central, eastern portion of the basin are largely composed of the Melbourne Airport. The commercial and natural land use types are distributed in the remaining areas, with commercial types filling in a majority of the space around the residential areas. Overall, relatively minor changes have occurred within the Crane Creek calibration basin from 2010 to 2020, with the exception of the conversions of approximately 4% of the total area from natural (scrub and uplands) to institutional or commercial types, which are particularly noticeable around the Melbourne Airport.

Table 9. Total area (in acres and percentage) of each land use consolidation type in the Crane Creek calibration basin for the 2010, 2015, and 2020 years.

Land Use Consolidation	Land Use Area (Acres)			Percent of Total Land Use (%)			Percent Change (%)	
	2010	2015	2020	2010	2015	2020	2015-2010	2020-2010
Citrus	20.27	17.03	17.03	0.37	0.31	0.31	-0.06	-0.06
Commercial	**995.60**	**997.45**	**1,063.32**	**18.22**	**18.26**	**19.46**	0.03	1.24
Dry Prairie	46.73	23.71	23.71	0.86	0.43	0.43	-0.42	-0.42
Field Crop	0.33	0.33	0.33	0.01	0.01	0.01	0.00	0.00
High Density Residential	**631.70**	**632.59**	**653.39**	**11.56**	**11.58**	**11.96**	0.02	0.40
Hydric Hammock	1.75	1.75	1.75	0.03	0.03	0.03	0.00	0.00
Improved Pasture	2.36	2.36	2.36	0.04	0.04	0.04	0.00	0.00
Industrial	281.29	254.21	255.31	5.15	4.65	4.67	-0.50	-0.48
Institutional	**791.25**	**876.14**	**909.04**	**14.48**	**16.04**	**16.64**	1.55	2.16
Low Density Residential	**553.02**	**556.06**	**560.61**	**10.12**	**10.18**	**10.26**	0.06	0.14
Medium Density Residential	**932.44**	**922.07**	**918.48**	**17.07**	**16.88**	**16.81**	-0.19	-0.26
Mesic Flatwoods	3.20	3.20	3.20	0.06	0.06	0.06	0.00	0.00
Mining	--	--	--	--	--	--	--	--
Open	50.68	30.22	85.26	0.93	0.55	1.56	-0.37	0.63
Other Agriculture	--	7.67	7.67	--	0.14	0.14	--	--
Rangeland	52.51	45.04	45.04	0.96	0.82	0.82	-0.14	-0.14
Recreational 1	0.18	0.18	0.18	0.00	0.00	0.00	0.00	0.00

Land Use Consolidation	Land Use Area (Acres)			Percent of Total Land Use (%)			Percent Change (%)	
	2010	2015	2020	2010	2015	2020	2015-2010	2020-2010
Recreational 2	20.56	20.56	20.56	0.38	0.38	0.38	0.00	0.00
Scrub	332.45	275.82	187.53	6.08	5.05	3.43	-1.04	-2.65
Transportation	153.14	168.19	167.94	2.80	3.08	3.07	0.28	0.27
Upland Flatwoods	209.52	164.64	141.52	3.83	3.01	2.59	-0.82	-1.24
Upland Mixed	--	59.13	--	--	1.08	--	--	--
Water	80.10	105.85	102.06	1.47	1.94	1.87	0.47	0.40
Wet Flatwoods	127.20	122.10	122.10	2.33	2.23	2.23	-0.09	-0.09
Wet Prairies	12.34	10.22	10.22	0.23	0.19	0.19	-0.04	-0.04
Wetland	164.95	167.02	164.94	3.02	3.06	3.02	0.04	0.00

**The top five land uses that make up a majority of the area have been bolded for each year. Percent change from the overall area between 2010 and 2015, as well as 2010 and 2020 have also been provided.*

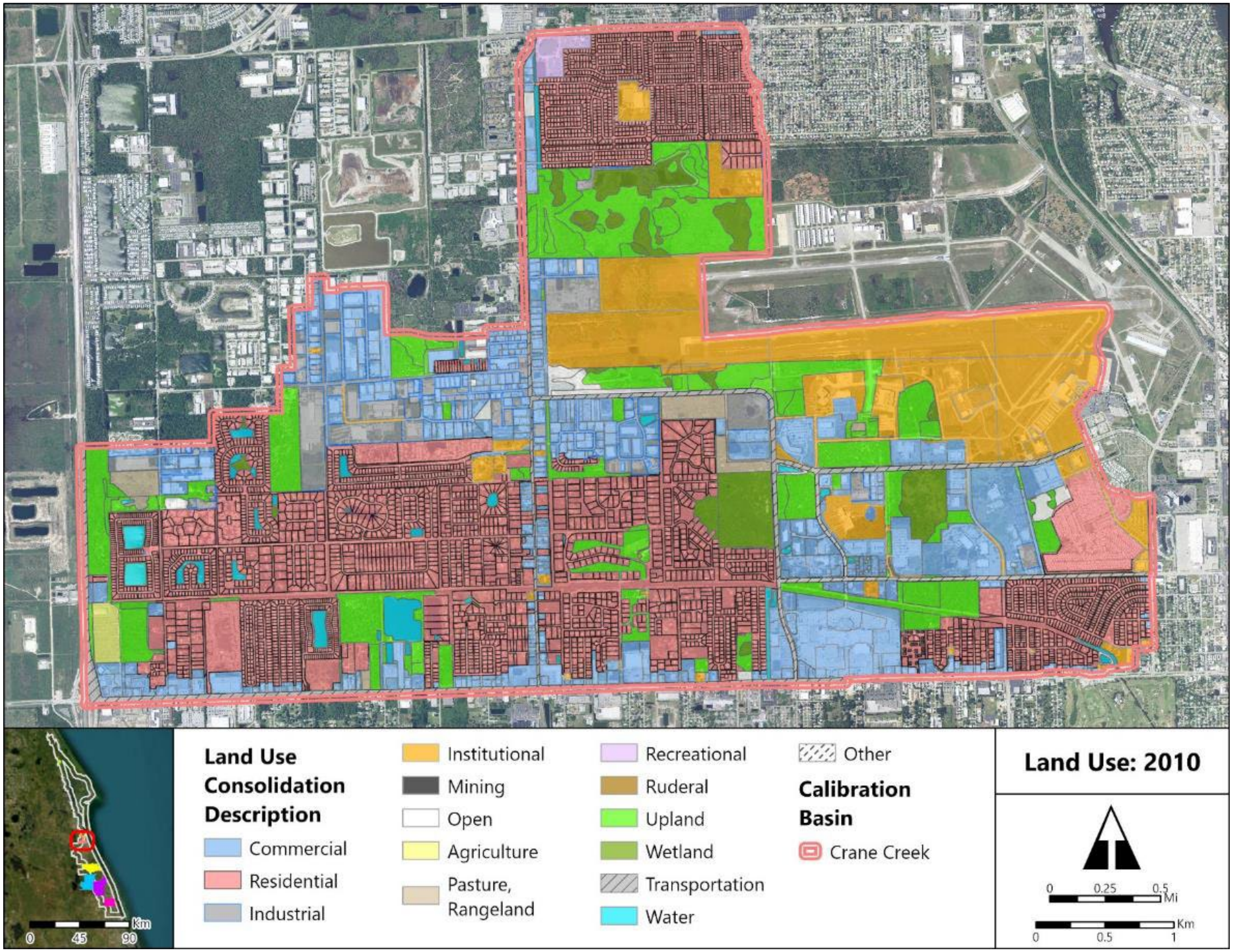

Figure 40. Land use within the Crane Creek calibration basin for 2010.

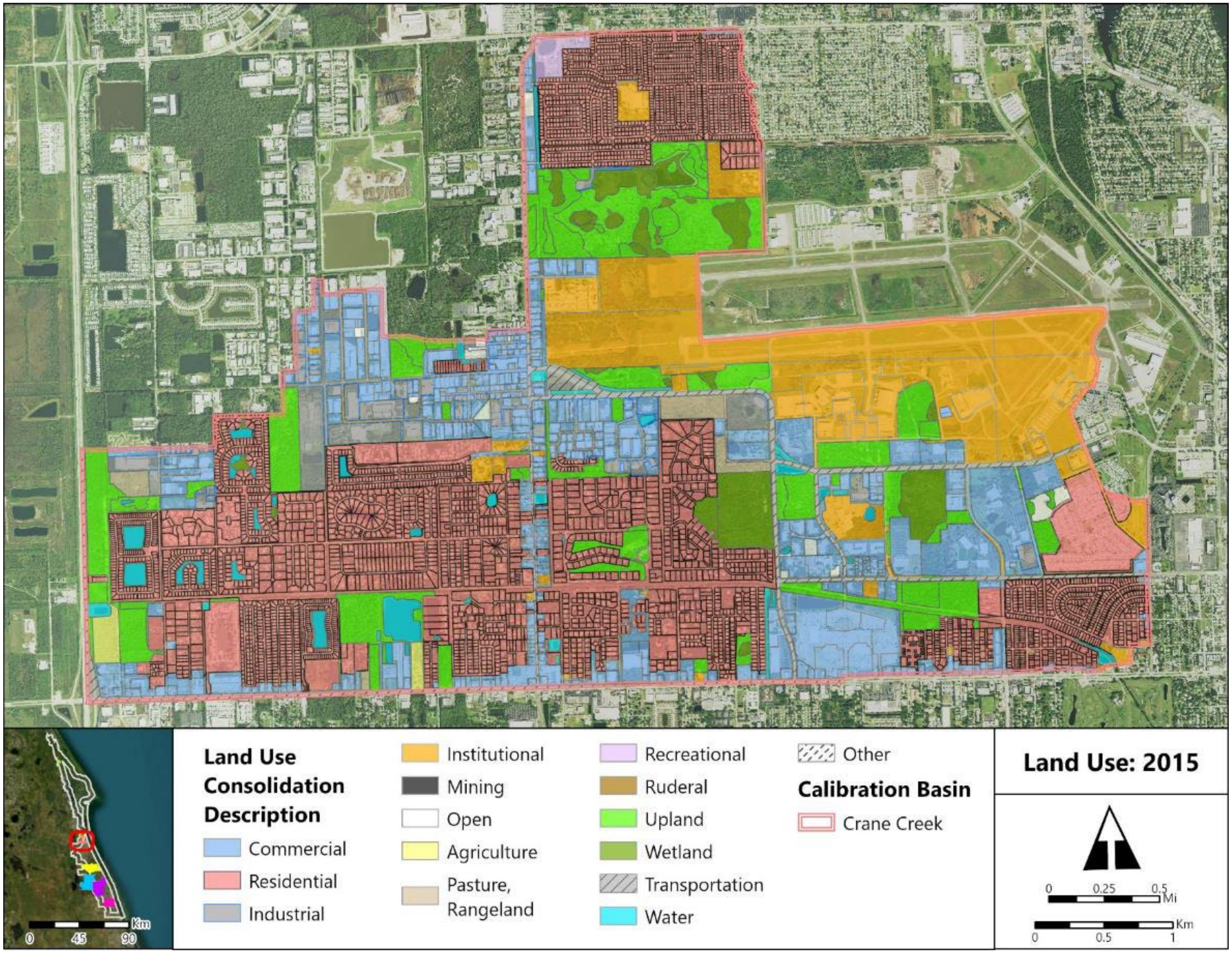

Figure 41. Land use within the Crane Creek calibration basin for 2015.

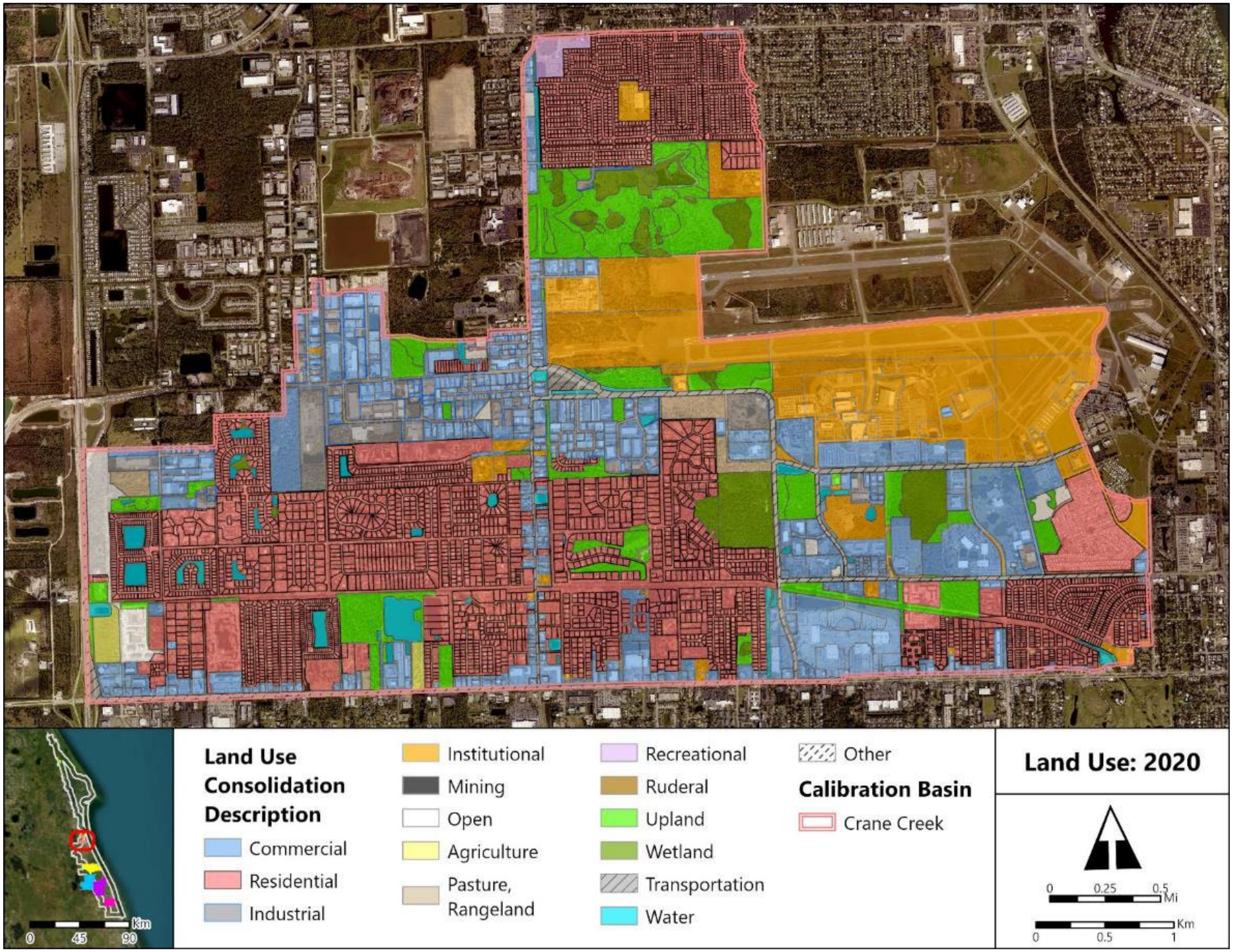

Figure 42. Land use within the Crane Creek calibration basin for 2020.

2.3.2 SOIL HYDROLOGIC GROUP

The Crane Creek calibration basin is primarily composed of the A/D hydrologic soil group (67%), followed by A (24%), B/D (4%), C/D (4%), D (2%), and water (<1%) (Figure 43). The A soils are located on the northern and eastern portions of the basin, the C/D soils are found along the western border with some centrally located patches, smaller patches of B/D soils are distributed throughout the basin, while the A/D soils encompass all other areas of the basin (Figure 44).

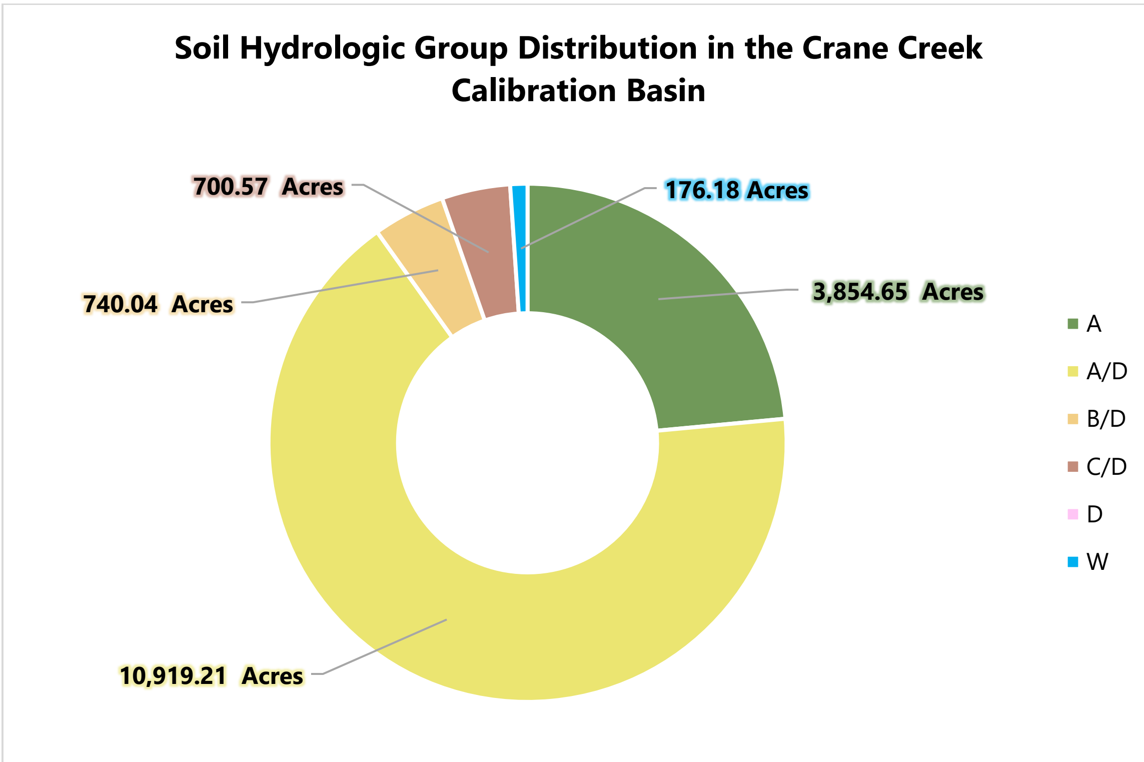

Figure 43. Pie chart (acres) of the soil hydrologic group distribution in the Crane Creek calibration basin using USDA NRCS data.

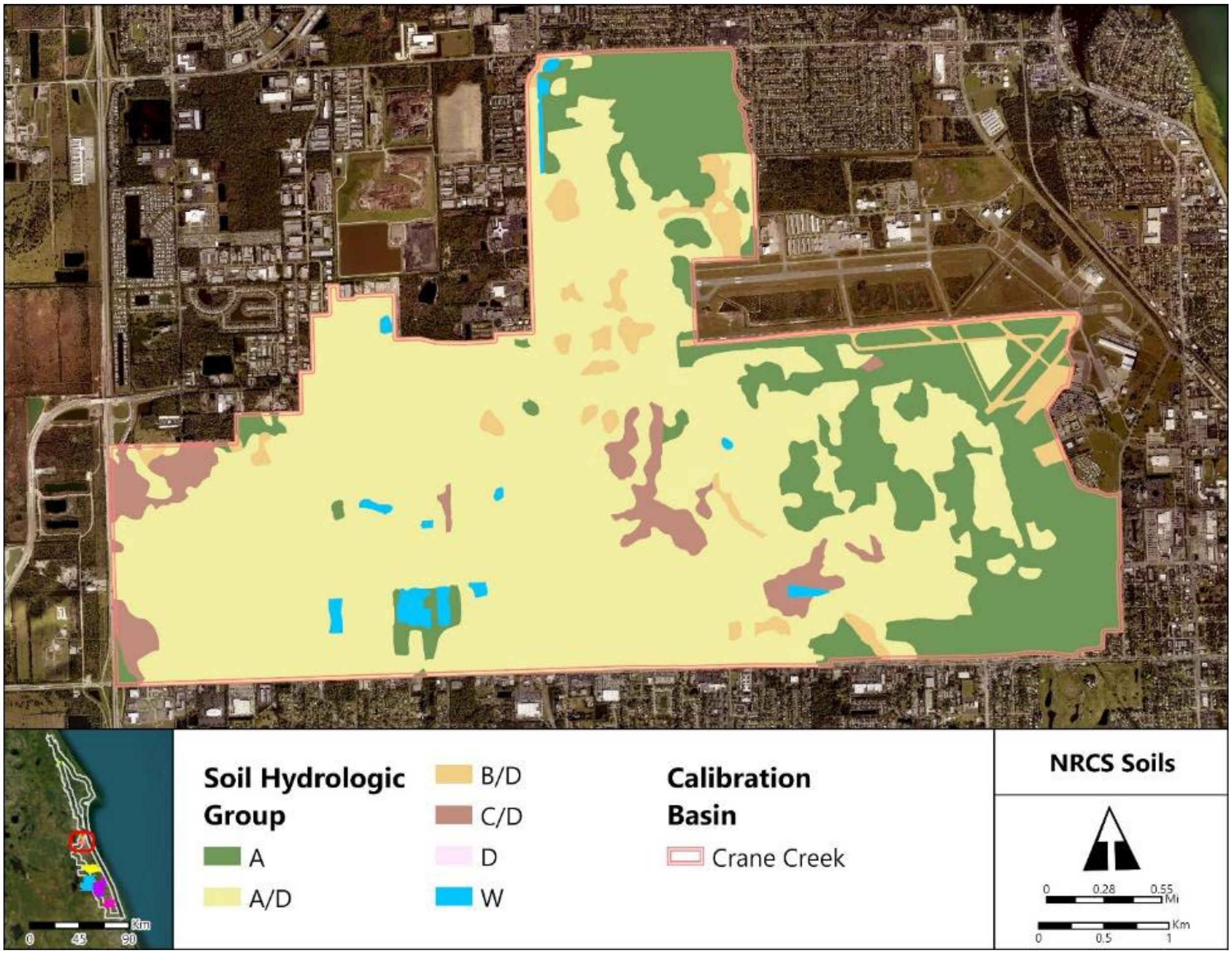

Figure 44. Distribution of soil hydrologic groups within the Crane Creek calibration basin.

2.3.3 PRECIPITATION

The annual total precipitation for Crane Creek ranges from the lowest annual total of 21 inches in 2010 to the highest annual total of 59 inches in 2017 (Figure 45). For all years, with the exception of 2013, the dry season has a lower total seasonal rainfall as compared to the wet seasons of the same years (Figure 46). The average monthly precipitation values are higher from May to October and lower from November to April (Figure 47). Maps for mean monthly precipitation (inches/month) during February and September across the POR in Crane Creek are provided in Figure 48 and Figure 49, respectively.

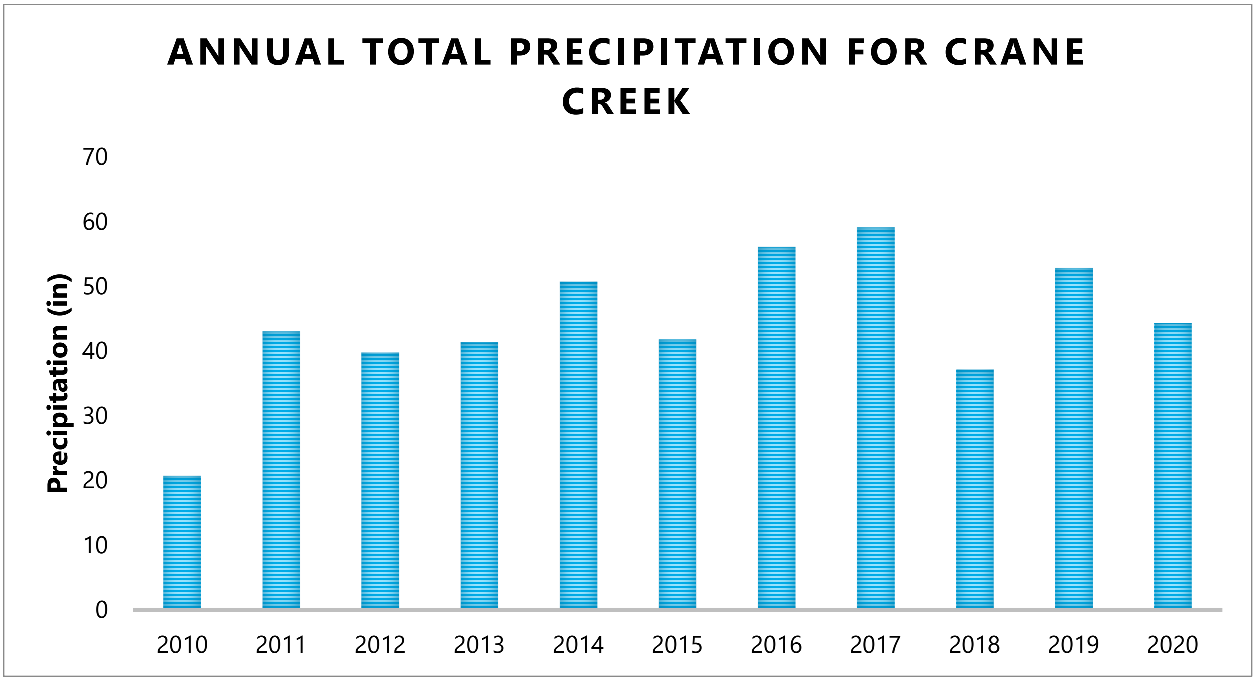

Figure 45. Annual total precipitation (in) for the Crane Creek calibration basin from 2010 to 2020 derived from SJRWMD NEXRAD data.

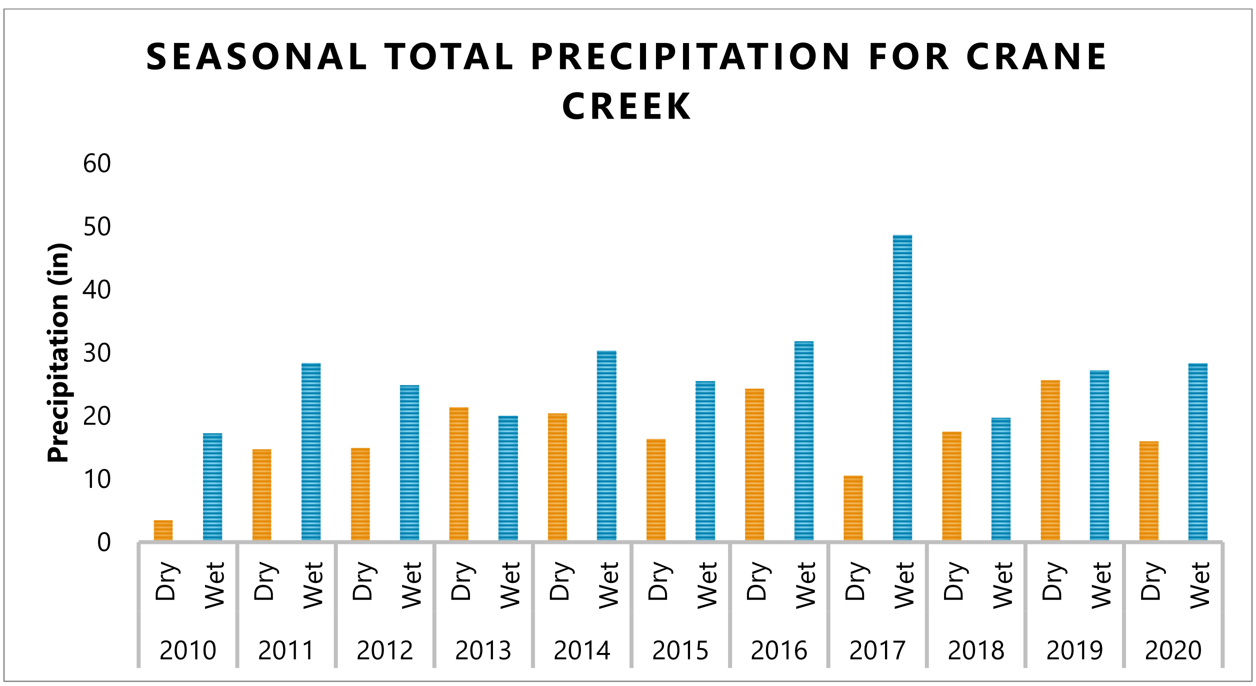

Figure 46. Seasonal total precipitation (in) for the Crane Creek calibration basin from 2010 to 2020 derived from SJRWMD NEXRAD data.

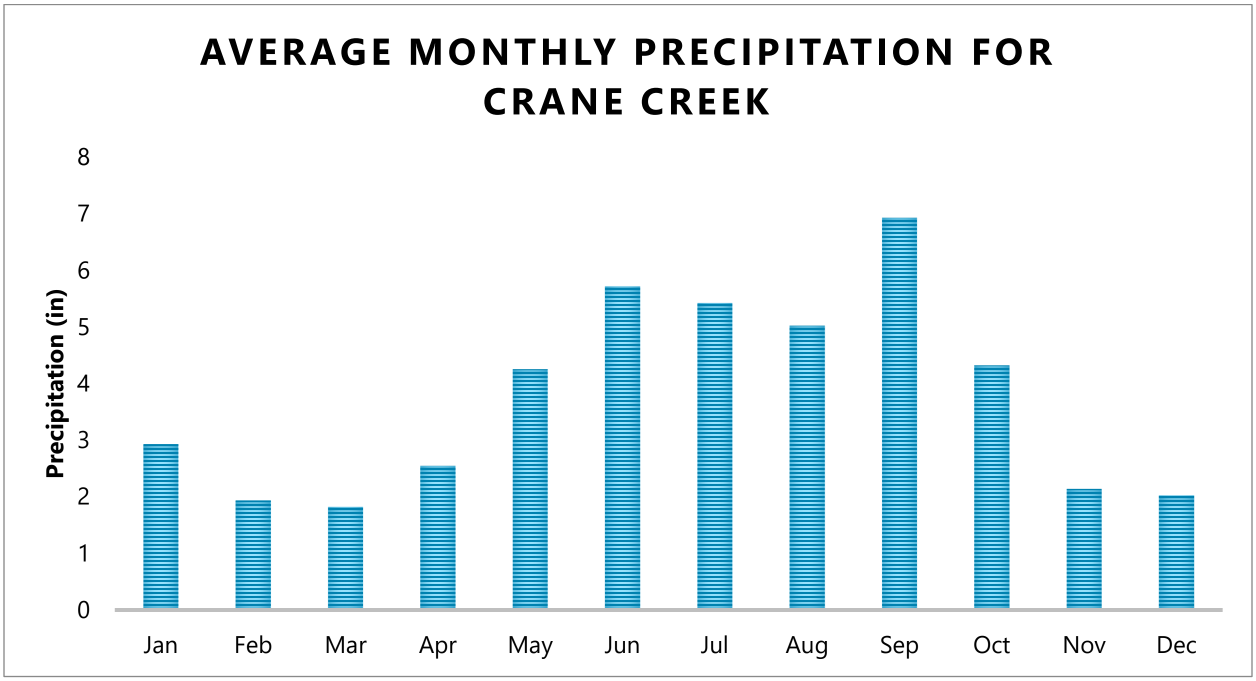

Figure 47. Average monthly precipitation (in) for the Crane Creek calibration basin derived from SJRWMD NEXRAD data.

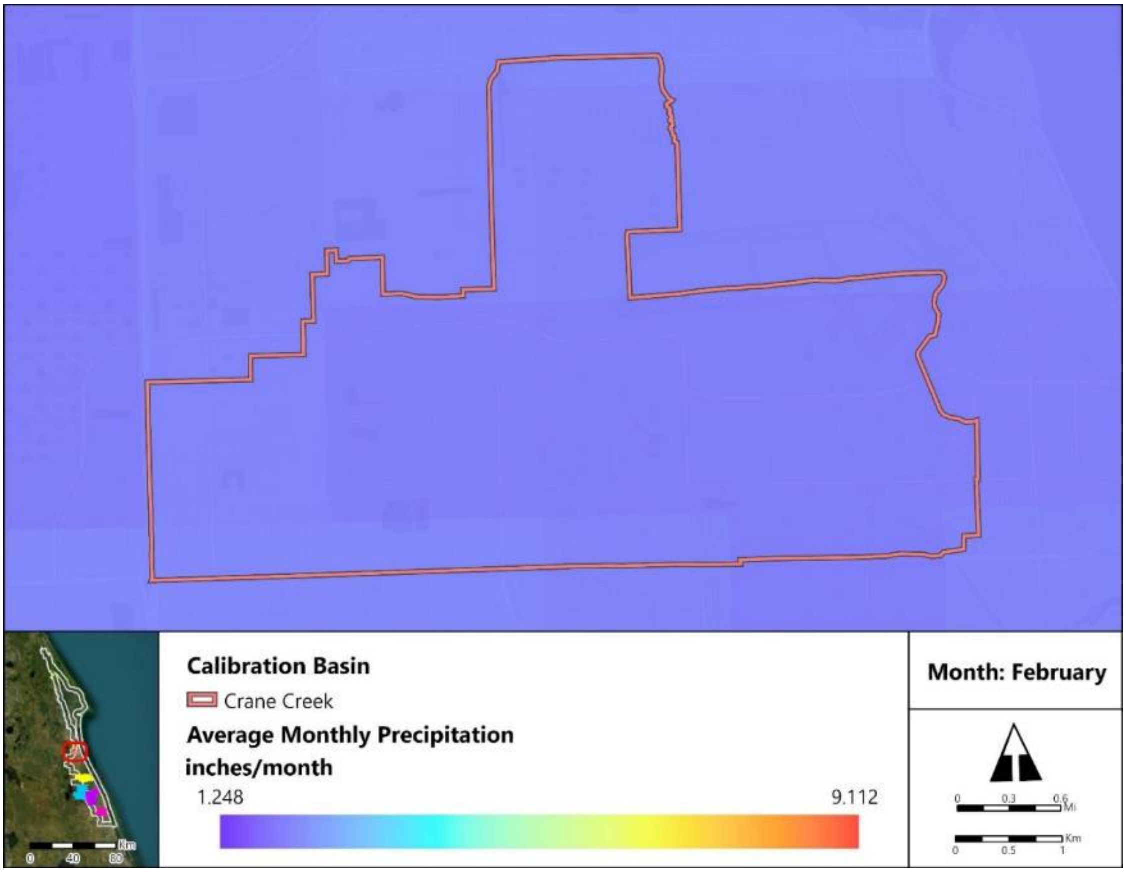

Figure 48. Average monthly precipitation (inches/month) for February across the period of record in the Crane Creek calibration basin.

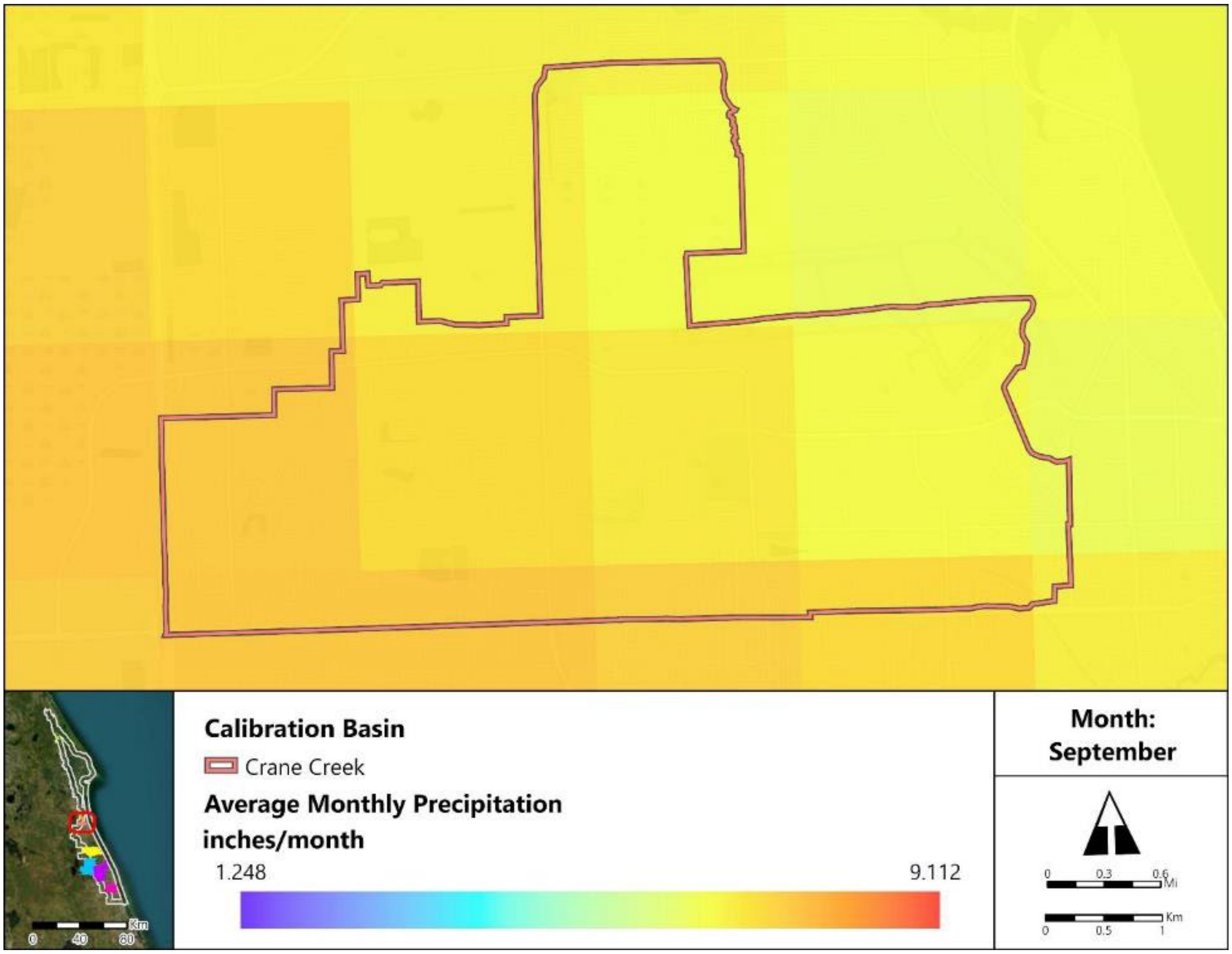

Figure 49. Average monthly precipitation (inches/month) for September across the period of record in the Crane Creek calibration basin.

2.3.4 ET

Summary statistics for the monthly mean ET in the Crane Creek calibration basin are provided as a boxplot (Figure 50). For Crane Creek, there is a lower variation in the wet and dry seasonal ET rates, and a general trend of increases through the wet season and decreases in the dry season is observed. The lowest median value and variability in ET rates are seen in the dry season, where there are generally lower temperatures. The greatest median ET and highest variability are seen in the wet season, where there are generally higher temperatures. The lowest median value was observed in January (1.07 mm/day), whereas the highest median was observed in September (2.24 mm/day). The highest variability was observed in July, with a 1.03 mm/day interquartile range difference, and the lowest variability was observed in October, with an interquartile range difference of 0.18 mm/day. Maps for mean monthly ET rates (mm/day) during February and September across the POR in the Crane Creek calibration basin are provided in Figure 51 and Figure 52, respectively.

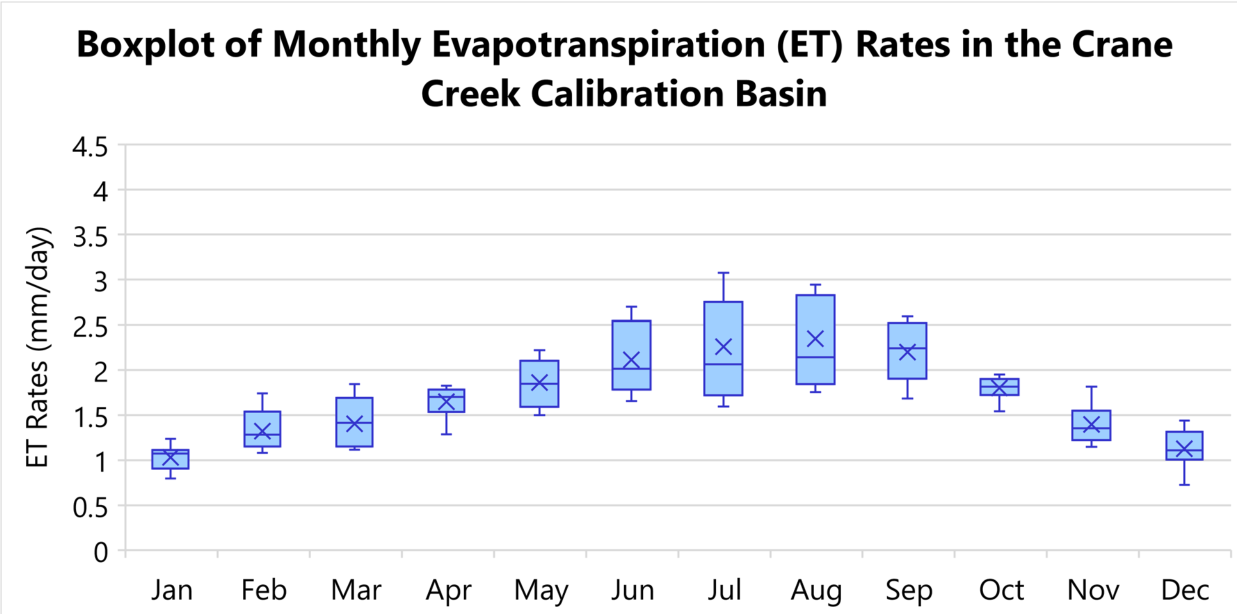

Figure 50. Boxplot of monthly mean ET rates in the Crane Creek calibration basin derived from NASA EarthData and the University of Montana data.

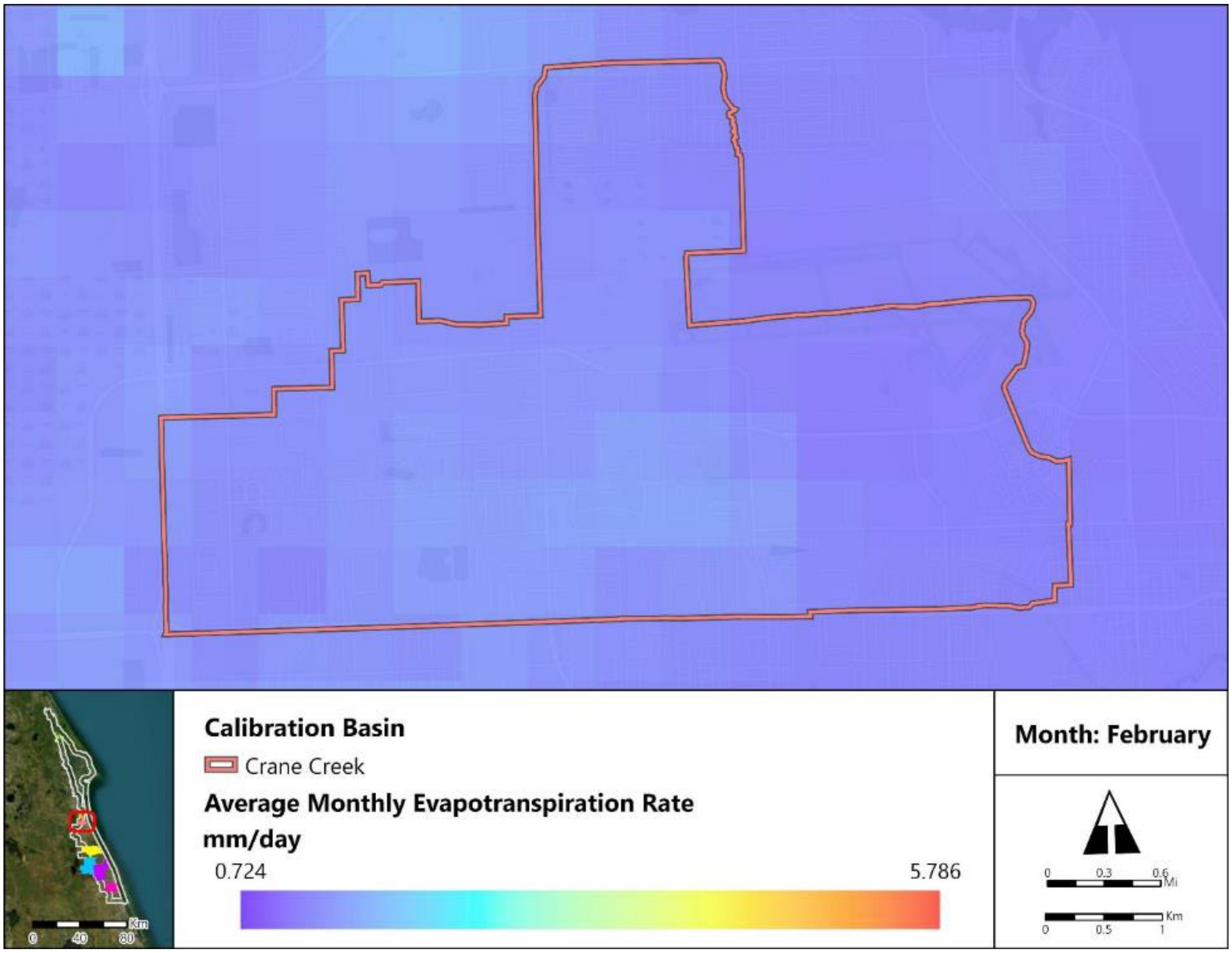

Figure 51. Average monthly ET rates (mm/day) for February across the period of record in the Crane Creek calibration basin.

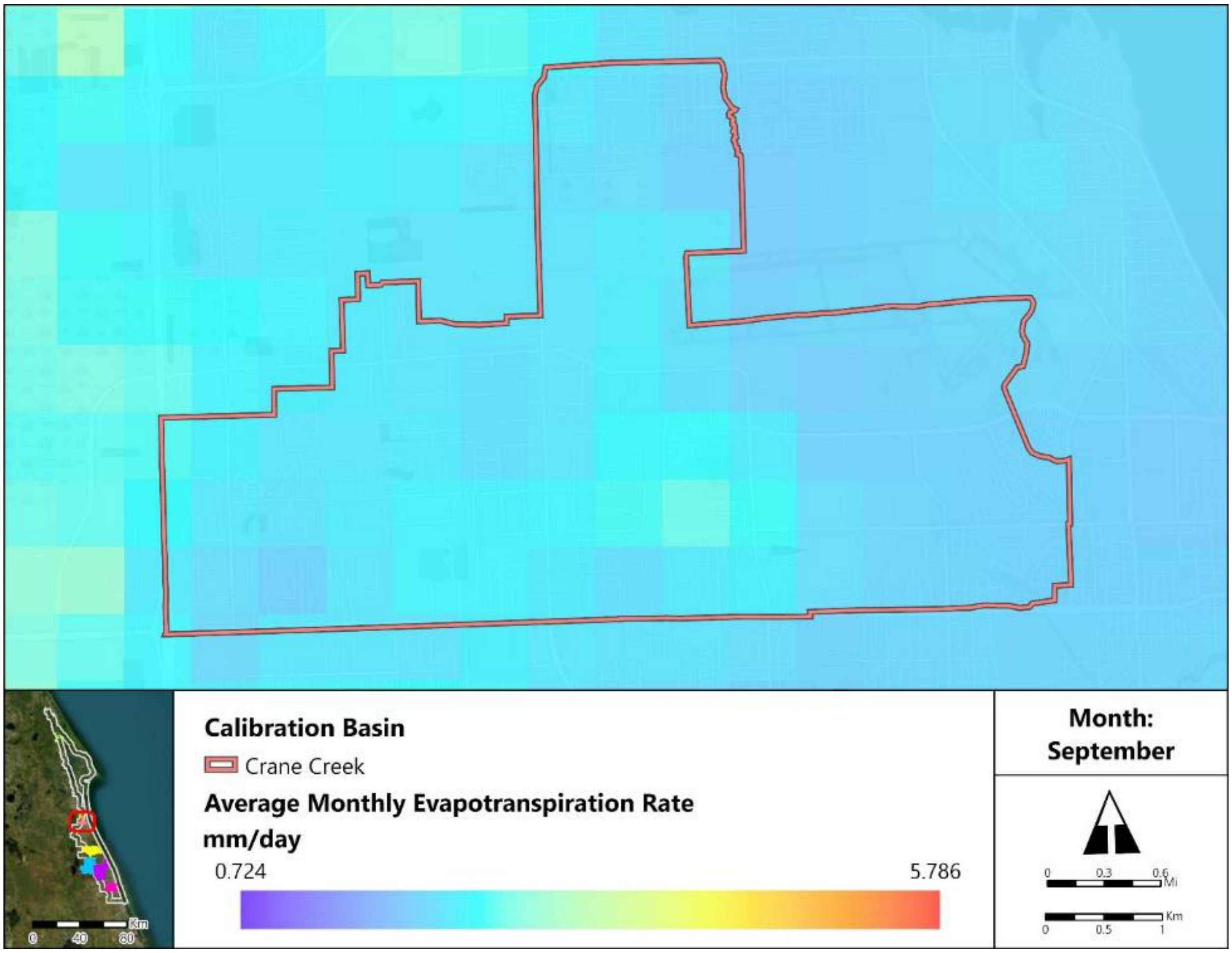

Figure 52. Average monthly ET rates (mm/day) for September across the period of record in the Crane Creek calibration basin.

2.3.5 TREATMENTS

Within Crane Creek, approximately 44% of the calibration basin's total area is treated (Table 10), with similar distributions between wet (20%) and dry treatments (23%). Overall, the largest changes occurred between 2010 and 2020, with approximately 2% increases in both treatment types resulting in an overall 4% increase in treated lands within the total area. This is likely a result of increases in institutional and residential land use types (Figure 53, Figure 54, Figure 55).

Table 10. Total area (acres) of each treatment type in the Crane Creek calibration basin for the 2010, 2015, and 2020 years.

Treatment Type	Treatment Area (Acres)			Percent of Total Basin Area (%)			Percent Change (%)	
	2010	2015	2020	2010	2015	2020	2015-2010	2020-2010
Dry	1,226.15	1,251.22	1,330.16	22.44	22.90	24.35	0.46	1.90
Wet	1,076.03	1,090.98	1,180.32	19.70	19.97	21.60	0.27	1.91
Total	*2,302.18*	*2,342.20*	*2,510.47*	*42.14*	*42.87*	*45.95*	*0.73*	*3.81*

**The percentage of the total basin area and the percent change from the overall area between 2010 and 2015, as well as 2010 and 2020 have also been provided.*

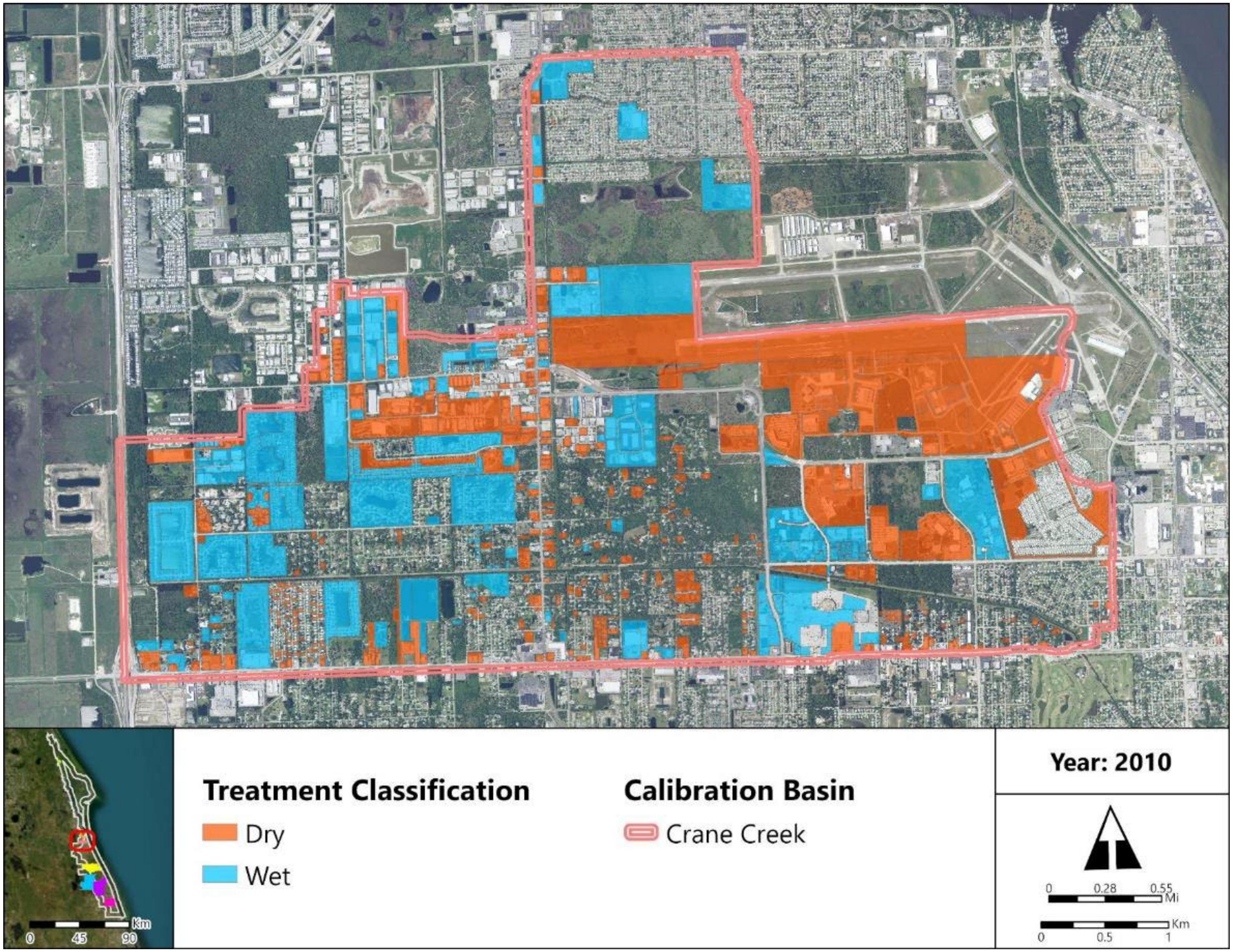

Figure 53. Treatments within the Crane Creek calibration basin for 2010.

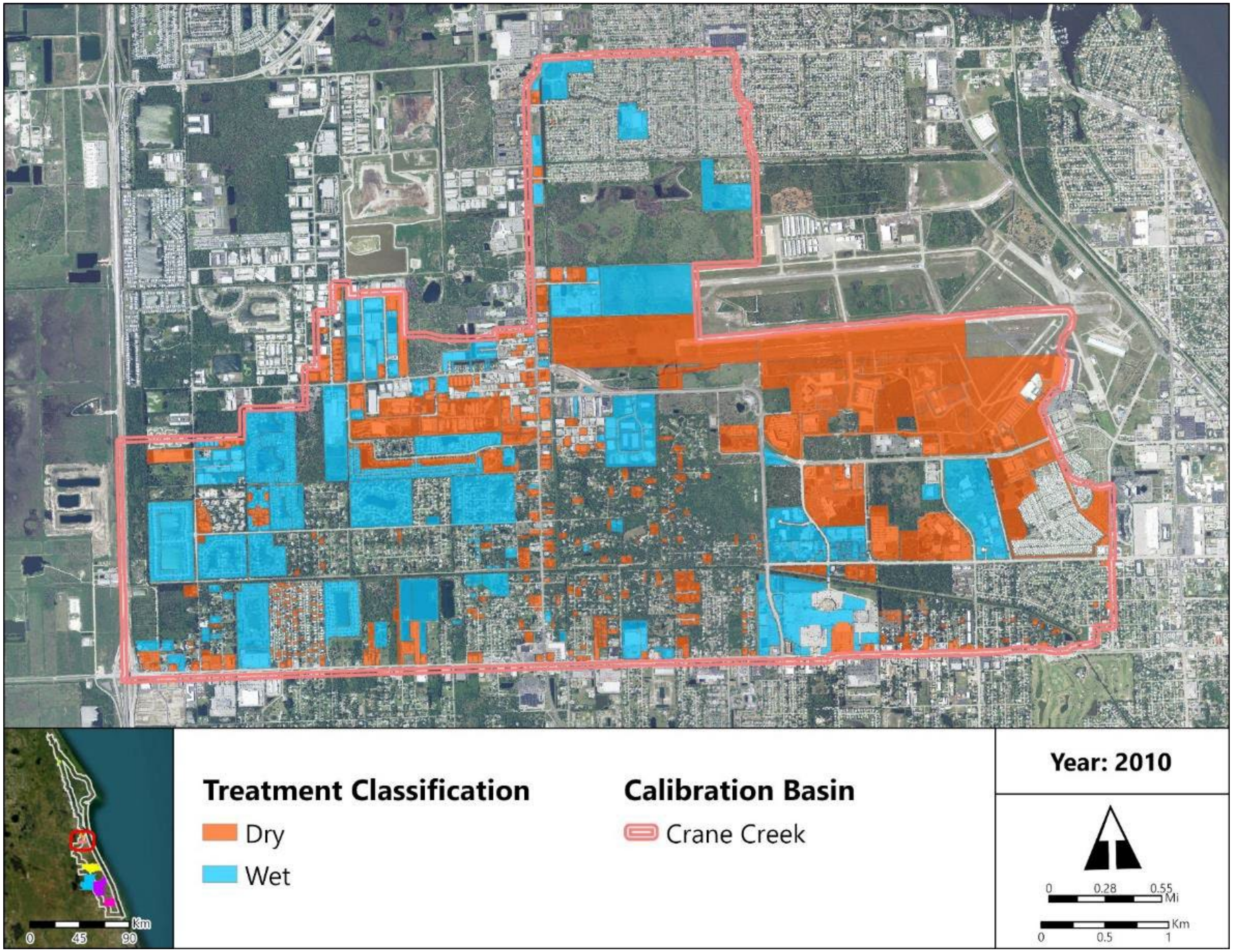

Figure 54. Treatments within the Crane Creek calibration basin for 2015.

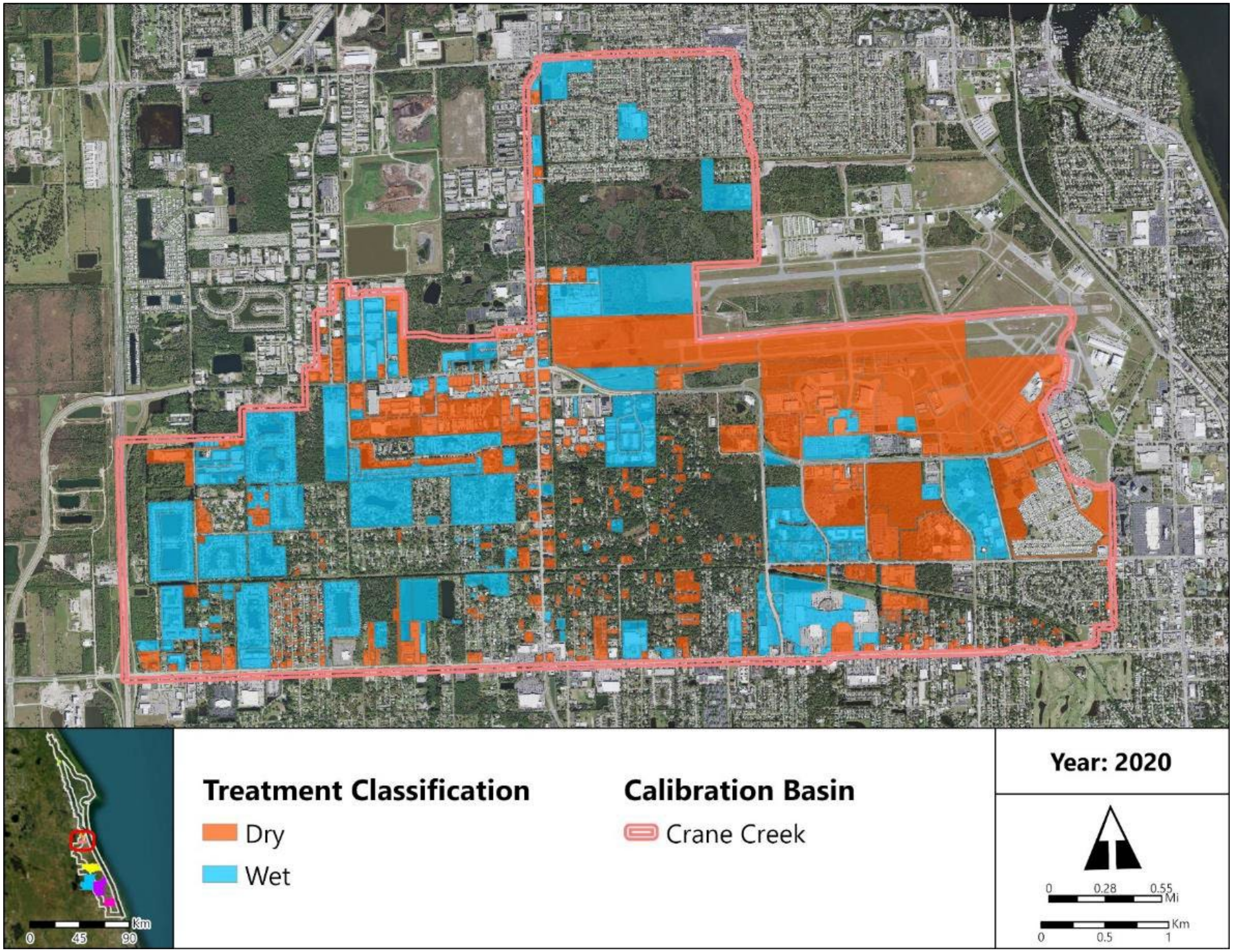

Figure 55. Treatments within the Crane Creek calibration basin for 2020.

2.3.6 Hydrology

The Crane Creek calibration basin volume is dominated by subsurface flow monthly (~81%), seasonally (~83% in the dry and ~78% in the west season), and annually (~80%) from 2010 to 2020. The average monthly volumes are higher from June to October, with lower volumes from November to May for the POR (Figure 57). The 2014, 2016, and 2017 wet seasons showed the highest volumes of discharge, and the lowest seasonal volumes were observed in the 2012 dry season (Figure 58). The greatest annual volumes were observed in 2014, 2016, and 2017 and the lowest volumes were observed in 2012, coinciding with the highest and lowest volumes observed in the seasonal data (Figure 56).

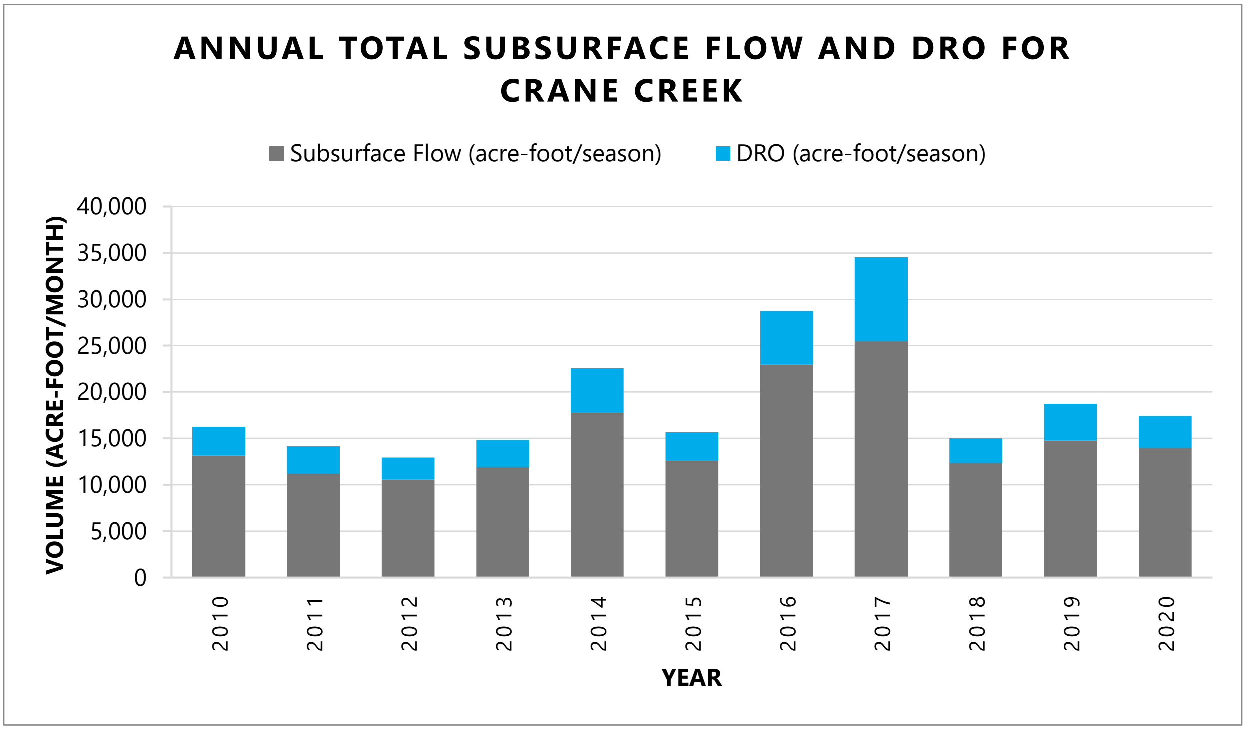

Figure 56. Annual subsurface flow (acre-foot/year) and DRO (acre-foot/year) for the Crane Creek calibration basin derived from USGS WHAT data.

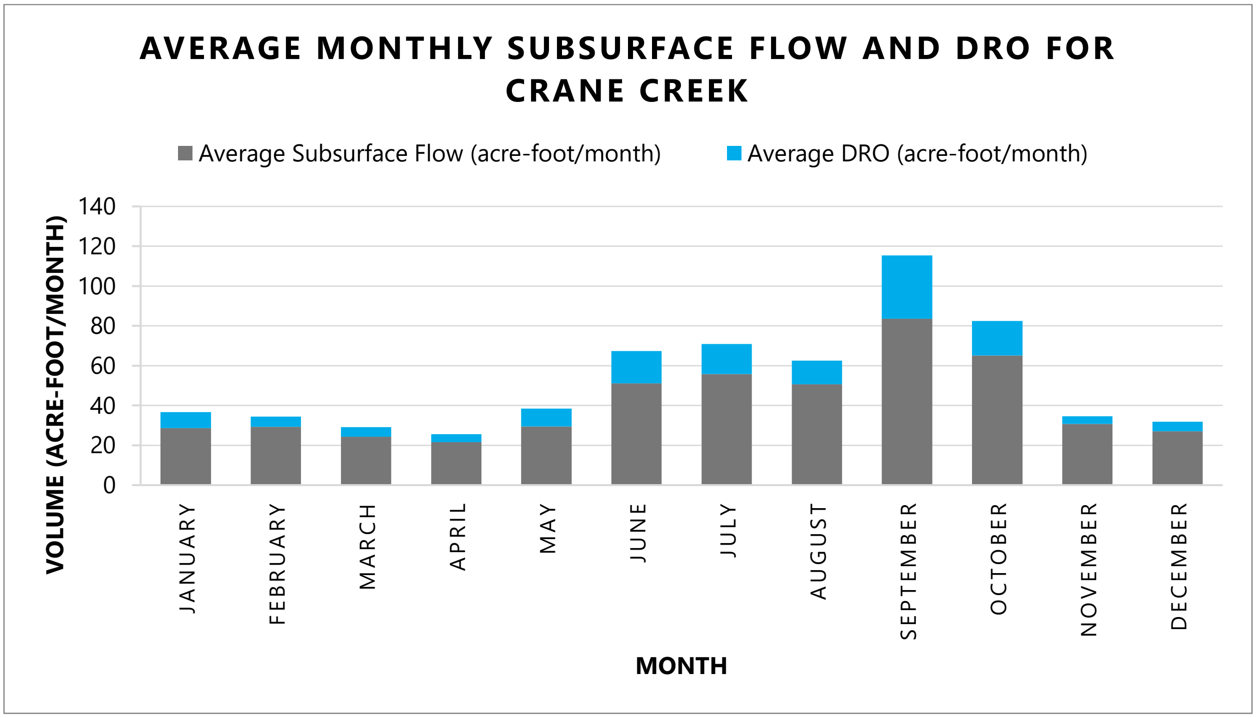

Figure 57. Average monthly subsurface flow (acre-foot/month) and DRO (acre-foot/month) for the Crane Creek calibration basin derived from USGS WHAT data.

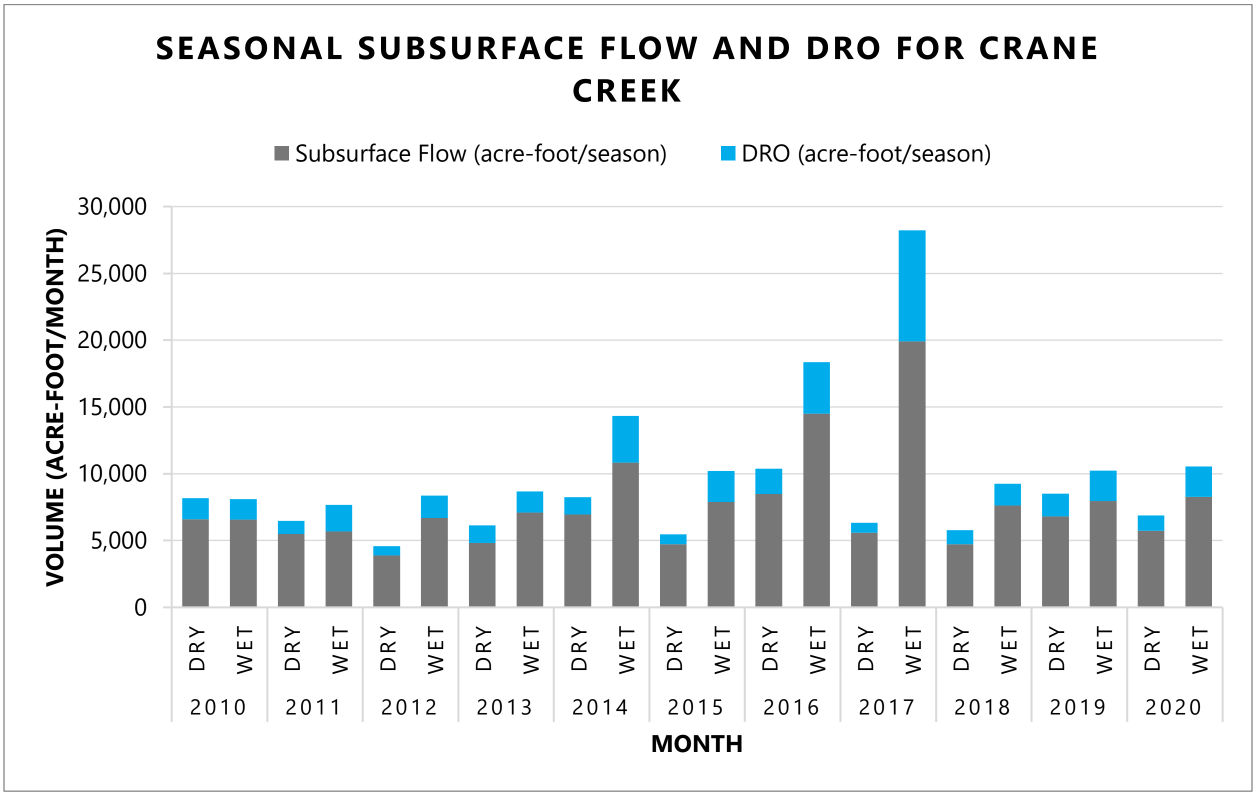

Figure 58. Seasonal subsurface flow (acre-foot/season) and DRO (acre-foot/season) for the Crane Creek calibration basin derived from USGS WHAT data.

2.3.7 Water Quality

From 2010 to 2020, there were a total of 125 samples collected from Crane Creek at CC03 by SJRWMD. No samples coincided with DRO conditions, 76 coincided with subsurface flow conditions, with the remaining 46 under mixed conditions (Table 11). Crane Creek's annual geometric mean subsurface flow concentrations for TN and TP showed two different patterns over the POR, with higher degrees of variability observed in TN concentrations. The annual geometric mean subsurface flow concentration for TP shows little variability from 2010 to 2020, with the concentrations ranging from 0.07 to 0.12 mg/L.

The highest annual geometric means in TN were observed in 2013, 2014, and 2015. There was an overall increasing trend through 2018 before beginning a decreasing trend through 2020 (Figure 60).

When inspecting observed data at a seasonal interval, the overall annual trends also remain consistent (Figure 59). Aside from 2013 and 2014, concentrations in subsurface seasonal geometric means are elevated during the dry season in comparison to the wet season for TN.

Table 11. Geometric means of annual TN (mg/L) and TP (mg/L) subsurface flow and DRO samples collected by SJRWMD from 2010 to 2020 at the Crane Creek station CC03. No samples were collected during DRO conditions.

Year	TN - DRO	TN - DRO	TN - Subsurface flow	TP - Subsurface flow
2010			0.851	0.068
2011			0.783	0.089
2012			0.827	0.084
2013			0.837	0.089
2014			0.909	0.096
2015			0.916	0.097
2016			0.874	0.110
2017			0.905	0.105
2018			0.916	0.117
2019			0.812	0.088
2020			0.768	0.098

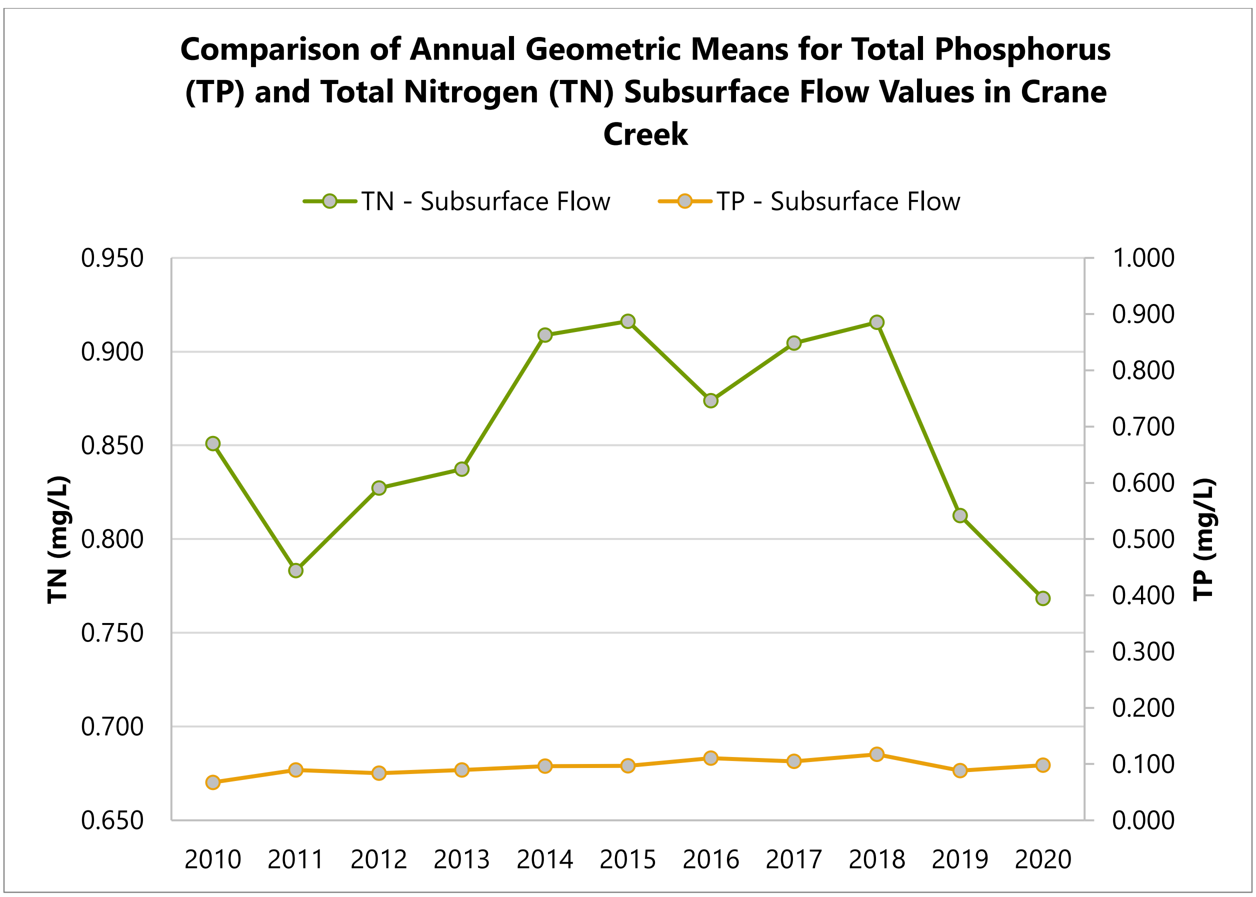

Figure 59. Comparision of the annual geometric means of TN (mg/L) and TP (mg/L) for subsurface between 2010 and 2020 for the Crane Creek calibration basin.

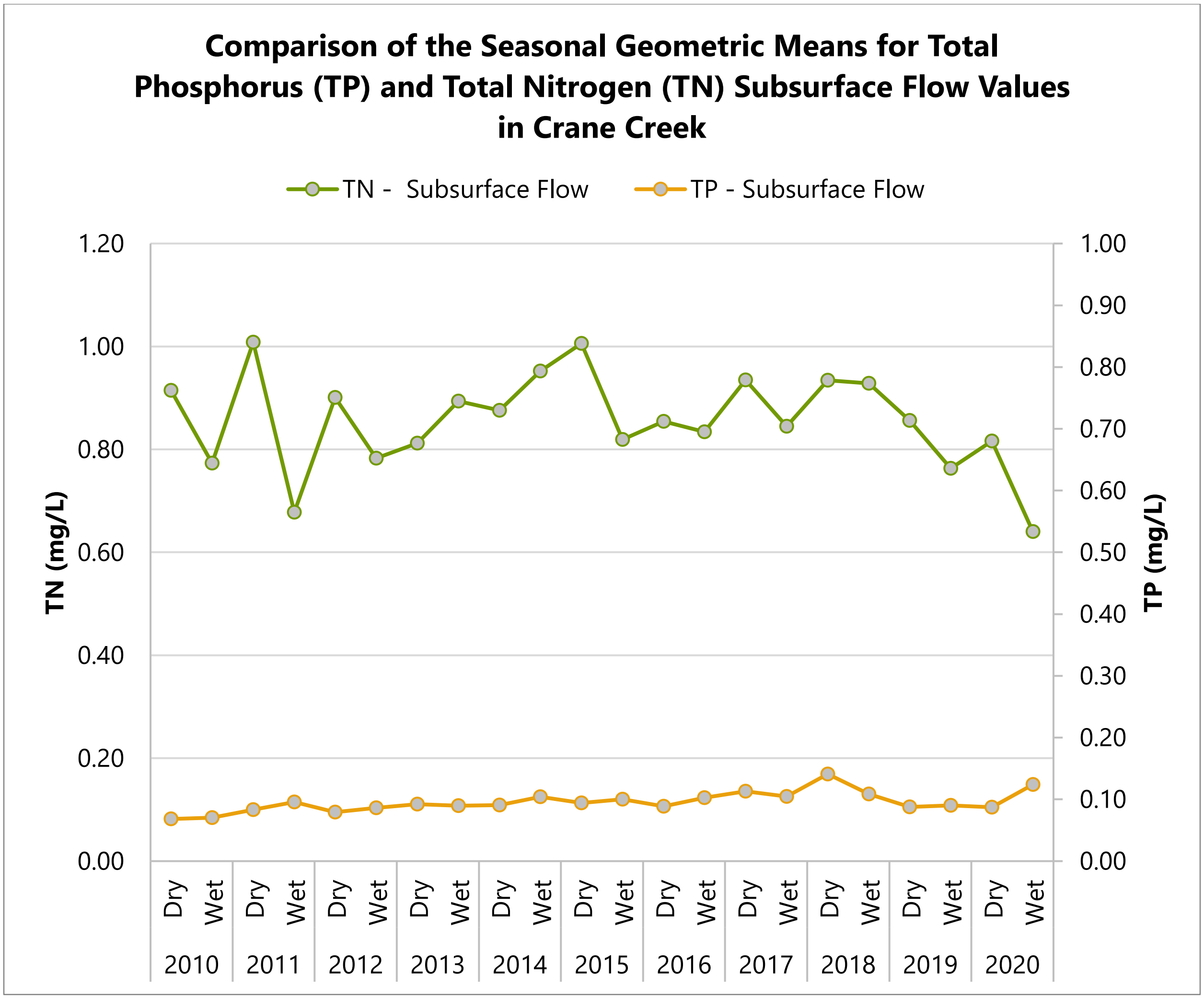

Figure 60. Comparision of the seasonal geometric means of TN (mg/L) and TP (mg/L) for subsurface between 2010 and 2020 for Crane Creek calibration basin.

2.4 Sebastian North Prong (SNP)

2.4.1 LULC Change

The SNP calibration basin is approximately 25,503 acres in sized and has been predominately composed of scrub (~17%), wetland (~14%), wet flatwoods (~12%), improved pasture (~11%), and rangeland (~7%) land use consolidation types (Table 12). Upland and wetlands are widely distributed all throughout the basin, although they are most concentrated along the southern and central areas (Figure 61, Figure 62, Figure 63). Pasture and rangelands are mainly distributed in the northwest corner and center of the basin, while residential areas are located in the northeast corner and larger platted lands are in the west. The residential areas are concentrated in the southwest region of the basin, as well as smaller neighborhoods within the northern and southeast corners. Within the SNP calibration basin, there has been an increase in the rangeland and open land use types as a result of the conversion from citrus fields, most notably in open land areas now occupied by the solar farms in the eastern portion of the basin. A portion of the increases in open lands were also conversions from natural scrub areas.

Table 12. Total area (in acres and percentage) of each land use consolidation type in the SNP calibration basin for the 2010, 2015, and 2020 years.

Land Use Consolidation	Land Use Area (Acres)			Percent of Total Land Use (%)			Percent Change (%)	
	2010	2015	2020	2010	2015	2020	2015-2010	2020-2010
Citrus	**2,072.46**	**1,714.06**	1,049.26	**8.13**	**6.72**	4.11	-1.41	-4.01
Commercial	31.62	31.65	31.65	0.12	0.12	0.12	0.00	0.00
Dry Prairie	732.30	808.97	831.67	2.87	3.17	3.26	0.30	0.39
Field Crop	5.18	--	--	0.02	--	--	--	--
High Density Residential	679.79	690.68	688.50	2.67	2.71	2.70	0.04	0.03
Hydric Hammock	165.18	165.21	165.21	0.65	0.65	0.65	0.00	0.00
Improved Pasture	**2,661.10**	**2,988.45**	**2,573.67**	**10.43**	**11.72**	**10.09**	1.28	-0.34
Industrial	52.77	46.76	49.44	0.21	0.18	0.19	-0.02	-0.01
Institutional	30.45	29.93	37.43	0.12	0.12	0.15	0.00	0.03
Low Density Residential	1,212.78	1,432.71	1,287.78	4.76	5.62	5.05	0.86	0.29
Medium Density Residential	63.52	79.35	82.39	0.25	0.31	0.32	0.06	0.07
Mesic Flatwoods	893.88	957.06	957.06	3.50	3.75	3.75	0.25	0.25
Mining	63.30	--	--	0.25	--	--	--	--
Open	710.87	849.30	1,481.83	2.79	3.33	5.81	0.54	3.02
Other Agriculture	70.54	9.45	9.39	0.28	0.04	0.04	-0.24	-0.24
Rangeland	1,866.38	1,615.23	**2,182.53**	7.32	6.33	**8.56**	-0.98	1.24
Recreational 1	30.14	30.14	30.11	0.12	0.12	0.12	0.00	0.00

Land Use Consolidation	Land Use Area (Acres)			Percent of Total Land Use (%)			Percent Change (%)	
	2010	2015	2020	2010	2015	2020	2015-2010	2020-2010
Recreational 2	56.18	52.73	52.73	0.22	0.21	0.21	-0.01	-0.01
Row Crops	0.12	8.75	8.75	0.00	0.03	0.03	0.03	0.03
Ruderal	--	197.12	197.12	--	0.77	0.77	--	--
Scrub	**4,699.76**	**4,217.00**	**4,194.66**	**18.43**	**16.54**	**16.45**	-1.89	-1.98
Transportation	106.49	106.48	106.48	0.42	0.42	0.42	0.00	0.00
Upland Flatwoods	910.82	881.45	871.39	3.57	3.46	3.42	-0.12	-0.15
Water	797.11	791.68	856.94	3.13	3.10	3.36	-0.02	0.23
Wet Flatwoods	**3,035.81**	**3,220.14**	**3,215.07**	**11.90**	**12.63**	**12.61**	0.72	0.70
Wet Prairies	795.56	618.60	617.97	3.12	2.43	2.42	-0.69	-0.70
Wetland	**3,514.88**	**3,766.85**	**3,730.75**	**13.78**	**14.77**	**14.63**	0.99	0.85
Xeric Hammock	244.18	193.40	193.40	0.96	0.76	0.76	-0.20	-0.20

The top five land uses that make up a majority of the area have been bolded for each year. Percent change from the overall area between 2010 and 2015, as well as 2010 and 2020 have also been provided.

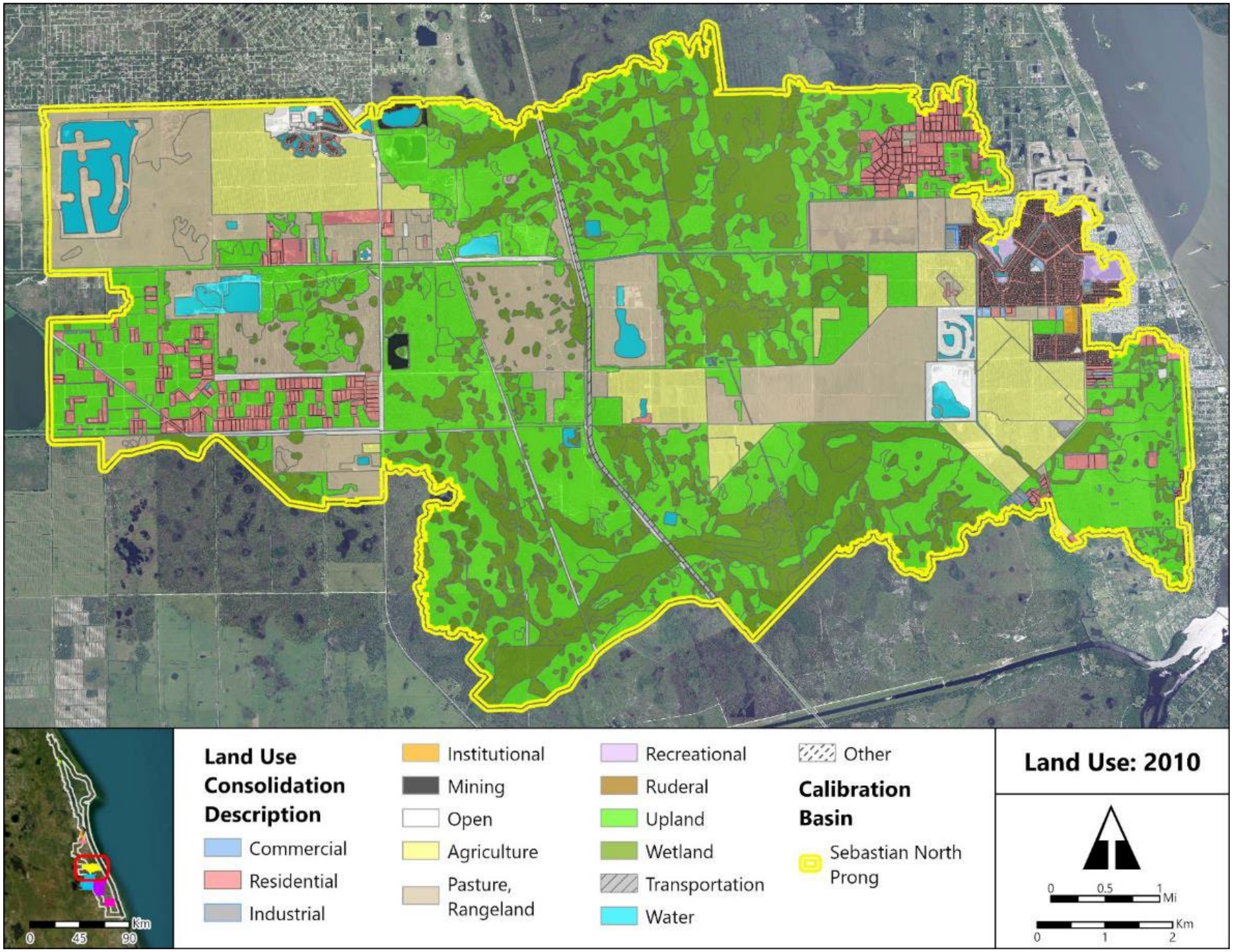

Figure 61. Land use within the SNP calibration basin for 2010.

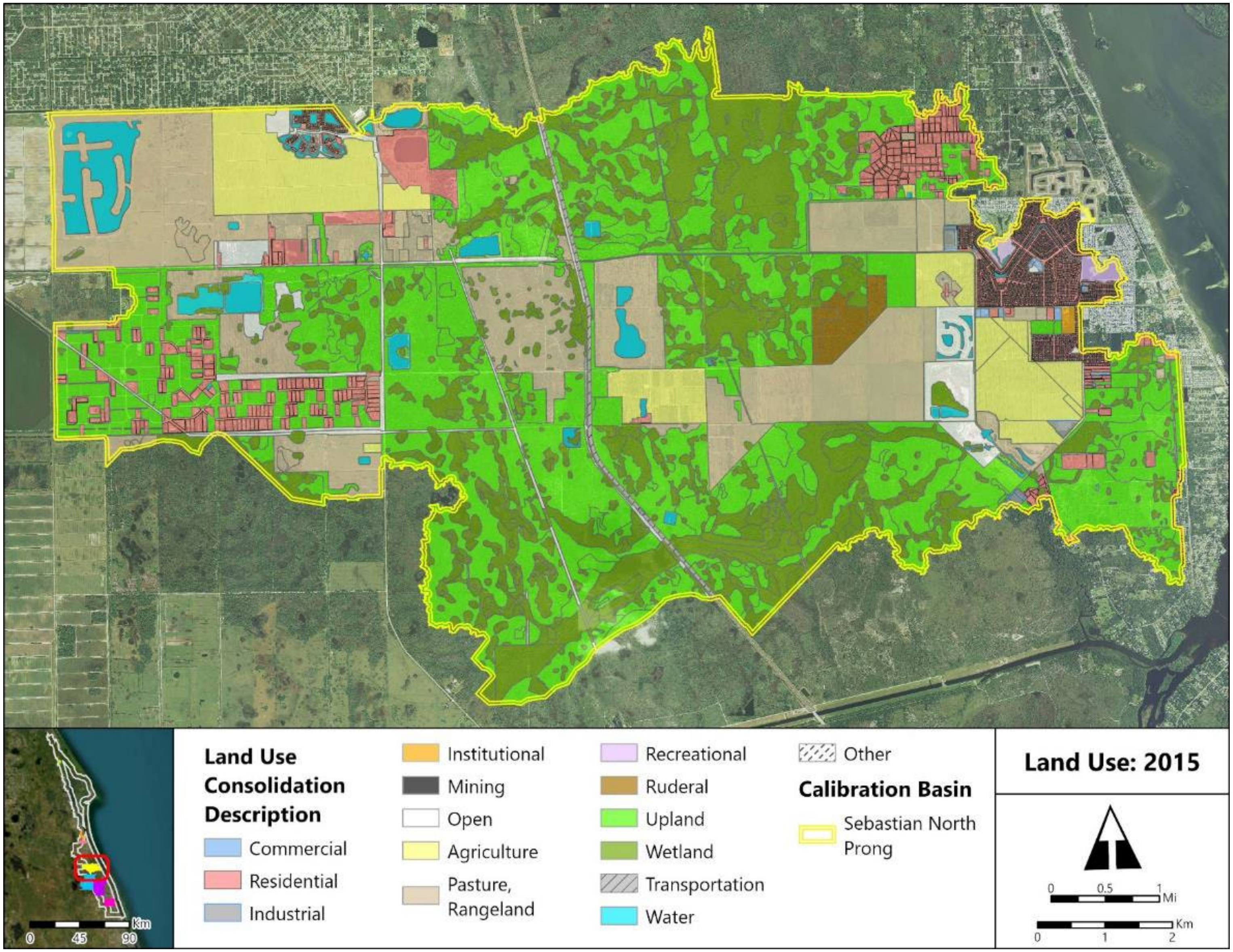

Figure 62. Land use within the SNP calibration basin for 2015.

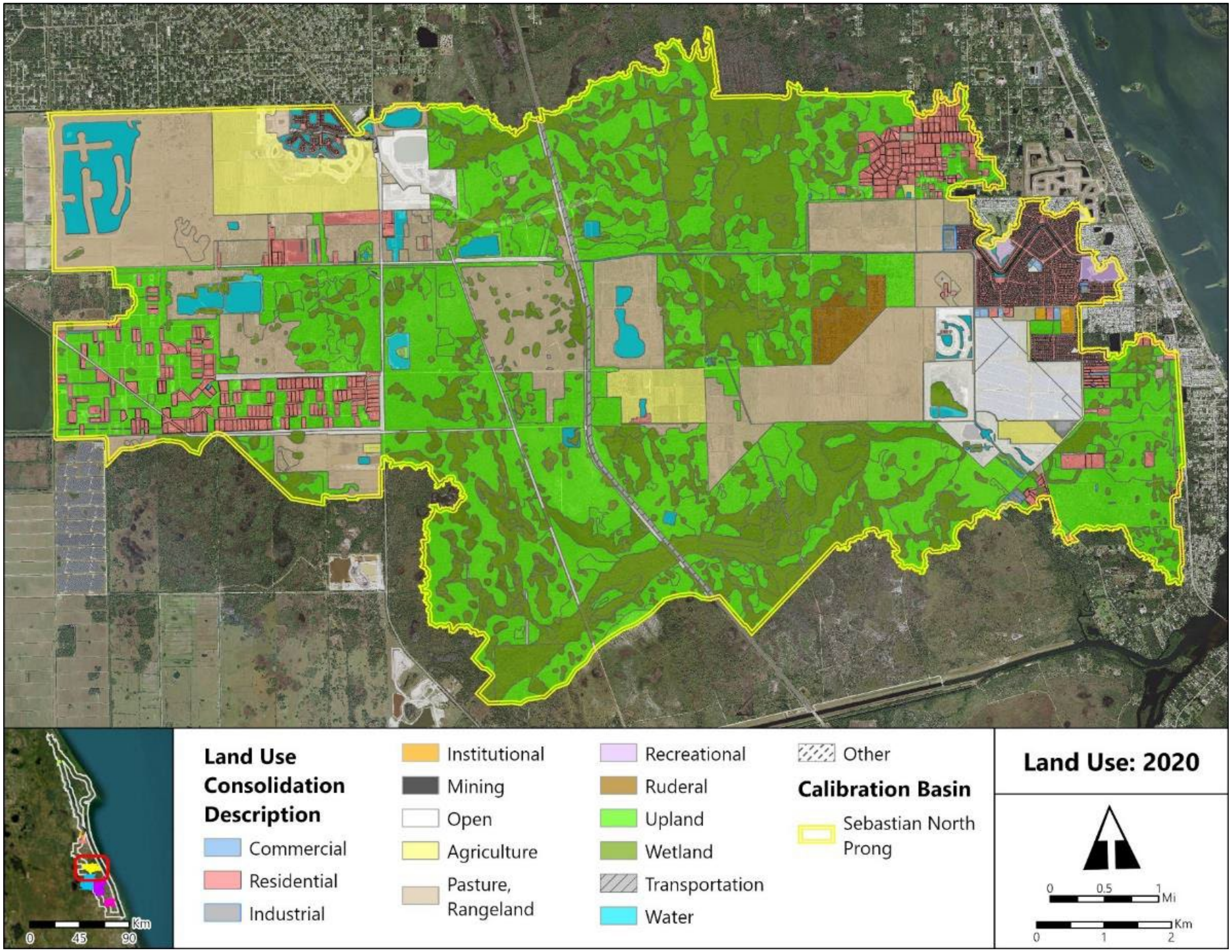

Figure 63. Land use within the SNP calibration basin for 2020.

2.4.2 Soil Hydrologic Group

The SNP calibration basin is primarily composed of the A/D (51%) and C/D (36%) hydrologic soil groups, followed by A (8%) and B/D (5%) soils, and water making up less than 1% of the total area (Figure 64). The C/D soils are located in the western portion of the basin with a large band that is centrally distributed (Figure 65). The A soil hydrologic group also has a vertical band in the center of the basin, as well as a large area in the southeast corner of the basin. The A/D soils fill in a majority of the remaining area, with smaller patches of B/D distributed throughout.

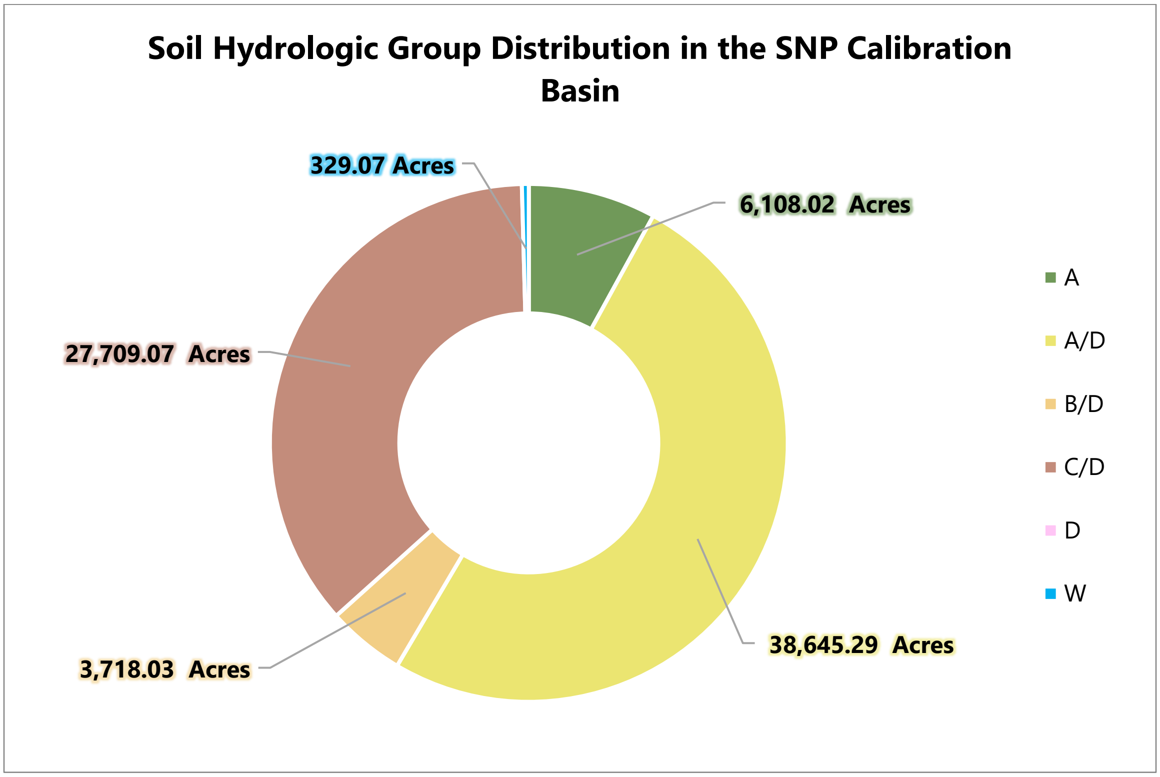

Figure 64. Pie chart (acres) of the soil hydrologic group distribution in the SNP calibration basin using USDA NRCS data.

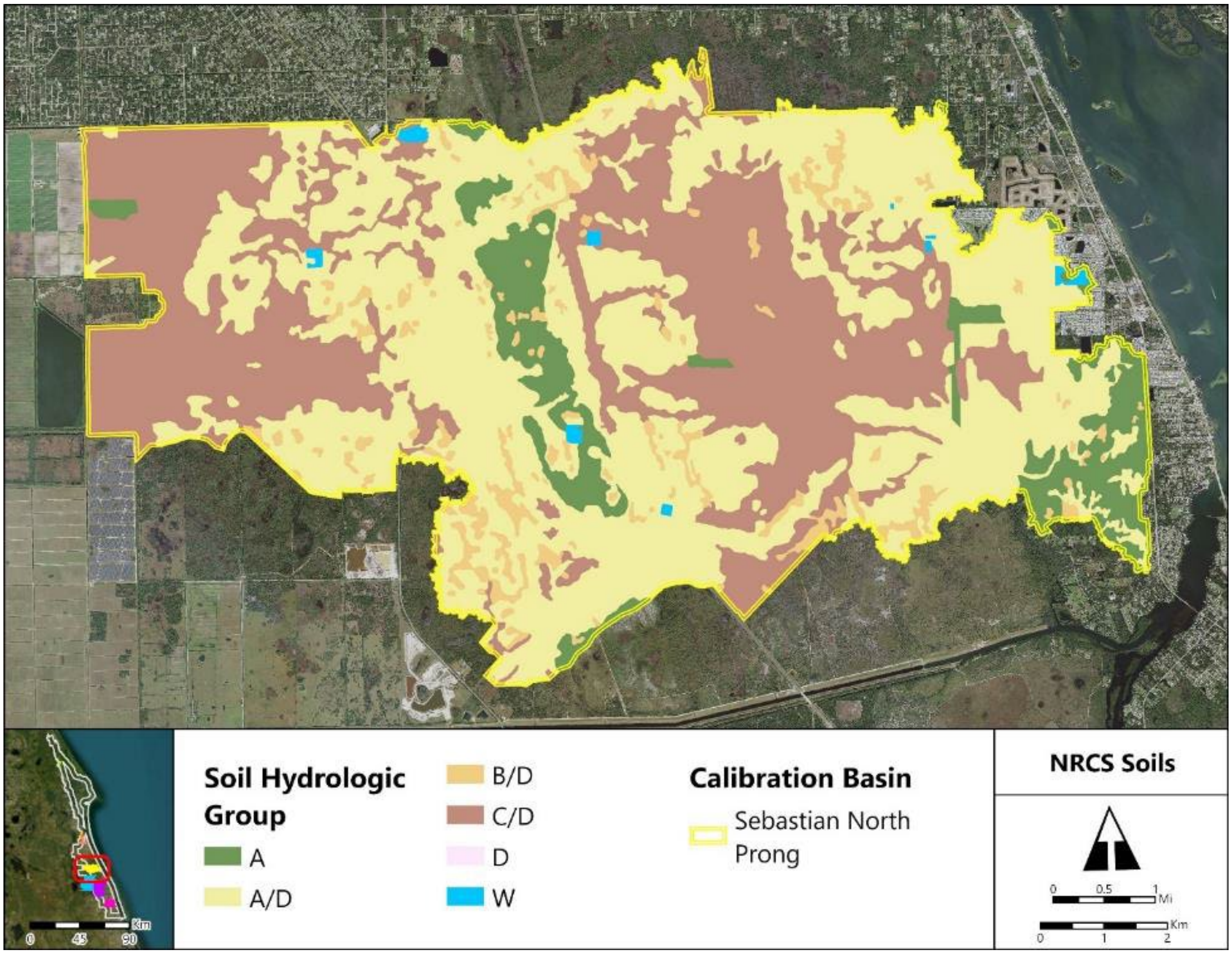

Figure 65. Distribution of soil hydrologic groups within the SNP calibration basin.

2.4.3 PRECIPITATION

The annual total precipitation for SNP ranges from the lowest annual total of 21 inches in 2010 to the highest annual total of 68 inches in 2017 (Figure 66). For all years, with the exception of 2018, the dry season has a lower total seasonal rainfall as compared to the wet seasons of the same years (Figure 67). The average monthly precipitation values are higher from May to October and lower from November to April (Figure 68). Maps for the monthly precipitation averages (inches/month) for February and September across the POR within the SNP are provided in Figure 69 and Figure 70, respectively.

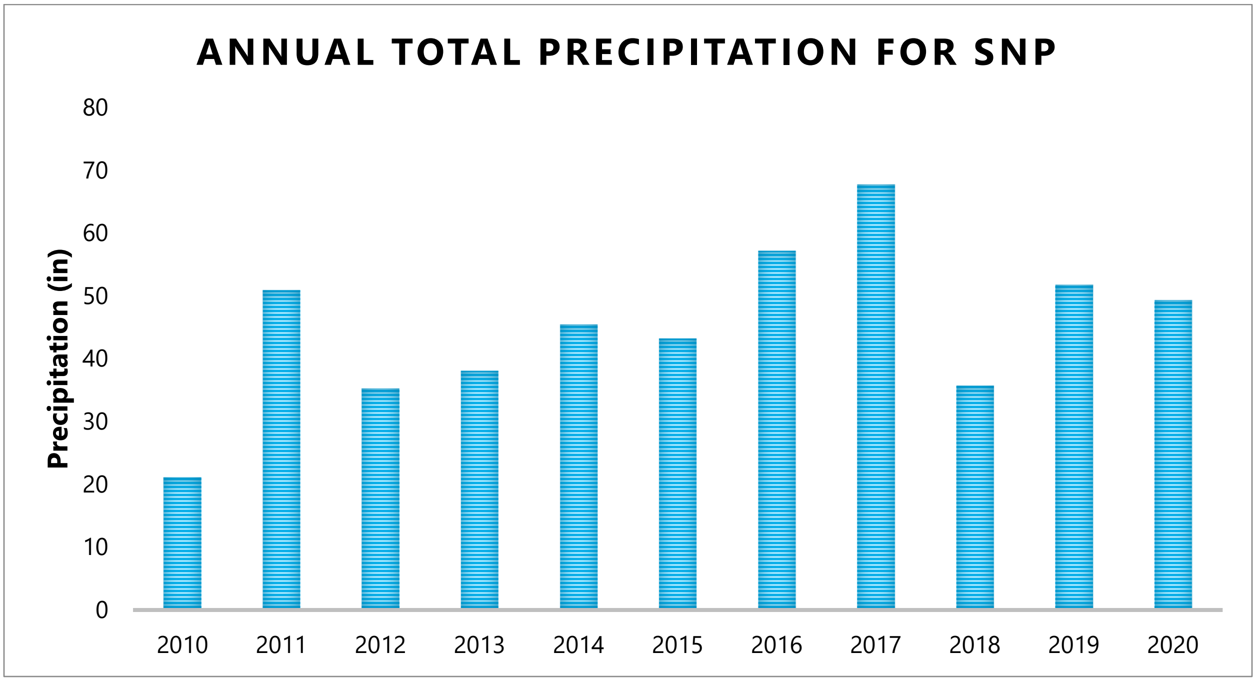

Figure 66. Annual total precipitation (in) for the SNP calibration basin from 2010 to 2020 derived from SJRWMD NEXRAD data.

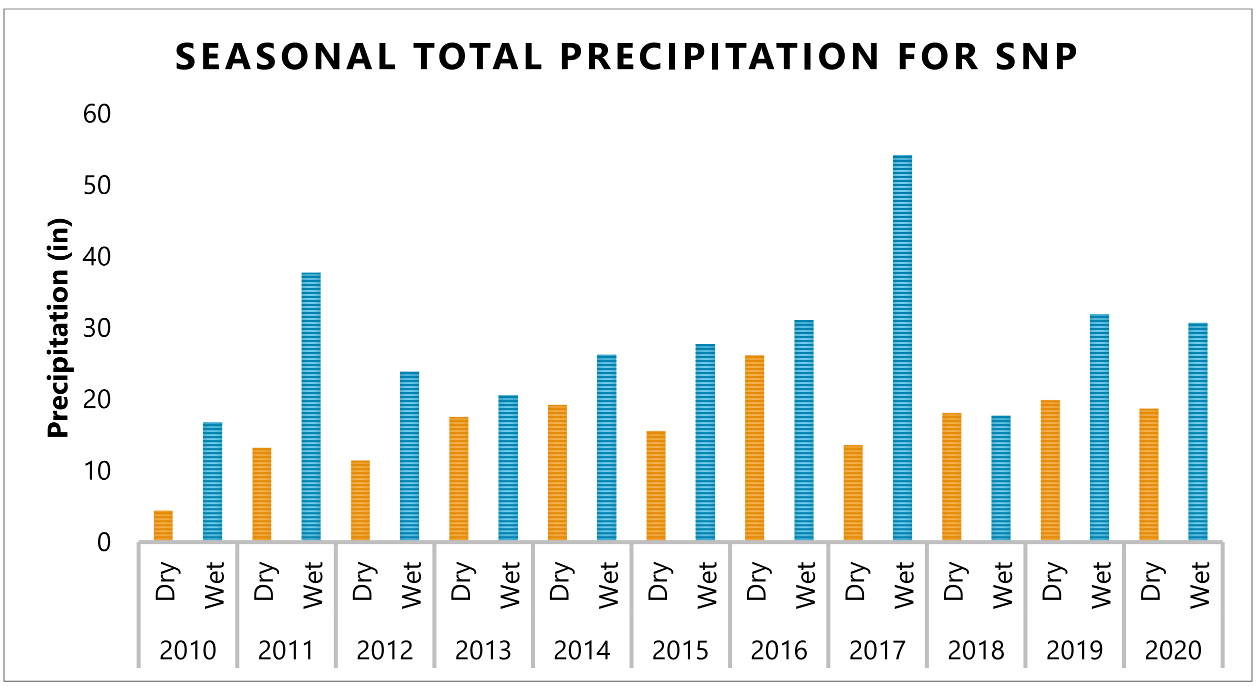

Figure 67. Seasonal total precipitation (in) for the SNP calibration basin from 2010 to 2020 derived from SJRWMD NEXRAD data.

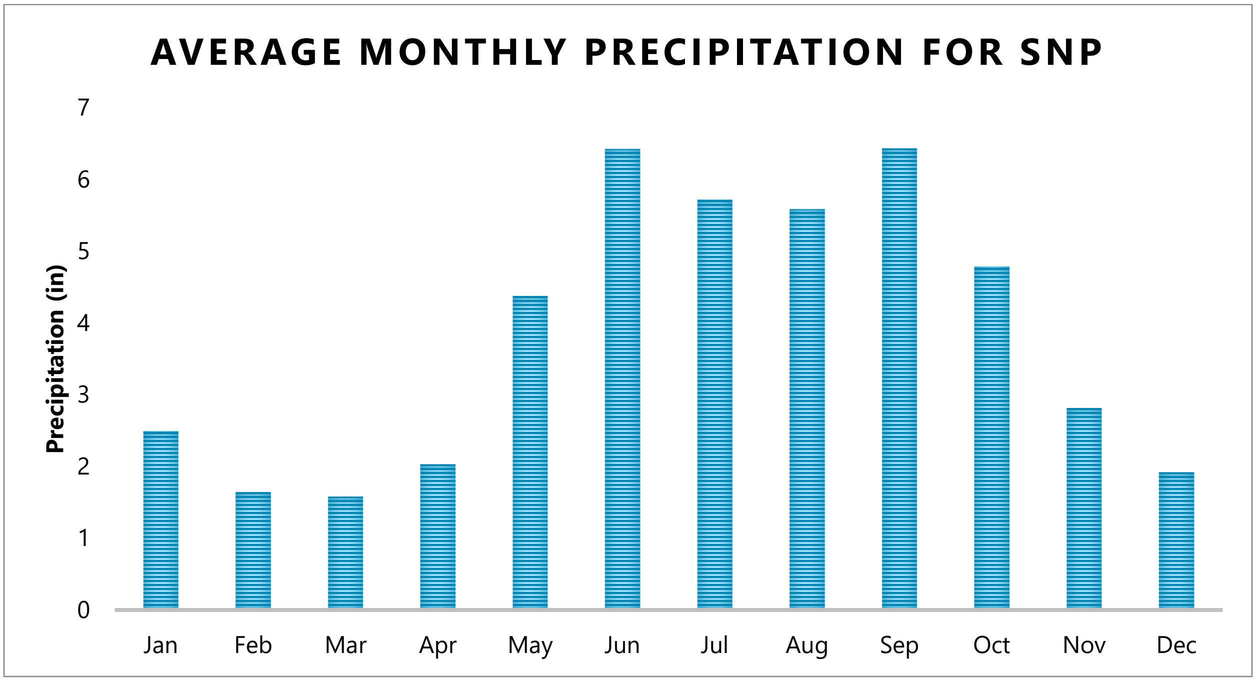

Figure 68. Average monthly precipitation (in) for the SNP calibration basin derived from SJRWMD NEXRAD data.

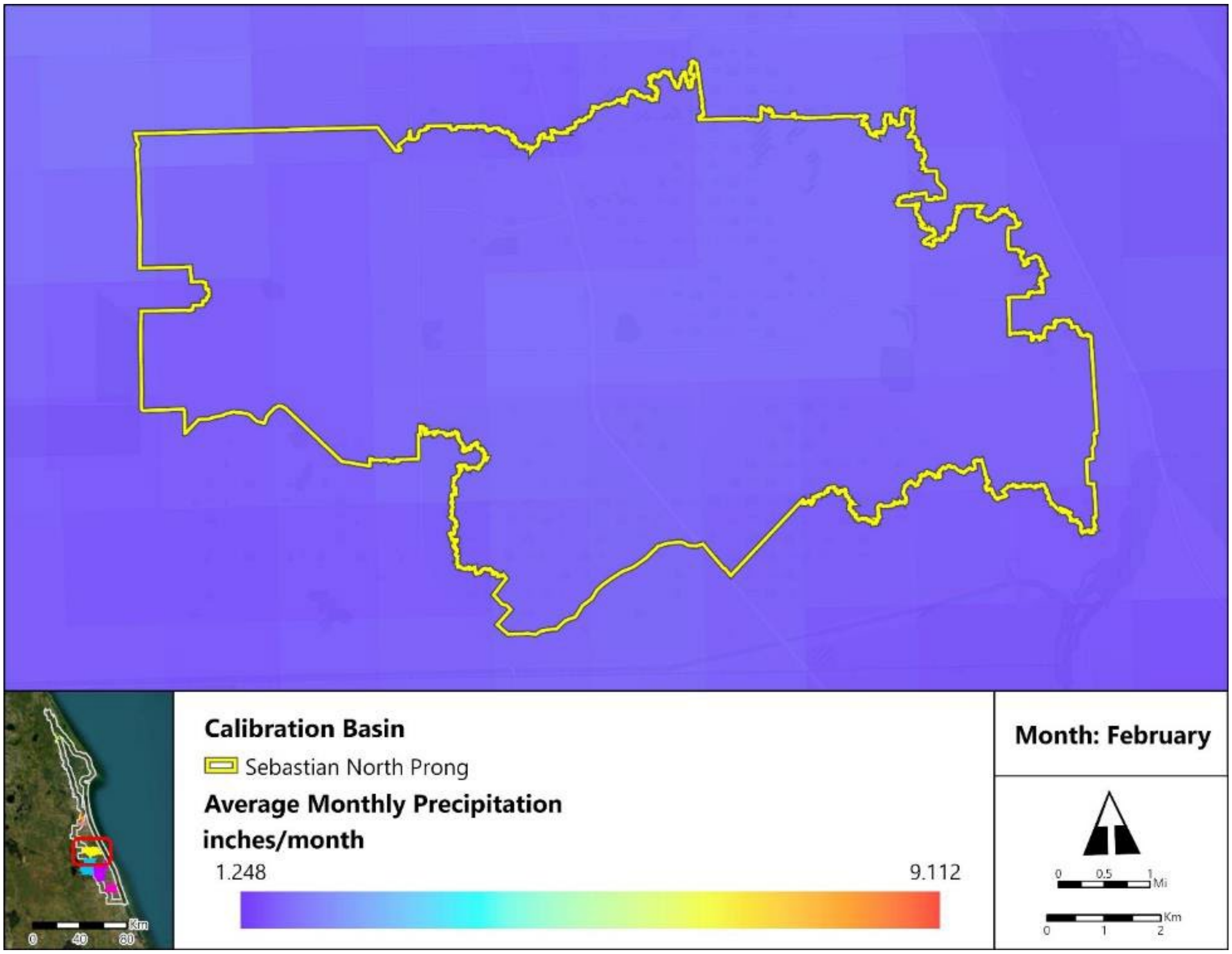

Figure 69. Average monthly precipitation (inches/month) for February across the period of record in the SNP calibration basin.

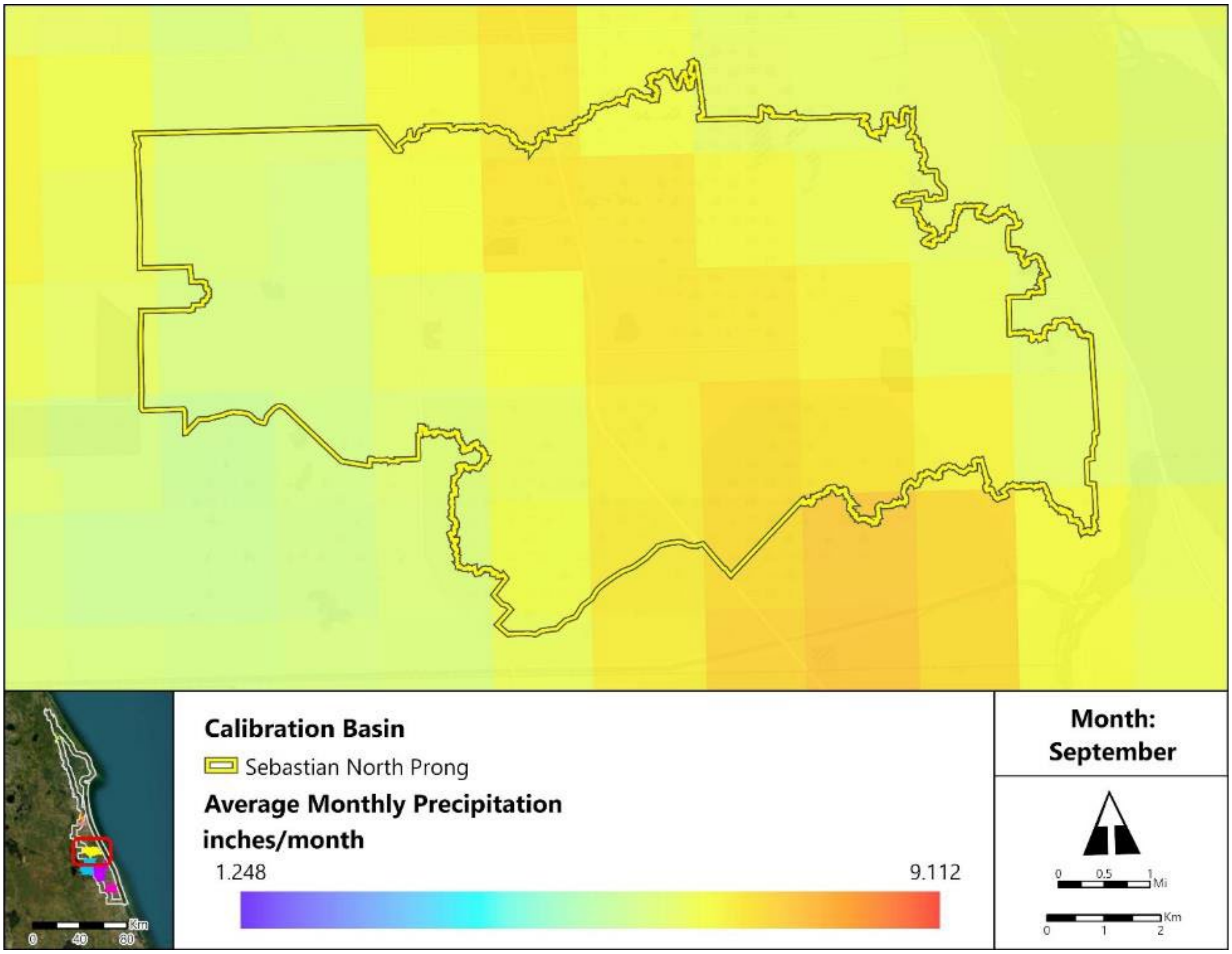

Figure 70. Average monthly precipitation (inches/month) for September across the period of record in the SNP calibration basin.

2.4.4 ET

Summary statistics for the monthly mean ET in the SNP calibration basin are provided as a boxplot (Figure 71). For SNP, there is a distinct difference in the wet and dry seasonal ET rates, as increasing rates are observed through the wet season and decrease in the dry season. The lowest median value and lowest variability in ET rates are seen in the dry season, where there are generally lower temperatures. The greatest median value and highest variability in ET rates are seen in the wet season, where there are generally higher temperatures. The lowest median value was observed in January (1.25 mm/day), whereas the highest median was observed in July (3.01 mm/day). The highest variability was observed in June, with a 0.73 mm/day difference in the interquartile range, and the lowest variability was observed in November, with a 0.18 mm/day difference within the interquartile range. Maps for mean monthly ET rates (mm/day) during February and September across the POR in the SNP calibration basin are provided in Figure 72 and Figure 73, respectively.

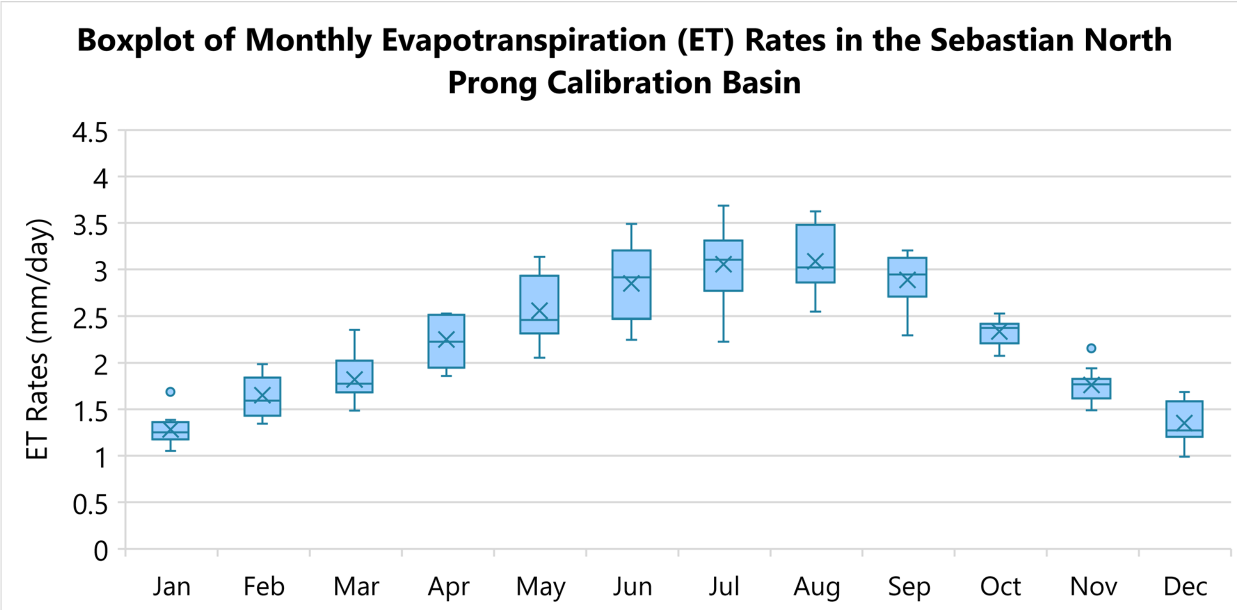

Figure 71. Boxplot of monthly mean ET rates in the SNP calibration basin.

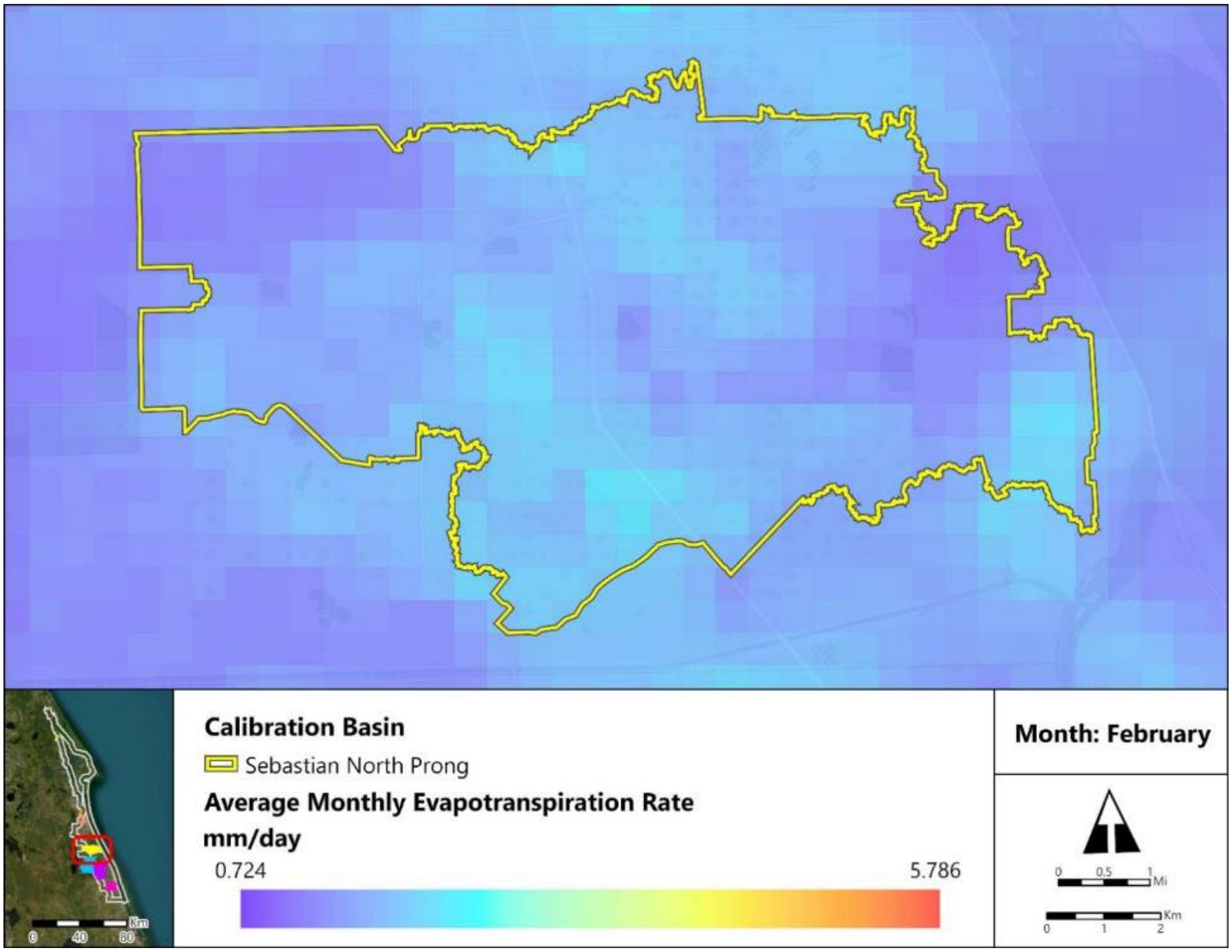

Figure 72. Average monthly ET rates (mm/day) for February across the period of record in the SNP calibration basin.

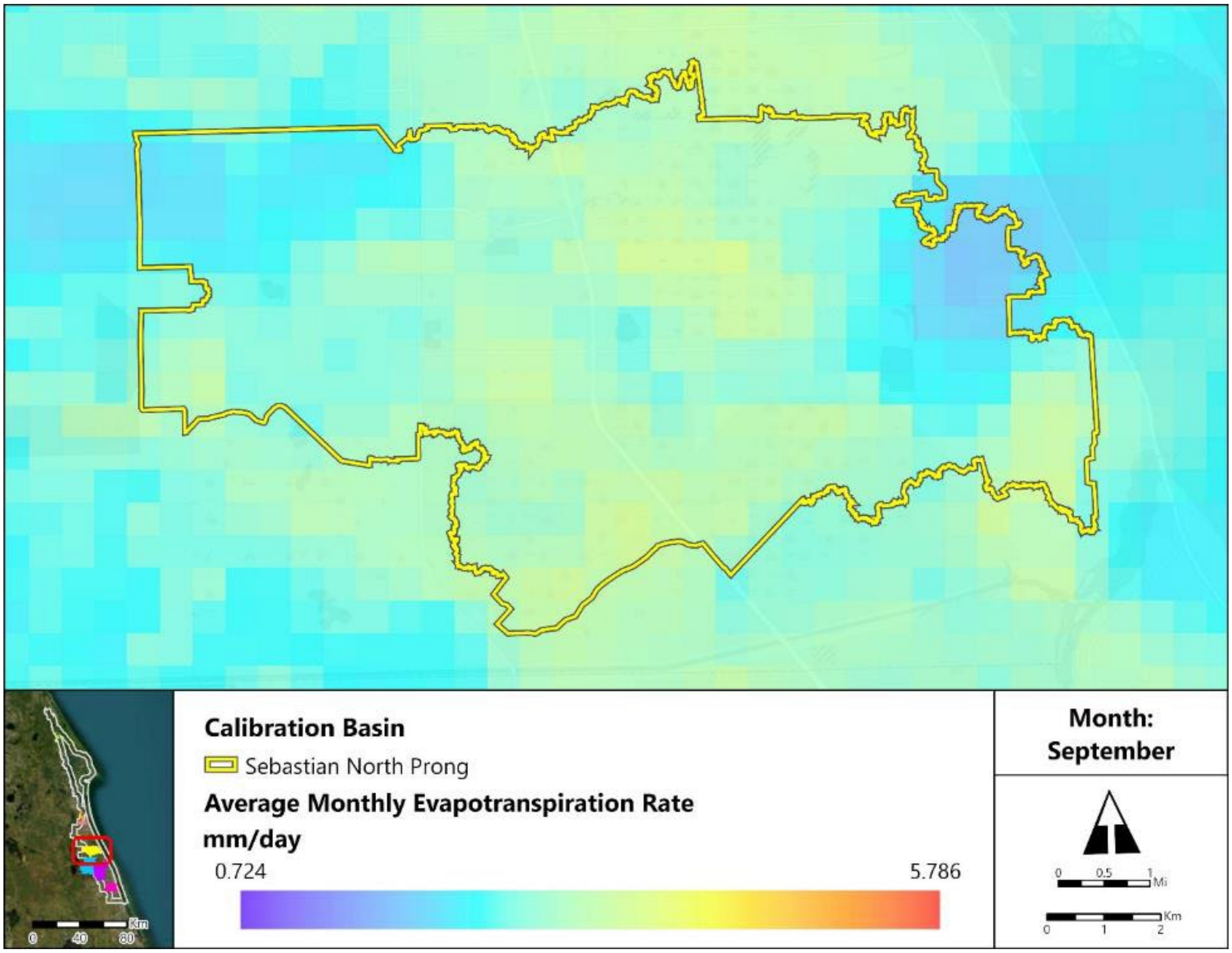

Figure 73. Average monthly ET rates (mm/day) for September across the period of record in the SNP calibration basin.

2.4.5 TREATMENTS

Within SNP, approximately 20% of the calibration basin's total area is treated (Table 13), with almost all of the treatments being composed of the wet type (20%). Overall, the largest changes occurred between 2010 and 2020, with approximately a 3% increase in the treated area, likely a result of increases in residential land use types (Figure 74, Figure 75, Figure 76).

Table 13. Total area (acres) of each treatment type in the SNP calibration basin for the 2010, 2015, and 2020 years.

Treatment Type	Treatment Area (Acres)			Percent of Total Basin Area (%)			Percent Change (%)	
	2010	2015	2020	2010	2015	2020	2015-2010	2020-2010
Dry	35.11	32.06	32.06	0.14	0.13	0.13	-0.01	-0.01
Wet	4,767.71	4,833.50	5,590.59	18.69	18.95	21.92	0.26	3.23
Total	*4,802.82*	*4,865.56*	*5,622.65*	*18.83*	*19.08*	*22.05*	*0.25*	*3.22*

**The percentage of the total basin area and the percent change from the overall area between 2010 and 2015, as well as 2010 and 2020 have also been provided.*

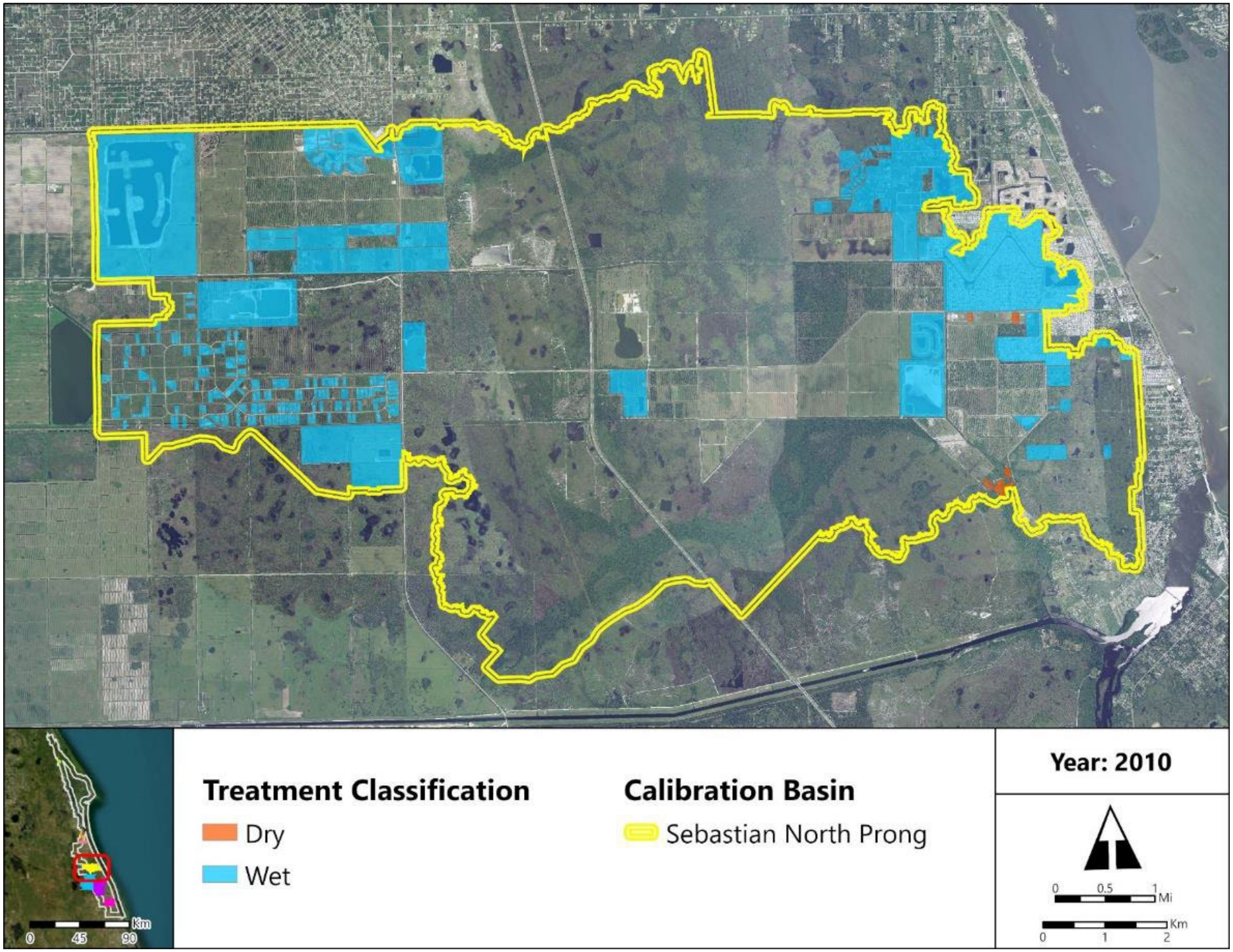

Figure 74. Treatments within the SNP calibration basin for 2010.

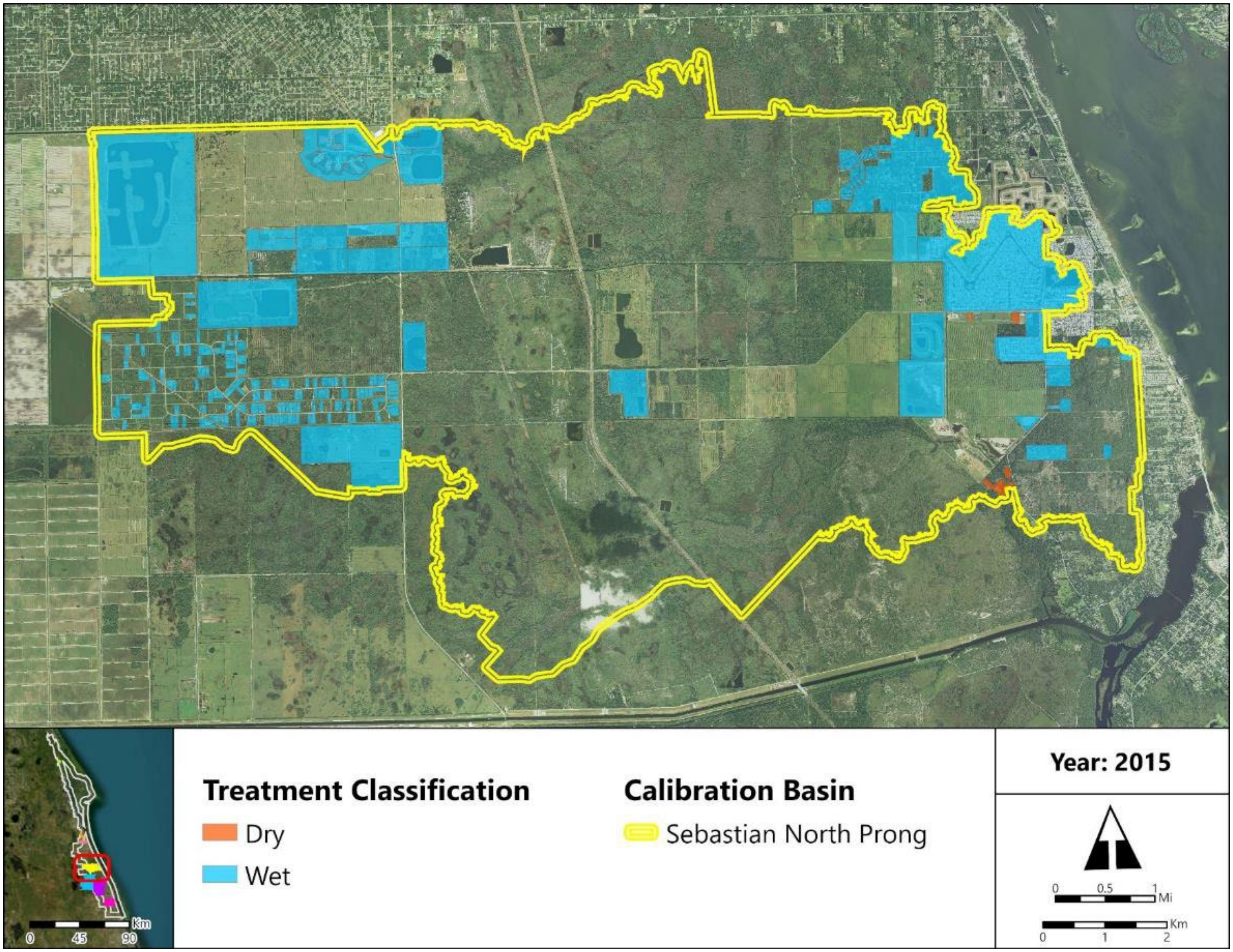

Figure 75. Treatments within the SNP calibration basin for 2015.

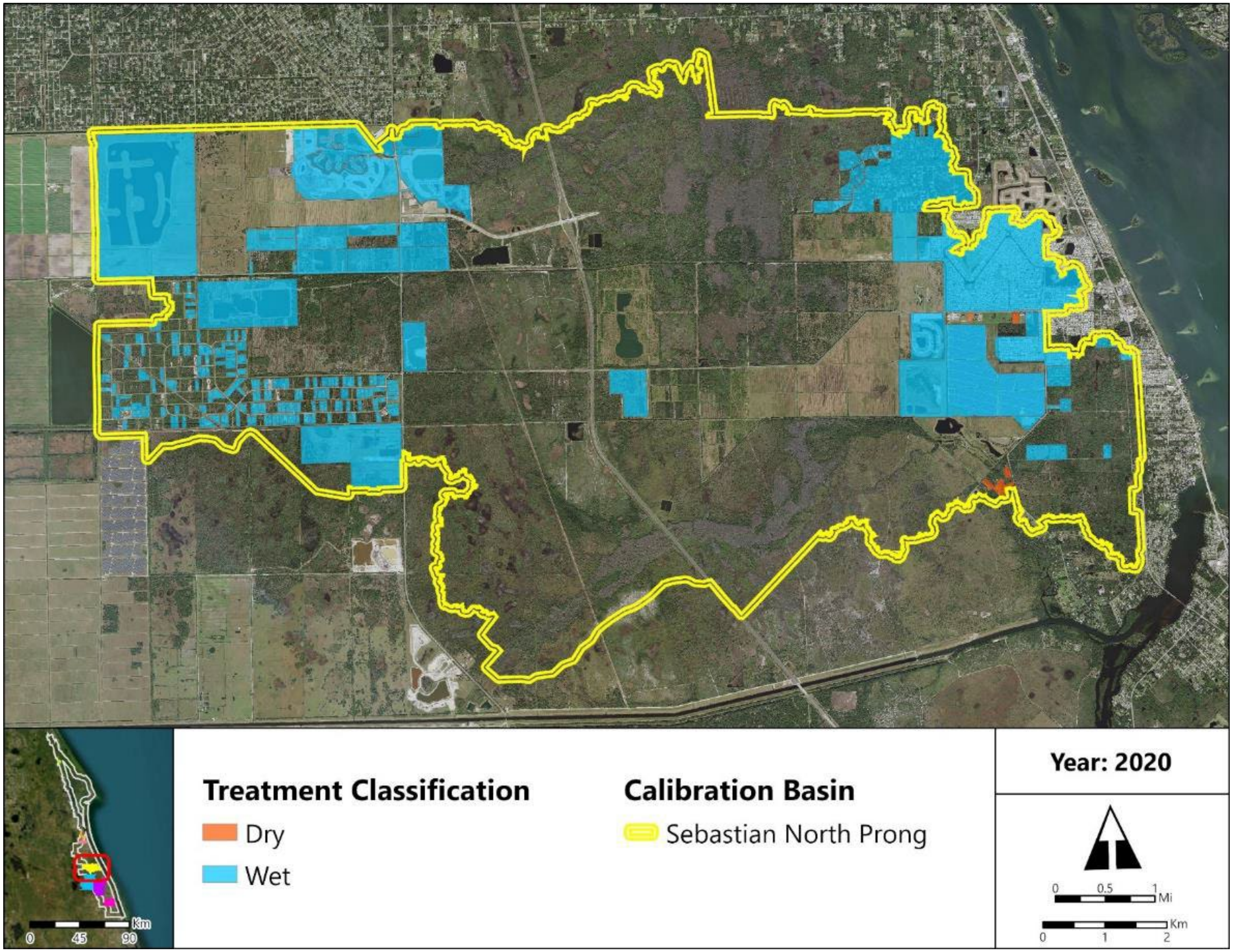

Figure 76. Treatments within the SNP calibration basin for 2020

2.4.6 Hydrology

The SNP calibration basin volume is dominated by subsurface flow monthly (~77%), seasonally (~81% in the dry season and ~74% in the wet season), and annually (76%) from 2010 to 2020. The average monthly volumes are higher from June to November, with lower volumes from December to May for the POR (Figure 79). The 2017 wet season showed the highest volumes of discharge, and the lowest seasonal volumes were observed in the 2010 dry season (Figure 78). The greatest annual volumes were observed in 2016 and 2017, and the lowest volumes were observed in 2012 (Figure 77).

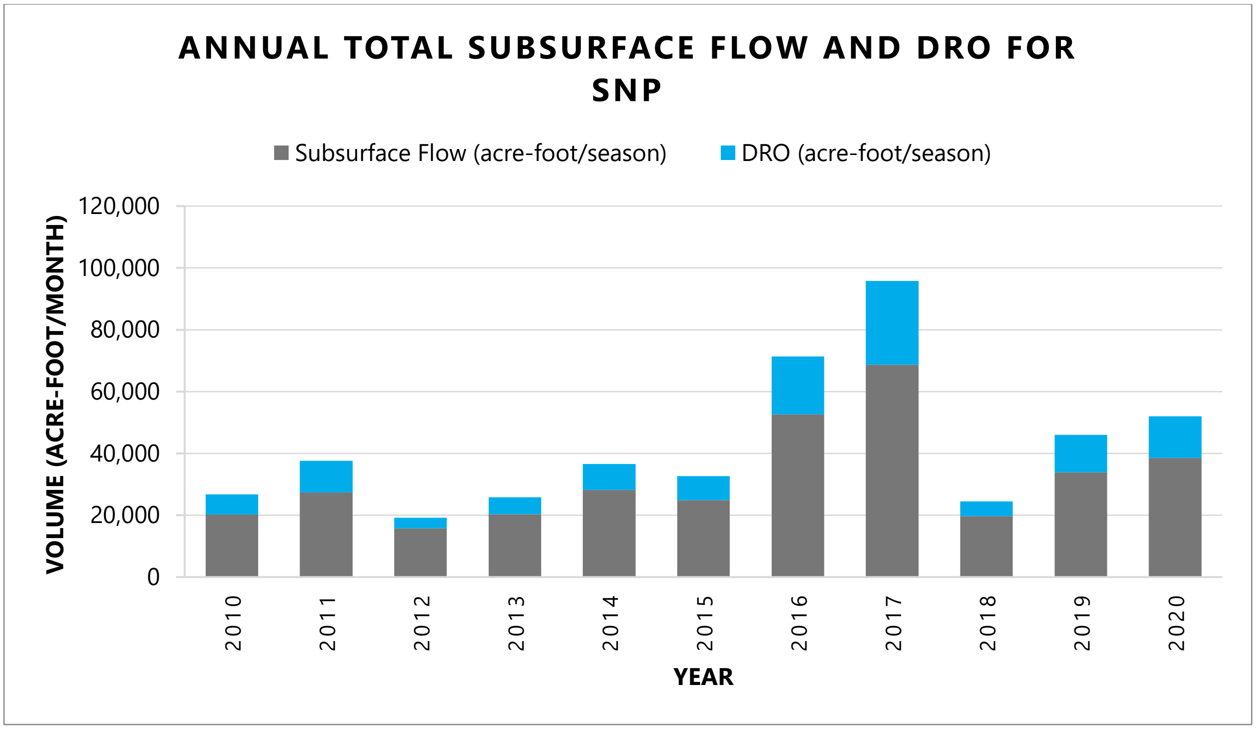

Figure 77. Annual subsurface flow (acre-foot/year) and DRO (acre-foot/year) for the SNP calibration basin derived from USGS WHAT data.

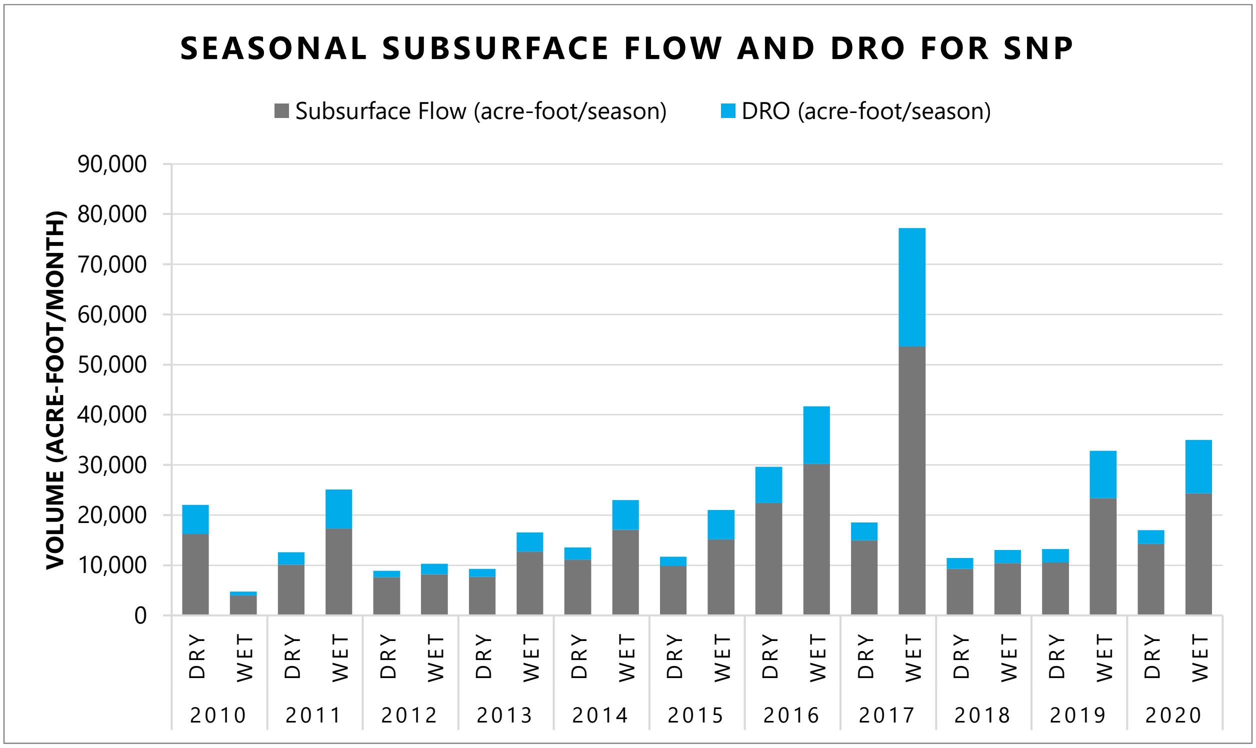

Figure 78. Seasonal subsurface flow (acre-foot/season) and DRO (acre-foot/season) for the SNP calibration basin derived from USGS WHAT data.

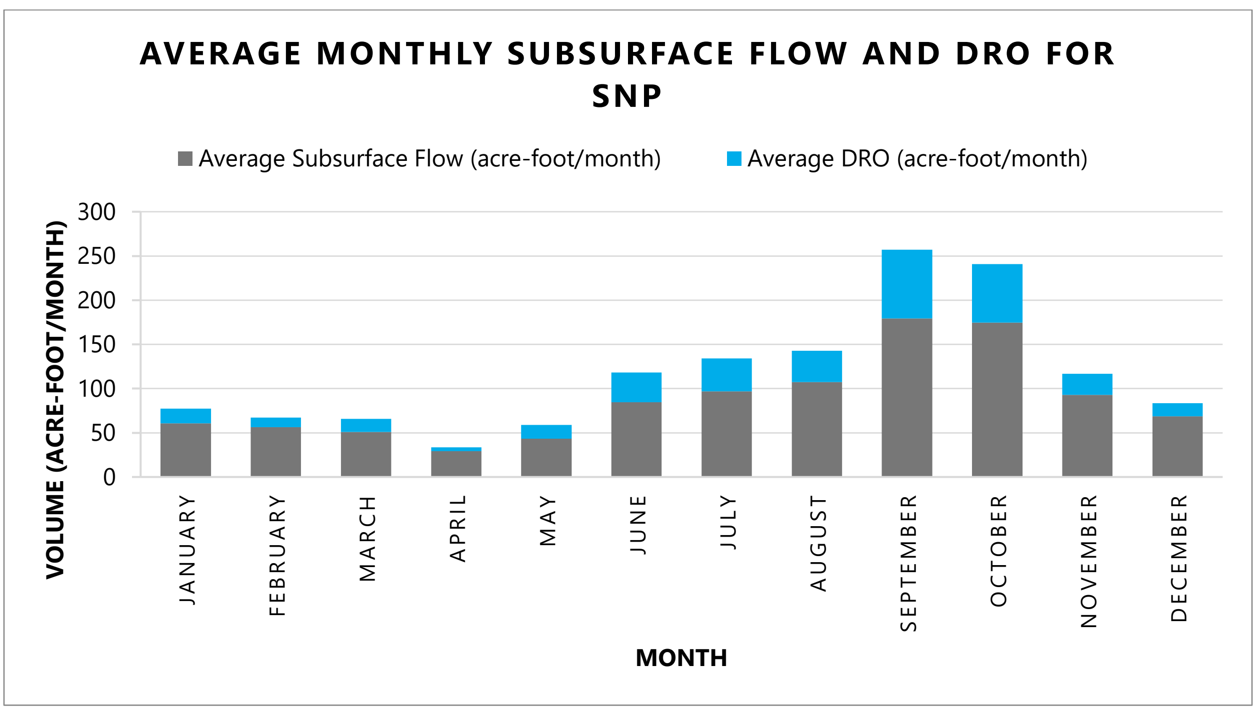

Figure 79. Average monthly subsurface flow (acre-foot/month) and DRO (acre-foot/month) for the SNP calibration basin derived from USGS WHAT data.

2.4.7 WATER QUALITY

From 2011 to 2020, there were a total of 112 samples collected from SNP at IRLSEBNP by SJRWMD; no samples were collected during 2010. Two samples coincided with DRO conditions, 81 coincided with subsurface flow conditions, and the remaining 29 were under mixed conditions (Table 14). As there are only two data points in 2011 and 2020, annual and seasonal trends in DRO concentrations for either nutrient are ineligible for interpretation.

In general, there is a higher degree of variability in geometric means for TN subsurface flow in comparison to TP (Figure 80). However, their respective time series showed similar trend patterns across the POR, with a decrease in concentrations observed from 2011 through 2013 and an increase in concentrations in 2014, followed by a general decrease in concentrations from 2015 through 2020. The highest geometric mean concentrations for both TN and TP were observed during 2011 and 2014.

Table 14. Geometric means of annual TN (mg/L) and TP (mg/L) subsurface flow and DRO samples collected by SJRWMD from 2010 to 2020 at the SNP station IRLSEBNP.

Year	TN - DRO	TP - DRO	TN - Subsurface flow	TP - Subsurface flow
2010				
2011	1.049	0.148	1.042	0.111
2012			0.837	0.079
2013			0.681	0.064
2014			1.002	0.122
2015			0.899	0.098
2016			0.951	0.095
2017			0.936	0.097
2018			0.803	0.082
2019			0.821	0.068
2020	1.006	0.169	0.822	0.077

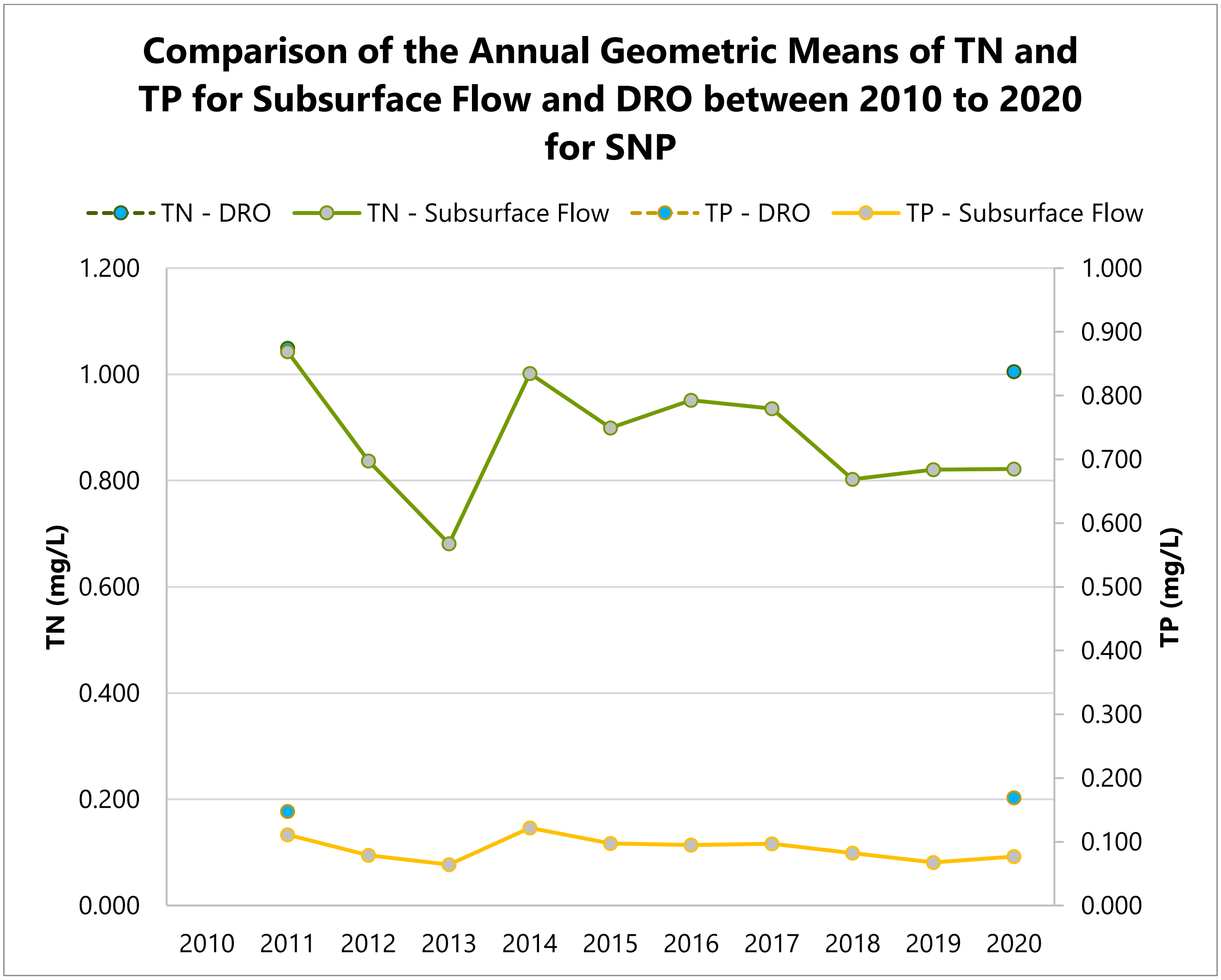

Figure 80. Comparison of the annual geometric means of TN (mg/L) and TP (mg/L) for subsurface flow and DRO between 2010 and 2020 for the SNP calibration basin.

Similar patterns in nutrient concentrations observed at the annual interval were also observed at the seasonal interval. Seasonal geometric mean TN and TP subsurface flow concentrations show a general pattern of lower concentrations in the dry season with higher concentrations in the wet season (Figure 81), with generally consistent fluctuations during the transition between seasons. Gaps in the time series data for DRO, as well as some subsurface flow points, are due to a lack of measured data at the monitoring location.

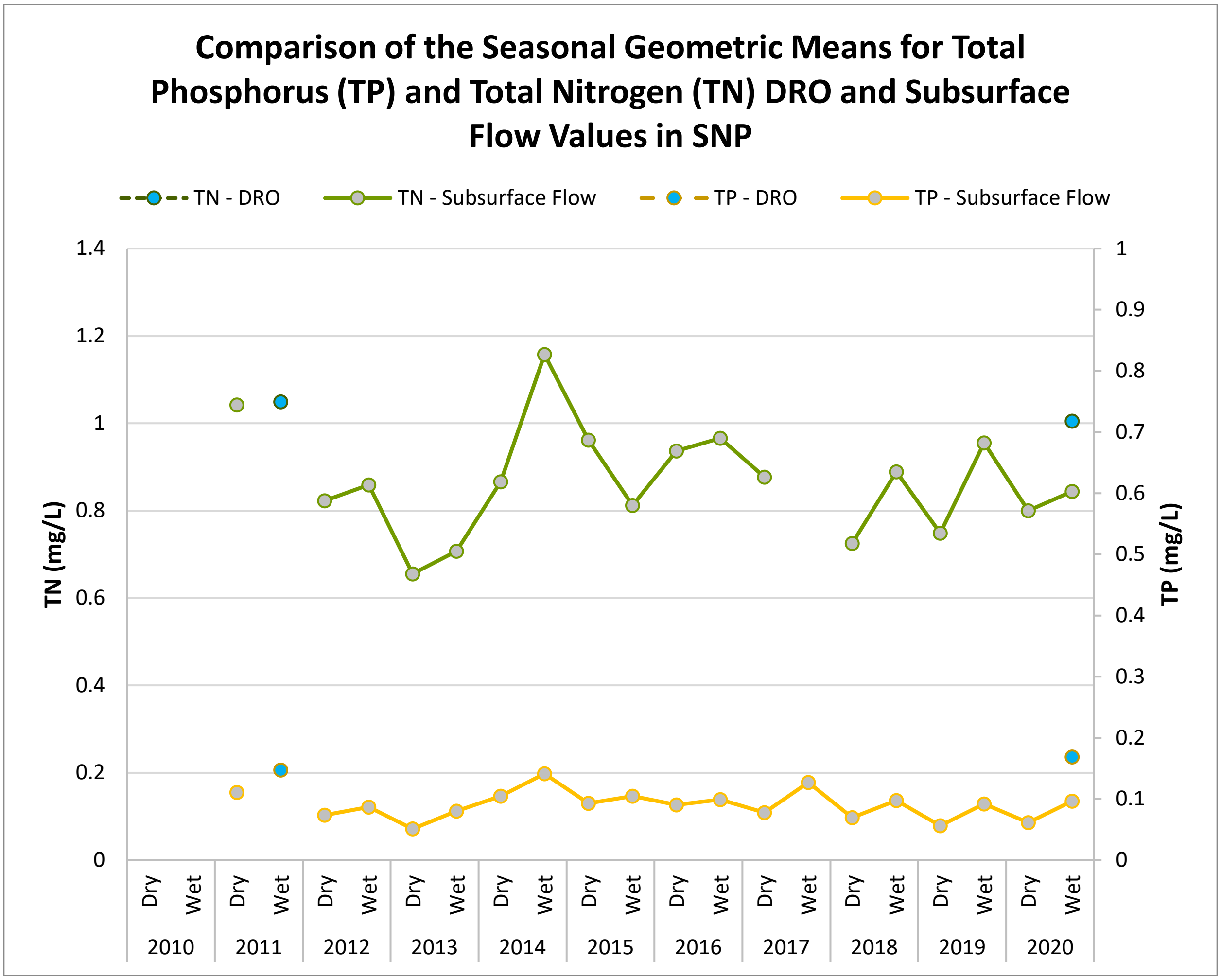

Figure 81. Comparision of the seasonal geometric means of TN (mg/L) and TP (mg/L) for subsurface flow and DRO between 2010 and 2020 for the SNP calibration basin.

2.5 Sebastian South Prong (SSP)

2.5.1 LULC Change

The SSP calibration basin is the second largest basin (~36,096 acres) and has been predominately composed of improved pasture (~18%), medium density residential (~13%), wetland (~9%), rangeland (~9%), and scrub (~9%) land use consolidation types (Table 15). The rangeland, pasture, wetland, and upland areas occupy a majority of the western portion of the basin, with the natural land use types laterally bisecting the rangeland and pasture lands (Figure 82, Figure 83, Figure 84). Agricultural, including abandoned citrus, are found in the central and southeastern regions of the basin, while residential areas are located in the northern portion of the basin, mainly from the central border to the eastern corner. Within the SSP calibration basin, the largest change is the abandonment of citrus fields (~14% decrease based on the total area), converting to either pasture, rangeland, other agricultural types, or reclassification to abandoned cropland which goes to the ruderal land use type.

Table 15. Total area (in acres and percentage) of each land use consolidation type in the SSP calibration basin for the 2010, 2015, and 2020 years.

Land Use Consolidation	Land Use Area (Acres)			Percent of Total Land Use (%)			Percent Change (%)	
	2010	2015	2020	2010	2015	2020	2015 - 2010	2020 - 2010
Citrus	**5,870.66**	971.80	934.14	**16.26**	2.69	2.59	-13.57	-13.68
Commercial	126.37	125.72	185.82	0.35	0.35	0.51	0.00	0.16
Dry Prairie	1,450.73	1,426.78	1,407.01	4.02	3.95	3.90	-0.07	-0.12
Field Crop	19.08	19.08	19.08	0.05	0.05	0.05	0.00	0.00
High Density Residential	210.25	217.15	224.35	0.58	0.60	0.62	0.02	0.04
Hydric Hammock	5.60	5.60	5.60	0.02	0.02	0.02	0.00	0.00
Improved Pasture	**5,757.11**	**6,932.00**	**6,813.99**	**15.95**	**19.21**	**18.88**	3.26	2.93
Industrial	43.31	38.52	38.37	0.12	0.11	0.11	-0.01	-0.01
Institutional	354.29	346.58	351.68	0.98	0.96	0.97	-0.02	-0.01
Low Density Residential	1,164.92	1,055.77	1,108.75	3.23	2.92	3.07	-0.30	-0.16
Medium Density Residential	**4,388.04**	**4,542.99**	**4,565.40**	**12.16**	**12.59**	**12.65**	0.43	0.49
Mesic Flatwoods	255.32	238.27	248.33	0.71	0.66	0.69	-0.05	-0.02
Mining	157.30	239.69	246.26	0.44	0.66	0.68	0.23	0.25
Open	803.58	647.93	519.04	2.23	1.80	1.44	-0.43	-0.79
Other Agriculture	124.94	548.11	530.03	0.35	1.52	1.47	1.17	1.12
Rangeland	**3,084.64**	**3,134.29**	**3,638.21**	**8.55**	**8.68**	**10.08**	0.14	1.53
Recreational 1	245.19	245.19	245.19	0.68	0.68	0.68	0.00	0.00

Land Use Consolidation	Land Use Area (Acres)			Percent of Total Land Use (%)			Percent Change (%)	
	2010	2015	2020	2010	2015	2020	2015 - 2010	2020 - 2010
Recreational 2	26.81	27.01	27.01	0.07	0.07	0.07	0.00	0.00
Ruderal	220.71	2,943.10	2,592.49	0.61	8.15	7.18	7.54	6.57
Scrub	3,079.58	**3,225.36**	**3,160.15**	8.53	**8.94**	**8.76**	0.40	0.22
Transportation	273.04	273.64	273.63	0.76	0.76	0.76	0.00	0.00
Upland Flatwoods	1,028.68	1,074.71	1,244.59	2.85	2.98	3.45	0.13	0.60
Upland Mixed	5.02	4.93	11.11	0.01	0.01	0.03	0.00	0.02
Water	688.18	736.36	761.61	1.91	2.04	2.11	0.13	0.20
Wet Flatwoods	2,766.09	2,673.88	2,622.80	7.66	7.41	7.27	-0.26	-0.40
Wet Prairies	801.59	811.43	1,023.96	2.22	2.25	2.84	0.03	0.62
Wetland	**3,136.76**	**3,581.82**	**3,289.21**	**8.69**	**9.92**	**9.11**	1.23	0.42
Xeric Hammock	6.80	6.91	6.80	0.02	0.02	0.02	0.00	0.00

**The top five land uses that make up a majority of the area have been bolded for each year. Percent change from the overall area between 2010 and 2015, as well as 2010 and 2020 have also been provided.*

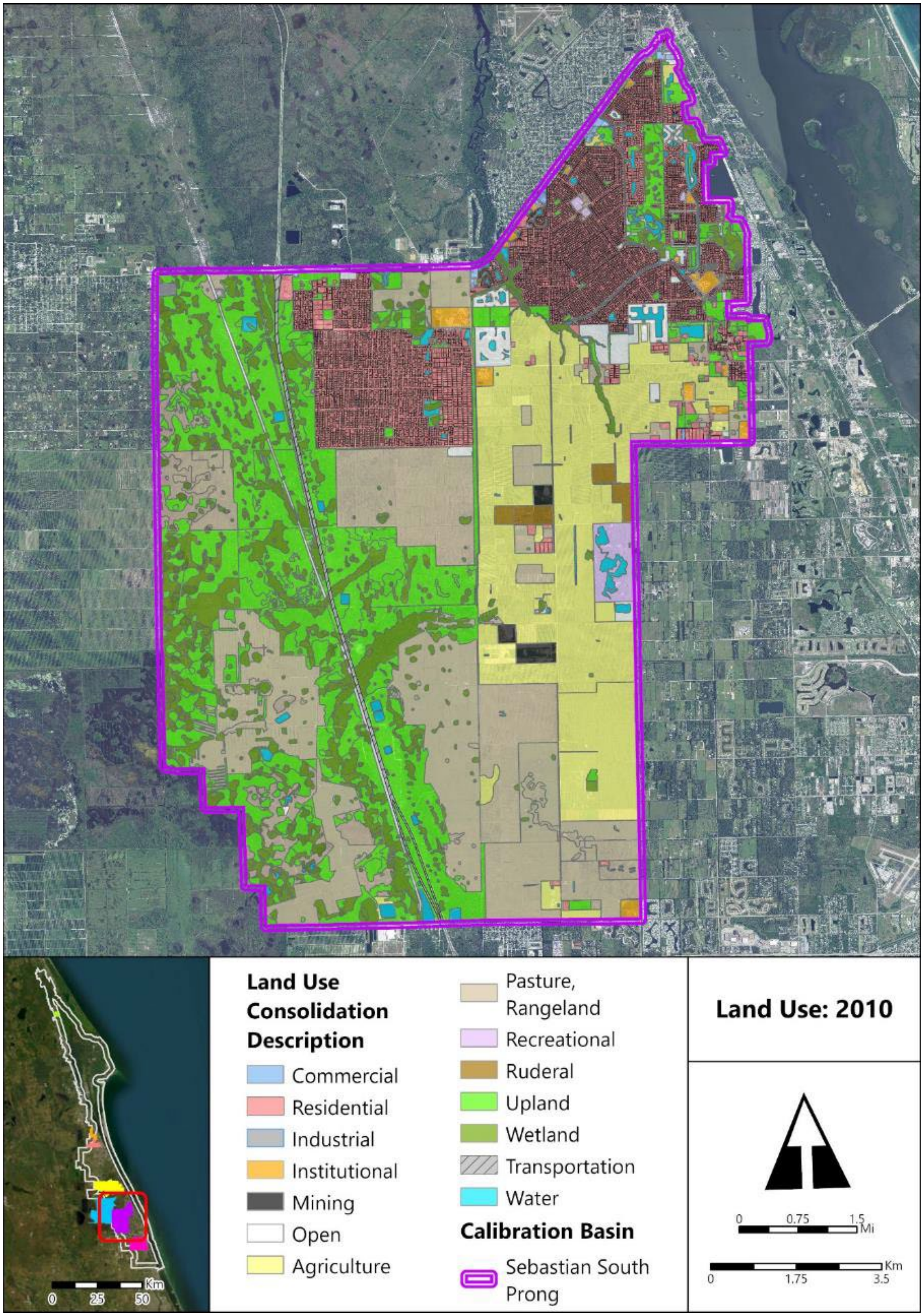

Figure 82. Land use within the SSP calibration basin for 2010.

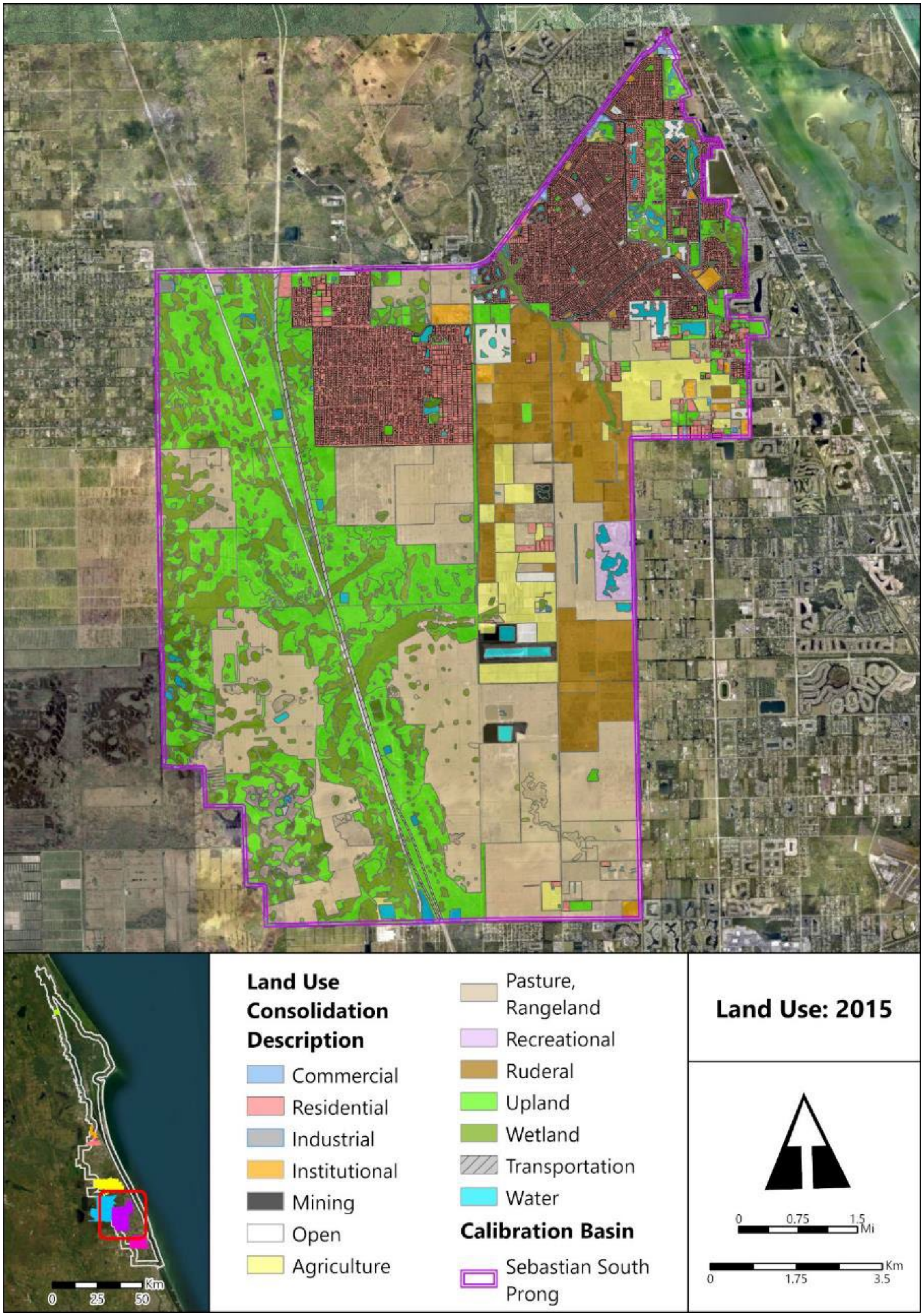

Figure 83. Land use within the SSP calibration basin for 2015.

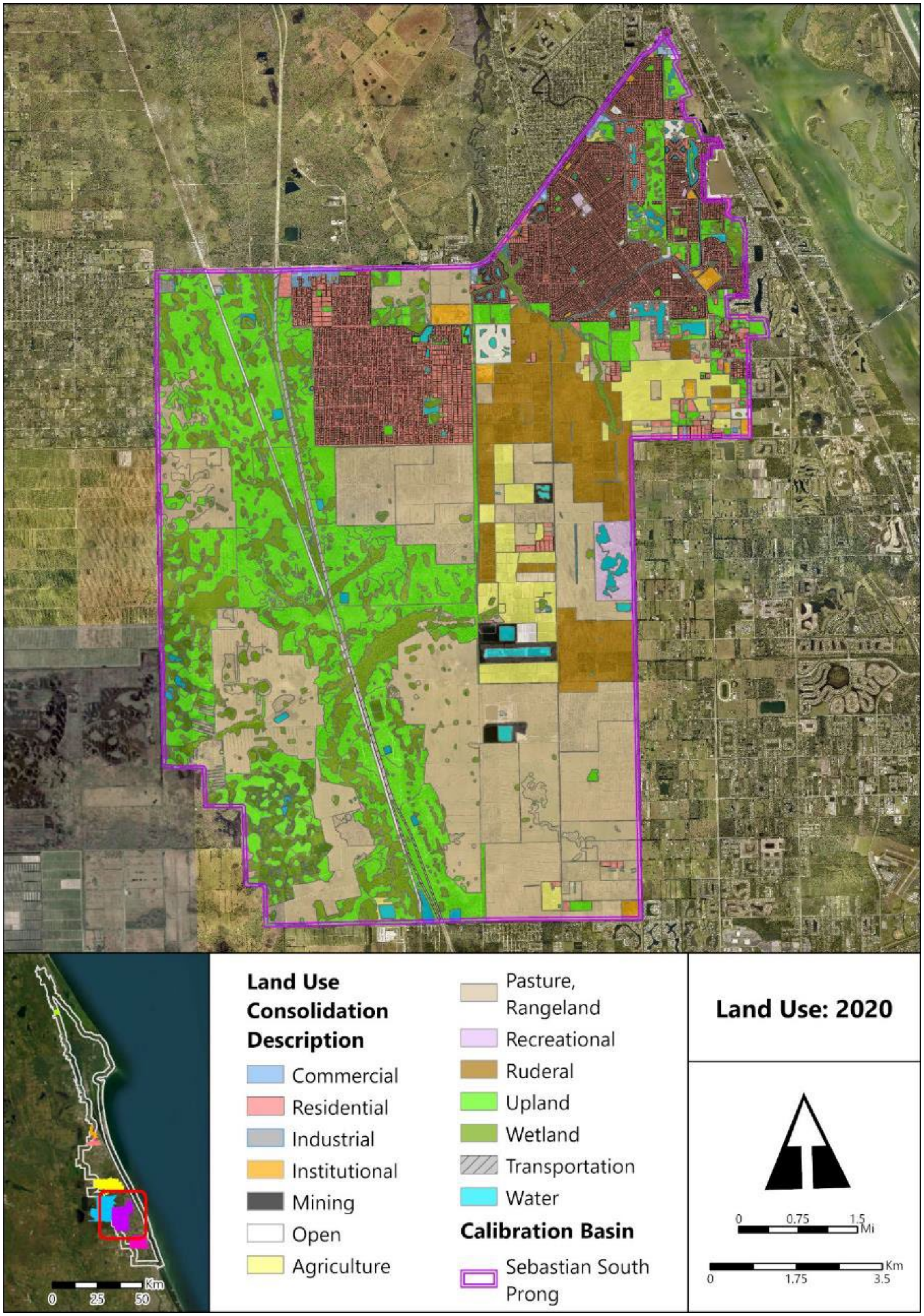

Figure 84. Land use within the SSP calibration basin for 2020.

2.5.2 Soil Hydrologic Group

The SSP calibration basin is primarily composed of the A/D (46%) and B/D (31%) hydrologic soil groups, followed by C/D (18%) and A (4%) soils, and water making up less than 1% of the total area (Figure 85). The B/D soils have two major patches in the central-southeast region, with one patch along the eastern border and one patch along the western border (Figure 86). The C/D soils are located in the southeastern portion of the basin, with larger patches in the center and north. There are two major bands of the A hydrologic soil group, one in the northeast corner and the other in the center of the southern portion. The A/D soils fill in a majority of the remaining area.

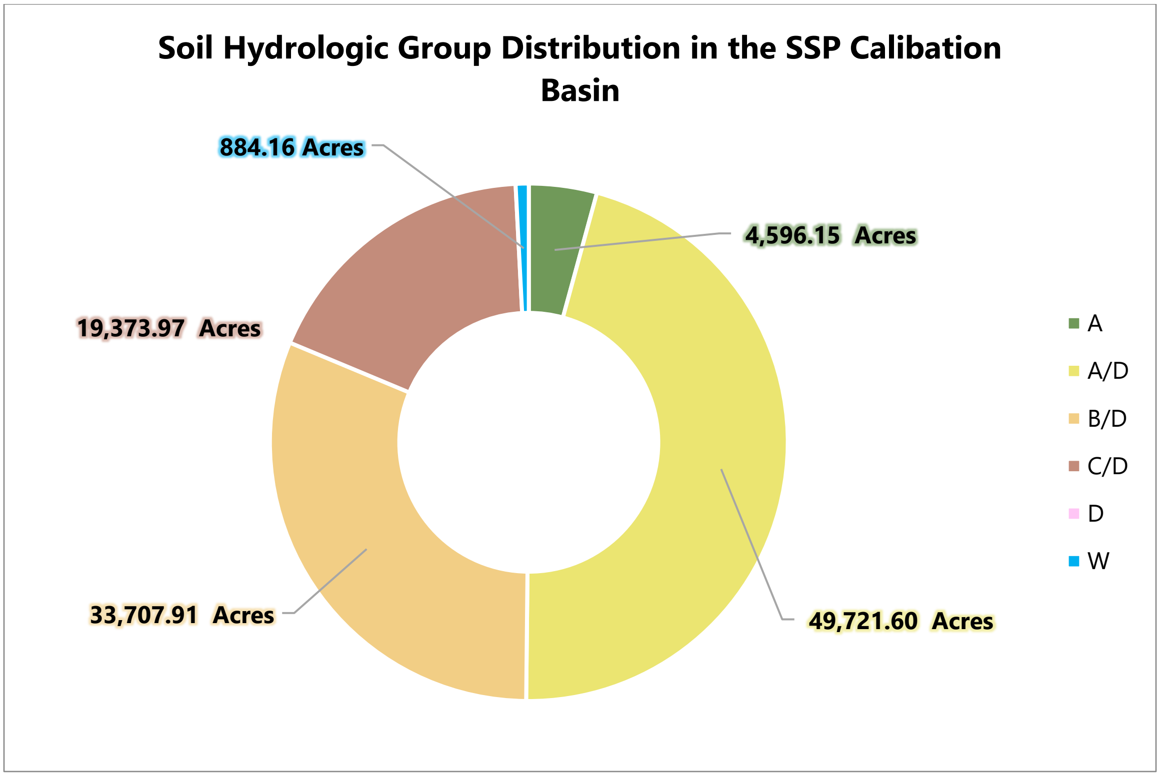

Figure 85. Pie chart (acres) of the soil hydrologic group distribution in the SSP calibration basin using USDA NRCS data.

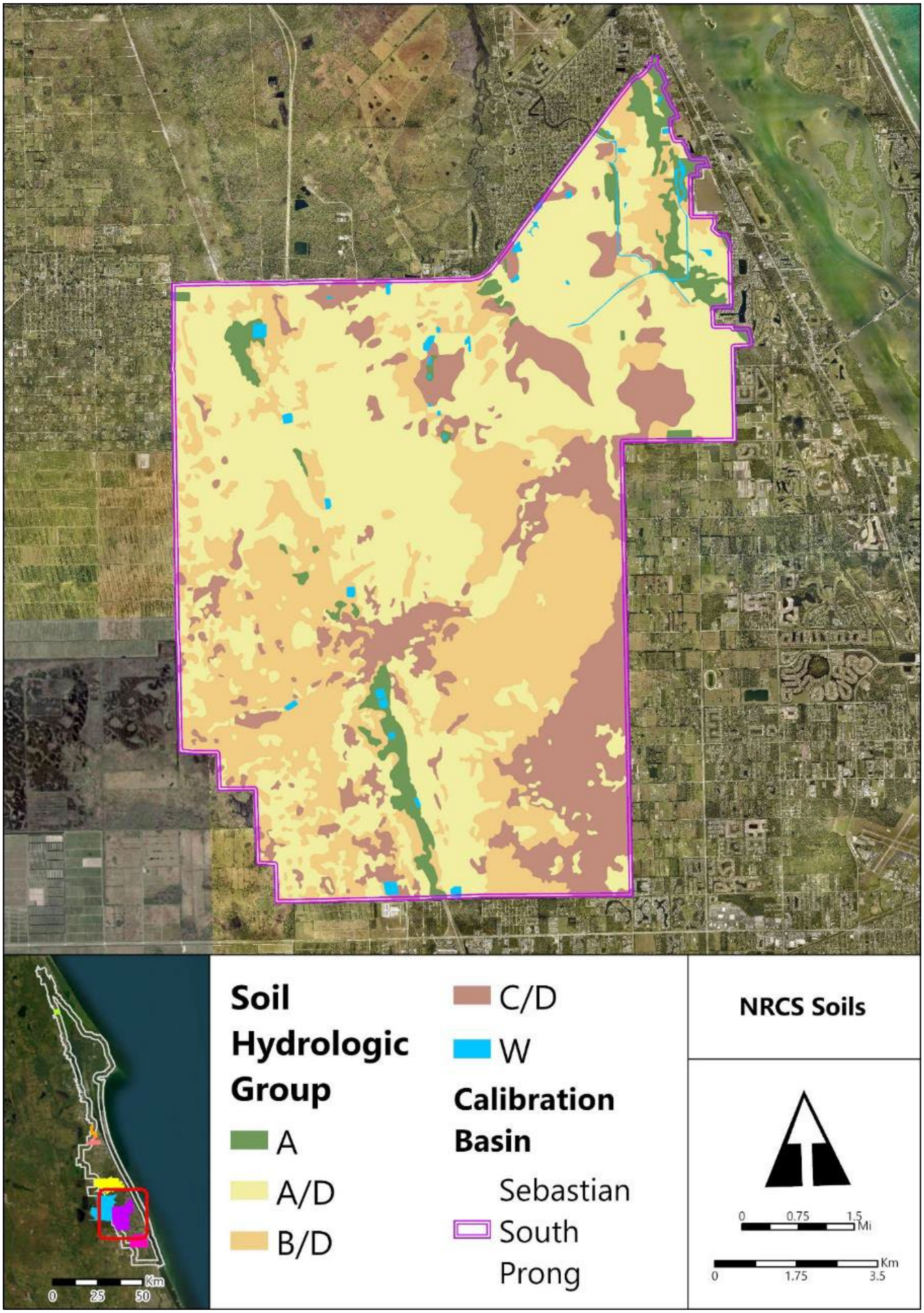

Figure 86. Distribution of soil hydrologic groups within the SSP calibration basin.

2.5.3 PRECIPITATION

The annual total precipitation for SSP ranges from the lowest annual total of 28 inches in 2010 to the highest annual total of 64 inches in 2017 (Figure 87). For all years, with the exception of 2018, the dry season has a lower total seasonal rainfall as compared to the wet seasons of the same years (Figure 88). The average monthly precipitation values are higher from May to October and lower from November to April (Figure 89). Maps for the monthly precipitation averages (inches/month) during February and September across the POR in the SSP calibration basin are provided in Figure 90 and Figure 91, respectively.

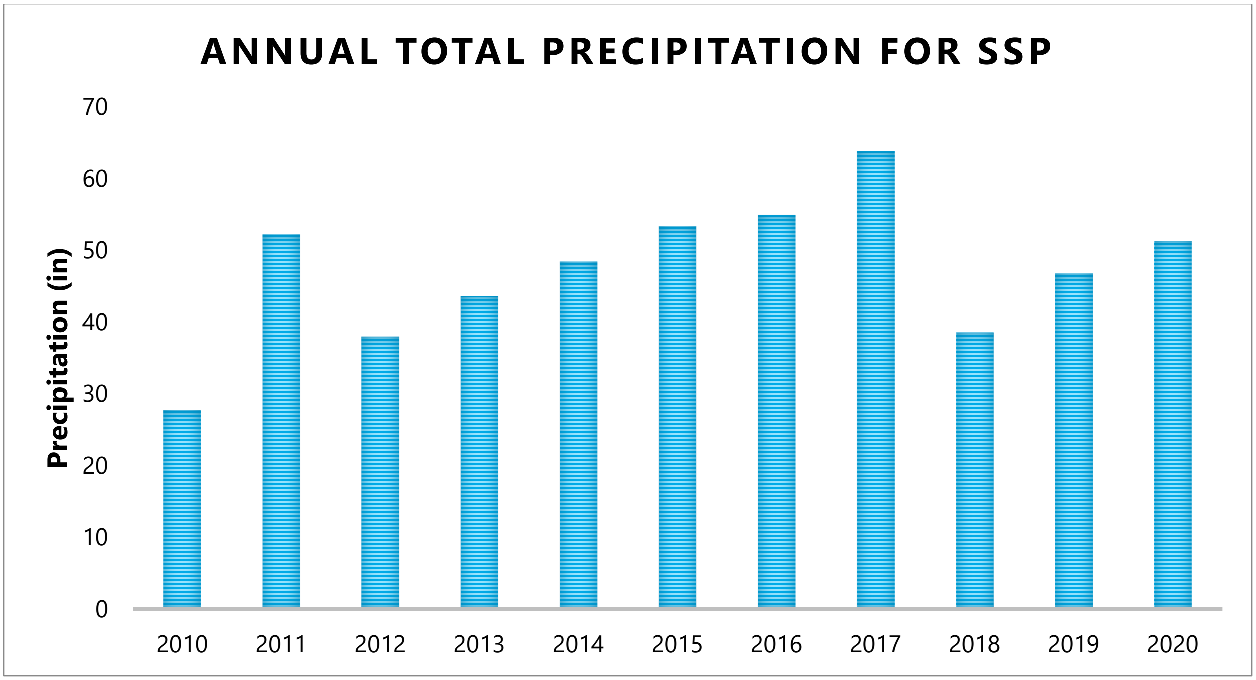

Figure 87. Annual total precipitation (in) for the SSP calibration basin from 2010 to 2020 derived from SJRWMD NEXRAD data.

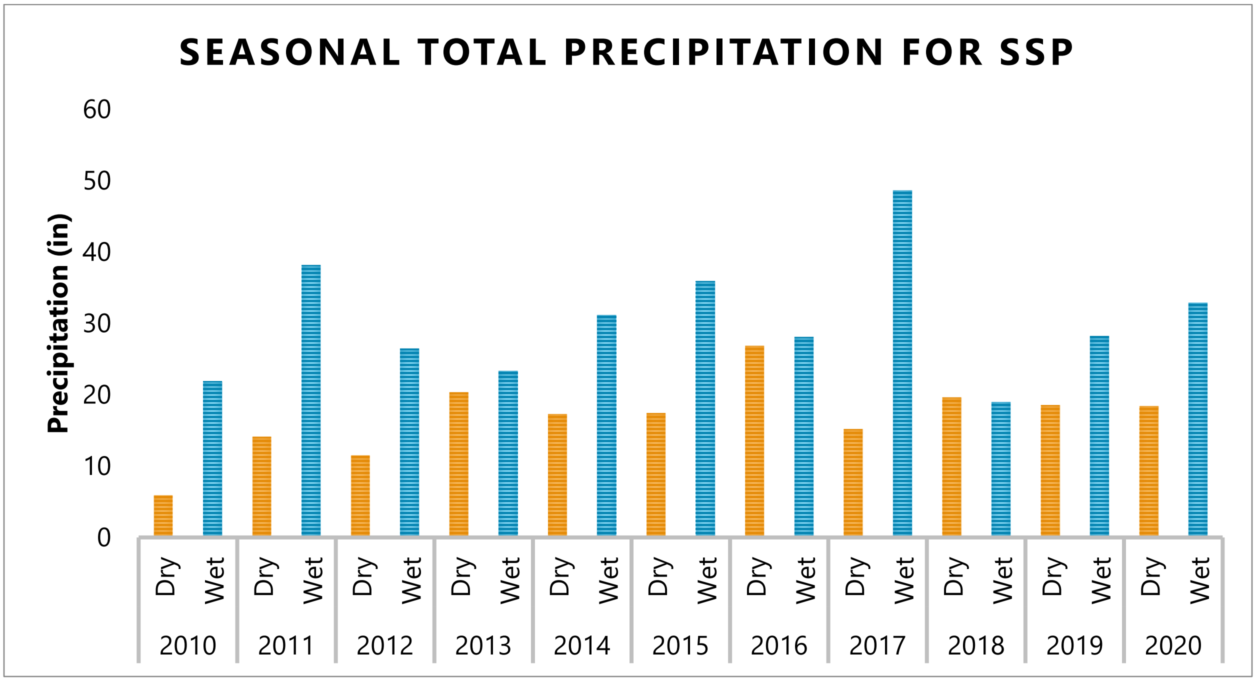

Figure 88. Seasonal total precipitation (in) for the SSP calibration basin from 2010 to 2020 derived from SJRWMD NEXRAD data.

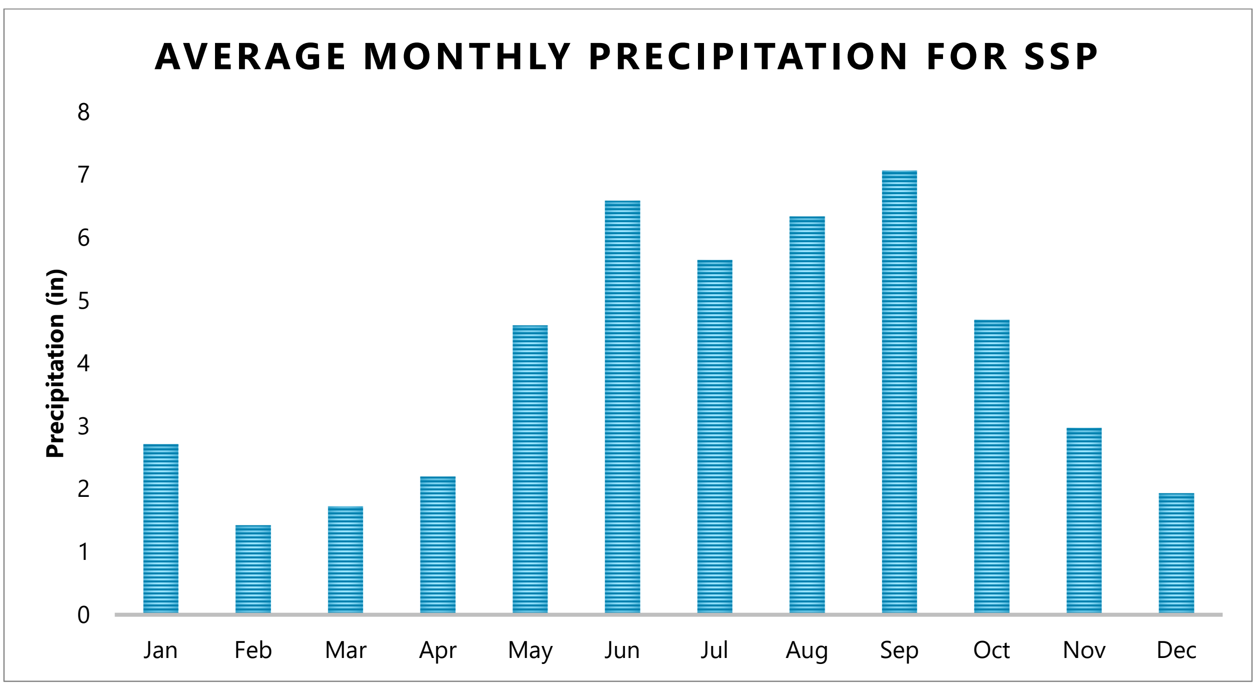

Figure 89. Average monthly precipitation (in) for the SSP calibration basin derived from SJRWMD NEXRAD data.

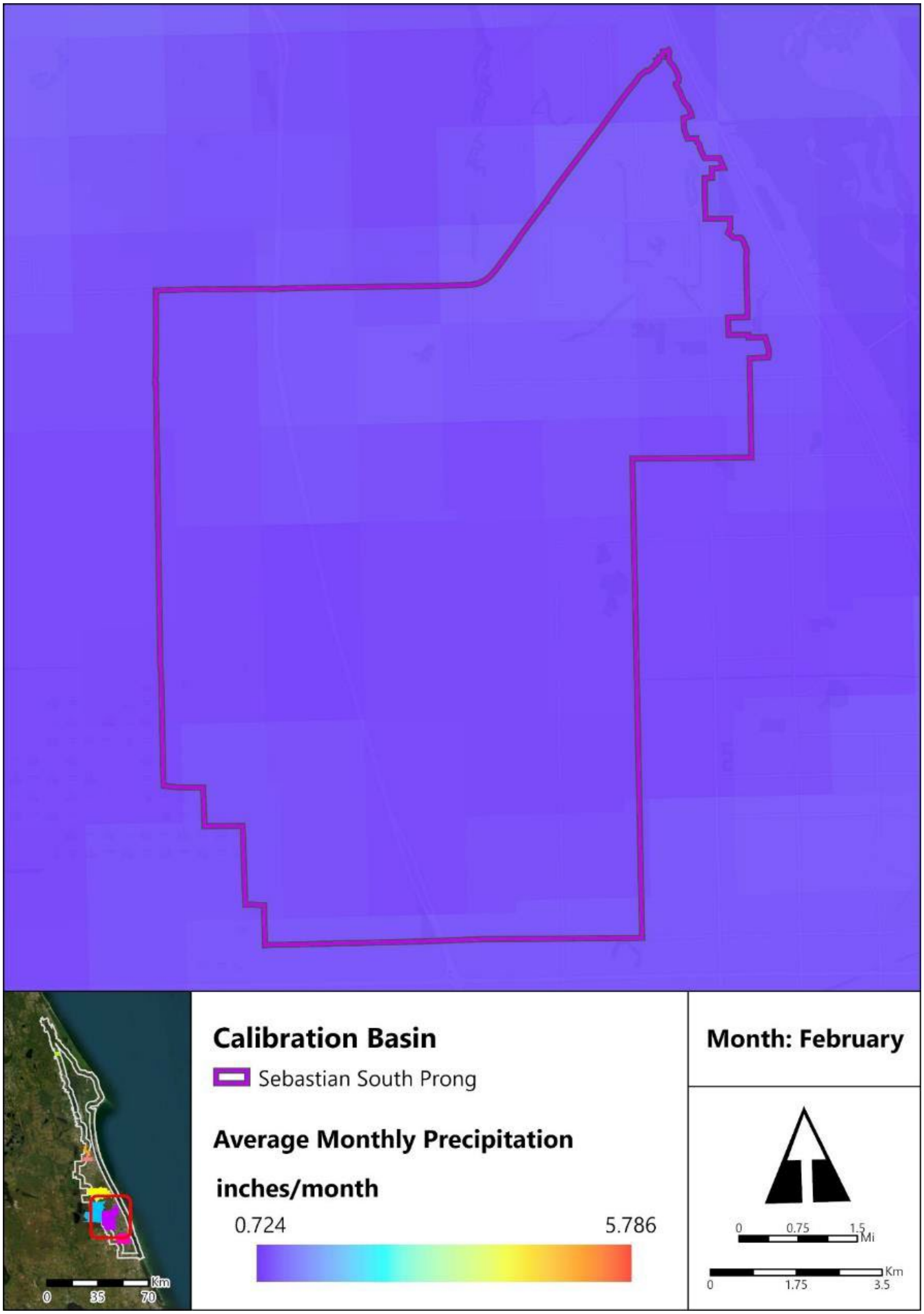

Figure 90. Average monthly precipitation (inches/month) for February across the period of record in the SSP calibration basin.

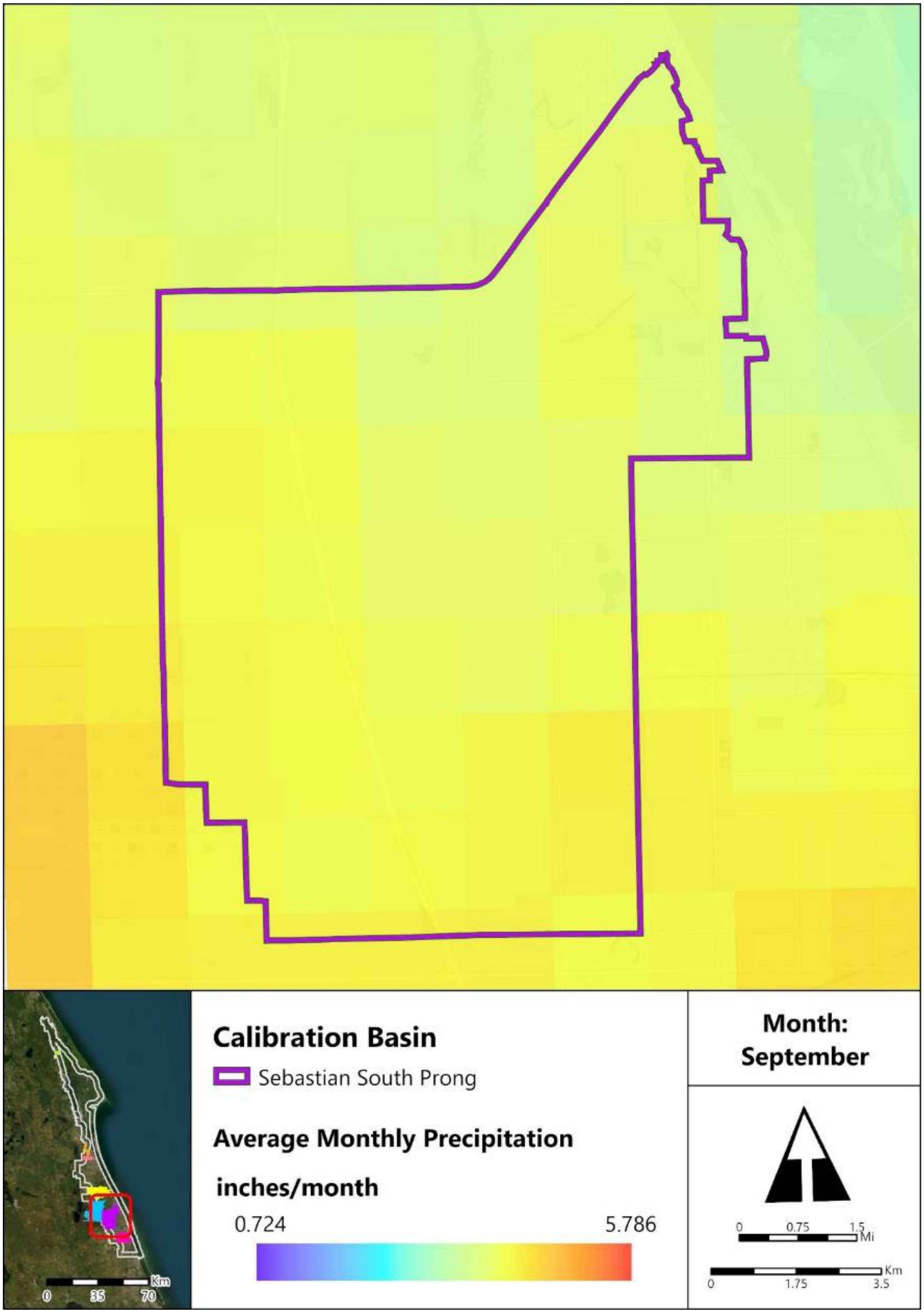

Figure 91. Average monthly precipitation (inches/month) for September across the period of record in the SSP calibration basin.

2.5.4 ET

Summary statistics for the monthly mean ET in the SSP calibration basin are provided as a boxplot (Figure 92). For SSP, there is a distinct difference in the wet and dry seasonal ET rates, with increasing through the wet season and decreasing rates in the dry season. The lowest median value and lowest variability in ET rates are seen in the dry season, where there are generally lower temperatures. The greatest median value and highest variability in ET rates are seen in the wet season, where there are generally higher temperatures. The lowest median value was observed in December (1.21 mm/day), whereas the highest median was observed in July (2.82 mm/day). The highest variability was observed in June, with an interquartile range difference of 0.85 mm/day, and the lowest variability was observed in October, with a 0.17 mm/day interquartile range difference. Maps for mean monthly ET rates (mm/day) during February and September across the POR in the SSP calibration basin are provided in Figure 93 and Figure 94, respectively.

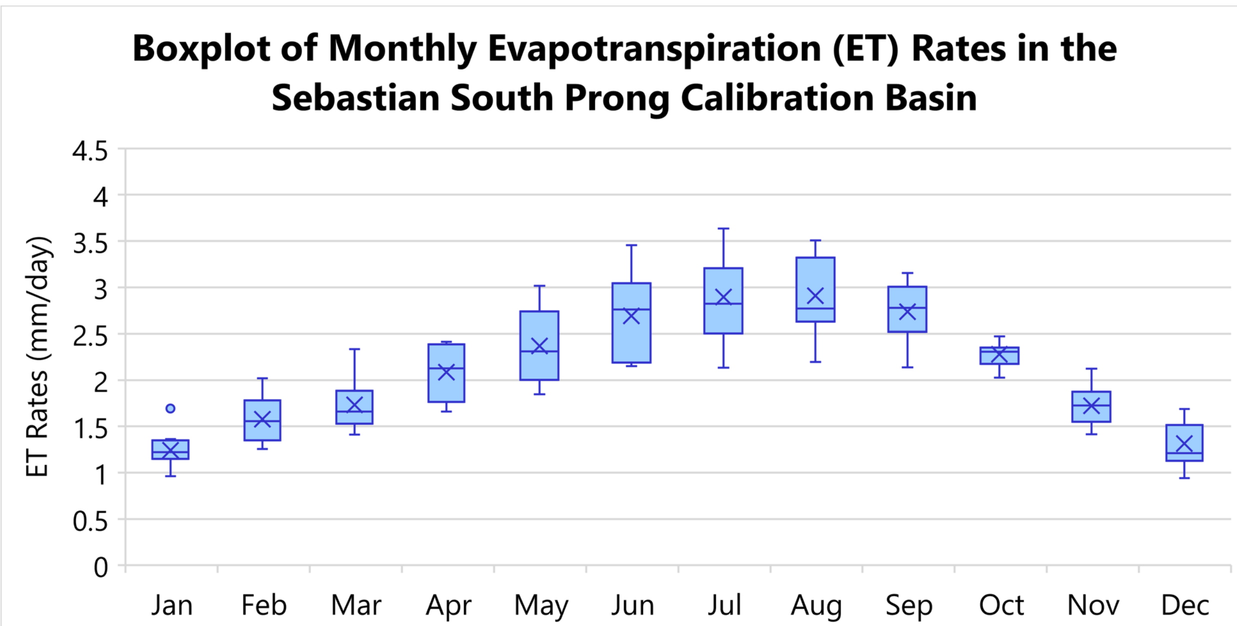

Figure 92. Boxplot of monthly mean ET rates in the SSP calibration basin derived from NASA EarthData and the University of Montana data.

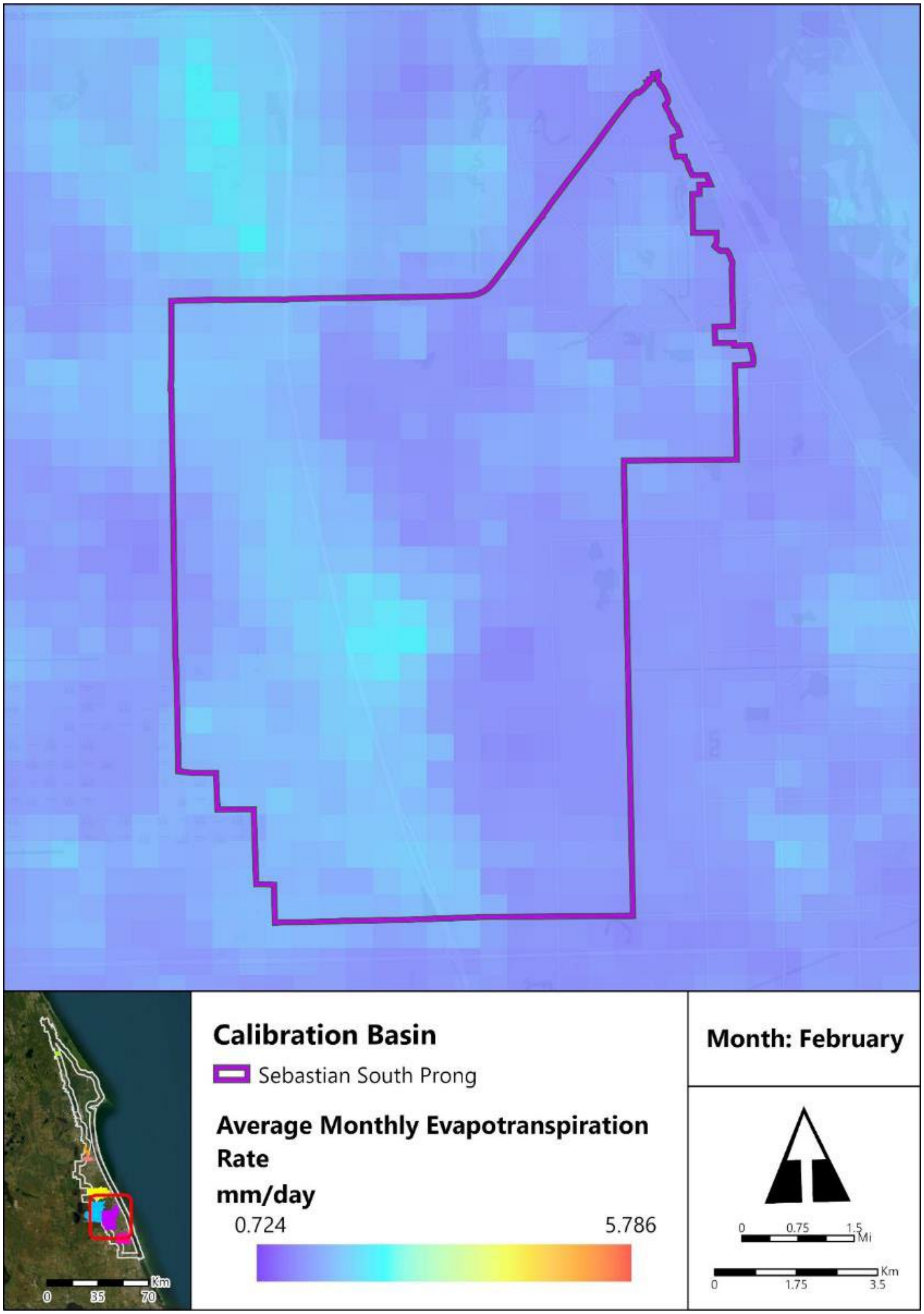

Figure 93. Average monthly ET rates (mm/day) for February across the period of record in the SSP calibration basin.

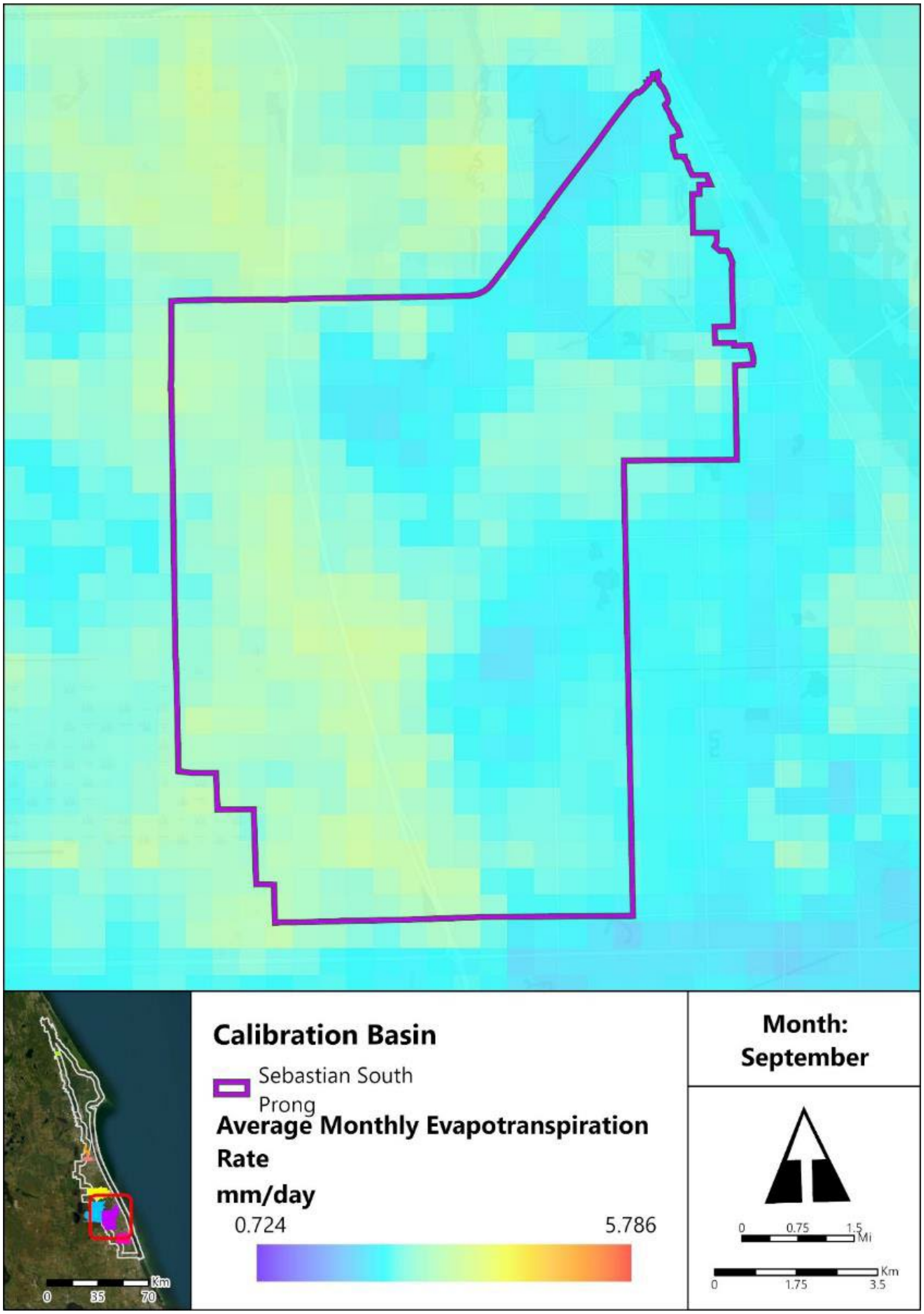

Figure 94. Average monthly ET rates (mm/day) for September across the period of record in the SSP calibration basin.

2.5.5 Treatments

Within SSP, approximately 17% of the calibration basin's total area is treated (Table 16), with a majority of the treated area using wet (~13%) versus dry treatments (~4%). Overall, very minimal changes have occurred across the three years of treatments, with less than 1% change in the treated area (Figure 95, Figure 96, Figure 97).

Table 16. Total area (acres) of each treatment type in the SSP calibration basin for the 2010, 2015, and 2020 years.

Treatment Type	Treatment Area (Acres)			Percent of Total Basin Area (%)			Percent Change (%)	
	2010	2015	2020	2010	2015	2020	2015-2010	2020-2010
Dry	1,409.62	1,409.62	1,414.29	3.91	3.91	3.92	0.00	0.01
Wet	4,543.31	4,543.82	4,548.80	12.59	12.59	12.60	0.00	0.02
Total	*5,952.93*	*5,953.44*	*5,963.09*	*16.49*	*16.49*	*16.52*	*0.00*	*0.03*

**The percentage of the total basin area and the percent change from the overall area between 2010 and 2015, as well as 2010 and 2020 have also been provided.*

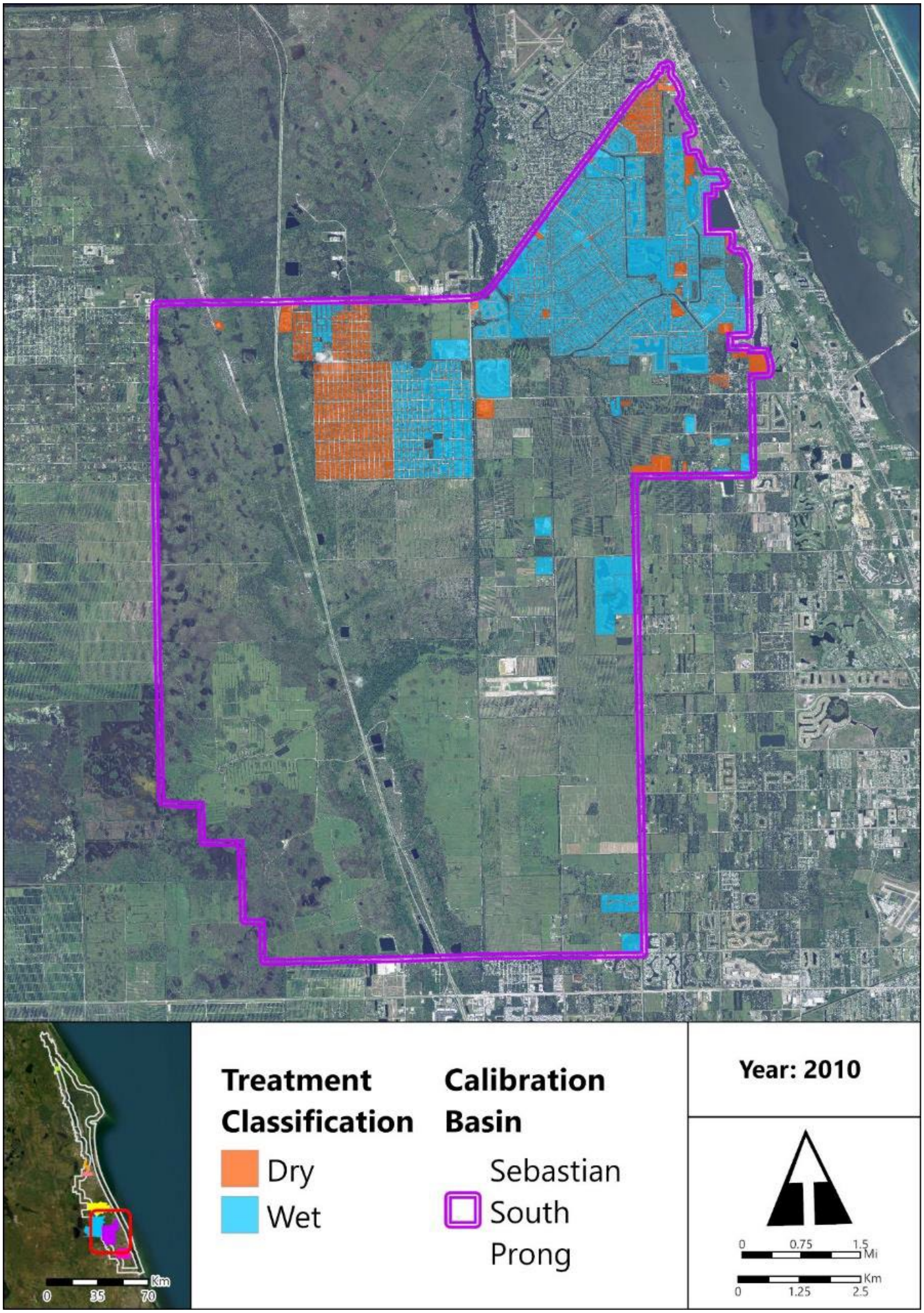

Figure 95. Treatments within the SSP calibration basin for 2010.

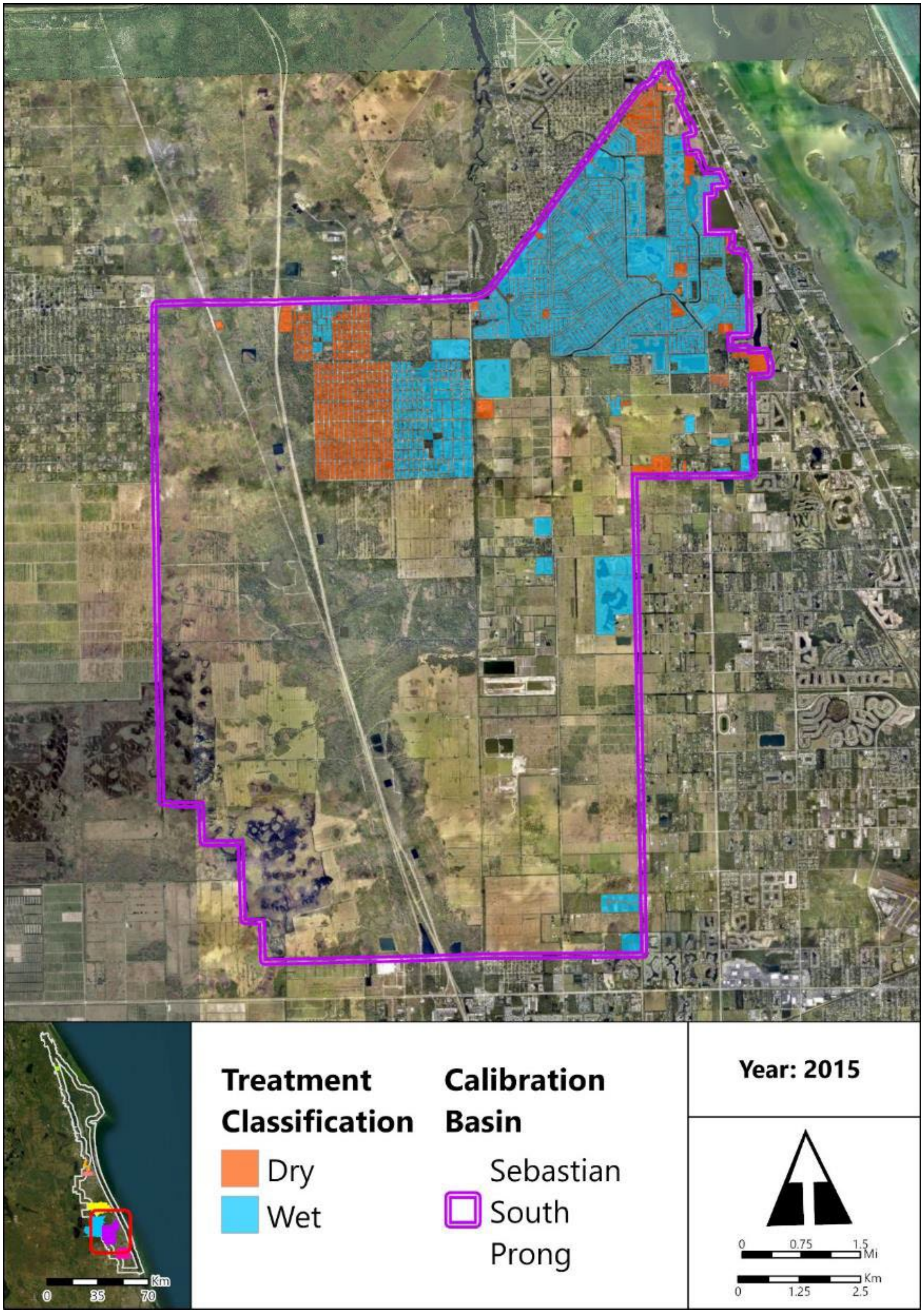

Figure 96. Treatments within the SSP calibration basin for 2015.

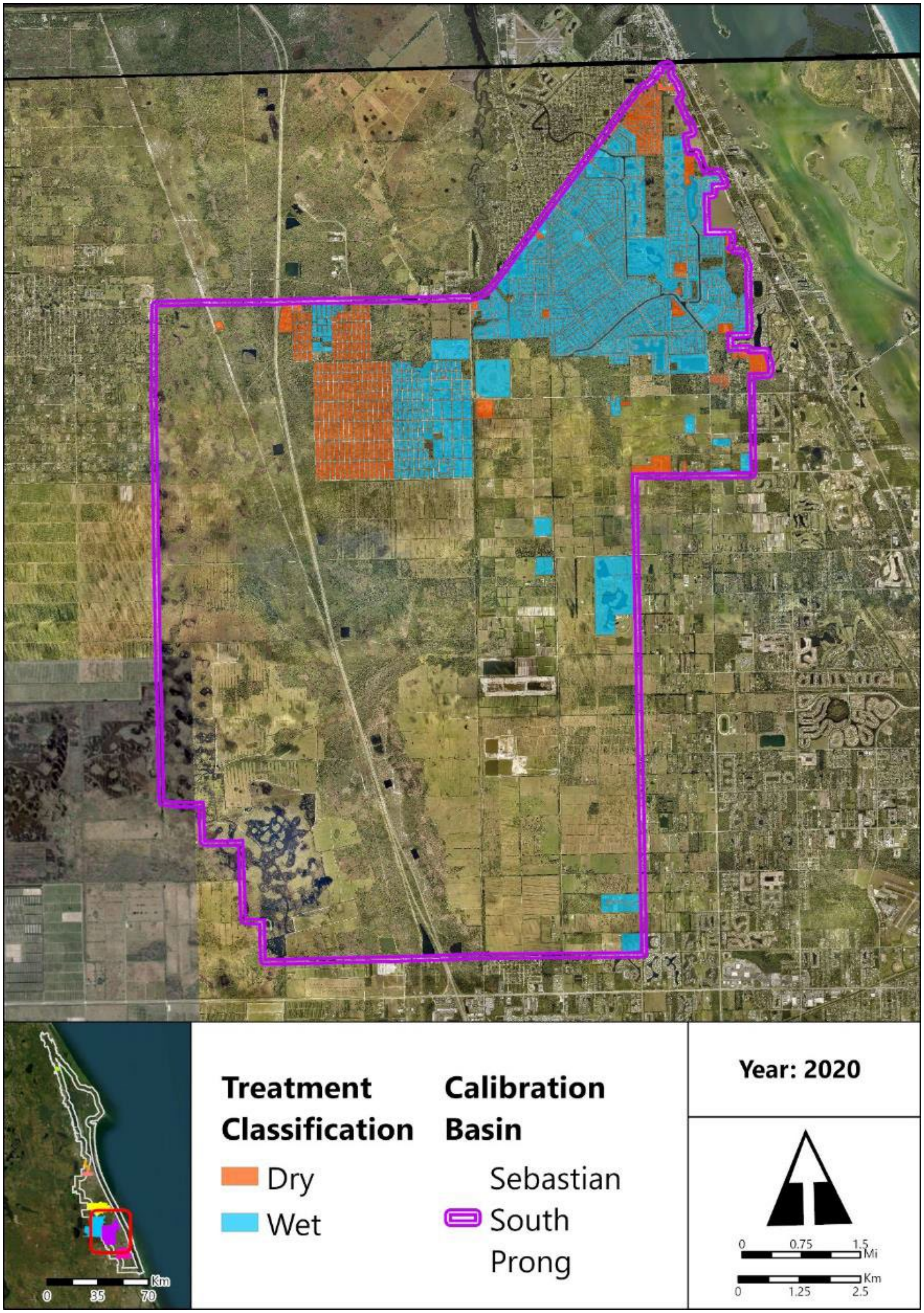

Figure 97. Treatments within the SSP calibration basin for 2020.

2.5.6 Hydrology

The SSP calibration basin volume is dominated by subsurface flow monthly (~77%), seasonally (~79% in the dry season and ~74% in the wet season), and annually (~76%) from 2010 to 2020. The average monthly volumes are higher from July to November, with lower volumes from December to June for the POR (Figure 98). The 2017 wet season showed the highest volumes of discharge, and the lowest seasonal volumes were observed in the 2012 dry season (Figure 99). The greatest annual volumes were observed in 2017, as the lowest volumes were observed in 2012, coinciding with the highest and lowest volumes observed in the seasonal data (Figure 100).

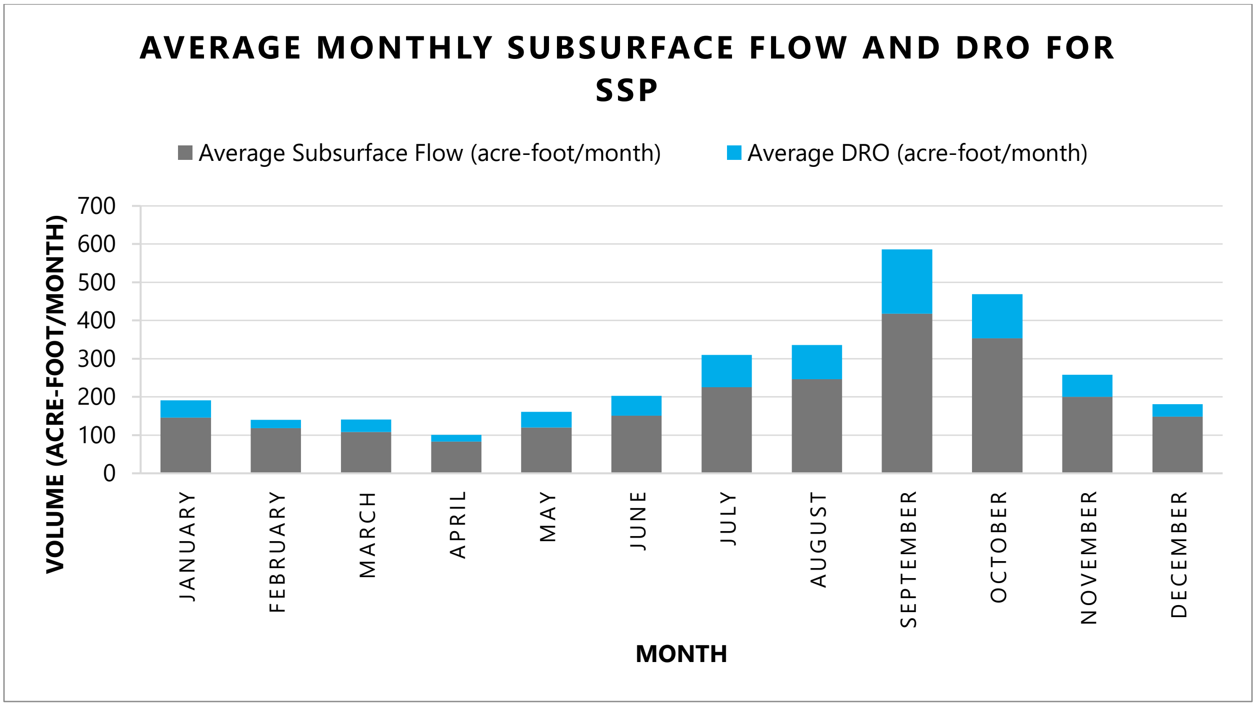

Figure 98. Average monthly subsurface flow (acre-foot/month) and DRO (acre-foot/month) for the SSP calibration basin derived from USGS WHAT data.

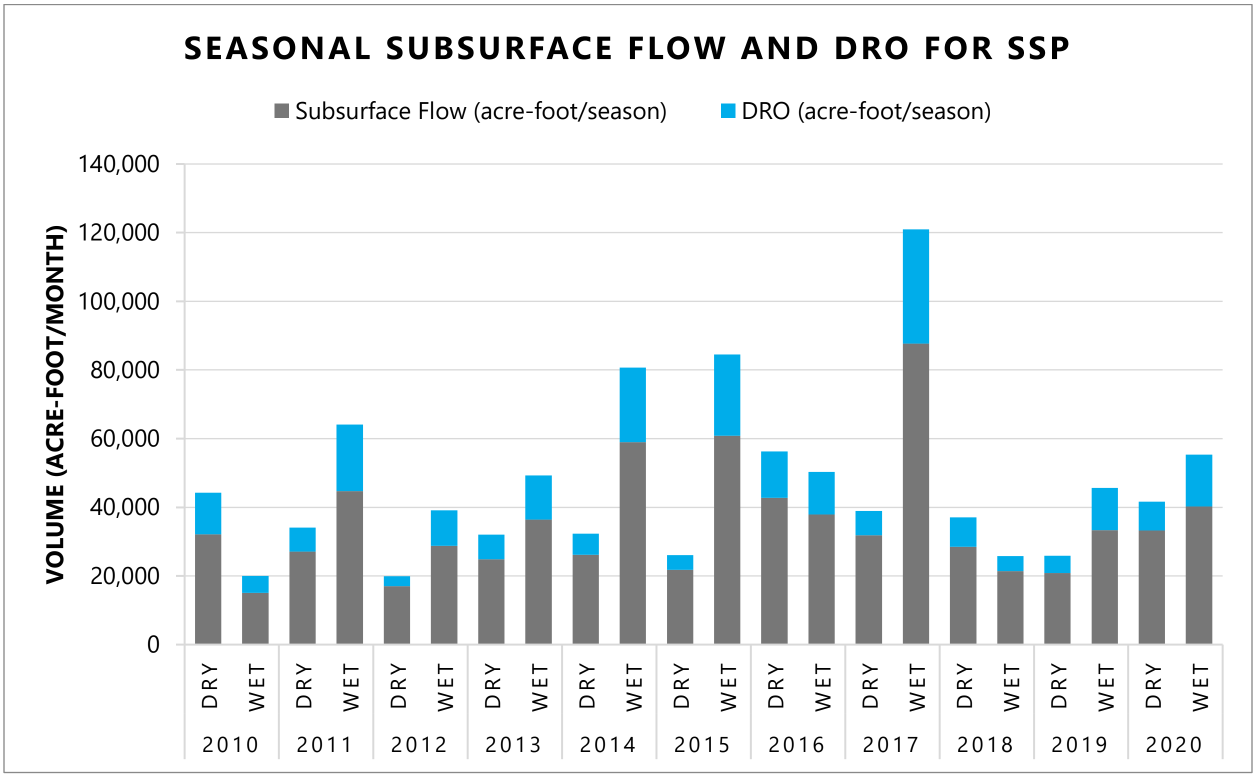

Figure 99. Seasonal subsurface flow (acre-foot/season) and DRO (acre-foot/season) for the SSP calibration basin derived from USGS WHAT data.

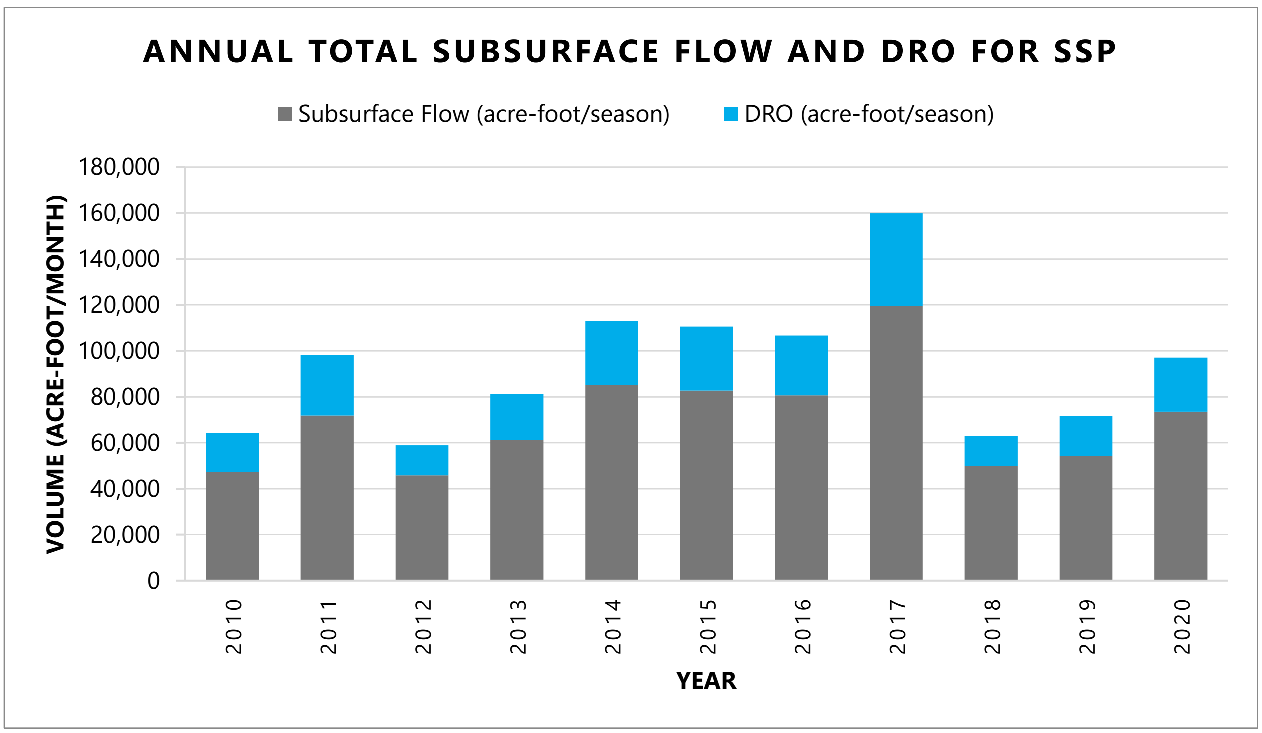

Figure 100. Annual subsurface flow (acre-foot/year) and DRO (acre-foot/year) for the SSP calibration basin derived from USGS WHAT data.

2.5.7 Water Quality

From 2013 to 2020, there were a total of 90 samples collected from the SSP at IRLSIR003 by SJRWMD; no samples were collected from 2010 to 2012. One sample coincided with DRO conditions, 60 coincided with subsurface flow conditions, and the remaining 29 were under mixed conditions (Table 17). As there is only a single data point in 2020 to represent DRO concentrations, annual and seasonal trends for either nutrient cannot be interpreted.

Minimal variations were observed in the annual mean TN and TP subsurface flow concentrations from 2013 to 2020, with TN ranging from 0.60 to 0.89 mg/L and TP ranging from 0.08 to 0.15 mg/L (Figure 101); the highest geometric mean concentrations for both TN and TP occurred in 2016. The seasonal mean TN and TP subsurface flow concentrations both show a pattern of elevated geometric mean concentrations in the wet season and lower concentrations in the dry season, with the exception of the TN subsurface flow concentration which increased between the 2019 wet into the 2019 dry season (Figure 102).

Table 17. Geometric means of annual TN (mg/L) and TP (mg/L) subsurface flow and DRO samples collected by SJRWMD from 2010 to 2020 at the SSP station IRLSIR003.

Year	TN - DRO	TP - DRO	TN - Subsurface flow	TP - Subsurface flow
2010				
2011				
2012				
2013			0.795	0.109
2014			0.759	0.143
2015			0.788	0.113
2016			0.886	0.153
2017			0.795	0.126
2018			0.775	0.112
2019			0.604	0.063
2020	0.958	0.139	0.734	0.078

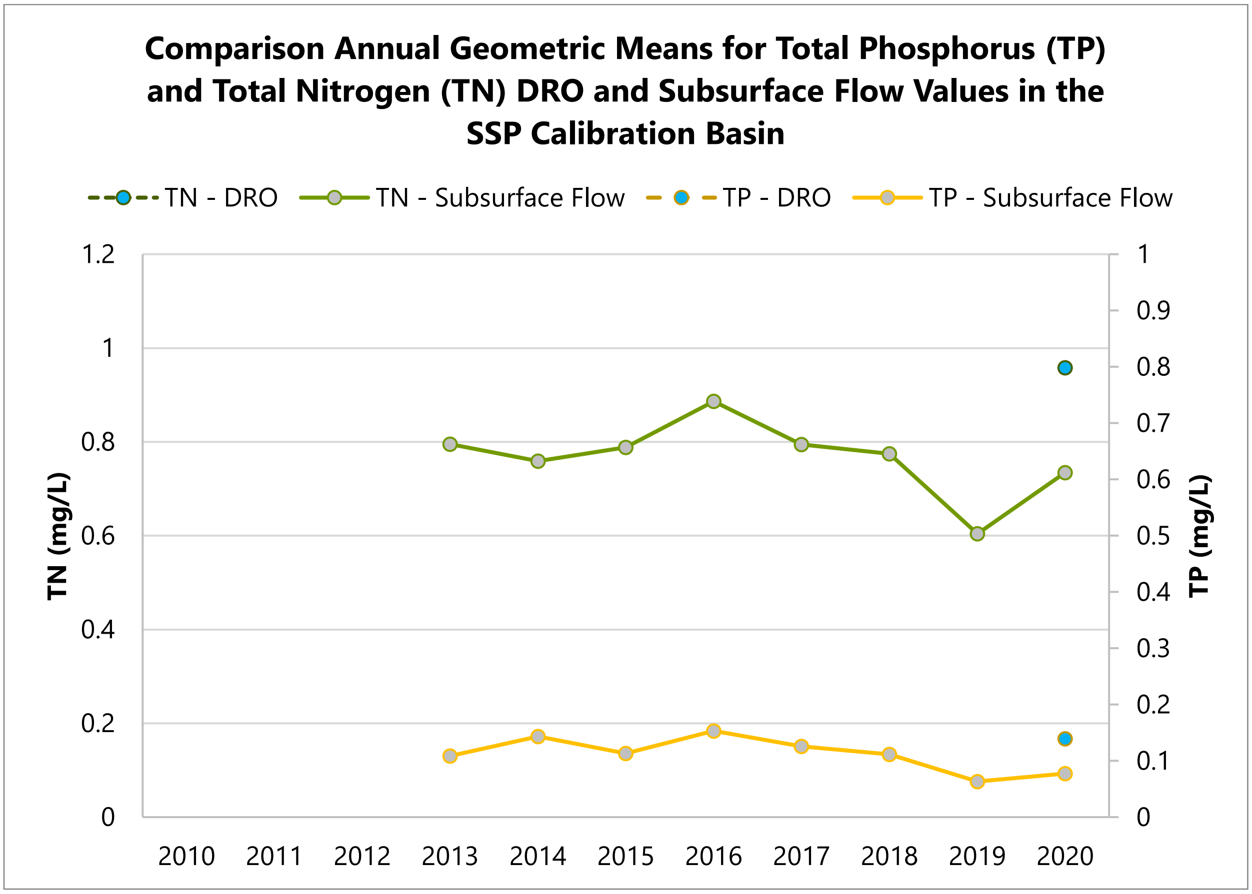

Figure 101. Comparison of the annual geometric means of TN (mg/L) and TP (mg/L) for subsurface flow and DRO between 2010 and 2020 for the SSP calibration basin.

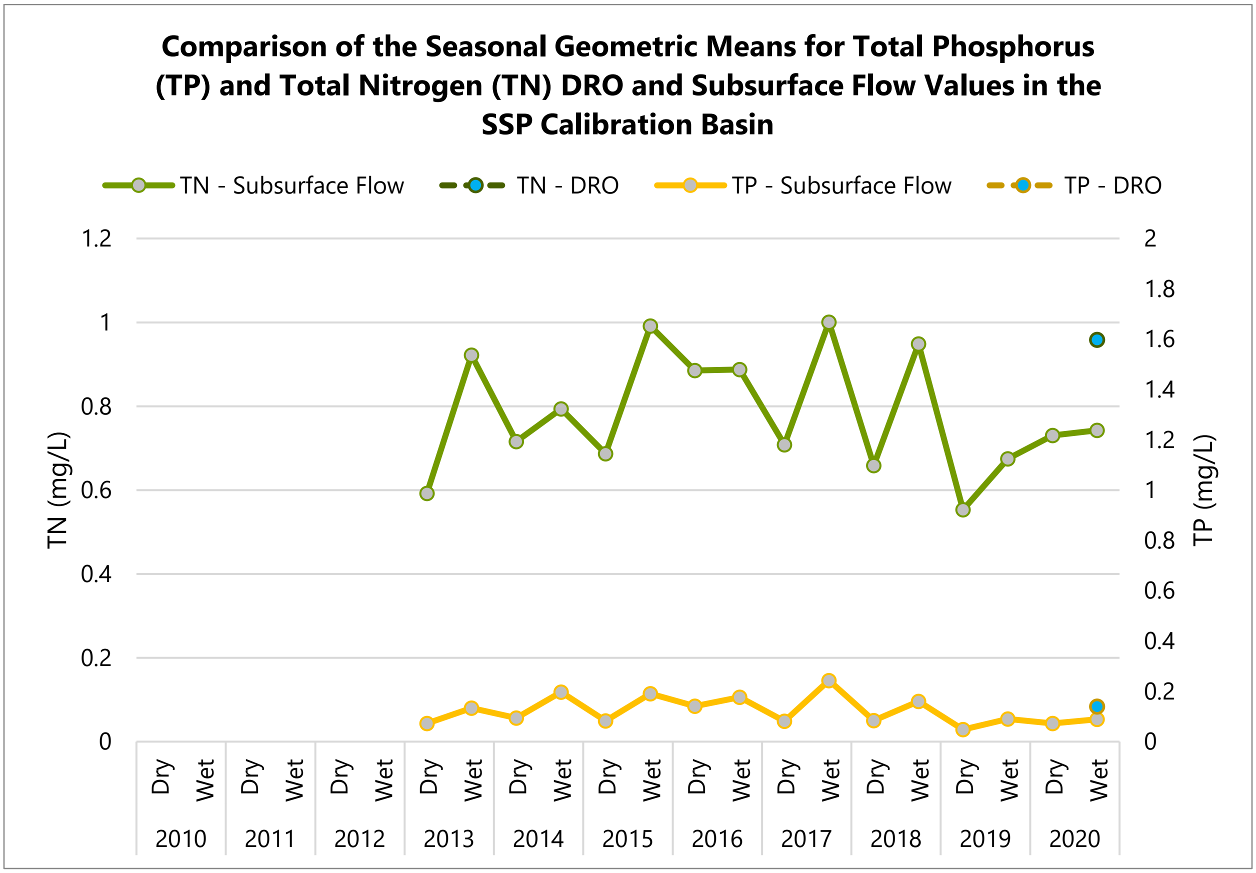

Figure 102. Comparison of the seasonal geometric means of TN (mg/L) and TP (mg/L) for subsurface flow and DRO between 2010 and 2020 for the SSP calibration basin.

2.6 FELLSMERE

2.6.1 LULC CHANGE

Fellsmere is the largest calibration basin (~36,360 acres) and has been predominately composed of citrus (~46%), low density residential (~9%), scrub (~8%), improved pasture (~8%), and wet flatwoods (~5%) land use consolidation types (Table 18). The agricultural lands encompass the western and southern regions of the basin, the natural (upland and wetland) types are located in the northeast corner, and the residential areas are found in the central region along the eastern border (Figure 103, Figure 104, Figure 105). Minor changes have occurred within the Fellsmere calibration basin from 2010 to 2020, such as the conversion of citrus or field crops to row crops or pasture lands, with some increases in low density residential areas.

Table 18. Total area (in acres and percentage) of each land use consolidation type in the Fellsmere calibration basin for the 2010, 2015, and 2020 years.

Land Use Consolidation	Land Use Area (Acres)			Percent of Total Land Use (%)			Percent Change (%)	
	2010	2015	2020	2010	2015	2020	2015 - 2010	2020 - 2010
Citrus	**17,154.56**	**16,628.57**	**16,597.29**	**47.18**	**45.73**	**45.65**	-1.45	-1.53
Commercial	70.22	118.03	121.21	0.19	0.32	0.33	0.13	0.14
Dry Prairie	350.13	372.30	290.13	0.96	1.02	0.80	0.06	-0.17
Field Crop	581.15	126.96	122.08	1.60	0.35	0.34	-1.25	-1.26
High Density Residential	81.94	90.07	91.97	0.23	0.25	0.25	0.02	0.03
Hydric Hammock	11.07	11.07	11.07	0.03	0.03	0.03	0.00	0.00
Improved Pasture	**2,426.95**	**3,167.33**	**3,072.91**	**6.67**	**8.71**	**8.45**	2.04	1.78
Industrial	295.34	437.22	458.80	0.81	1.20	1.26	0.39	0.45
Institutional	118.36	104.77	104.91	0.33	0.29	0.29	-0.04	-0.04
Low Density Residential	**3,060.96**	**3,272.75**	**3,527.42**	**8.42**	**9.00**	**9.70**	0.58	1.28
Medium Density Residential	642.10	634.20	633.63	1.77	1.74	1.74	-0.02	-0.02
Mesic Flatwoods	542.49	537.72	521.21	1.49	1.48	1.43	-0.01	-0.06
Mining	--	4.71	4.71	--	0.01	0.01	--	--
Open	703.59	652.47	680.33	1.94	1.79	1.87	-0.14	-0.06
Other Agriculture	1,032.79	262.35	262.36	2.84	0.72	0.72	-2.12	-2.12
Rangeland	661.12	642.09	651.85	1.82	1.77	1.79	-0.05	-0.03
Recreational 2	53.27	56.76	44.71	0.15	0.16	0.12	0.01	-0.02
Row Crops	539.99	1,403.10	1,409.38	1.49	3.86	3.88	2.37	2.39
Ruderal	370.65	287.21	294.68	1.02	0.79	0.81	-0.23	-0.21
Scrub	**3,070.43**	**2,997.48**	**3,053.96**	**8.44**	**8.24**	**8.40**	-0.20	-0.05

Land Use Consolidation	Land Use Area (Acres)			Percent of Total Land Use (%)			Percent Change (%)	
	2010	2015	2020	2010	2015	2020	2015 - 2010	2020 - 2010
Transportation	33.09	33.09	33.09	0.09	0.09	0.09	0.00	0.00
Upland Flatwoods	773.08	779.62	759.97	2.13	2.14	2.09	0.02	-0.04
Upland Mixed	--	60.71	--	--	0.17	--	--	--
Water	322.78	360.28	337.95	0.89	0.99	0.93	0.10	0.04
Wet Flatwoods	**1,997.51**	**1,795.80**	**1,724.92**	**5.49**	**4.94**	**4.74**	-0.55	-0.75
Wet Prairies	225.84	181.10	179.50	0.62	0.50	0.49	-0.12	-0.13
Wetland	1,210.44	1,314.38	1,342.09	3.33	3.61	3.69	0.29	0.36
Xeric Hammock	30.29	28.02	28.02	0.08	0.08	0.08	-0.01	-0.01

**The top five land uses that make up a majority of the area have been bolded for each year. Percent change from the overall area between 2010 and 2015, as well as 2010 and 2020 have also been provided.*

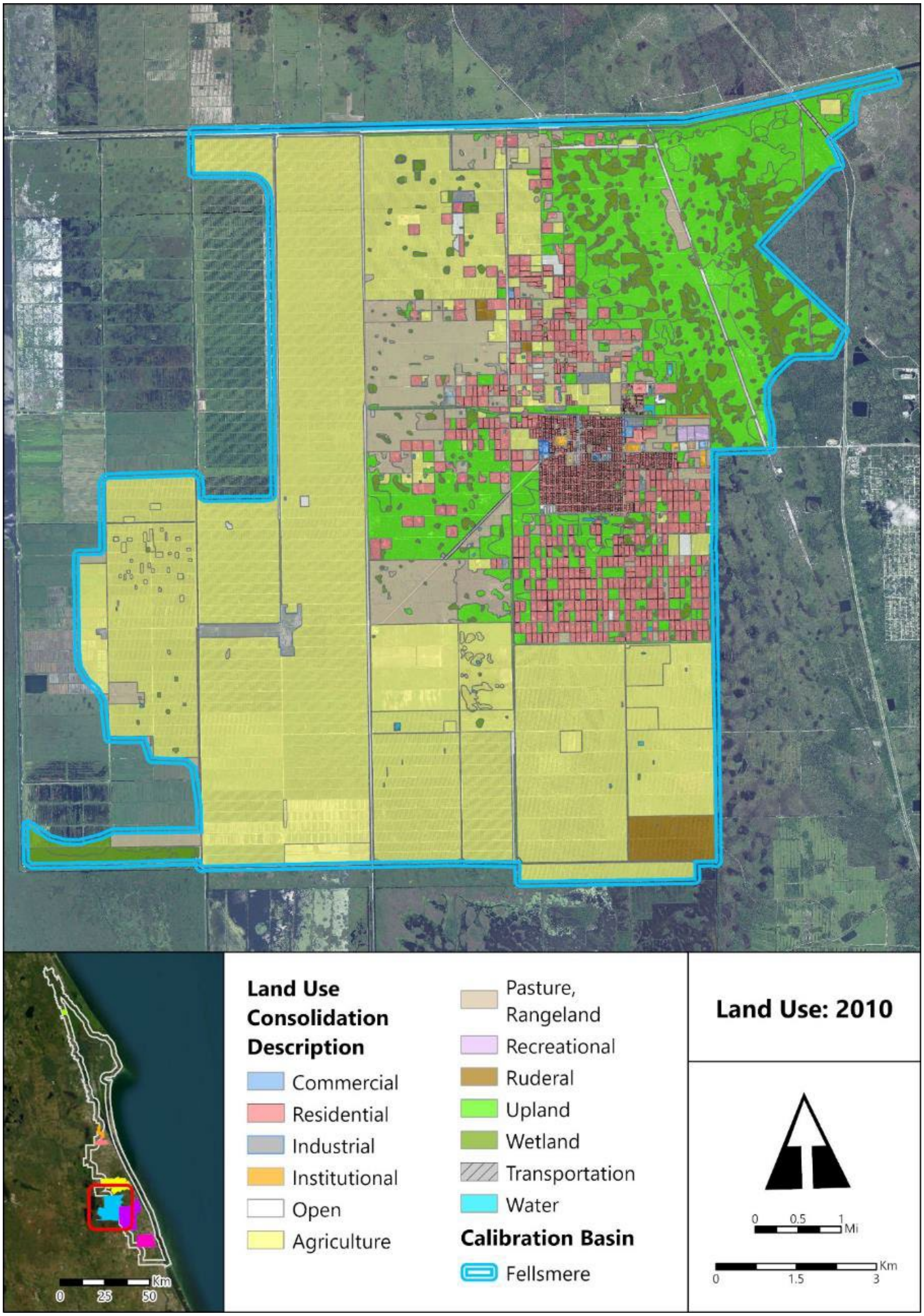

Figure 103. Land use within the Fellsmere calibration basin for 2010.

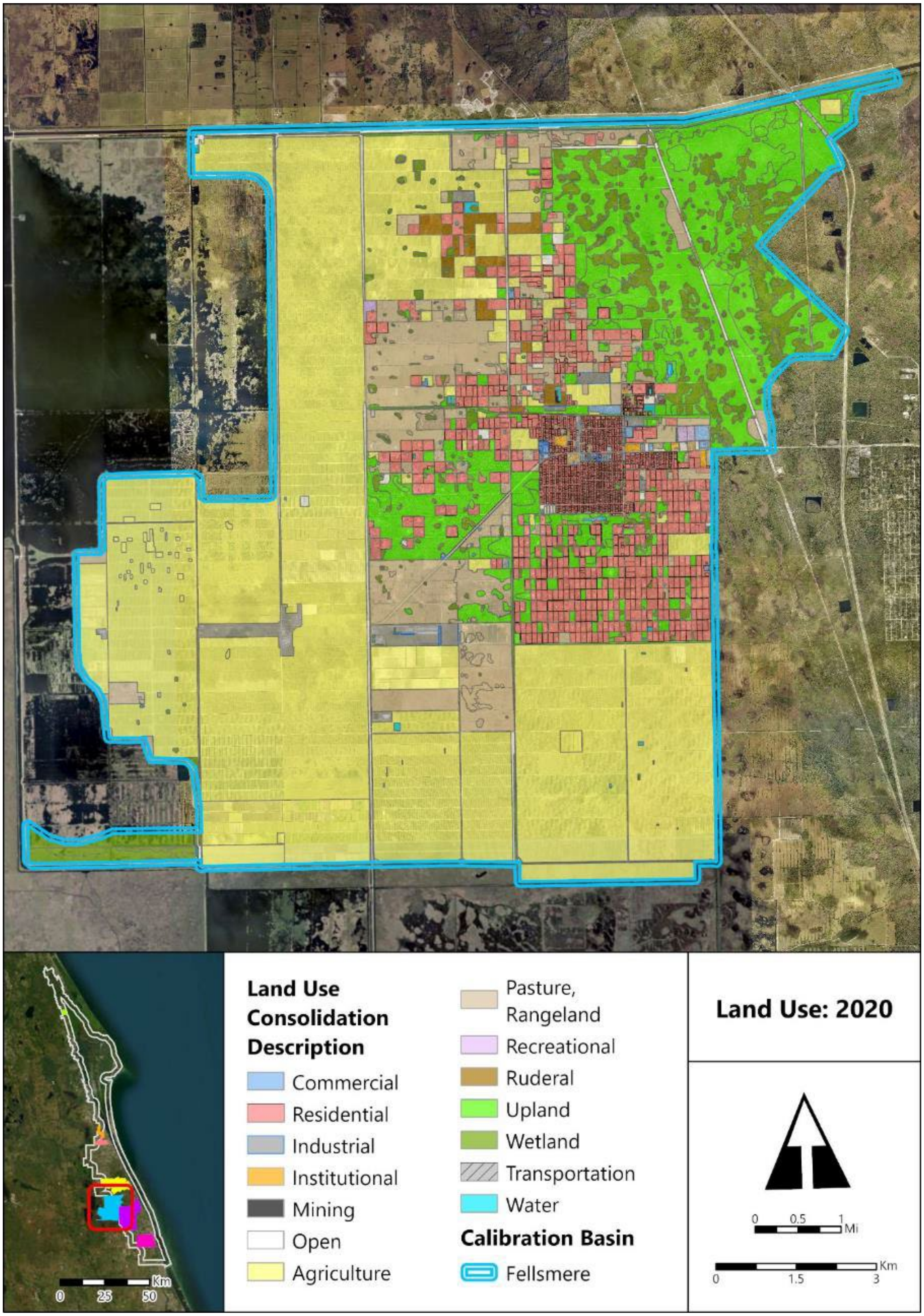

Figure 104. Land use within the Fellsmere calibration basin for 2015.

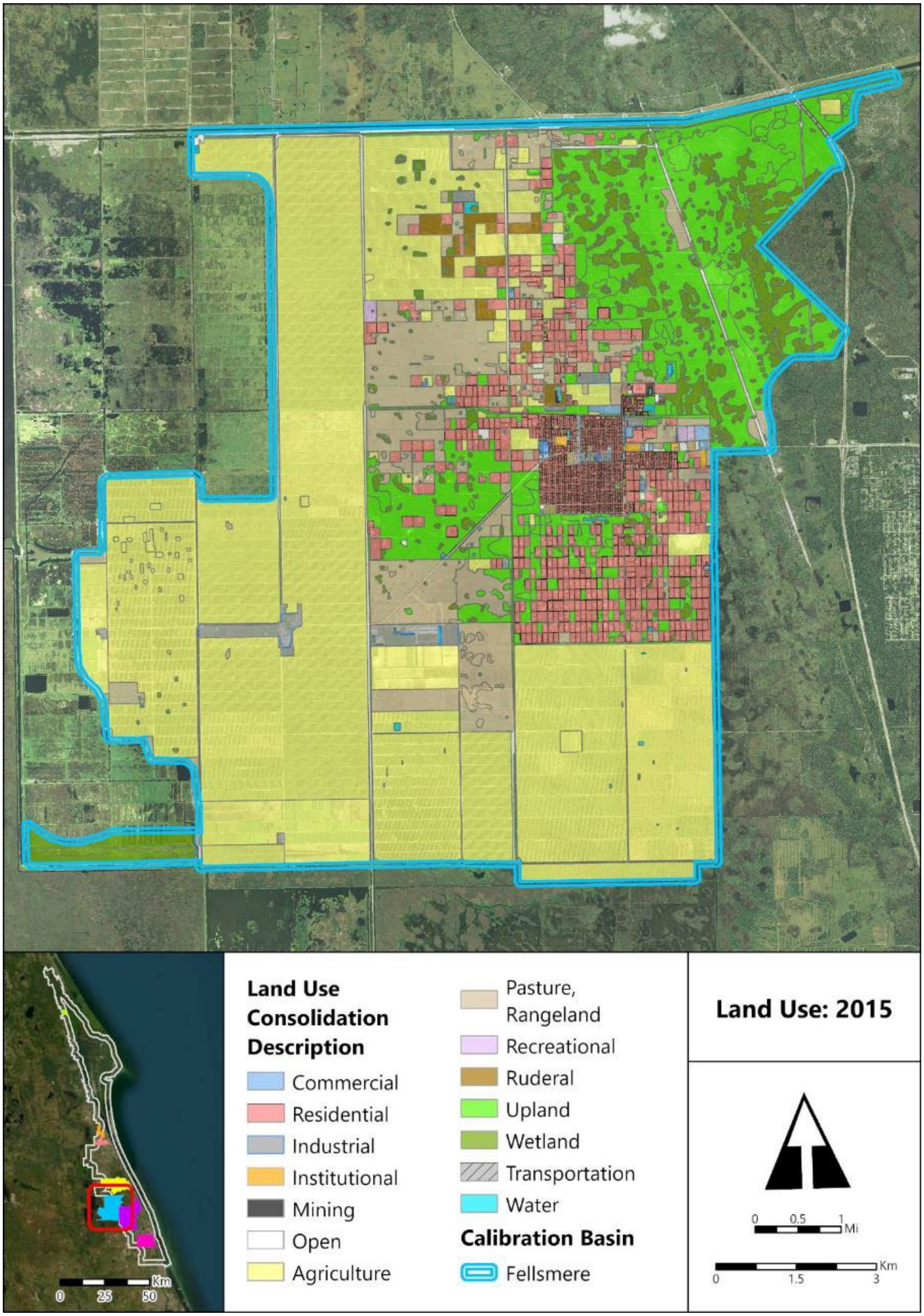

Figure 105. Land use within the Fellsmere calibration basin for 2020.

2.6.2 Soil Type

The Fellsmere calibration basin is primarily composed of the A/D (38%), B/D (36%), and C/D (24%) hydrologic soil groups (Figure 106); the remaining soils (A and water) make up approximately 2% of the total basin area. The C/D soils are located in the central to the southwestern portion of the basin, the B/D soils have two major patches along the central-southeast region, and there are small patches of A soils distributed in the northeast corner (Figure 107). The A/D soils fill in a majority of the remaining area.

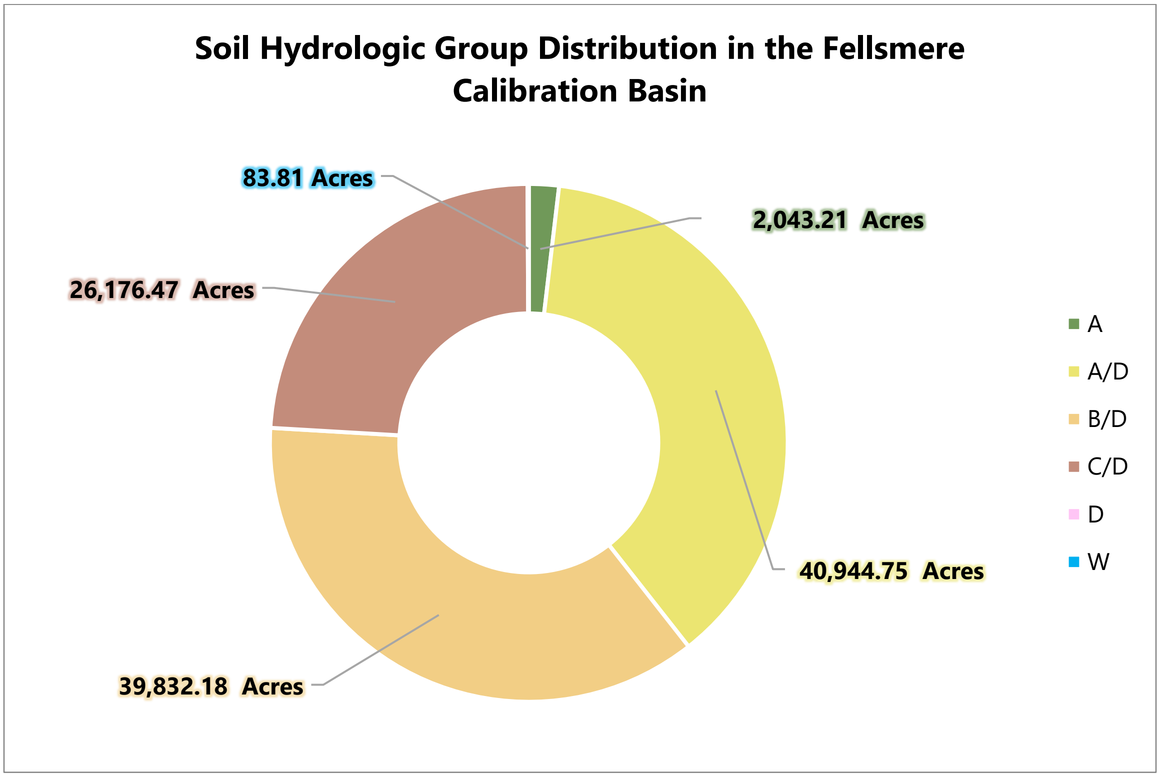

Figure 106. Pie chart (acres) of the soil hydrologic group distribution in the Fellsmere calibration basin using USDA NRCS data.

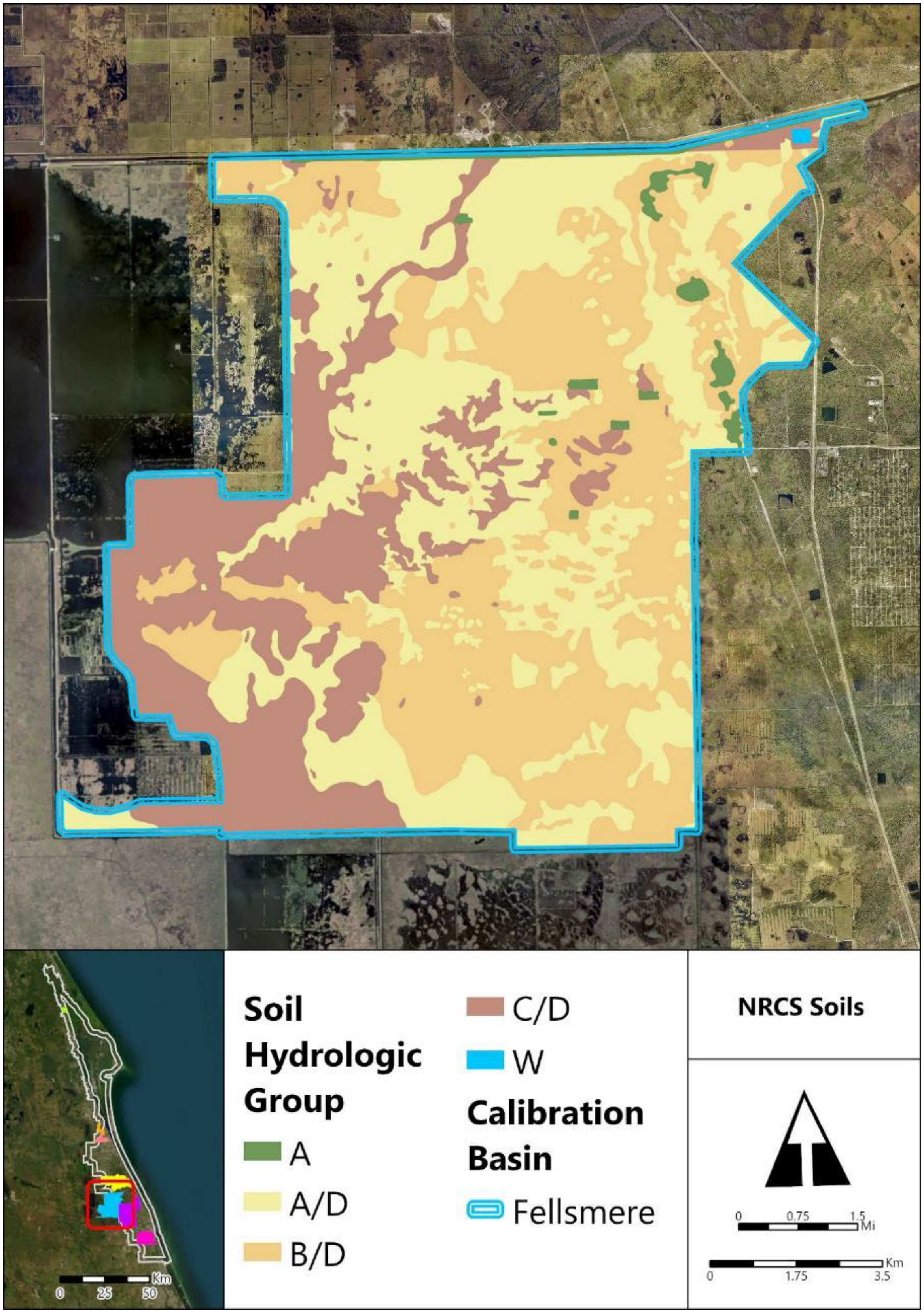

Figure 107. Distribution of soil hydrologic groups within the Fellsmere calibration basin.

2.6.3 PRECIPITATION

The annual total precipitation for Fellsmere ranges from the lowest annual total of 31 inches in 2010 to the highest annual total of 62 inches in 2017 (Figure 108). For all years, the dry season has a lower total seasonal rainfall as compared to the wet seasons of the same years (Figure 109). The average monthly precipitation values are higher from May to October and lower from November to April (Figure 110). Maps for the monthly precipitation averages (inches/month) during February and September across the POR for the Fellsmere calibration basin are provided in Figure 111 and Figure 112, respectively.

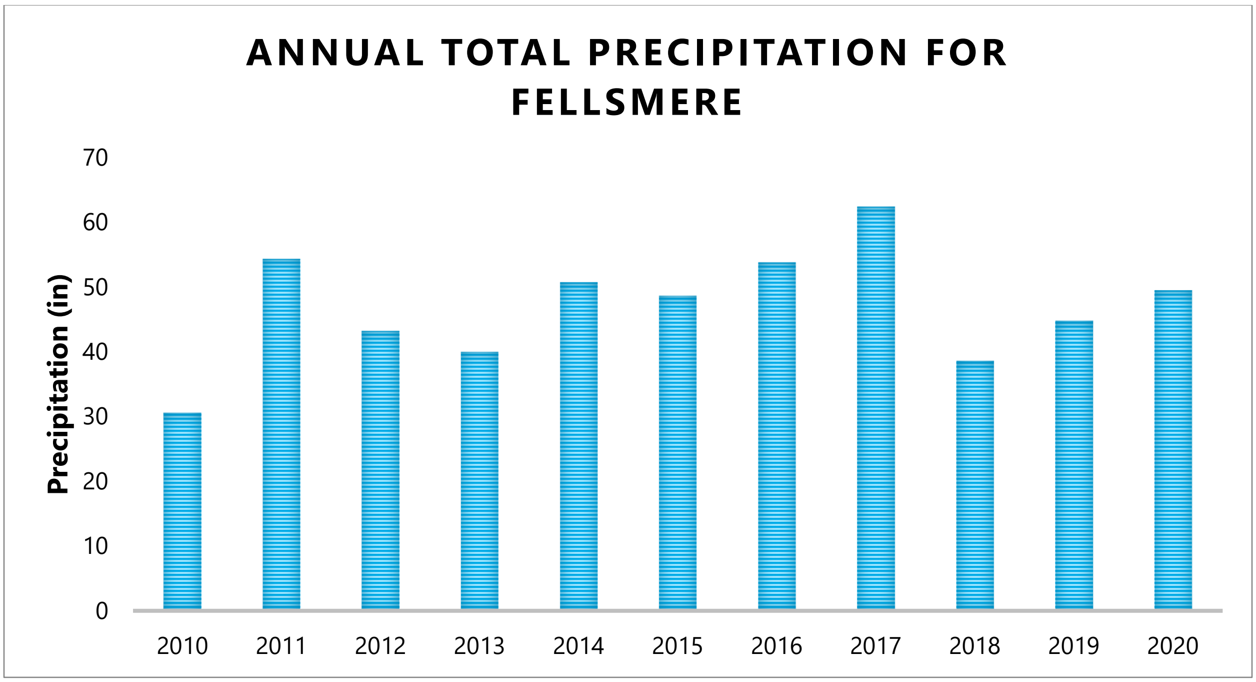

Figure 108. Annual total precipitation (in) for the Fellsmere calibration basin from 2010 to 2020 derived from SJRWMD NEXRAD data.

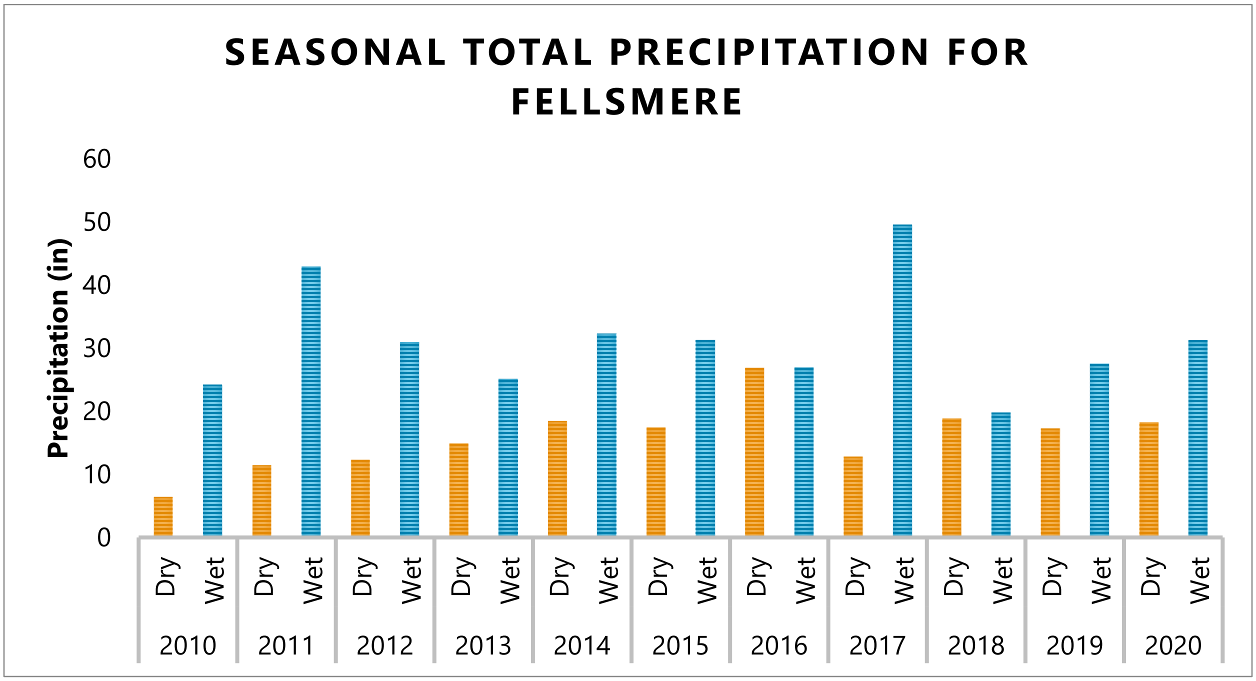

Figure 109. Seasonal total precipitation (in) for the Fellsmere calibration basin from 2010 to 2020 derived from SJRWMD NEXRAD data.

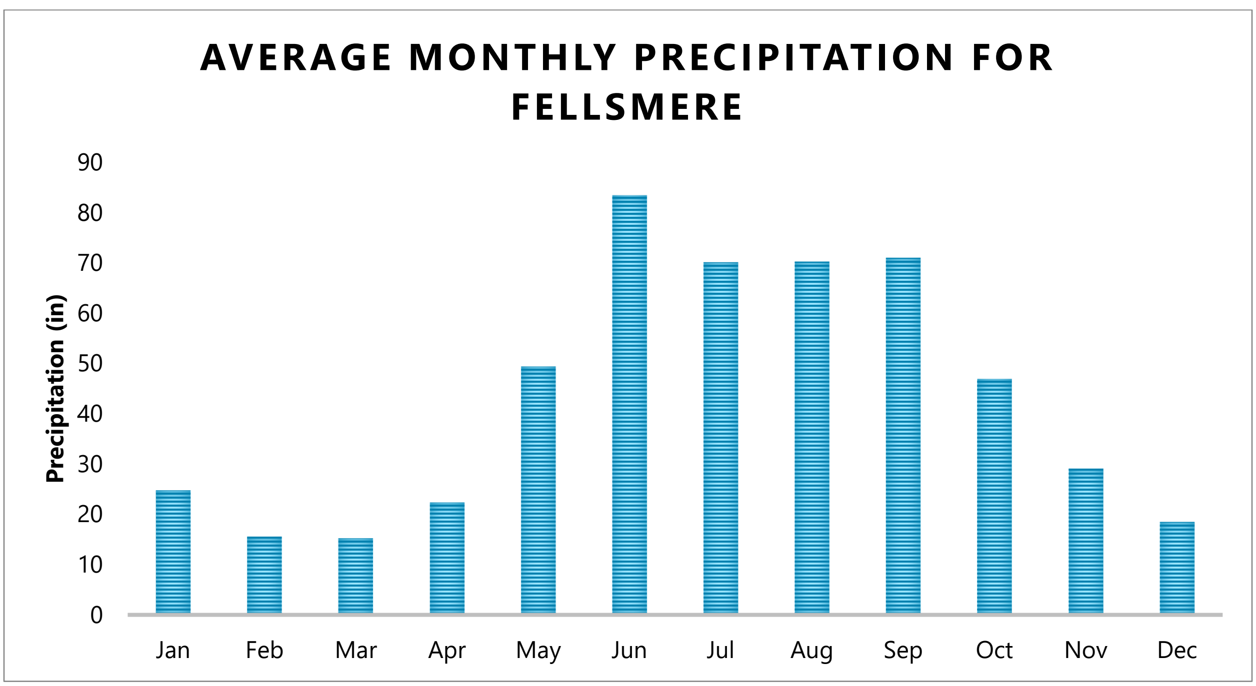

Figure 110. Average monthly precipitation (in) for the Fellsmere calibration basin derived from SJRWMD NEXRAD data.

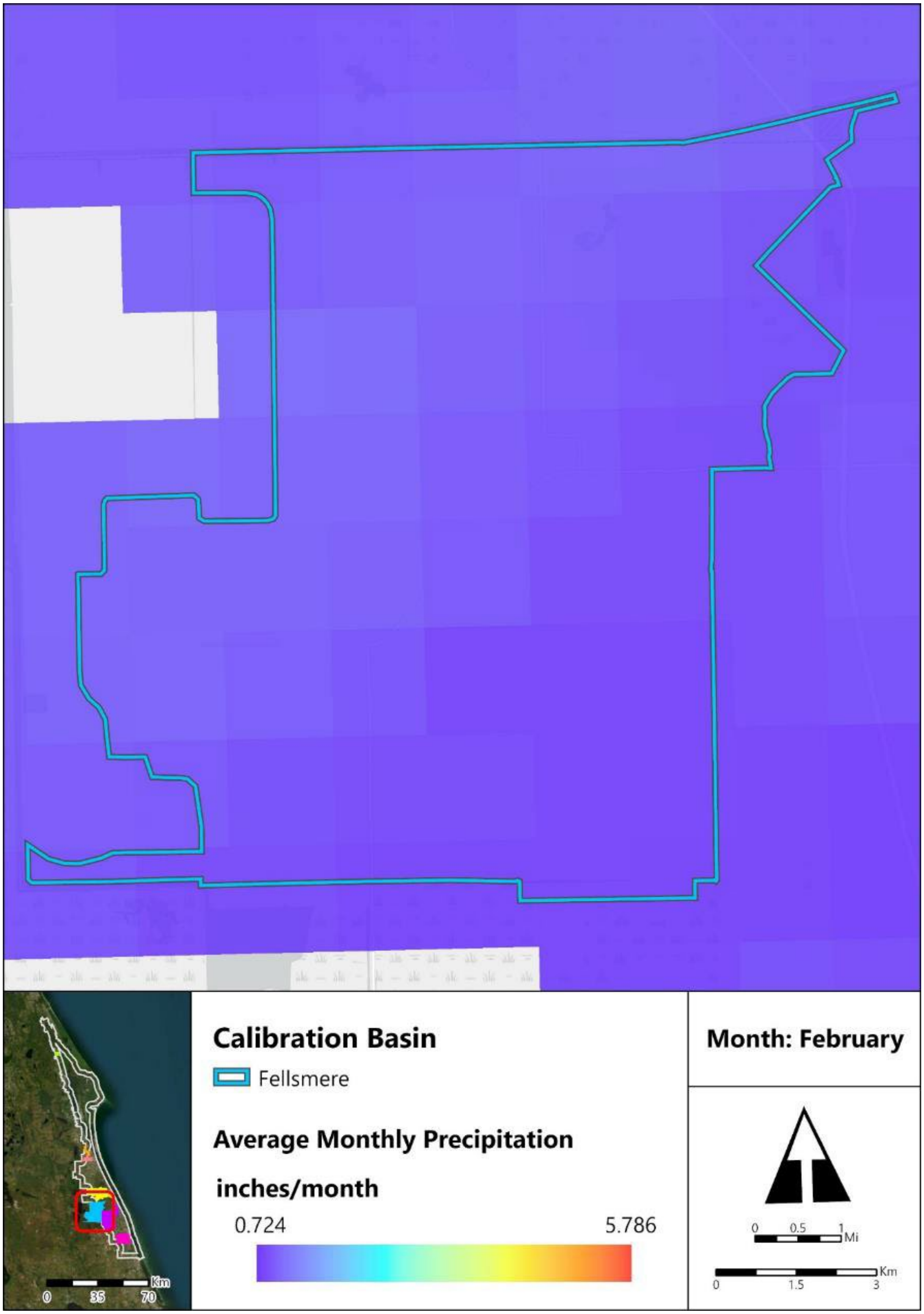

Figure 111. Average monthly precipitation (inches/month) for February across the period of record in the Fellsmere calibration basin.

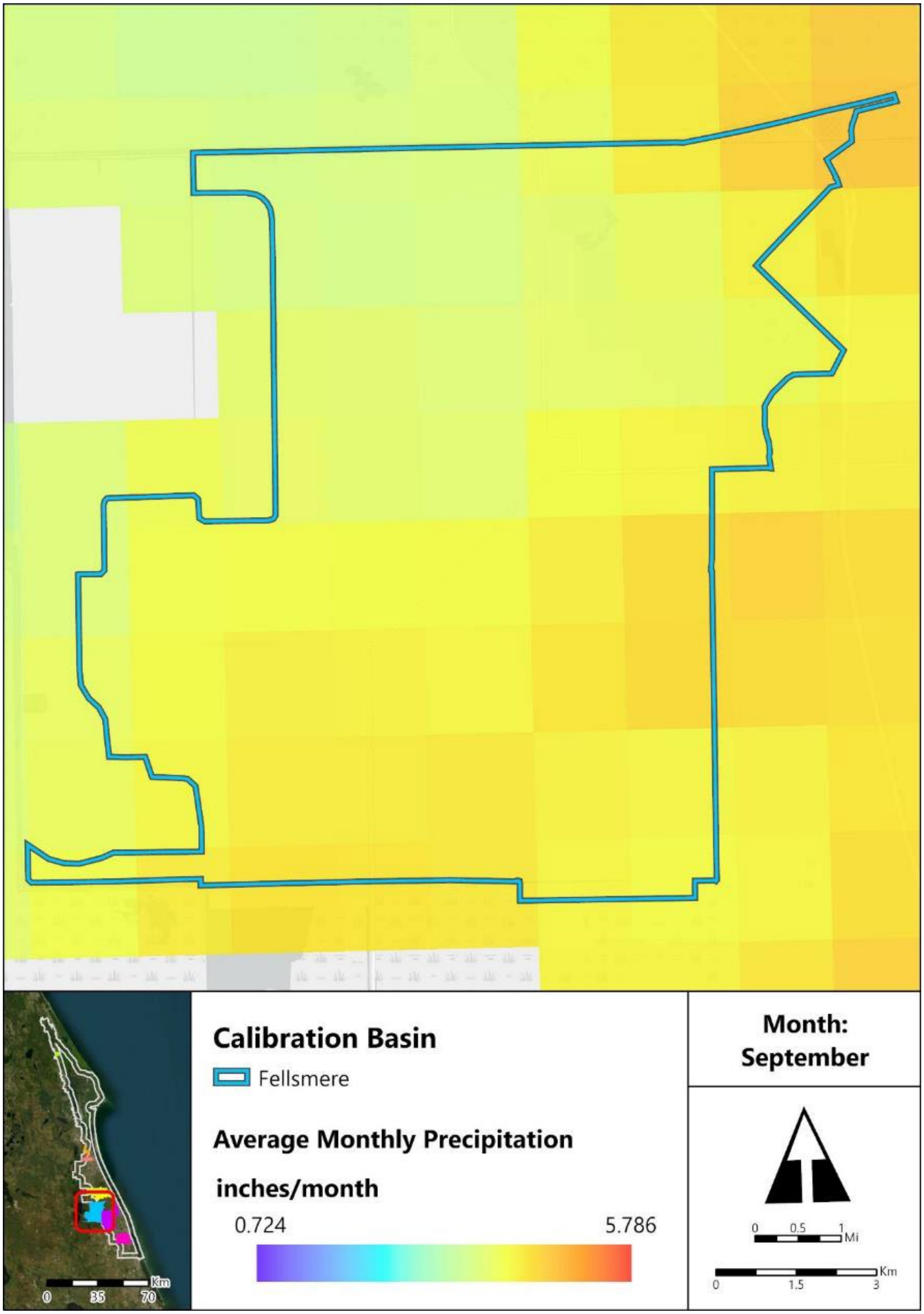

Figure 112. Average monthly precipitation (inches/month) for September across the period of record in the Fellsmere calibration basin.

2.6.4 ET

Summary statistics for the monthly mean ET in the Fellsmere calibration basin are provided as a boxplot (Figure 113). There is a lower variation in the wet and dry seasonal ET rates than in some of the previously described calibration basins, with an observed general trend of increases in ET rates through the wet season and decreases in the dry season. The lowest median value and lowest variability in ET rates are seen in the dry season, where there are generally lower temperatures. The greatest median ET and highest variability are seen in the wet season, where there are generally higher temperatures. The lowest median value was observed in January and December (1.27 mm/day), whereas the highest median was observed in July and August (2.95 mm/day). The highest variability was observed in May, with a 0.72 mm/day difference within the interquartile range, and the lowest variability was observed in January, with a 0.11 mm/day interquartile range difference. Maps for mean monthly ET rates (mm/day) during February and September across the POR in the Fellsmere calibration basin are provided in Figure 114 and Figure 115, respectively.

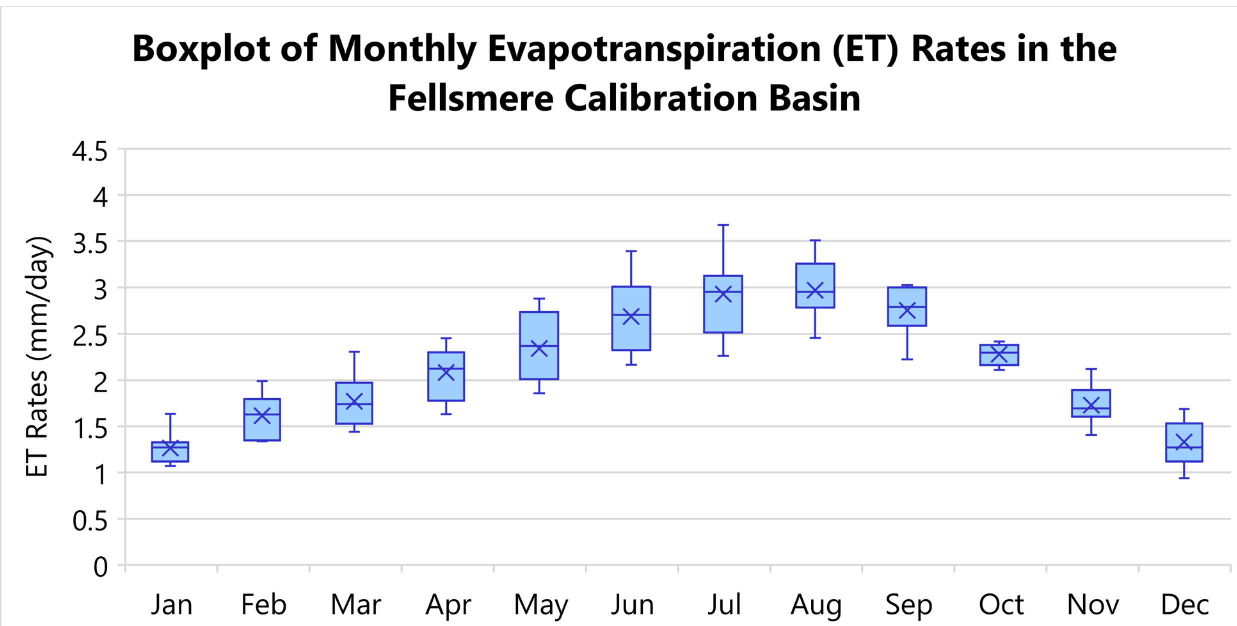

Figure 113. Boxplot of monthly mean ET rates in the Fellsmere calibration basin derived from NASA EarthData and the University of Montana data.

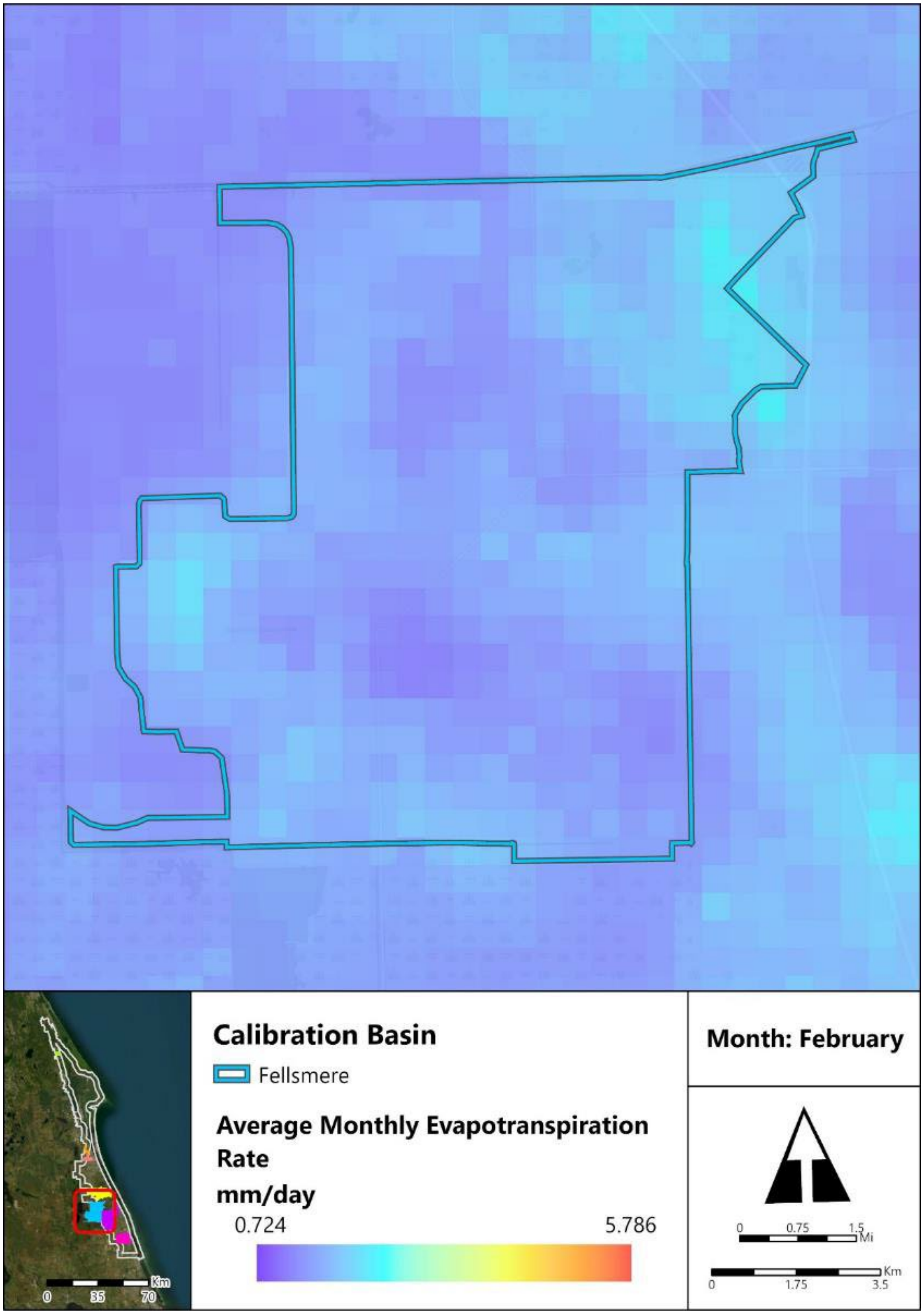

Figure 114. Average monthly ET rates (mm/day) for February across the period of record in the Fellsmere calibration basin.

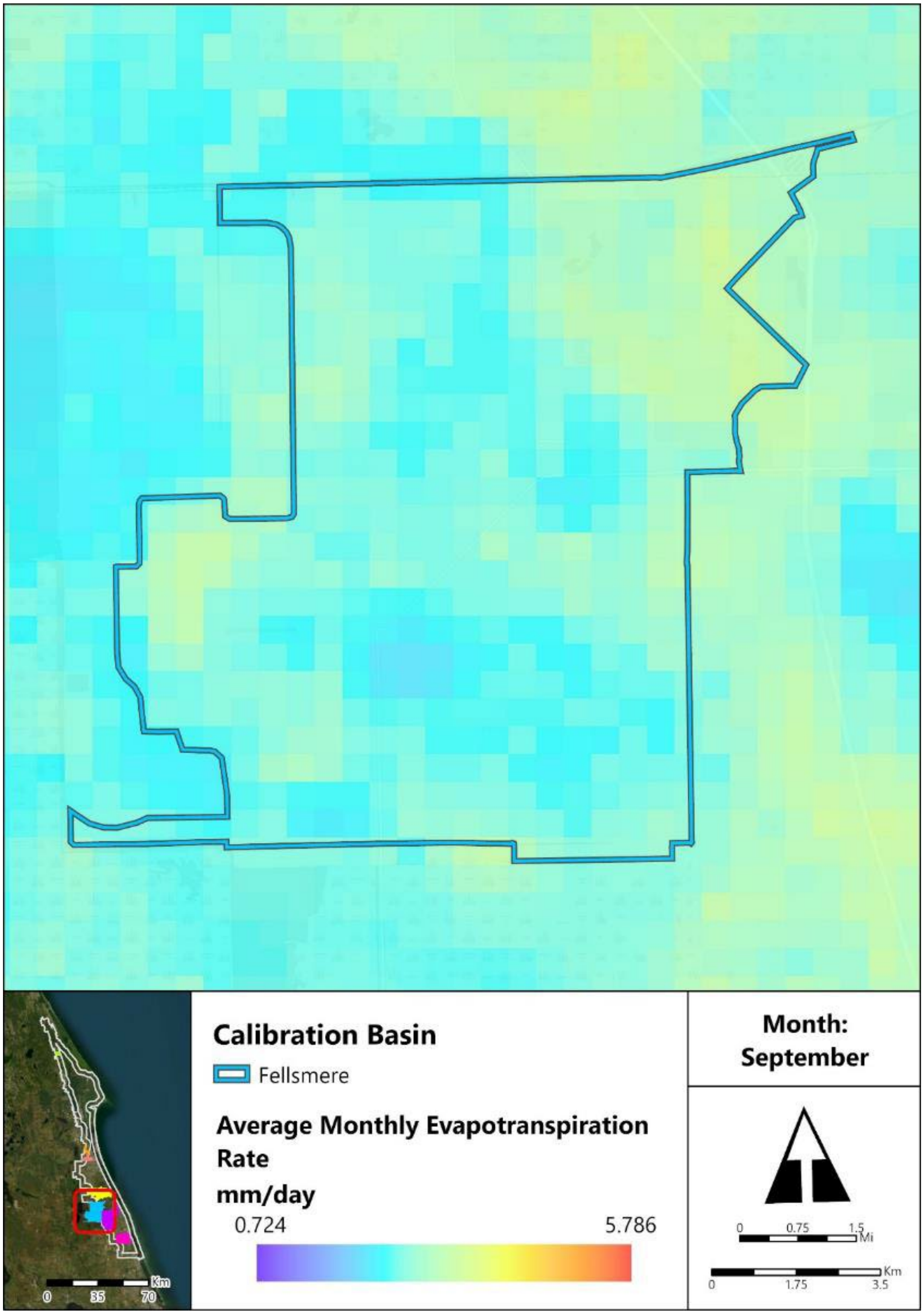

Figure 115. Average monthly ET rates (mm/day) for February across the period of record in the Fellsmere calibration basin.

2.6.5 TREATMENTS

Within Fellsmere, approximately 15% of the basin's total area is treated (Table 19), with almost all the treatments being composed of the wet type (13%). Overall, minimal changes occurred within the Fellsmere calibration basin, but the largest changes occurred between 2010 and 2020, with approximately a 1% increase in the treated area using wet treatments, likely a result of increases in residential land use types (Figure 116, Figure 117, Figure 118).

Table 19. Total area (acres) of each treatment type in the Fellsmere calibration basin for the 2010, 2015, and 2020 years.

Treatment Type	Treatment Area (Acres)			Percent of Total Basin Area (%)			Percent Change (%)	
	2010	2015	2020	2010	2015	2020	2015-2010	2020-2010
Dry	1,001.10	1,035.87	1,049.09	2.75	2.85	2.89	0.10	0.13
Wet	4,447.69	4,589.37	4,773.24	12.23	12.62	13.13	0.39	0.90
Total	*5,448.79*	*5,625.23*	*5,822.33*	*14.99*	*15.47*	*16.01*	*0.49*	*1.03*

**The percentage of the total basin area and the percent change from the overall area between 2010 and 2015, as well as 2010 and 2020 have also been provided.*

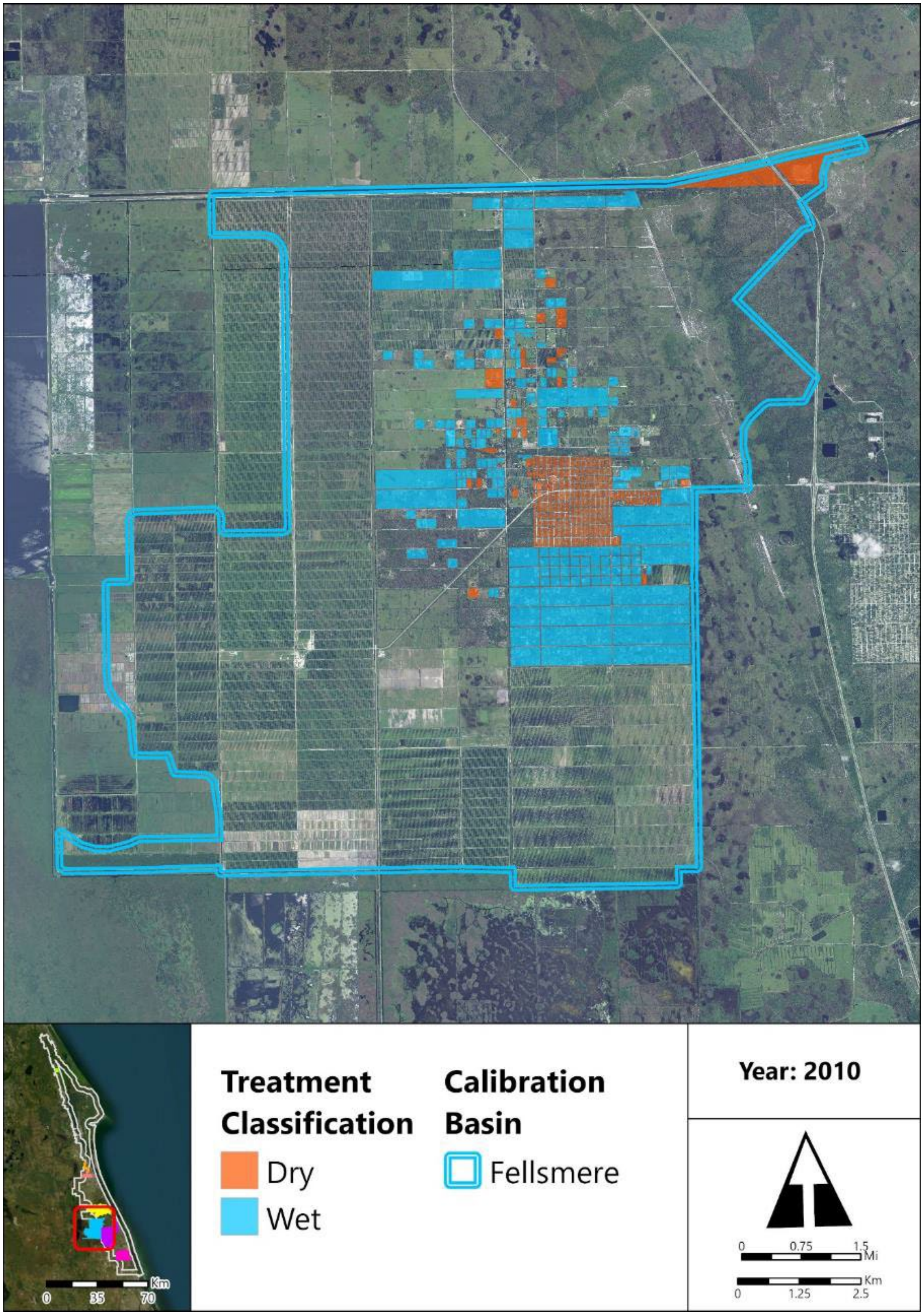

Figure 116. Treatments within the Fellsmere calibration basin for 2010.

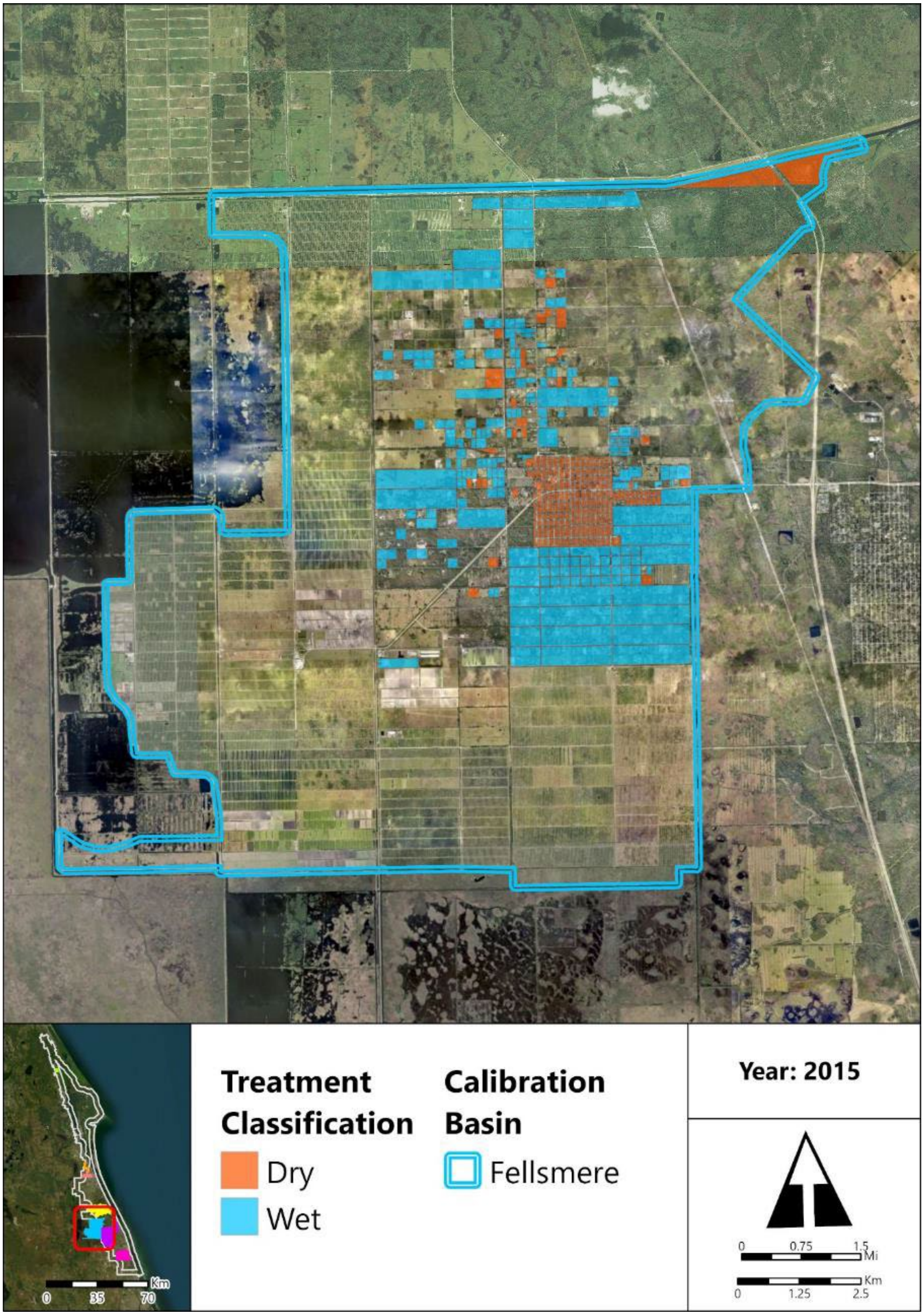

Figure 117. Treatments within the Fellsmere calibration basin for 2015.

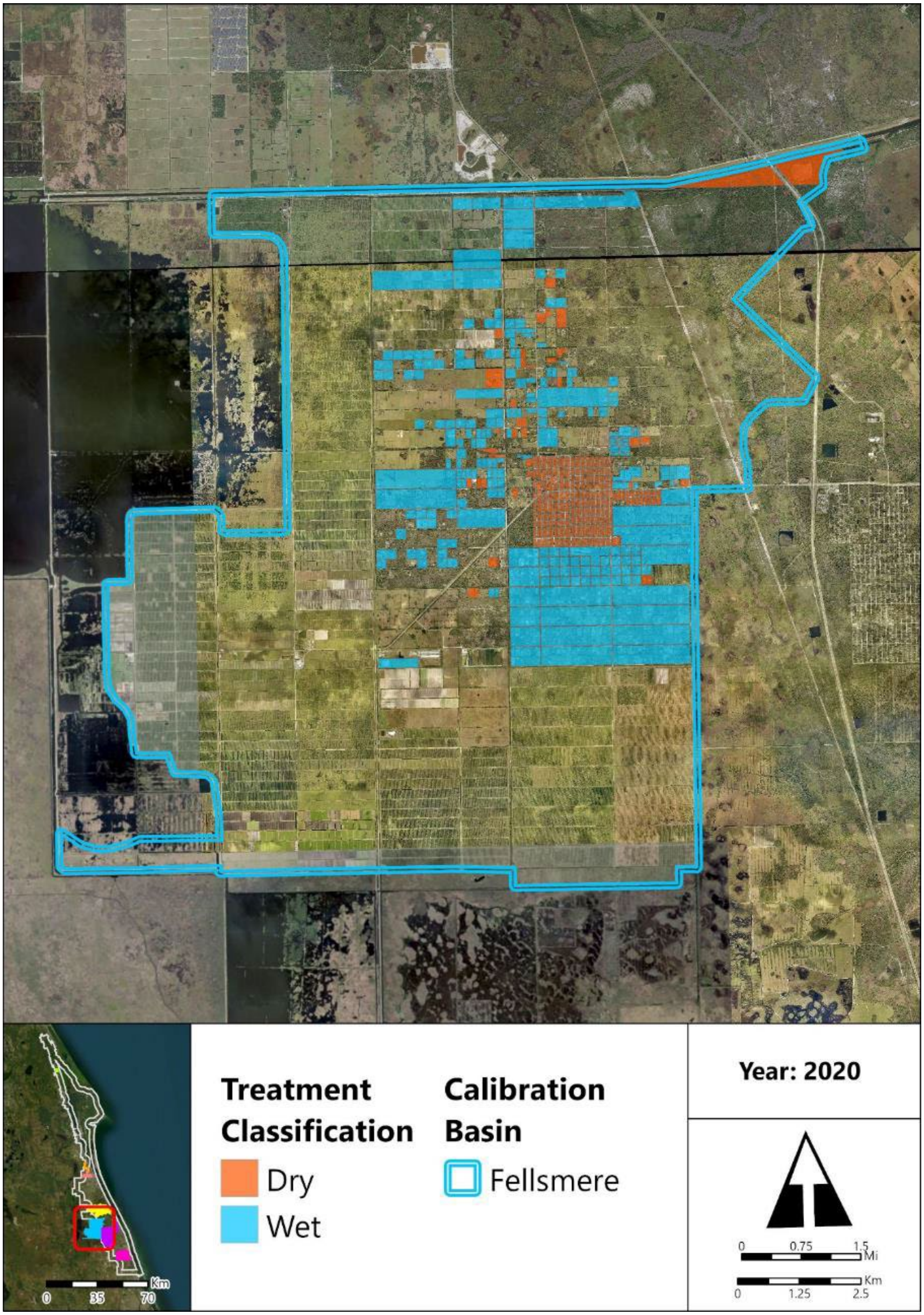

Figure 118. Treatments within the Fellsmere calibration basin for 2020.

2.6.6 Hydrology

The Fellsmere calibration basin volume is dominated by subsurface flow monthly (~77%), seasonally (~79% in the dry season and ~74% in the wet season), and annually (~76%) from 2010 to 2020. The average monthly volumes are higher from June to November, with lower volumes from December to May for the POR (Figure 119). The 2011 and 2017 wet seasons showed the highest volumes of discharge, and the lowest seasonal volumes were observed in the 2011 and 2013 dry seasons as well as the 2018 wet season (Figure 120). The greatest annual volumes were observed to increase from 2010 through 2017, with a sharp decrease in annual volumes in 2018, followed by an increasing trend from 2018 through 2020 (Figure 121).

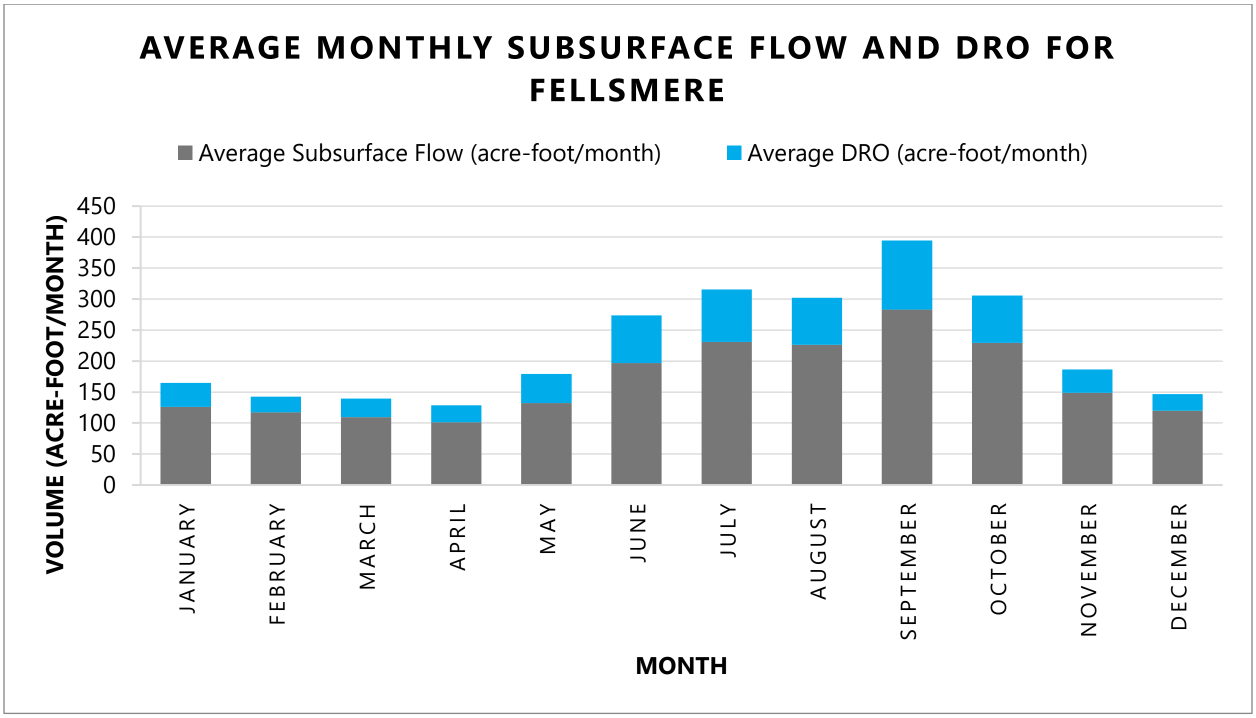

Figure 119. Average monthly subsurface flow (acre-foot/month) and DRO (acre-foot/month) for the Fellsmere calibration basin derived from USGS WHAT data.

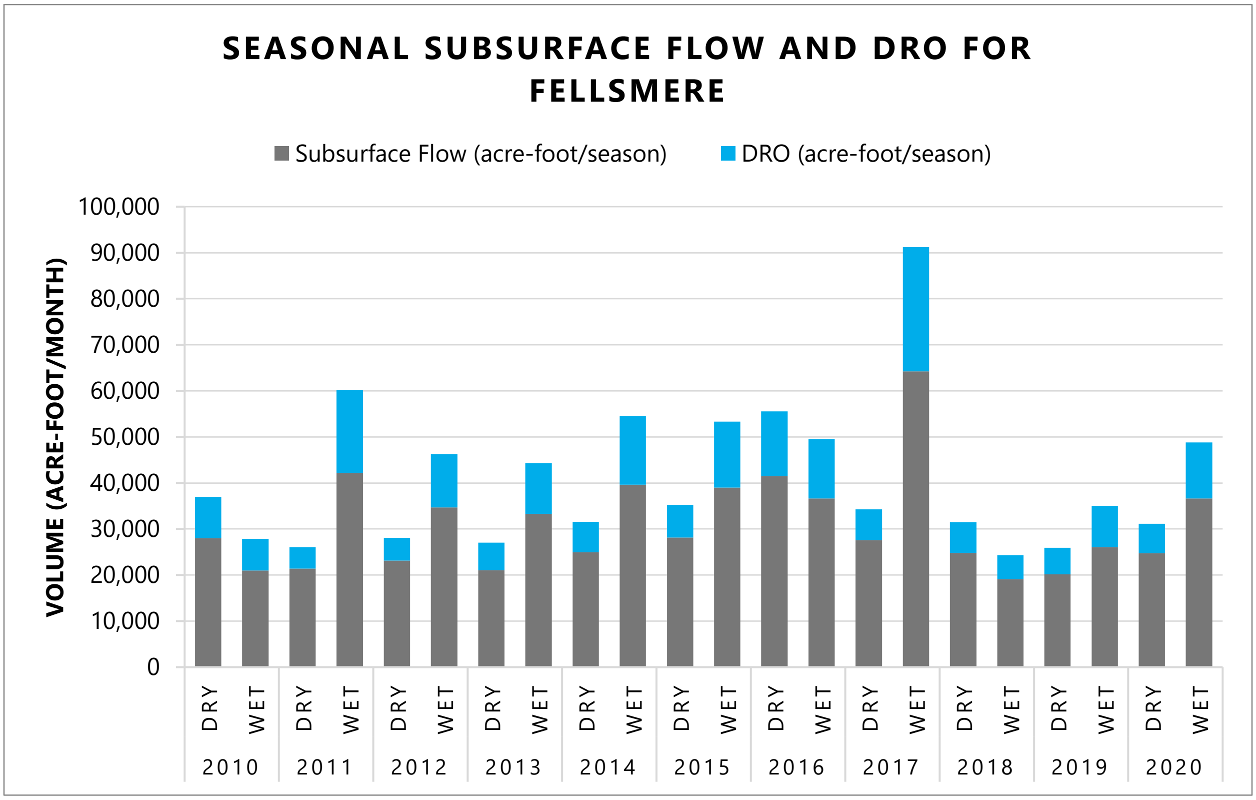

Figure 120. Seasonal subsurface flow (acre-foot/season) and DRO (acre-foot/season) for the Fellsmere calibration basin derived from USGS WHAT data.

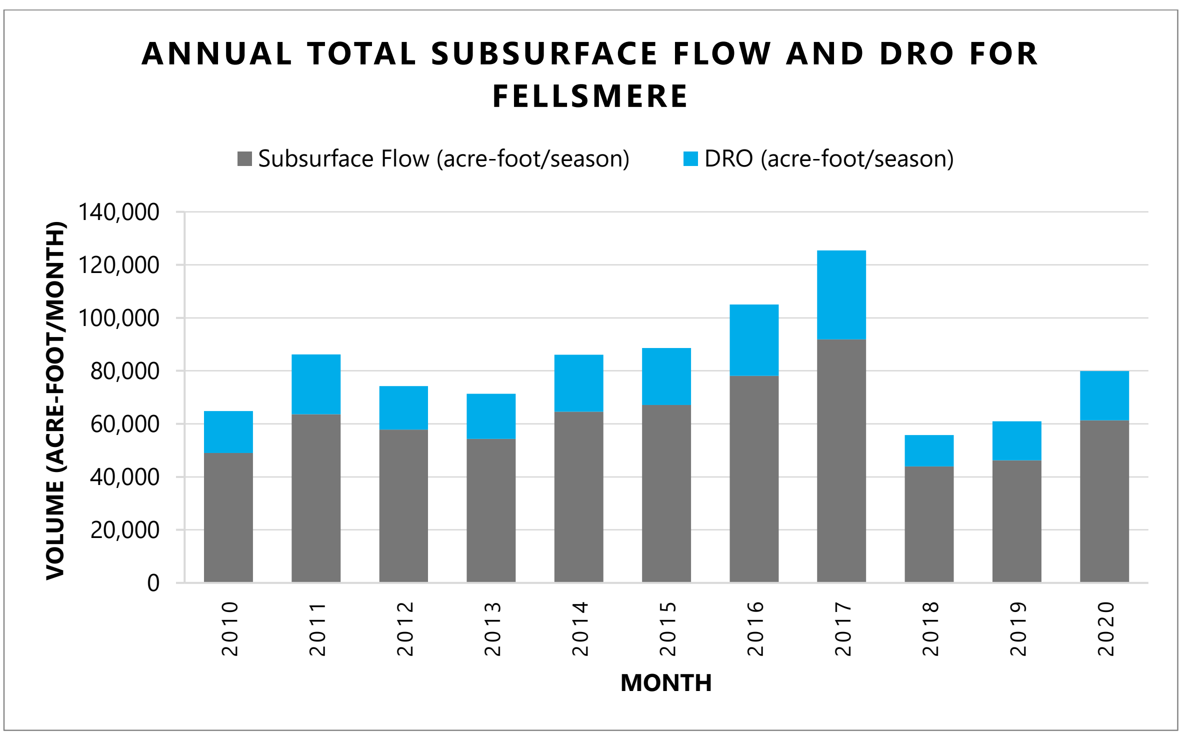

Figure 121. Annual subsurface flow (acre-foot/year) and DRO (acre-foot/year) for the Fellsmere calibration basin derived from USGS WHAT data.

2.6.7 Water Quality

From 2011 to 2020, there were a total of 112 samples collected from the Fellsmere Canal at IRLUPSFW by SJRWMD; no samples were collected during 2010. Three samples coincided with DRO conditions, 70 coincided with subsurface flow conditions, and the remaining 39 were under mixed conditions (Table 20). As there are only three data points (2011, 2013, and 2016) for DRO concentrations across the POR, annual and seasonal trends for either nutrient cannot be interpreted.

The annual mean TN subsurface flow concentrations from 2011 to 2020 appeared to be on an overall downward trend, albeit the increase in geometric mean concentration in 2015 was the only one to reach above 1.0 mg/L (Figure 122). Variability in annual geometric mean TP subsurface flow concentrations is lower than those observed in TN, only ranging from 0.09 to 0.17 mg/L. in concentration. Although no trends can be determined, the singular data points for DRO concentrations of both nutrients are higher than those observed for subsurface flow.

Table 20. Geometric means of annual TN (mg/L) and TP (mg/L) subsurface flow and DRO samples collected by SJRWMD from 2010 to 2020 at the Fellsmere station IRLUPSFW.

Year	TN - DRO	TP - DRO	TN - Subsurface flow	TP - Subsurface flow
2010				
2011	0.968	0.279	0.934	0.122
2012			0.819	0.101
2013	1.531	0.353	0.833	0.090
2014			0.838	0.115
2015			1.131	0.165
2016	1.534	0.249	0.986	0.149
2017			0.820	0.167
2018			0.717	0.107
2019			0.657	0.086
2020			0.777	0.108

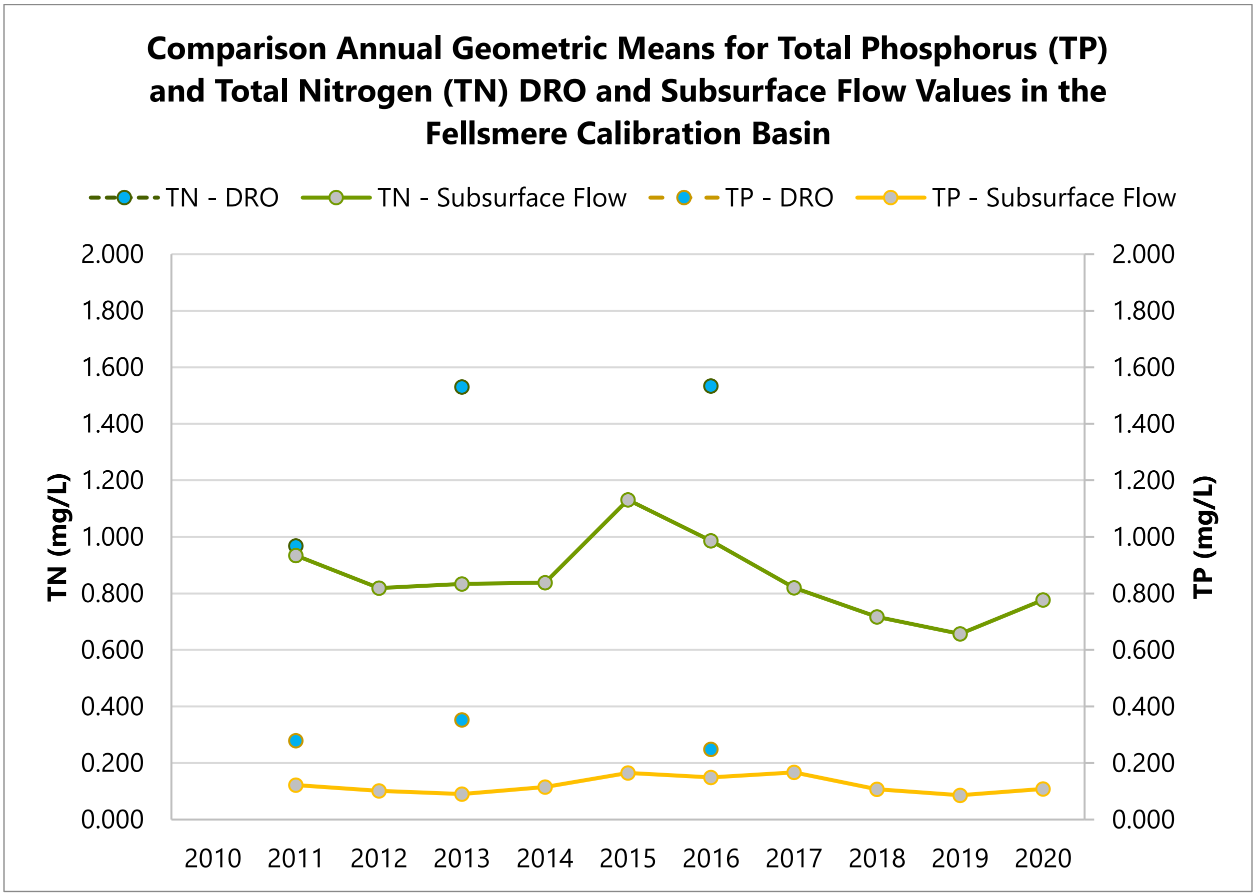

Figure 122. Comparison of the annual geometric means of TN (mg/L) and TP (mg/L) for subsurface flow and DRO between 2010 and 2020 for the Fellsmere calibration basin.

Although there is a higher degree of variability in geometric mean concentrations of TN, similar patterns in seasonal geometric mean concentrations of subsurface flow are observed for TN and TP throughout the POR (Figure 123). Additionally, both nutrients have lower concentrations in the dry season and higher concentrations in the wet season, with the exception of the seasonal TN subsurface flow concentration increase between the 2015 wet into the 2015 dry season.

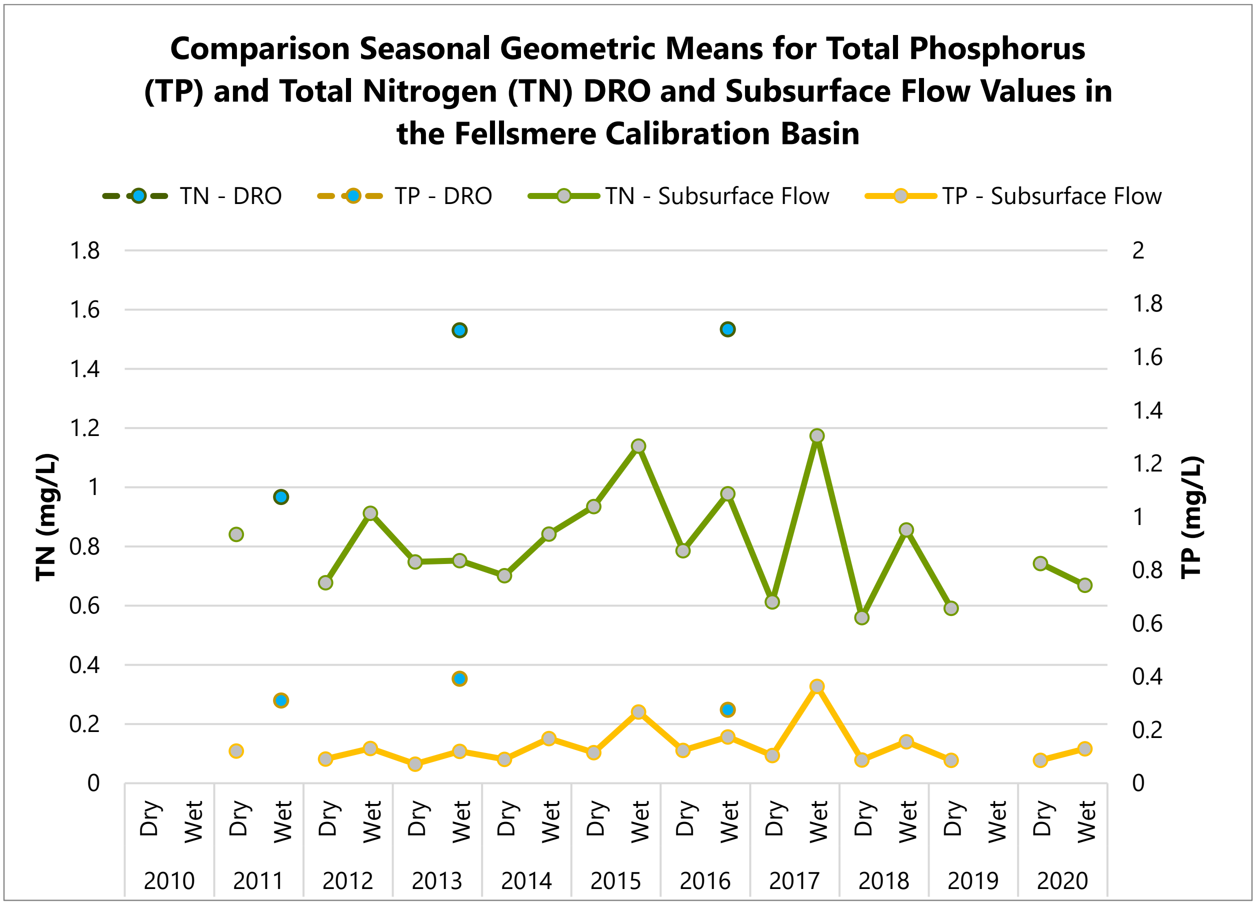

Figure 123. Comparison of the seasonal geometric means of TN (mg/L) and TP (mg/L) for subsurface flow and DRO between 2010 and 2020 for the Fellsmere calibration basin.

2.7 South Canal

2.7.1 LULC Change

The South Canal calibration basin has been predominately composed of medium density residential (~24%), low density residential (~16%), improved pasture (~15%), high density residential (~6%), and upland flatwoods (~5%) land use consolidation types (Table 21). The agricultural, pasture, and rangelands encompass the southwestern regions of the basin, the natural (i.e., upland) types are located in the central-eastern portion of the basin, and the residential areas are found in the central to northeast portion as well as the southeast corner (Figure 103, Figure 104, Figure 105). Changes that have occurred within the South Canal calibration basin are primarily due to a change in classification from open to pasture lands by the SJRWMD from 2010 to 2015 within the western side of the basin, as well as the conversion of citrus or field and row crops to pasture lands, with some increases in residential areas.

Table 21. Total area (in acres and percentage) of each land use consolidation type in the South Canal calibration basin for the 2010, 2015, and 2020 years.

Land Use Consolidation	Land Use Area (Acres)			Percent of Total Land Use (%)			Percent Change (%)	
	2010	2015	2020	2010	2015	2020	2015 - 2010	2020 - 2010
Citrus	**1,536.42**	437.54	447.65	**8.99**	2.56	2.62	-6.43	-6.37
Commercial	359.14	391.79	399.65	2.10	2.29	2.34	0.19	0.24
Dry Prairie	241.83	472.65	359.64	1.42	2.77	2.11	1.35	0.69
Field Crop	396.92	7.08	--	2.32	0.04	--	-2.28	--
High Density Residential	937.46	**977.24**	**1,090.40**	5.49	**5.72**	**6.38**	0.23	0.90
Hydric Hammock	--	--	--	--	--	--	--	--
Improved Pasture	**1,867.46**	**2,908.10**	**3,040.74**	**10.93**	**17.02**	**17.80**	6.09	6.87
Industrial	139.55	165.30	160.33	0.82	0.97	0.94	0.15	0.12
Institutional	539.46	428.10	453.43	3.16	2.51	2.65	-0.65	-0.50
Low Density Residential	**2,666.97**	**2,748.06**	**2,962.11**	**15.61**	**16.08**	**17.34**	0.47	1.73
Medium Density Residential	**4,046.46**	**4,113.62**	**4,309.63**	**23.68**	**24.07**	**25.23**	0.39	1.55
Mesic Flatwoods	--	--	--	--	--	--	--	--
Mining	--	--	--	--	--	--	--	--
Open	**1,067.47**	595.44	422.38	**6.25**	3.48	2.47	-2.76	-3.77
Other Agriculture	193.21	482.86	322.96	1.13	2.83	1.89	1.70	0.76
Rangeland	338.10	608.39	500.29	1.98	3.56	2.93	1.58	0.95
Recreational 1	146.11	145.86	145.86	0.86	0.85	0.85	0.00	0.00
Recreational 2	16.75	90.37	90.37	0.10	0.53	0.53	0.43	0.43

Land Use Consolidation	**Land Use Area (Acres)**			**Percent of Total Land Use (%)**			**Percent Change (%)**	
	2010	**2015**	**2020**	**2010**	**2015**	**2020**	**2015 - 2010**	**2020 - 2010**
Row Crops	276.16	15.88	15.88	1.62	0.09	0.09	-1.52	-1.52
Ruderal	191.24	415.94	382.25	1.12	2.43	2.24	1.32	1.12
Scrub	314.38	299.81	250.12	1.84	1.75	1.46	-0.09	-0.38
Transportation	74.66	77.07	77.06	0.44	0.45	0.45	0.01	0.01
Upland Flatwoods	817.30	**825.02**	**787.95**	4.78	**4.83**	**4.61**	0.05	-0.17
Upland Mixed	--	0.49	--	--	0.00	--	--	--
Water	541.04	584.03	566.74	3.17	3.42	3.32	0.25	0.15
Wet Flatwoods	203.99	130.39	122.62	1.19	0.76	0.72	-0.43	-0.48
Wet Prairies	17.02	12.55	12.15	0.10	0.07	0.07	-0.03	-0.03
Wetland	153.36	148.92	155.39	0.90	0.87	0.91	-0.03	0.01
Xeric Hammock	4.76	4.73	4.73	0.03	0.03	0.03	0.00	0.00
Total	*17,087.24*	*17,087.24*	*17,087.24*	*100*	*100*	*100*		

**The top five land uses that make up a majority of the area have been bolded for each year. Percent change from the overall area between 2010 and 2015, as well as 2010 and 2020 have also been provided.*

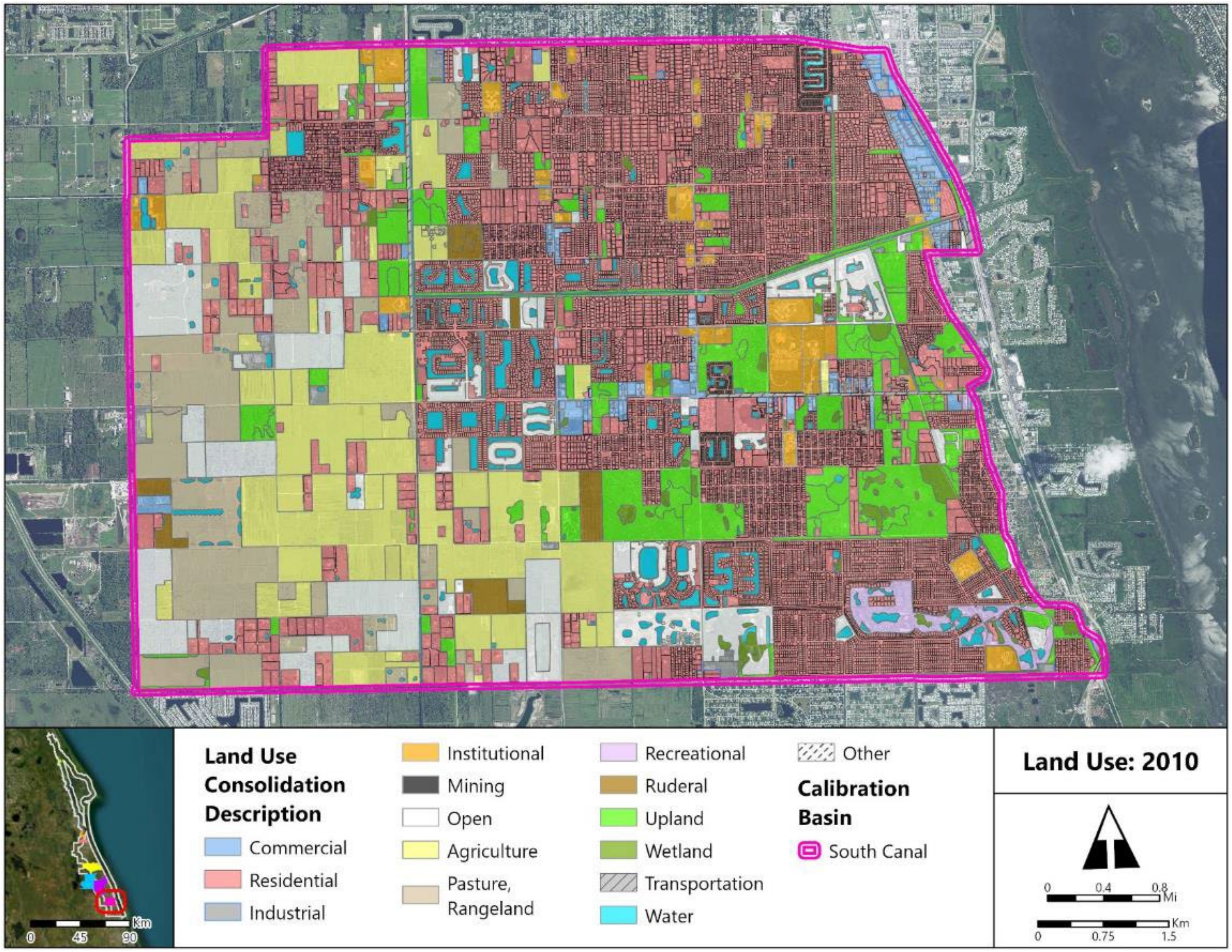

Figure 124. Land use within the South Canal calibration basin for 2010.

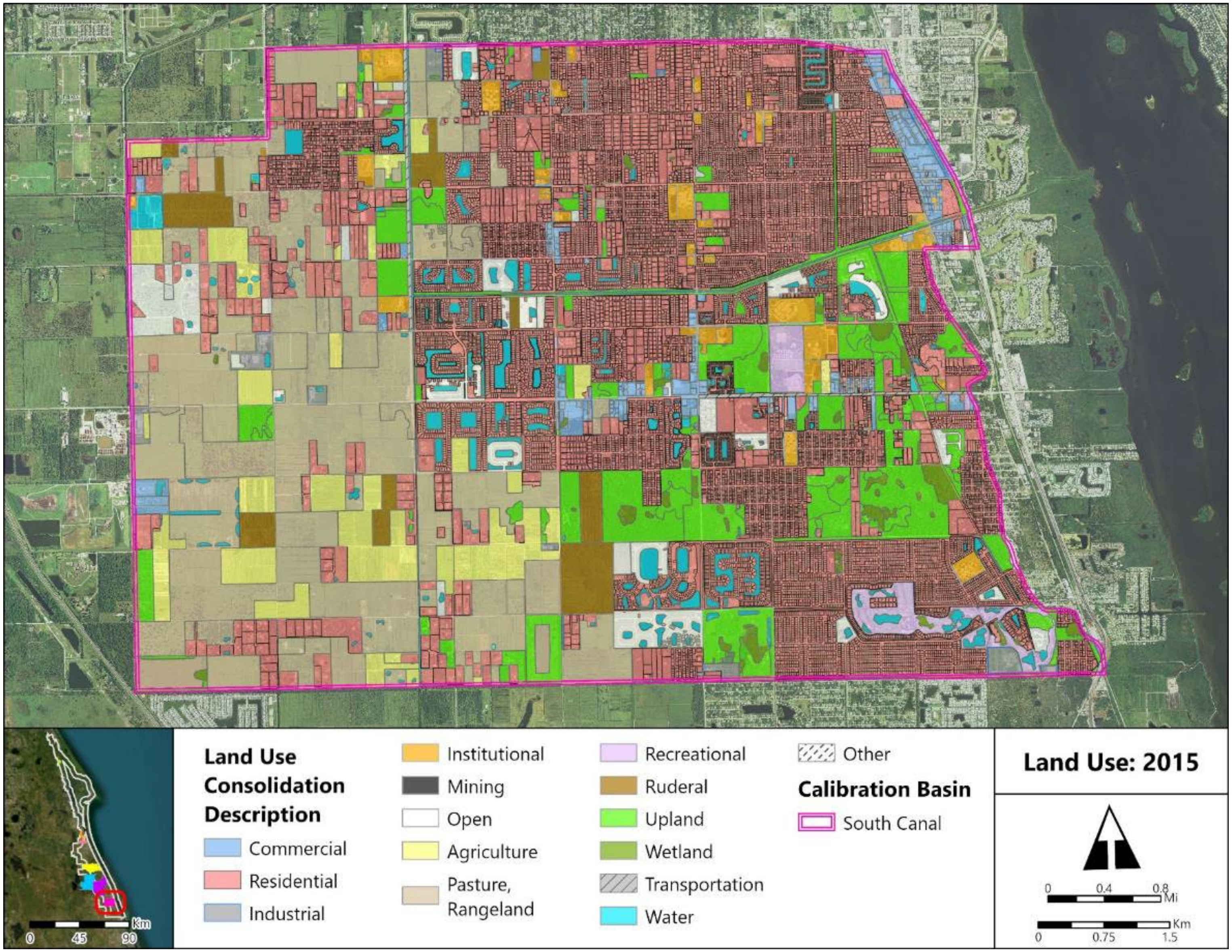

Figure 125. Land use within the South Canal calibration basin for 2015.

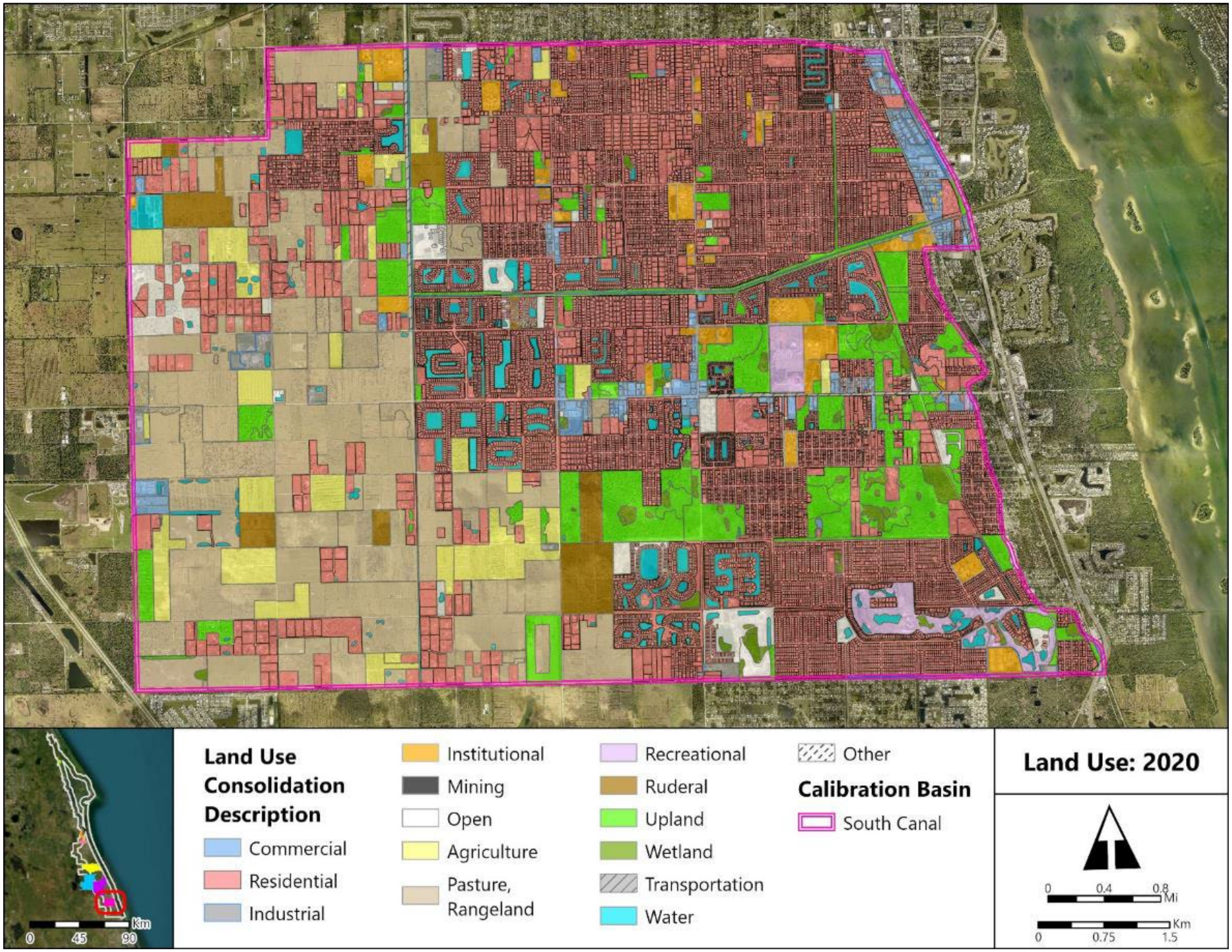

Figure 126. Land use within the South Canal calibration basin for 2020.

2.7.2 Soil Hydrologic Group

The South Canal calibration basin is primarily composed of the A/D (41%), B/D (26%), and C/D (25%) hydrologic soil groups, followed by the A soils (7%) and water which is less than 1% of the total basin area (Figure 127). The C/D soils are concentrated in the central to the western portion of the basin, the B/D soils have two major patches along the western and central region portion, and the A soils are distributed along the easter border (Figure 128). The A/D soils fill in a majority of the remaining area.

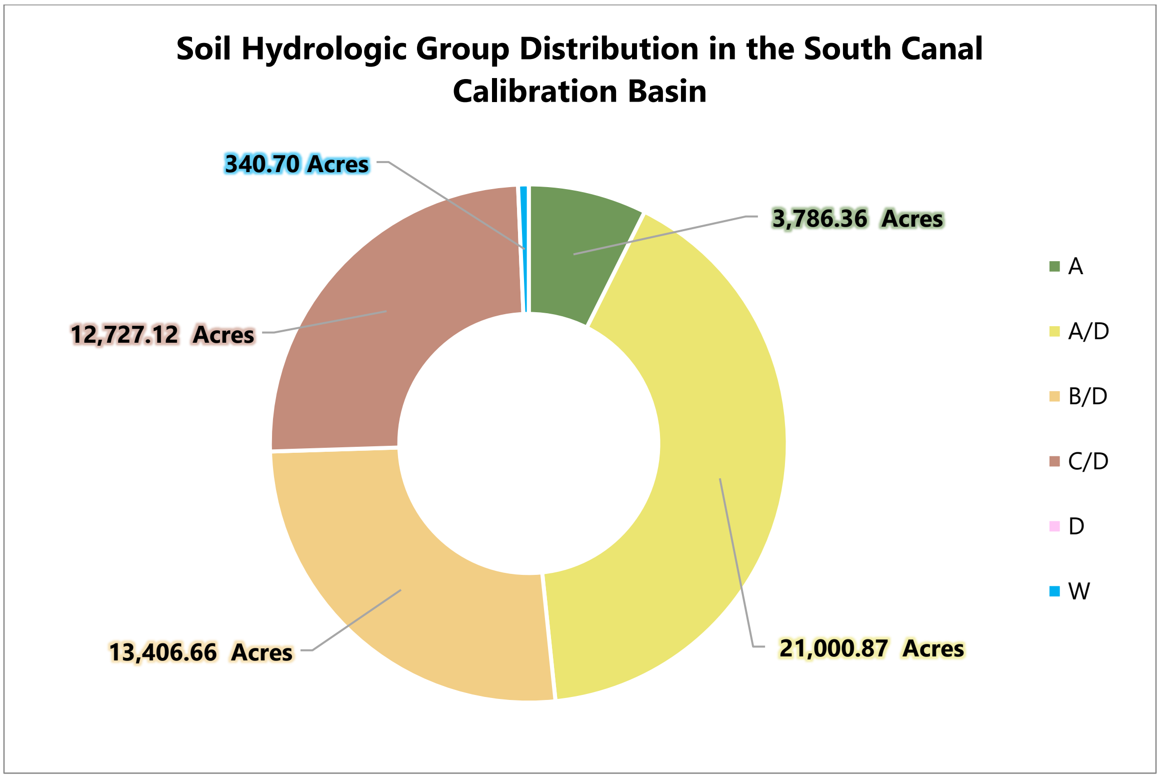

Figure 127. Pie chart (acres) of the soil hydrologic group distribution in the South Canal calibration basin using USDA NRCS data.

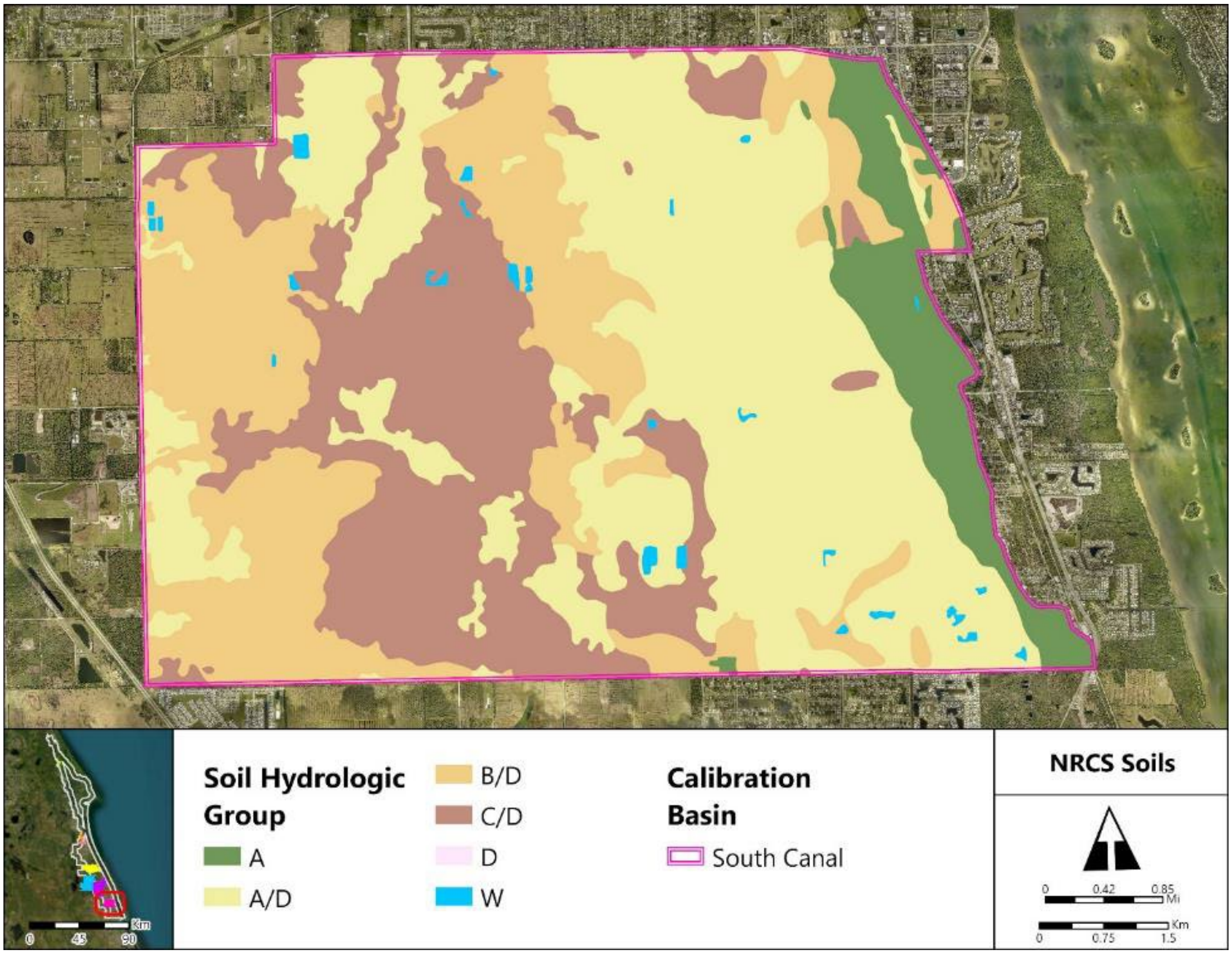

Figure 128. Distribution of soil hydrologic groups within the South Canal calibration basin.

2.7.3 Precipitation

The annual total precipitation for South Canal ranges from the lowest annual total of 23 inches in 2010 to the highest annual total of 64 inches in 2020 (Figure 129). For all years, the dry season has a lower total seasonal rainfall as compared to the wet seasons of the same years (Figure 130). The average monthly precipitation values are higher from May to October and lower from November to April (Figure 131). Maps for the monthly precipitation averages (inches/month) in February and September across the POR in the South Canal calibration basin are provided in Figure 132 and Figure 133, respectively.

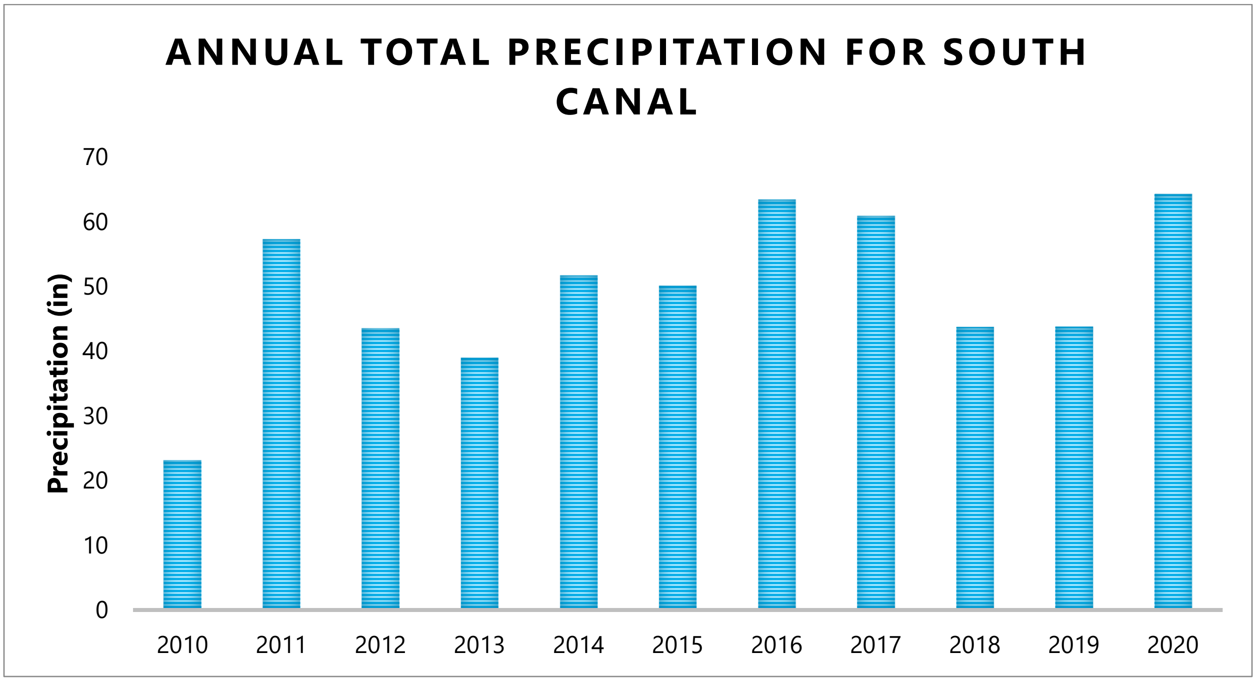

Figure 129. Annual total precipitation (in) for the South Canal calibration basin from 2010 to 2020 derived from SJRWMD NEXRAD data.

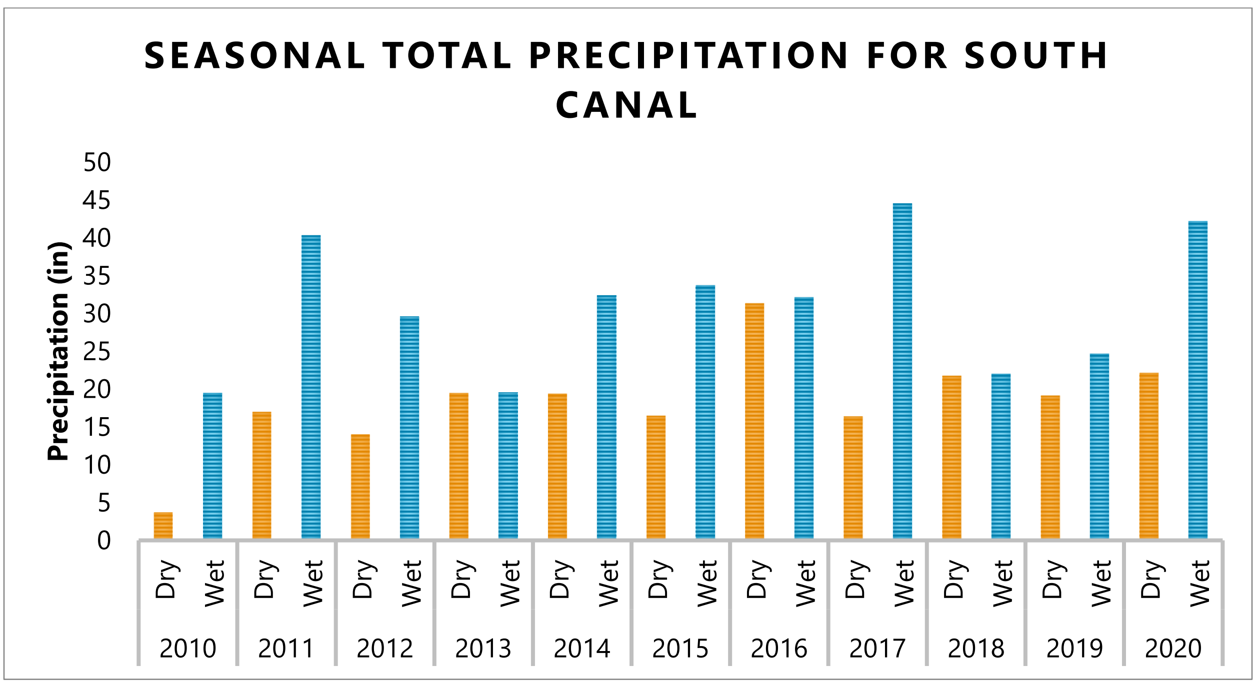

Figure 130. Seasonal total precipitation (in) for the South Canal calibration basin from 2010 to 2020 derived from SJRWMD NEXRAD data.

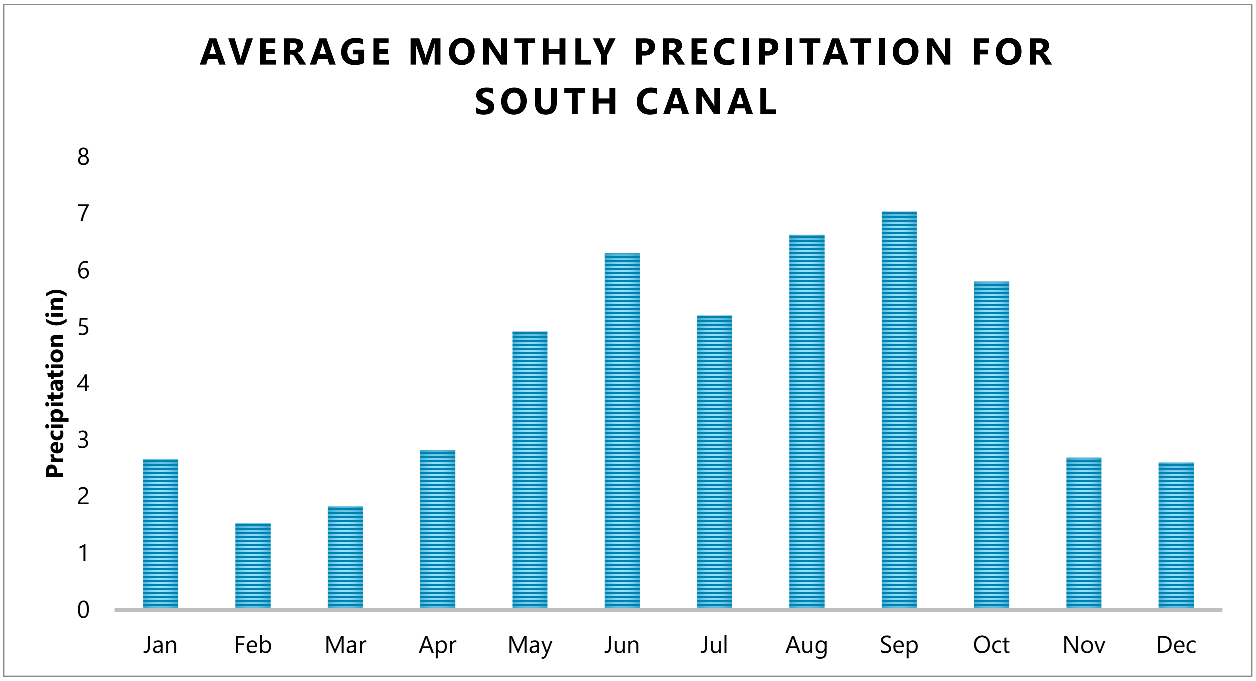

Figure 131. Average monthly precipitation (in) for the South Canal calibration basin derived from SJRWMD NEXRAD data.

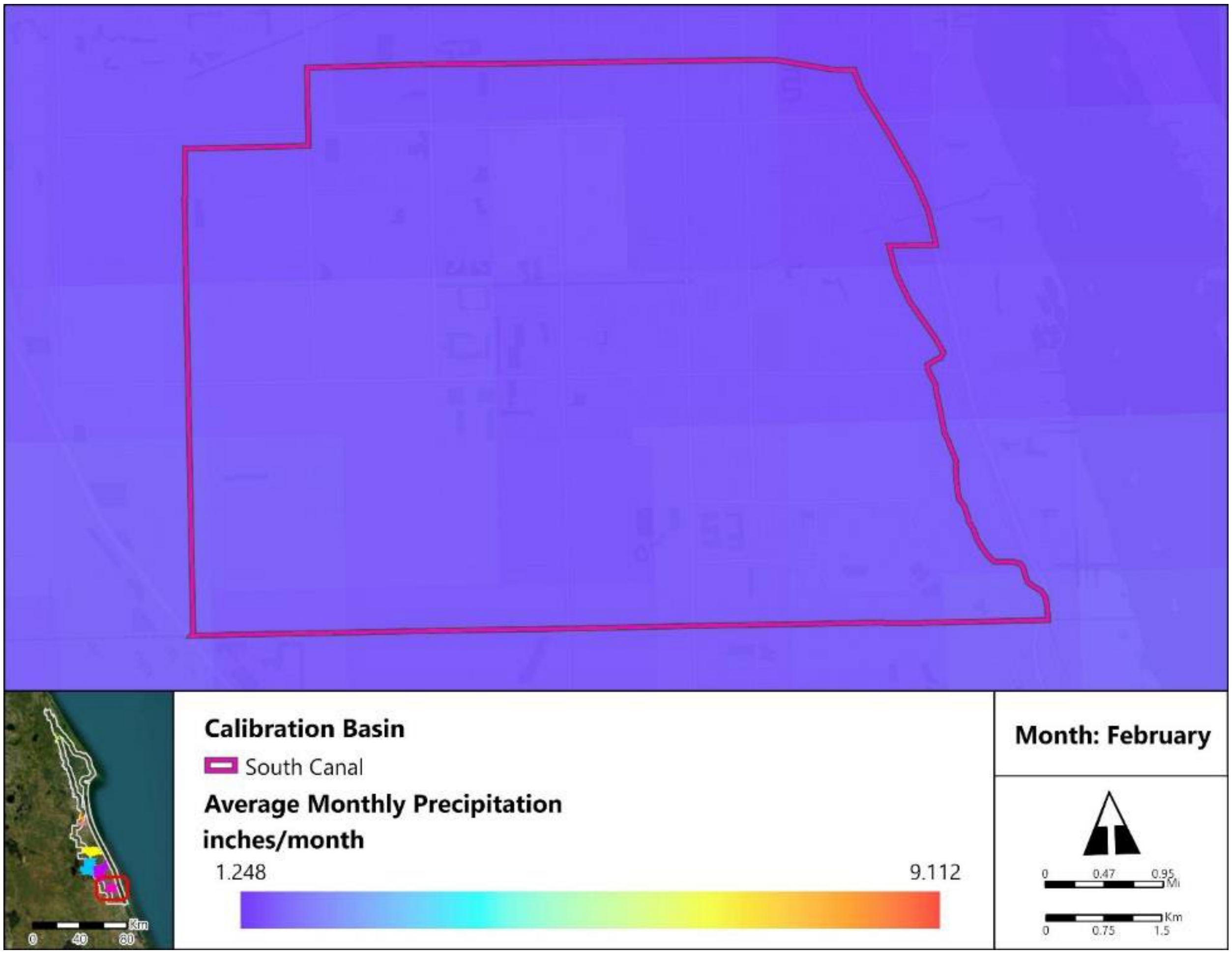

Figure 132. Average monthly precipitation (inches/month) for February across the period of record in the South Canal calibration basin.

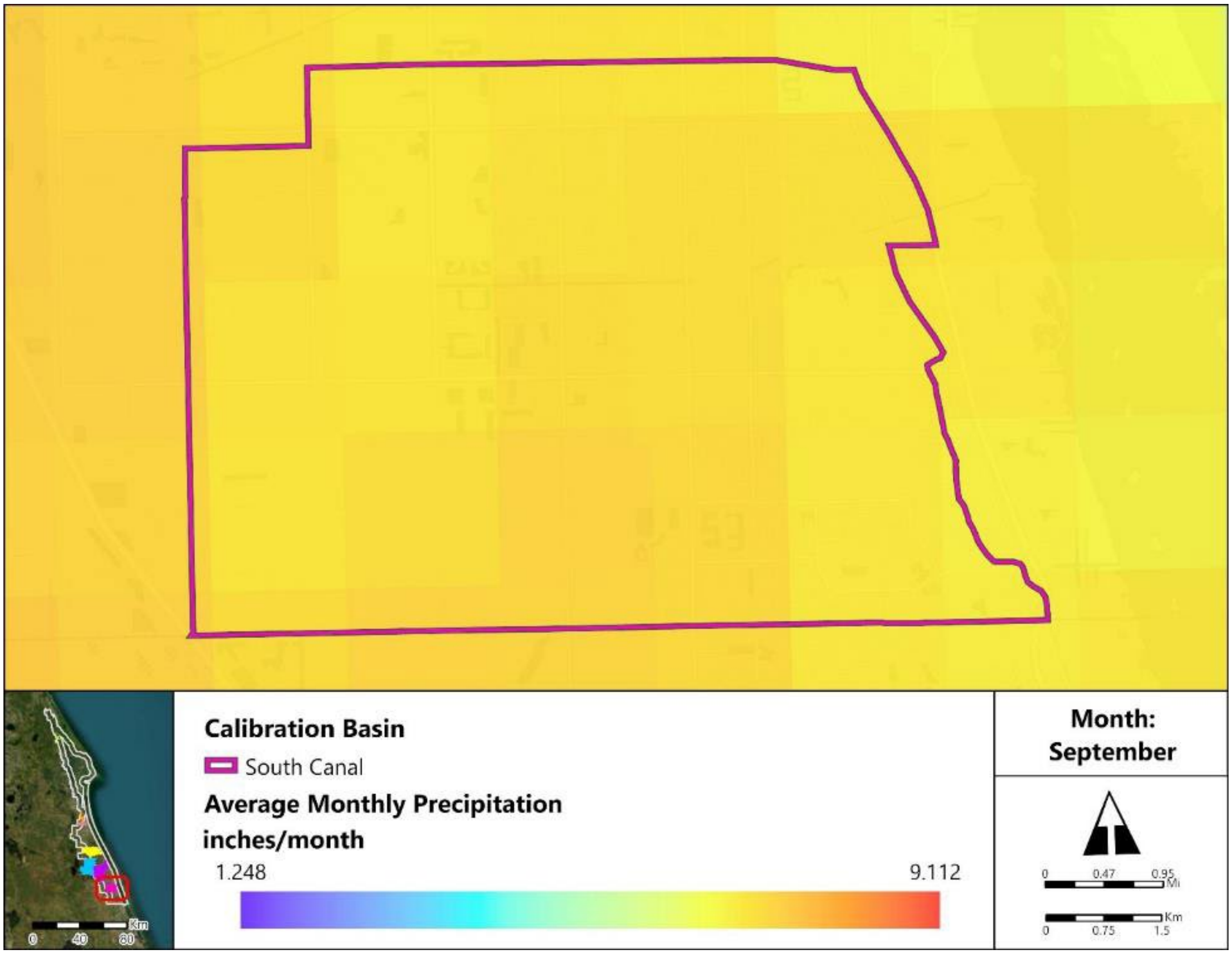

Figure 133. Average monthly precipitation (inches/month) for September across the period of record in the South Canal calibration basin.

2.7.4 ET

Summary statistics for the monthly mean ET in the South Canal calibration basin are provided as a boxplot (Figure 134). For South Canal, there is a lower variation in the wet and dry seasonal ET rates, albeit a trend is observed with increases in ET rates through the wet season and decreases in the dry season. The lowest median values and lowest variability in ET rates are seen in the dry season, where there are generally lower temperatures. The greatest median value and highest variability in ET rates are seen in the wet season, where there are generally higher temperatures. The lowest median value was observed in January (1.07 mm/day), whereas the highest medians were observed in August (2.44 mm/day). The highest variability was observed in May, with an interquartile range difference of 0.91 mm/day, and the lowest variability was observed in January, with a 0.28 mm/day difference in the interquartile range. Maps for mean monthly ET rates (mm/day) during February and September across the POR in the South Canal calibration basin are provided in Figure 135 and Figure 136, respectively.

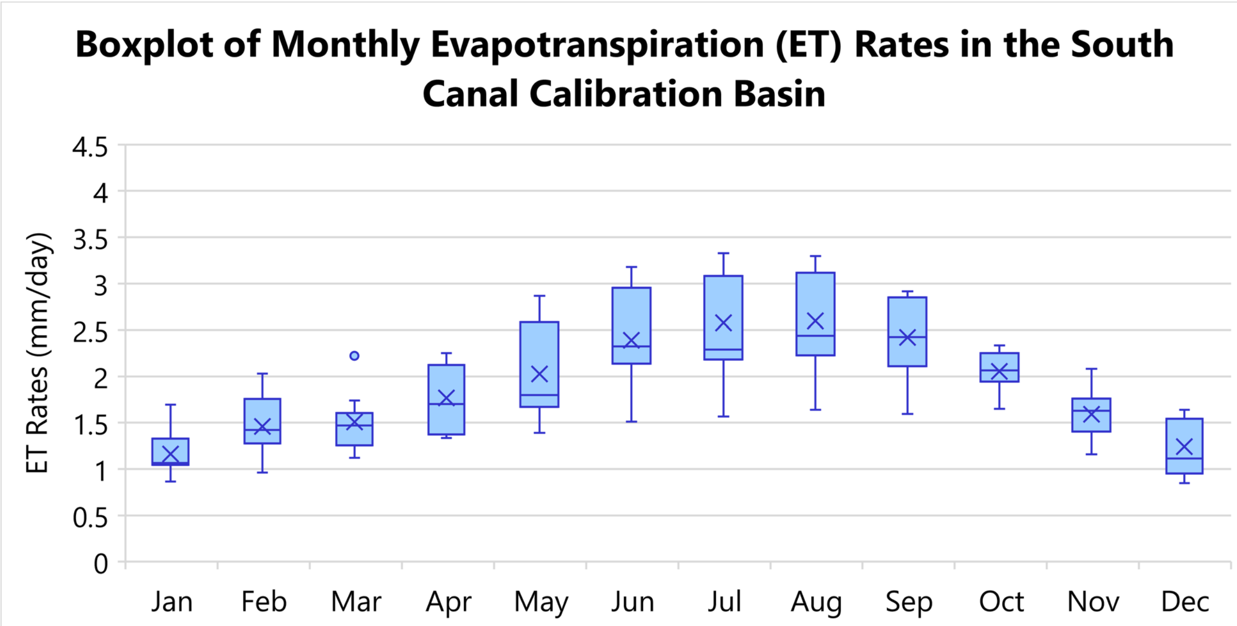

Figure 134. Boxplot of monthly mean ET rates in the South Canal calibration basin derived from NASA EarthData and the University of Montana data.

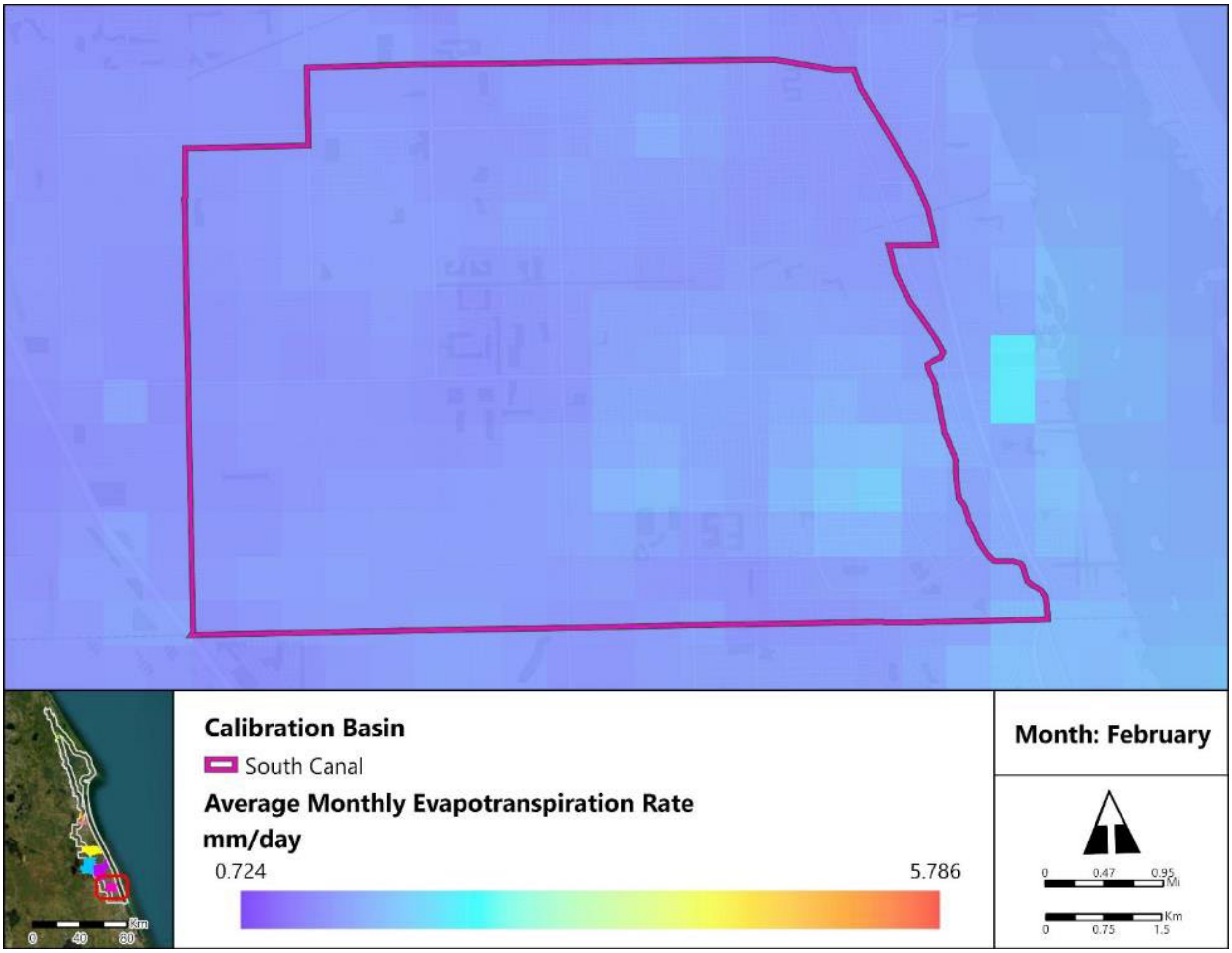

Figure 135. Average monthly ET rates (mm/day) for February across the period of record in the South Canal calibration basin.

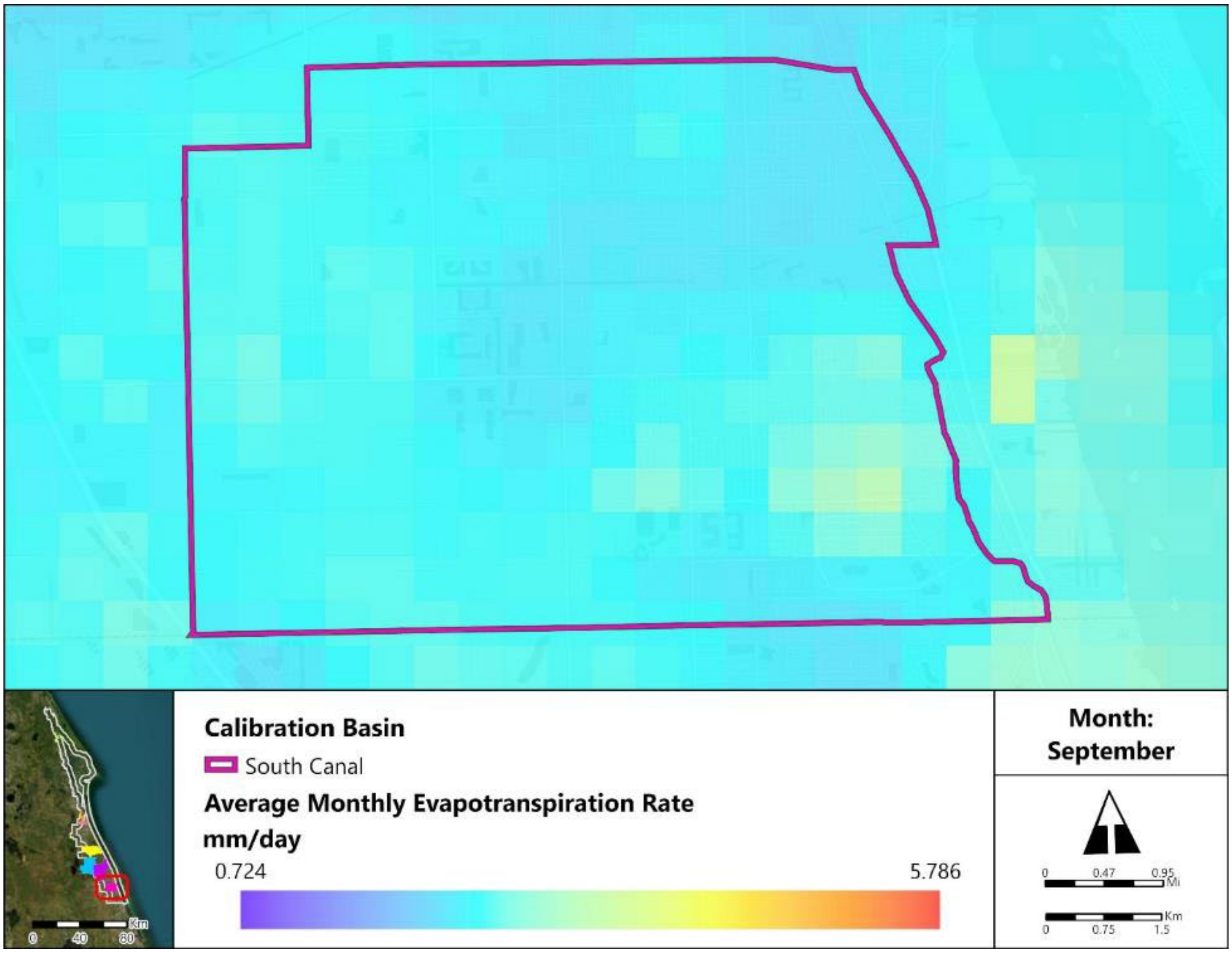

Figure 136. Average monthly ET rates (mm/day) for September across the period of record in the South Canal calibration basin.

2.7.5 TREATMENTS

Within South Canal, approximately 48% of the calibration basin's total area is treated (Table 22), with most of the treatments being composed of the wet type (35%) versus a dry treatment (14%). Overall, the largest changes occurred between 2010 and 2020, with a 2.6% increase in the treated area using wet treatments, a result of increases in residential land use types (Figure 137, Figure 138, Figure 139).

Table 22. Total area (acres) of each treatment type in the South Canal calibration basin for the 2010, 2015, and 2020 years.

Treatment Type	Treatment Area (Acres)			Percent of Total Basin Area (%)			Percent Change (%)	
	2010	2015	2020	2010	2015	2020	2015-2010	2020-2010
Dry	2,296.26	2,311.73	2,320.18	13.44	13.53	13.58	0.09	0.14
Wet	5,762.15	5,867.96	6,202.39	33.72	34.34	36.30	0.62	2.58
Total	*8,058.42*	*8,179.69*	*8,522.57*	*47.16*	*47.87*	*49.88*	*0.71*	*2.72*

The percentage of the total basin area and the percent change from the overall area between 2010 and 2015, as well as 2010 and 2020 have also been provided.

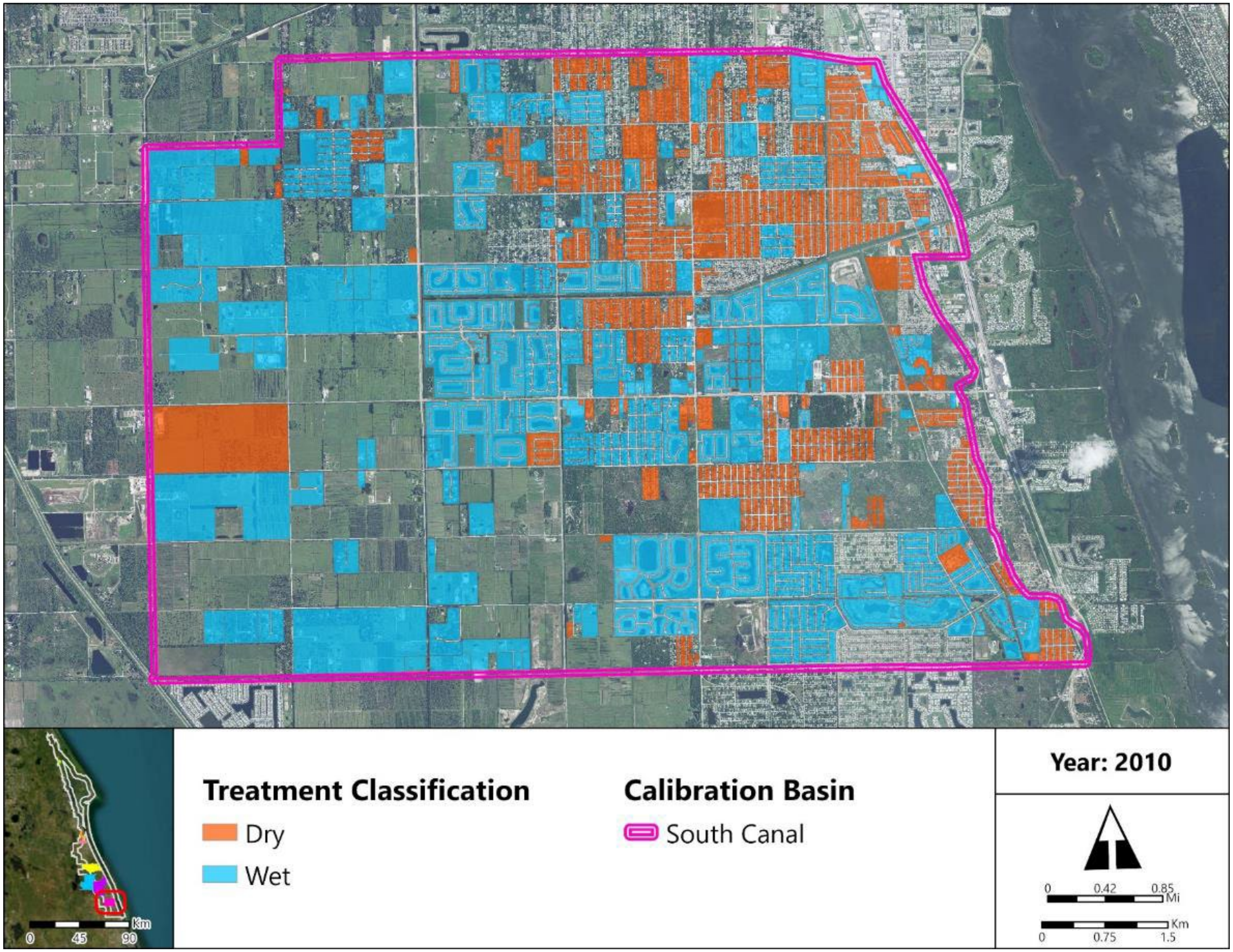

Figure 137. Treatments within the South Canal calibration basin for 2010.

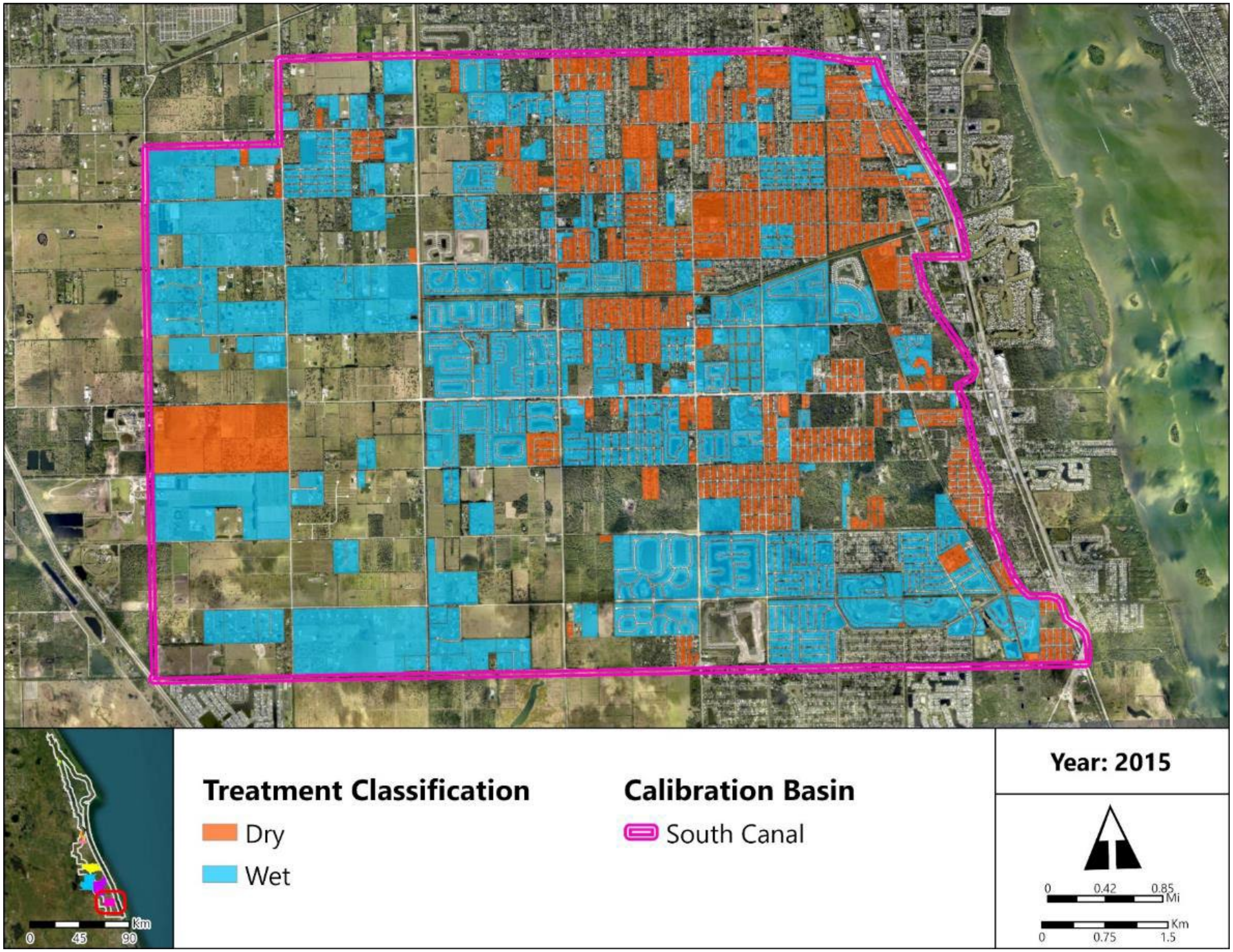

Figure 138. Treatments within the South Canal calibration basin for 2015.

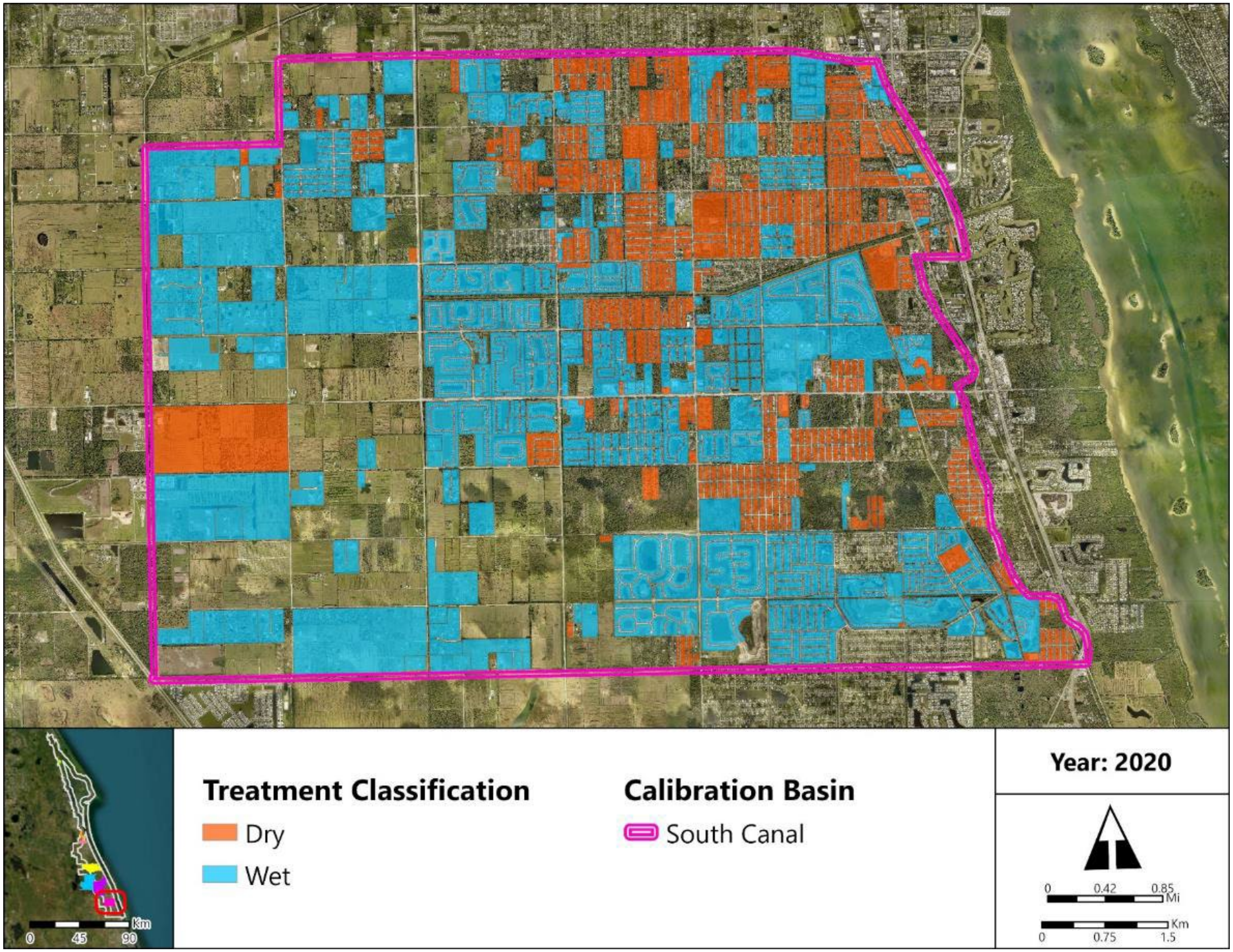

Figure 139. Treatments within the South Canal calibration basin for 2020.

2.7.6 Hydrology

The South Canal calibration basin volume is dominated by subsurface flow monthly (~76%), seasonally (~78% in the dry season and ~72% in the wet season), and annually (~76%) from 2010 to 2020. The average monthly volumes are higher from June to October, with lower volumes from November to May for the POR (Figure 140). The 2017 and 2020 wet seasons showed the highest volumes of discharge, and the lowest seasonal volumes were observed in the 2010 wet season (Figure 141). The greatest annual volumes were observed in 2017 and 2020, as the lowest volumes were observed in 2010, coinciding with the highest and lowest volumes observed in the seasonal data (Figure 142).

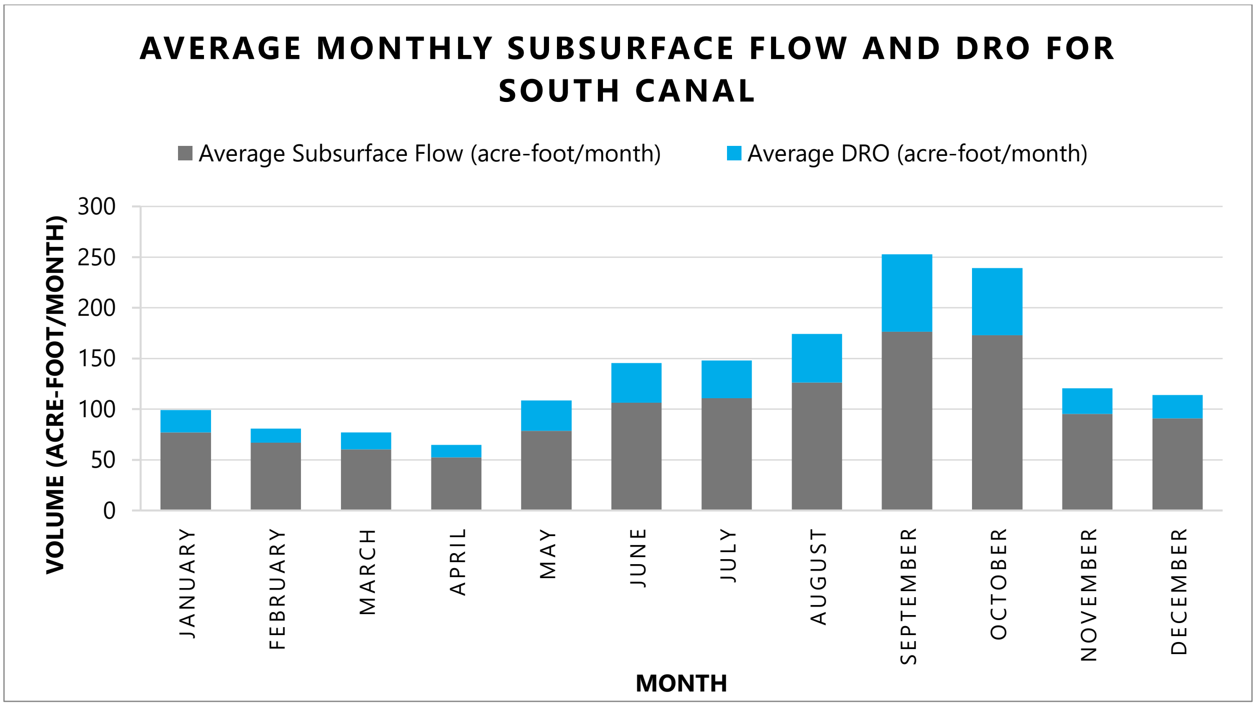

Figure 140. Average monthly subsurface flow (acre-foot/month) and DRO (acre-foot/month) for the South Canal calibration basin derived from USGS WHAT data.

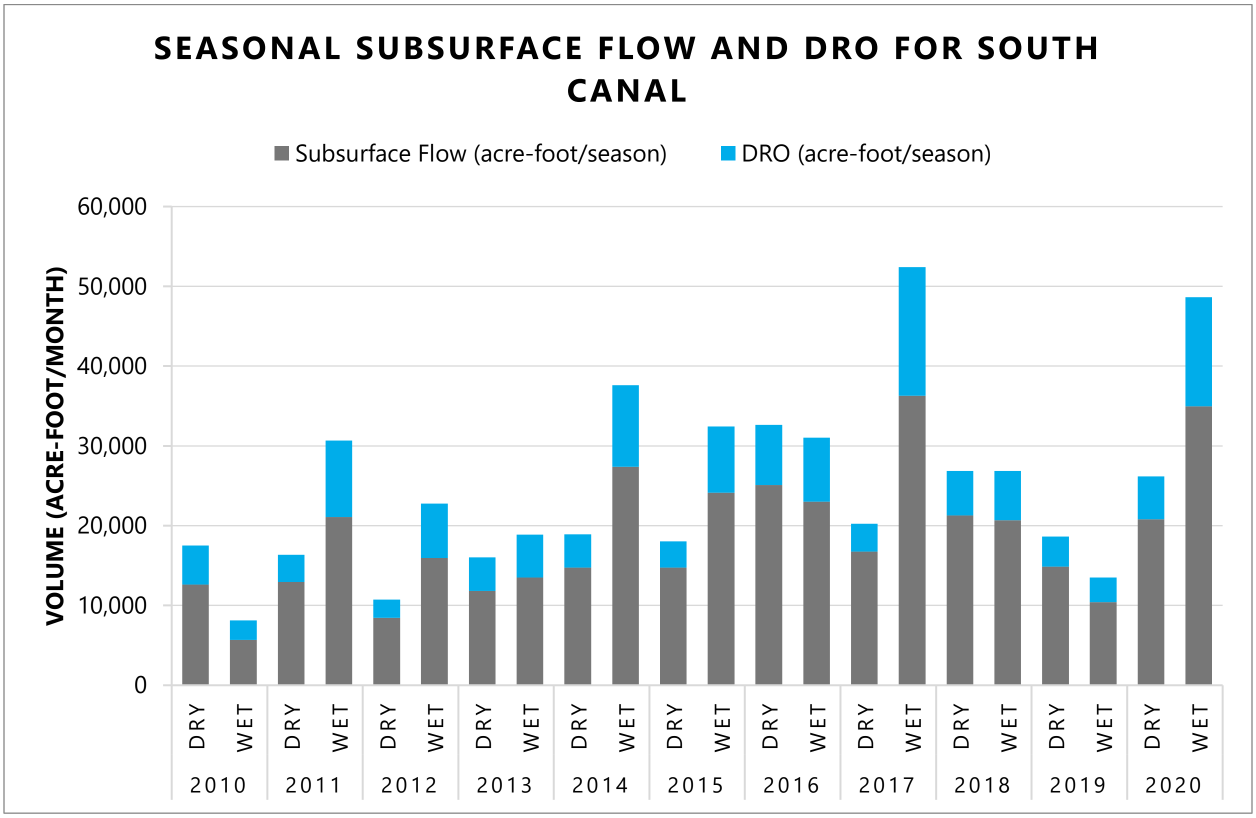

Figure 141. Seasonal subsurface flow (acre-foot/season) and DRO (acre-foot/season) for the South Canal calibration basin derived from USGS WHAT data.

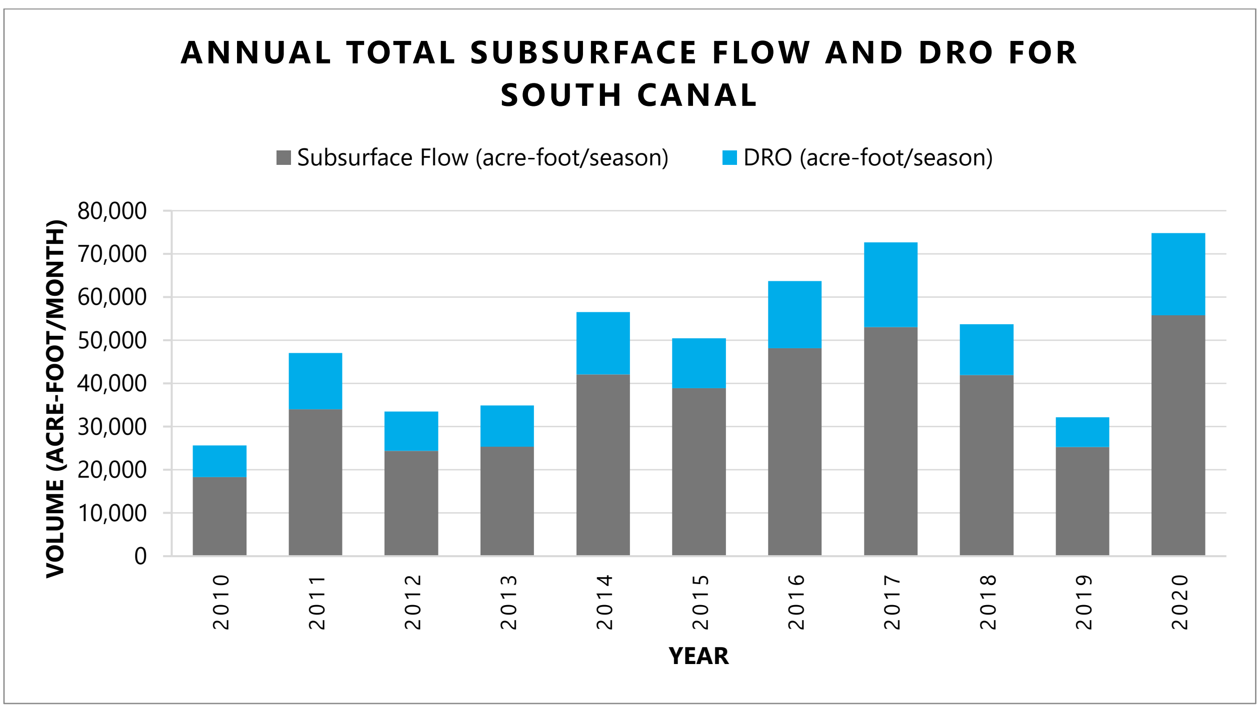

Figure 142. Annual subsurface flow (acre-foot/year) and DRO (acre-foot/year) for the South Canal calibration basin derived from USGS WHAT data.

2.7.7 Water Quality

From 2010 to 2020, there were a total of 132 samples collected from the Vero Beach South Canal at IRLVSC by SJRWMD. Six samples coincided with DRO conditions, 85 coincided with subsurface flow conditions, and the remaining 41 were under mixed conditions (Table 23). A pattern is unable to be determined with the annual and seasonal TN and TP DRO concentrations as there are too few data points.

In general, there is a higher degree of variability for TN subsurface flow in comparison to TP, whose geometric means show to be extremely similar. Although geometric mean concentrations of subsurface flow for TN and TP are not extremely variable within themselves, there does appear to be a steady decrease in annual geometric mean concentrations are observed from 2010 to 2020 (Figure 143).

Table 23. Geometric means of annual TN (mg/L) and TP (mg/L) subsurface flow and DRO samples collected by SJRWMD from 2010 to 2020 at the South Canal station IRLVSC.

Year	TN - DRO	TP - DRO	TN - Subsurface flow	TP - Subsurface flow
2010		0.148	1.186	0.149
2011	1.600	0.515	1.133	0.148
2012	1.513	0.242	1.037	0.138
2013	1.520	0.464	0.853	0.129
2014			1.029	0.143
2015			1.021	0.159
2016			1.065	0.133
2017			0.930	0.150
2018	1.435	0.323	0.906	0.122
2019			0.746	0.091
2020	1.434	0.305	0.935	0.104

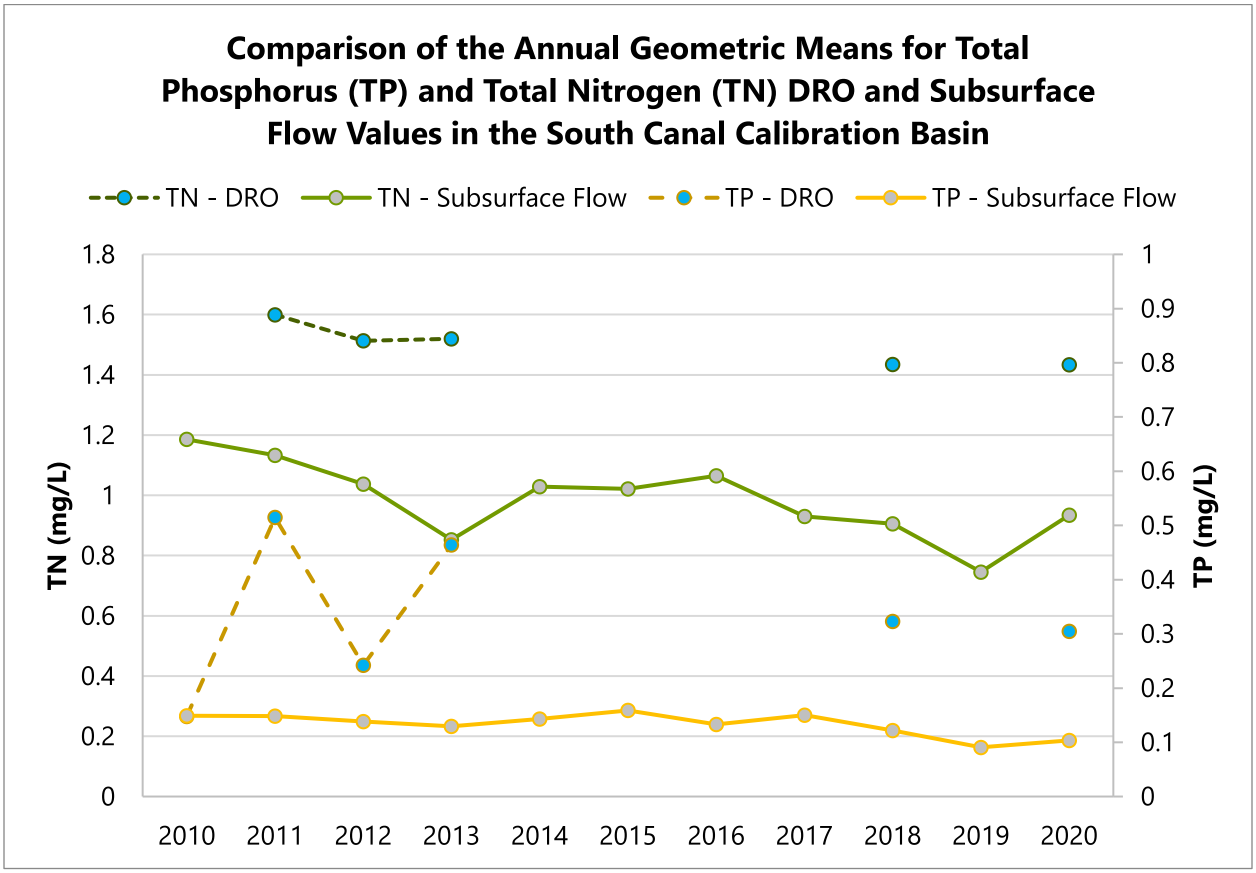

Figure 143. Comparison of the annual geometric means of TN (mg/L) and TP (mg/L) for subsurface flow and DRO between 2010 and 2020 for the South Canal calibration basin.

At a seasonal interval, geometric mean TN concentrations appear to follow a similar pattern to the other stations, with lower concentrations in the dry season and higher concentrations in the wet season (Figure 144). Seasonal geometric mean TN subsurface flow concentrations appear to be decreasing from the 2010 wet season through the 2013 wet season, then begin to increase from the 2013 wet season through the 2015 dry season, then transition into a period of seasonal fluctuations. As with the annual geometric mean concentrations, there is little variation in the seasonal TP subsurface flow; however, a small pattern of concentration being higher in the wet season and lower in the dry season can be observed.

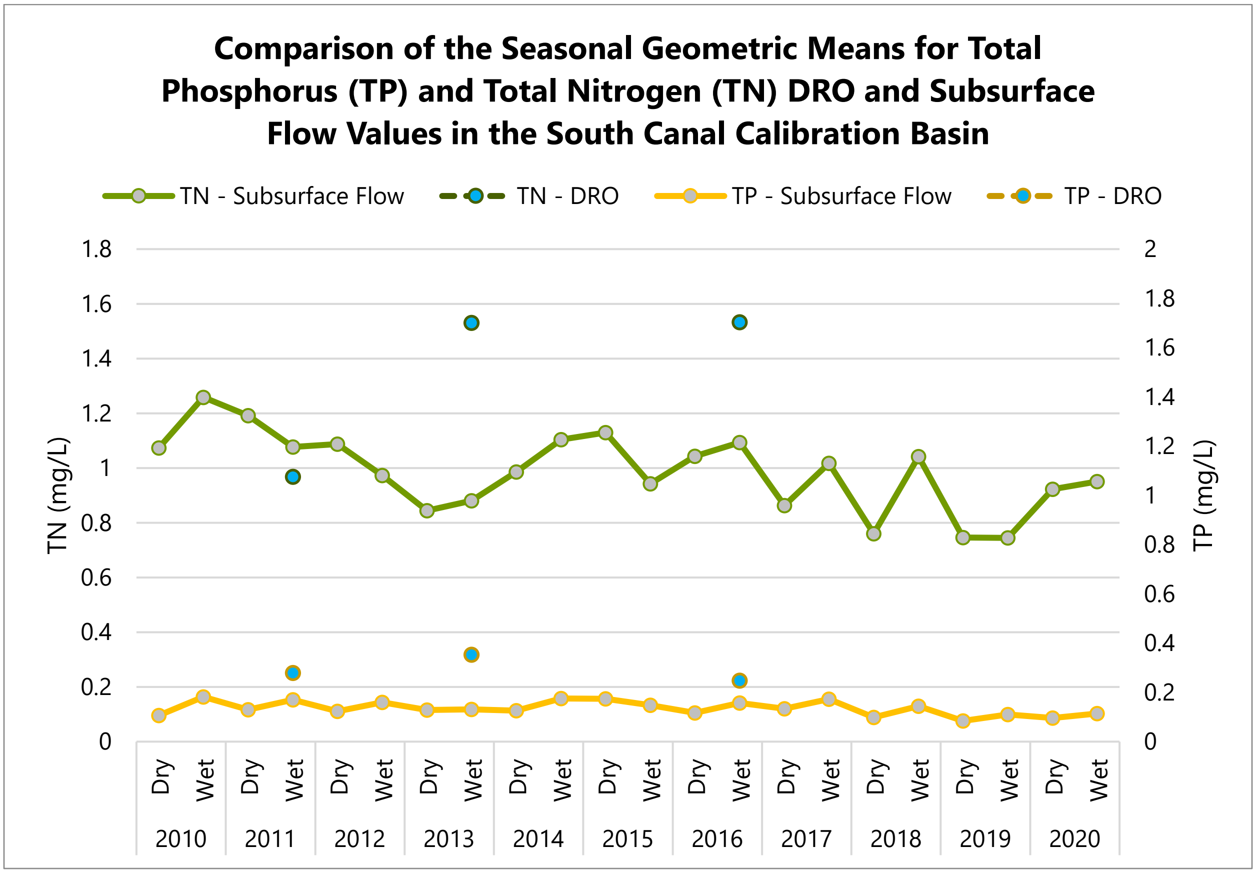

Figure 144. Comparison of the seasonal geometric means of TN (mg/L) and TP (mg/L) for subsurface flow and DRO between 2010 and 2020 for the South Canal calibration basin.

3 REFERENCES

Applied Ecology, Inc. 2022. SWIL v5 Task 1 Update; Data evaluation for the runoff model component. Final Memorandum Report submitted to the Florida Department of Environmental Protection for Agreement PO511181.

Hydrologic Data. St. Johns River Water Management District Hydrologic Data Search Tool. SJRMWD. (2021). Retrieved January 26, 2022, from https://www.sjrwmd.com/data/hydrologic/.

National Water Dashboard. United States Geological Survey. (n.d.). Retrieved January 26, 2022, from https://dashboard.waterdata.usgs.gov/app/nwd/?region=lower48&aoi=defaul